



THE UNIVERSITY OF
WAIKATO
Te Whare Wānanga o Waikato

Research Commons

<http://researchcommons.waikato.ac.nz/>

Research Commons at the University of Waikato

Copyright Statement:

The digital copy of this thesis is protected by the Copyright Act 1994 (New Zealand).

The thesis may be consulted by you, provided you comply with the provisions of the Act and the following conditions of use:

- Any use you make of these documents or images must be for research or private study purposes only, and you may not make them available to any other person.
- Authors control the copyright of their thesis. You will recognise the author's right to be identified as the author of the thesis, and due acknowledgement will be made to the author where appropriate.
- You will obtain the author's permission before publishing any material from the thesis.

**ANALYSIS OF MULTIBEAM SONAR DATA FOR
BENTHIC HABITAT CHARACTERIZATION OF THE
PORT OF TAURANGA, NEW ZEALAND**

A thesis
submitted in partial fulfilment
of the requirements for the degree

of

**Master Of Sciences
in Earth and Ocean Sciences**

at

The University of Waikato

by

SEBASTIEN O. C. BOULAY



THE UNIVERSITY OF
WAIKATO
Te Whare Wānanga o Waikato

2012

ABSTRACT

Tauranga Harbour is a mesotidal lagoon located within the Bay of Plenty, New Zealand, and is subject to an ongoing maintenance dredging program to remove mud deposits coming from various sources in the catchment. At the southern end of the commercial port, the Tauranga Bridge Marina was built adjacent to the bridge causeway, with 500 floating concrete berths, enclosed by concrete floating breakwaters. It is proposed to convert these floating breakwaters into solid ones to stop waves entering the marina. This is expected to influence tidal circulation around the Tauranga bridge causeway, and potentially affect sedimentation and marine habitats. The region is an important source of "kai moana" (seafood) for local iwi, and is a source of juvenile shellfish for the large beds located on the flood tidal delta and surrounding channels.

This study investigates the impact of the successive harbour constructions on the local sedimentology. The overall goal of the mapping part of this project is to identify and locate the different seabed facies and features within the study site, which may be affected by the sediment transport potentially resulting from the past and future harbour developments.

To investigate the impacts of the harbour modifications, a habitat-mapping survey using acoustic mapping techniques was undertaken in July and August 2011. The hydrographic survey was simultaneously performed using a multibeam echosounder (Kongsberg-Simrad EM3000) and a Starfish 452F sidescan sonar. The backscatter/imagery data from both systems was then used for habitat mapping, using a combination of Angular Response Analysis and image-based segmentation. An underwater camera survey and seabed sampling were also performed to ground-truth the morphologies identified from the acoustic backscatter analysis. The most recent habitat map was then compared to the previous studies to identify changes in response to the different modifications of the estuary.



Overview of the dredged Tauranga Stella Passage and the Sulphur Point Container Wharf.

ACKNOWLEDGEMENTS

This project would not have been possible without the help and inspiration from many people and I would like to show them all the gratitude they deserve. First, 'Merci' to my parents for their encouragements even though being on the other side of the world was never easy. Thank you to Valerie for her never-ending support over the course of this thesis. Thank you also to all my friends for always cheering me up when I would turn into the grumpiest guy in the Southern Hemisphere.

Sincere thanks to my advisor, Dr Willem de Lange, for setting up this whole project when my first thesis topic was cancelled and I thought about giving up. Thank you for helping me define the topic of this thesis, your assistance in the fieldwork organization and your directions during the thesis writing. Also, thank you for doing a great job in the early 80s that I could get the inspiration from!

I am particularly grateful to Dirk Immenga. Thank you for your foresight, your organization, for sharing your knowledge, for introducing me to so many people here in New Zealand, for making me a part of the Coastal Marine Group and for never giving up on teaching me how to tie up the boat! Thanks also to the staff of the Earth & Ocean Sciences Department (Chris McKinnon, Dean Sandwell, Sydney Wright, Dr Karin Bryan, Dr Cam Nelson) and my fellow students. I would also like to thank Alexandre Schimel for mentoring me into the darkness of the multibeam sonars and the habitat mapping concepts.

Thank you to Peter McComb from MetOcean Solutions Ltd and Greg Cox from Discovery Marine Ltd for trusting me on various projects during my rare spare times.

I want to express my gratitude to the Australasian Hydrographic Society for awarding me the 2010 AHS Student Award. Thank you also to the GEOHAB committee for the Student Travel Award that allowed me to present my work at the 2011 annual conference in Helsinki, Finland. Finally, the Broad Memorial Fund is gratefully acknowledged for providing financial support for this thesis.

Thank you to the Tauranga Bridge Marina staff for their support during the fieldwork. Thank you Glen Nicholson at Tonkin & Taylor for sharing the Northern Breakwater Assessment Report. Thank you Geoff Shipton and Tony Ramirez at Triton Imaging and Chris Elliott at Quester Tangent for providing trial versions of their programs. Thank you also to the Tauranga City Library staff for digging up the old engineering reports.

This thesis is dedicated to the memory of my grandfather Ollivier.

TABLE OF CONTENTS

ABSTRACT	I
ACKNOWLEDGEMENTS.....	III
TABLE OF CONTENTS.....	IV
LIST OF FIGURES	VII
LIST OF TABLES	XVI
CHAPTER 1 - INTRODUCTION	1
1.1. PORT OF TAURANGA: CURRENT SITUATION.....	1
1.2. PORT OF TAURANGA: PLANNED MODIFICATIONS.....	6
1.3. TAURANGA BRIDGE MARINA PLANNED MODIFICATIONS	9
1.4. STUDY AIM AND OBJECTIVES	12
1.5. THESIS STRUCTURE	13
1.6. REFERENCES.....	14
CHAPTER 2 - PREVIOUS STUDIES OF THE TAURANGA HARBOUR. 15	
2.1. INTRODUCTION.....	15
2.2. PHYSICAL SETTING	15
2.3. A PRELIMINARY ASSESSMENT OF SOME ASPECTS OF THE ECOLOGY OF TAURANGA HARBOUR - 1974	17
2.4. SEDIMENT DYNAMICS OF TAURANGA HARBOUR AND THE TAURANGA INLET - 1976	18
2.5. TAURANGA HARBOUR STUDY - 1985	20
2.5.1. <i>Bathymetry</i>	20
2.5.2. <i>Hydrodynamic Modelling</i>	21
2.5.3. <i>Sediment Transport Modelling</i>	22
2.5.4. <i>Morphological Study</i>	22
2.6. TAURANGA HARBOUR BRIDGE: ENVIRONMENTAL ASSESSMENT - 1985	28
2.7. WAVE CLIMATE AND SEDIMENT TRANSPORT WITHIN TAURANGA HARBOUR IN THE VICINITY OF PILOT BAY - 1988	32
2.8. PORT OF TAURANGA LTD CHANNEL DEEPENING AND WIDENING DREDGING PROGRAMME: ENVIRONMENTAL ASSESSMENT - 1991... 35	
2.9. SEDIMENTATION OF THE ENTRANCE CHANNEL OF THE TAURANGA HARBOUR - 1999	38
2.10. EVALUATION OF AN INNER SHELF SITE OFF TAURANGA HARBOUR, NEW ZEALAND, FOR DISPOSAL OF MUDDY SANDY DREDGED SEDIMENTS - 1999.....	40
2.11. BENTHIC COMMUNITIES OF THE STELLA PASSAGE REGION - 1999 .. 42	
2.12. THE POPULATION DYNAMICS AND PRODUCTION OF PAPHIES AUSTRALIS (PIPI) IN THE SOUTHERN BASIN, TAURANGA HARBOUR - 2001	45
2.13. CHANGE IN GEOMORPHOLOGY, HYDRODYNAMICS AND SURFACIAL SEDIMENTS OF THE TAURANGA ENTRANCE TIDAL DELTA SYSTEM - 2009	47
2.14. TAURANGA BRIDGE MARINA: NORTHERN BREAKWATER ASSESSMENT OF ENVIRONMENTAL EFFECTS - 2009.....	51
2.15. CONCLUSION	54
2.16. REFERENCES.....	55

CHAPTER 3 - BENTHIC HABITAT MAPPING AND ACOUSTIC SEABED CLASSIFICATION	57
3.1. INTRODUCTION.....	57
3.2. BACKGROUND OF SEABED CHARACTERIZATION	57
3.2.1. <i>Habitat ecological definition</i>	57
3.2.2. <i>Acoustic Seabed Classification</i>	58
3.2.3. <i>Various approaches to Acoustic Seabed Classification</i>	58
3.3. ACOUSTIC SEABED MAPPING TECHNIQUES	60
3.3.1. <i>Introduction to underwater acoustics</i>	60
3.3.2. <i>Sidescan Sonars</i>	61
3.3.3. <i>Single-beam echosounders</i>	62
3.3.4. <i>Multibeam echosounders</i>	63
3.3.4.1. <i>Bathymetry measurement by MBES</i>	64
3.3.4.2. <i>Backscatter and mosaic</i>	65
3.3.4.3. <i>Angular Response</i>	66
3.4. CLASSIFICATION METHODS AND ALGORITHMS	68
3.4.1. <i>Introduction</i>	68
3.4.2. <i>Image-based and Texture Analysis</i>	69
3.4.3. <i>Angular Response Analysis</i>	69
3.4.4. <i>Geocoder</i>	70
3.4.4.1. <i>Mosaic Creation and Acoustic Signal Corrections</i>	70
3.4.4.2. <i>Angular Range Analysis and model inversion</i>	71
3.4.5. <i>Combined approach</i>	74
3.5. CONCLUSION	75
3.6. REFERENCES	76
CHAPTER 4 - SURFICIAL SEDIMENT AND SHELL COVERAGE FOR GROUND-TRUTHING	80
4.1. INTRODUCTION.....	80
4.2. SEDIMENT SAMPLING	80
4.2.1. <i>Method</i>	80
4.2.2. <i>Grain Size Analysis</i>	83
4.2.2.1. <i>Dry Sieving</i>	84
4.2.2.2. <i>Laser Diffraction</i>	84
4.2.3. <i>Results and Spatial Variation</i>	85
4.2.3.1. <i>Laser Diffraction</i>	85
4.2.3.2. <i>Dry Sieving</i>	86
4.3. UNDERWATER VIDEO SURVEY	89
4.3.1. <i>Method</i>	89
4.3.2. <i>Shell Coverage</i>	90
4.3.3. <i>Species identified</i>	92
4.4. SUMMARY	95
4.5. REFERENCES	98
CHAPTER 5 - BENTHIC HABITAT MAPPING AND ACOUSTIC SEABED CLASSIFICATION	99
5.1. INTRODUCTION.....	99
5.2. SIDESCAN SONAR SURVEY	99
5.2.1. <i>Method</i>	99
5.2.2. <i>Mosaic Creation</i>	102
5.3. MULTIBEAM ECHOSOUNDER SURVEY	105
5.3.1. <i>Method</i>	105
5.3.2. <i>Bathymetry processing</i>	107
5.3.3. <i>Mosaic creation</i>	112
5.4. IMAGE-BASED CLASSIFICATION	115
5.4.1. <i>Erdas Imagine</i>	115
5.4.2. <i>ArcGis Spatial Analyst</i>	117
5.4.3. <i>Image Based Analysis Results</i>	118
5.5. ANGULAR RESPONSE ANALYSIS	120
5.6. CORRELATION OF THE VARIOUS DATASETS	126

5.7.	BENTHIC HABITAT MAP CREATION	131
5.8.	CONCLUSIONS	133
5.9.	REFERENCES:.....	135
CHAPTER 6 - DISCUSSION AND CONCLUSIONS.....		136
6.1.	OVERVIEW	136
6.2.	COMPARISON TO PREVIOUS STUDIES	136
6.2.1.	<i>Stella Passage</i>	139
6.2.2.	<i>Town Reach and Tauranga Bridge Marina</i>	141
6.2.3.	<i>Summary</i>	143
6.3.	GEOCODER	145
6.3.1.	<i>Angular Response Analysis versus ground-truthing</i>	145
6.3.2.	<i>Limitations of Geocoder</i>	146
6.4.	SUMMARY OF THE VARIOUS CLASSIFICATION METHODS	147
6.5.	ACHIEVEMENTS OF THE STUDY	148
6.6.	RECOMMENDATIONS FOR FUTURE RESEARCH.....	150
6.7.	REFERENCES	151
 APPENDICES:		
GRAIN SIZE ANALYSIS, LASER DIFFRACTION.....		152
GRAIN SIZE ANALYSIS, SIEVING.		173
GROUNDTRUTHING DATA SUMMARY		194
SEDIMENT GRAB SAMPLES		197
UNDERWATER VIDEOS SNAPSHOTS		199

LIST OF FIGURES

Overview of the dredged Tauranga Stella Passage and the Sulphur Point Container Wharf.....	ii
Figure 1.1: Tauranga, located in the Bay of Plenty on the North Island of New Zealand.....	2
Figure 1.2: Map of the main Tauranga Harbour shipping channels and geographic features (Aerial photo source: Bay of Plenty Regional Council).....	3
Figure 1.3: Nautical chart of Tauranga region (Source: Land Information New Zealand, www.linz.govt.nz).....	4
Figure 1.4: 3D view of the Tauranga Stella Passage, Town Reach and Bridge Marina. Image created using the multibeam echosounder survey performed in July 2011 by the University of Waikato. Depths are 6 times vertically exaggerated. This chart clearly shows the current dredged area in the deep (dark blue) part of the Stella Passage. Depths are expressed in meters relative to Mean Sea Level (Moturiki Vertical Datum). (Aerial photo source: Bay of Plenty Regional Council).....	5
Figure 1.5: Planned future expansion of the Container Terminal (Photo Source: Port of Tauranga).....	7
Figure 1.6: Widening and Deepening shipping channels program (Source: Bay of Plenty Regional Council, Resource Consent N°65806).....	8
Figure 1.7: Northern floating pontoon of the Tauranga Bridge Marina.	10
Figures 1.8 & 1.9: Proposed breakwater plan (top) and section (bottom) (Source: Northern Breakwater Assessment of Environmental Effects 2010) ..	11
Figure 2.1: Aerial photograph of the Tauranga Harbour taken in 1975?. (Source: Davies-Colley, 1976).....	16
Figure 2.2: Underwater photograph of coarse shelly sediment, Southwest of the Centre Bank. Shells are mainly cockles (<i>Chione stutchburyi</i>), pipis (<i>Amphideam australe</i>) and various gastropods. These shells are the main roughness element on the seabed. (Photo: Wayne Ruegg from Davies-Colley, 1976).....	19

Figure 2.3: Underwater photograph of a relatively fine sandy sediment bed, Northeast of the Central Bank. The sediment bed is deformed by the action of tidal currents into small sinuous and linguoid ripples. (Photo: John White from Davies-Colley, 1976)	19
Figure 2.4 (Left): Distribution of the bedforms within Tauranga Harbour. (Source: Davies-Colley, 1976)	19
Figure 2.5 (Below): Echosounder profiles across sand dunes located within harbour channels. (Source: Davies-Colley, 1976)	19
Figure 2.6: Bathymetry changes between 1852 and 1983. Note the deepening of the west side of the Stella Passage and the reclamation on Sulphur Point. (Source: Barnett, 1985)	20
Figures 2.7, 2.8 and 2.9: Residual current vectors showing net current circulation averaged over a complete tidal cycle in the Stella Passage in 1970 (a), 1983 (b) and after completion of the dredging programme (c) (Source: Black, 1984)	21
Figure 2.10, 2.11, 2.12 And 2.13: Sedimentation patterns in the Stella Passage in 1970 (a), 1983 (b) and after completion of the dredging programme for a medium sand on a spring tidal range (c) and averaged over a year (d). Erosion is crosshatched; accretion is dotted. (Source: Black, 1984)	22
Figure 2.14: Klein sidescan sonar system (towfish) and Uniboom Seismic profiler. (Source: de Lange, 2011)	23
Figure 2.15: Single-beam echosounder recording onboard the BOPHB work vessel “Mahi”. (Source: de Lange, 2011)	23
Figure 2.16: Underwater photography and sediment sampling locations. (Source: Healy, 1985)	24
Figure 2.17: Tauranga Harbour sidescan track. (Source: Healy, 1985)	25
Figure 2.18: Tauranga Harbour sidescan example. The section 60 to 70 from Fig. 2.17 is represented here. (Source: Healy, 1985)	25
Figure 2.19: Tauranga Harbour bottom sediment facies. (Source: Healy, 1985) .	26
Figure 2.20: Vertical view of the Stella Passage, Town Reach, Sulphur Point and Waipu Bay. (Source: Healy, 1985)	27
Figure 2.21: Sulphur Point reclamation (looking south-east) during construction of the boat marina in 1981. (Source: Healy, 1985)	27

Figure 2.22: Shellfish sampling stations. (Source: Beca Carter Hollings and Ferner Ltd, 1985)	30
Figure 2.23: Ecology and Resources of the Tauranga Bridge area. (Source: Beca Carter Hollings and Ferner Ltd, 1985)	31
Figure 2.24: Shell lag facies made of fresh pipi (<i>Paphies australis</i>), turret shell (<i>Maoricolpus roseus</i>) and white rock shell (<i>Thais orbita</i>). (Source: de Lange, 1988).....	33
Figure 2.25: Very shelly sand facies, pipi and turret shells cover 50-80% of the seabed. (Source: de Lange, 1988)	33
Figure 2.26: Shelly sand facies, shell fragments and occasional live horse mussel and scallop cover 20-50% of the seabed. (Source: de Lange, 1988) .	33
Figure 2.27: Silty sand facies, finer undisturbed sediment with occasional cockles and horse mussels. (Source: de Lange, 1988)	33
Figure 2.28: Sand waves and megaripples facies. (Source: de Lange, 1988).....	33
Figure 2.29: Bottom sediment distribution for the Pilot Bay region. (Source: de Lange, 1988).....	34
Figure 2.30: Historic sediment sampling site locations (Source: Healy <i>et al</i> , 1991)	36
Figure 2.31: Stella Passage mud probe investigations and interpreted sediment types. (Source: Healy <i>et al</i> , 1991)	36
Figure 2.32: Core D76. (Source: Healy <i>et al</i> , 1991)	37
Figure 2.33: Core D75. (Source: Healy <i>et al</i> , 1991)	37
Figures 2.34, 2.35 and 2.36: Vibratory coring device, Core D76 stratigraphy and Core 75 stratigraphy. (Source: Healy <i>et al</i> , 1991).....	37
Figure 2.37: The Klein 595 system on board the Port of Tauranga Kairuri IV work vessel. (Source: Kruger, 1999)	38
Figure 2.38: Ebb tidal delta bottom sediment facies map. (Source: Kruger, 1999)	39
Figure 2.39: Sonograph from the Klein 595 showing medium-sand dunes and a shell lag. (Source: Kruger, 1999)	39

Figure 2.40: Interpretation of the features from the sidescan sonar survey on the proposed disposable ground. (Source: Michels & Healy, 1999).....	41
Figure 2.41: Sampling sites and macrofaunal community composition. (Source: Butler, 1999).....	43
Figure 2.42: Total number of individuals for the Bivalvia taxonomic group. (Source: Butler, 1999).....	44
Figure 2.43: Pearson's correlation coefficients between the pipi descriptors and the environmental conditions. Top value is Pearson's coefficient. Bottom value is p-value. Significant correlations are in bold. (Source: Gouk, 2011).....	46
Figure 2.44: Mean spring tide peak flood velocity vector plot for 2006 (top) and 1954 (bottom). (Source: Brannigan, 2009)	48
Figure 2.45: Sidescan sonar mosaic of the Tauranga Harbour in 2007. (Source: Brannigan, 2009).....	49
Figure 2.46: Surficial sediment and shell coverage map of the Tauranga Harbour in 2007. (Source: Brannigan, 2009)	50
Figure 2.47: Comparison of 2007 and 1983 surficial sediment and shell coverage maps for the Tauranga Harbour. (Source: Brannigan, 2009)	50
Figure 2.48: Existing bathymetry plan and core samples locations. (Source: Tonkin & Taylor Ltd, 2009).....	52
Figure 2.49: Peak flood tide currents after construction of the breakwater. (Source: Tonkin & Taylor Ltd, 2009)	53
Figure 2.50: Peak ebb tide currents after construction of the breakwater. (Source: Tonkin & Taylor Ltd, 2009).....	53
Figure 3.1: Strategies for the production of benthic habitat maps (Source: (Brown et al., 2011))	59
Figure 3.2: Beam pattern of a sidescan sonar (Source: (Penrose et al., 2005))	62
Figure 3.3: Single-beam echosounder for seabed interpretation (Source: (Anderson et al., 2007)).....	63
Figure 3.4: Multibeam echosounder principle (Source: (Anderson et al., 2007))..	65
Figure 3.5: Principle of the angular dependence of reflected energy (Source: (Dugelay, Graffigne, & Augustin, 1996)	67

Figure 3.6: Stacked backscatter angular response ranges from one side of an EM3000 multibeam sonar. The dashed lines represent the slope and the white circle the intercept. (Source: (Fonseca & Mayer, 2007)	73
Figure 3.7: Example of model fitting (blue) on the raw time series angular response on portside (red) and starboard (blue) in a version of Geocoder implemented in IVS Fledermaus. The manual modifications of the ARA parameters with ground-truthing data allow the model inversion.	73
Figure 3.8: Second stage of the unsupervised segmentation based on the angular response, here presented as a histogram instead of a curve. Following this stage, the two segments on the left will be aggregated. Source: (Schimel et al., in preparation)	75
Figure 4.1: Sediment sampling and underwater video locations. (Aerial photo source: Bay of Plenty Regional Council)	81
Figure 4.2: Sediment sampling setup on the University of Waikato's survey vessel <i>Tai Rangahau</i> . The capstan hauling the Ponar grab sampler through the pulley on the davit (visible on top) is located on the left behind the operator.....	82
Figures 4.3, 4.4, 4.5 and 4.6: Examples of sediment samples from the Port of Tauranga. Sites 14 (left) and 23 (right) are shown on the top; 21 (left) and 37 (right) are displayed on the bottom line.	82
Figure 4.7: "Octagon" sieve shaker fitted with the 6 different grain sizes sieves.	84
Figure 4.8: Overall laser diffraction particle size distribution of the Tauranga Harbour sediment samples. We can notice the clear dominance of the sand class (Phi values between -1 and 4).	85
Figure 4.9: Percentage of each sediment class in the combined Tauranga samples.	86
Figure 4.10: Overall frequency distribution histogram of the Tauranga sediment samples obtained from dry sieving, not including the gravel fraction. Note the importance of the fine sand class. (Phi 2 to 3). Graph produced with Gradistat.	87
Figure 4.11: Overall cumulative frequency of the Tauranga sediment samples obtained from dry sieving, not including the gravel fraction (> 2 mm). Graph produced with Gradistat.	87
Figure 4.12: Surficial sediment map of the Stella Passage, Town Reach and Bridge Marina areas of Tauranga Harbour derived from grab samples.	

The colour-coded clusters group similar sampling sites and do not mean to represent the actual sediment class boundaries of the area. . 88

Figure 4.13: Underwater video camera fitted on the weighted frame (about 50 cm × 50 cm), sitting on the back deck of the University of Waikato survey vessel *Tai Rangahau*. 89

Figure 4.14: Sand: very little or no shells (<20%) at Site 1..... 90

Figure 4.15: Shelly sand (20-50%) at Site 4..... 90

Figure 4.16: Very Shelly Sand (50-80%) at Site 21..... 90

Figure 4.17: Shell Lag (>80%) at Site 40. 90

Fig 4.18: Surficial shell coverage derived from underwater video analysis in the Tauranga Harbour. The colour-coded clusters group similar sampling sites and do not represent the actual shell coverage boundaries of the area. 91

Figure 4.19 & 4.20: Pipi (Left) and turret shell (right) spatial distributions..... 93

Figure 4.21 & 4.22: Cockle (Left) and starfish (right) spatial distributions. 93

Figure 4.23: Locations of the shell coverage disagreements between the sediment samples and underwater videos. The numbers are the sample location number (Fig. 4.1), and the colours indicate the level of disagreement. 97

Figures 5.1, 5.2 & 5.3: Installation of the Starfish 452F (bottom right) sidescan sonar on the hull of the University of Waikato survey vessel *Tai Rangahau*” (left). The top-right photo presents the simple survey station required to operate this equipment on the survey vessel. 100

Figure 5.4: Screenshot of the Starfish Scanline acquisition software. 100

Figure 5.5: Sidescan sonar survey coverage of Stella Passage and Town Reach, Tauranga Harbour, based on the navigation recording (July 2011). 101

Figure 5.6: Sidescan sonar reflectivity mosaic of the Port of Tauranga (July 2011). 103

Figures 5.7 to 5.12: Preview of identifiable facies based on sidescan sonar reflectivity. The top row shows the area around the Tauranga Harbour Bridge’s east end. The left image shows the rock wall of the artificial bank and several mooring concrete blocks and chains (darks spots). The centre and right pictures show the sand waves and sediment type

clear delineation just north of the Bridge gap. The bottom line presents seabed images around the Bridge Marina. The left image is the Marina entrance showing clear reflections on the piles. The centre and right image present the northern breakwater and the sediment patches and sand waves aligned with the Whareroa inlet.....	104
Figures 5.13 & 5.14: University of Waikato survey vessel <i>Tai Rangahau</i> (left) showing the Kongsberg EM3000 fitted on a bow pole (right).....	105
Figure 5.15: Multibeam echosounder (Kongsberg-Simrad EM3000) survey coverage of the Port of Tauranga (August 2011).....	106
Figure 5.16: Bathymetry of the Port of Tauranga based on the multibeam echosounder survey performed in August 2011 (water depth based on Moturiki Chart Datum).....	108
Figures 5.17 & 5.18: 3D side views of the Tauranga Harbour bathymetry survey (August 2011), with a 6 times vertical exaggeration. The dredging marks, the deep areas (purple) and the uneven seafloor of the Marina are here clearly visible.....	109
Figure 5.19: Slope factor derived from the bathymetry.....	110
Figures 5.20 & 5.21: Photos of the Port of Tauranga in August 2011 showing the propeller wash from the ship’s bow thrusters (top) or the tugboats (bottom). These could explain the deep areas adjacent to the wharves.	111
Figures 5.22 & 5.23: Multibeam echosounder backscatter mosaics using “trend” (left) and “flat” (right) AVG filters. The “trend” method clearly shows fewer artefacts.	113
Figure 5.24: Multibeam echosounder backscatter distribution in the Tauranga Harbour (August 2011).	113
Figure 5.25: Multibeam echosounder backscatter mosaic of the Tauranga Harbour, based on the survey performed in August 2011.....	114
Figures 5.26, 5.27 & 5.28: Results of the various classification methods of the MBES backscatter on ERDAS Imagine: unsupervised classification with 4 classes (left), unsupervised classification with 11 classes (centre) and supervised classification with 4 classes (right).	116
Figures 5.29 & 5.30: Results of the various classification methods of the SSS reflectivity on ERDAS Imagine: unsupervised classification with 4 classes (left) and unsupervised classification with 11 classes (right).	116

Figures 5.31, 5.32 & 5.33: Results of the various classification methods of the MBES backscatter on ArcGis Spatial Analyst: unsupervised classification with 4 classes (left), unsupervised classification with 11 classes (centre) and supervised classification with 4 classes (right).	117
Figures 5.34, 5.35 & 5.36: Results of the various classification methods of the SSS reflectivity on ArcGis Spatial Analyst: unsupervised classification with 4 classes (left), unsupervised classification with 11 classes (centre) and supervised classification with 4 classes (right).	118
Figures 5.37 & 5.38: Classes distribution resulting of the Unsupervised Classification of the MBES backscatter on Erdas Imagine (top) and ArcGis Spatial Analyst (bottom). Both methods were performed on the grey-scale mosaic of the MBES data obtained from the Port of Tauranga in July 2011.	119
Figure 5.39: Screenshot of the Fledermaus Geocoder Toolbox.	122
Figure 5.40: Beam pattern extraction in FMGT. The observed signal (backscatter measurement) in green is compared to the model in blue chosen according to the ground-truthing results. The residual beam pattern signal in brown can then be extracted for latter compensation.	122
Figures 5.41, 5.42 & 5.43: Angular Response signatures in the Tauranga Harbour for gravel (top), very fine sand (centre) and clay (bottom). The near, far and outer ranges show very distinct shapes depending on the seabed type.	123
Figure 5.44: Angular Response Analysis results and their spatial distribution in the Tauranga Harbour based on Kongsberg-Simrad EM3000 multibeam echosounder backscatter data.	124
Figure 5.45: Distribution of the 11 sediment classes resulting from the Angular Response Analysis of the MBES backscatter in the Port of Tauranga. The sandy classes are here clearly dominant.	125
Figure 5.46: Phi results of the Angular Response Analysis for every ground-truthing station.	125
Figure 5.47: Scatter plot matrix of the environment variables and analysis results for the ground-truthing locations (July 2011): Water Depth (m), Slope (degrees, derived from water depth), MBES Backscatter (dB), Sidescan Sonar mosaic pixel intensity, Shell Coverage (density index from 1 to 4), Mean Grain Size from the Laser Sizer (μm), Sediment Type from the sieving (Phi) and the Sediment Type from the ARA (Phi). The colour code represents the Phi classes obtained from the ARA.	128

Figure 5.48: Pearson’s linear correlation table of the variables extracted for every ground-truthing station of the Tauranga Harbour (2011). The shading increases according to the correlation values.....	129
Figure 5.49: Comparison of the grain size results from the Angular Response Analysis and the dry sieving of the sediment samples of the Tauranga Harbour (July 2011).	129
Figure 5.50: Scatter plot and linear regression of the dry sieving results against the ARA Phi for the Port of Tauranga (July 2011).	130
Figure 5.51: Scatter plot and linear regression of the dry sieving results against the backscatter values for the Port of Tauranga (July 2011).....	130
Figure 5.52: Scatter plot and linear regression of the ARA phi results against the backscatter values for the Port of Tauranga (July 2011).....	130
Figure 5.53: Final benthic habitat map of the Tauranga Harbour (July 2011). ..	132
Figure 6.1: Final distribution of the 7 seabed classes of the benthic habitat map of the Tauranga Harbour, July-August 2011.....	137
Figure 6.2: Sidescan sonar paper recordings of the Tauranga Harbour Study (Healy, 1985).....	137
Figure 6.3: Tauranga Harbour Study (Healy, 1985) sediment facies map derived from a sidescan sonar survey and sediment sampling.....	138

LIST OF TABLES

Table 1.1: Planned quantity of excavation (Source: Bay of Plenty Regional Council, Resource Consent N°65806).	9
Table 4.1: Udden-Wentworth sediment classification scale in terms of phi units and mm.....	83
Table 4.2: Summary of species found in the sediment samples and underwater videos of the Port of Tauranga.	94
Table 4.3: Summary of shell densities and sediment types obtained from both sediment samples and underwater video, expressed on a scale from 0 (no shell) to 2 (dense coverage). The agreement factor is the difference between both indexes and represents the repeatability of the results between bot datasets. The shell coverage class column provides a final finer definition of the type of shell density similar to the 1985 study by Healy (1985) and de Lange (1988).....	96
Table 6.1: Summary of the advantages and disadvantages for manual and automatic classifications of acoustic seabed data.	147

CHAPTER 1 - INTRODUCTION

1.1. PORT OF TAURANGA: CURRENT SITUATION

The Tauranga Harbour is a mesotidal lagoon situated within the Bay of Plenty, New Zealand (Fig. 1.1) (Spiers, Healy, & Winter, 2009). With an annual cargo handling of more than 13 million tonnes, the Port of Tauranga represents the largest export and second largest import port in New Zealand (Port of Tauranga Limited, 2009). Panepane Point in the West and the Mount Maunganui headland in the East both form the natural entrance to the harbour. The marked navigation channels (Fig. 1.2) include the Cutter Channel leading to the Maunganui Roads Channel and Wharves and eventually to the Stella Passage in the South. The “Tauranga Container Terminal”, located on the west side of the Stella Passage, offers a berthing length of 600 m with rail-mounted gantry cranes. The Mount Maunganui Quayside presents an overall length of 2060 m of berth to accommodate bulk and liquid cargo ships, and passenger vessels.

The channels used by the Port of Tauranga are subject to an on-going maintenance dredging program to remove mud deposits coming from various sources in the catchment. The first dredging was conducted in 1968 in order to reroute shipping through the Cutter Channel, bypassing the Pilot Bay Channel and removing a sharp turn that had caused the grounding of at least one vessel. A further capital dredging program was completed in July 1992, deepening the main navigation channel to an average depth of 13.0 m high water and 11.7 m low water, and removing an estimated total volume of 5 Mm³ of sediment (Mathew, 1997). The current maintenance dredging operations aim to maintain this average depth in the area.

The Tauranga Bridge Marina was built in 1995, following the construction in 1988 of the Tauranga Bridge and causeway linking Mount Maunganui and the Sulphur Point wharves. It is located at the southern extent of the Stella Passage, on the shallow shelf know as the “Town Reach Channel”, showing an average depth of 3 to 5 m below chart datum (Figs. 1.3 & 1.4). The Marina offers a total of

560 berths within an overall extent of around 550 m North-South and 280 m East-West (Tonkin & Taylor Ltd, 2010).



Figure 1.1: Tauranga, located in the Bay of Plenty on the North Island of New Zealand.



Figure 1.2: Map of the main Tauranga Harbour shipping channels and geographic features (Aerial photo source: Bay of Plenty Regional Council)

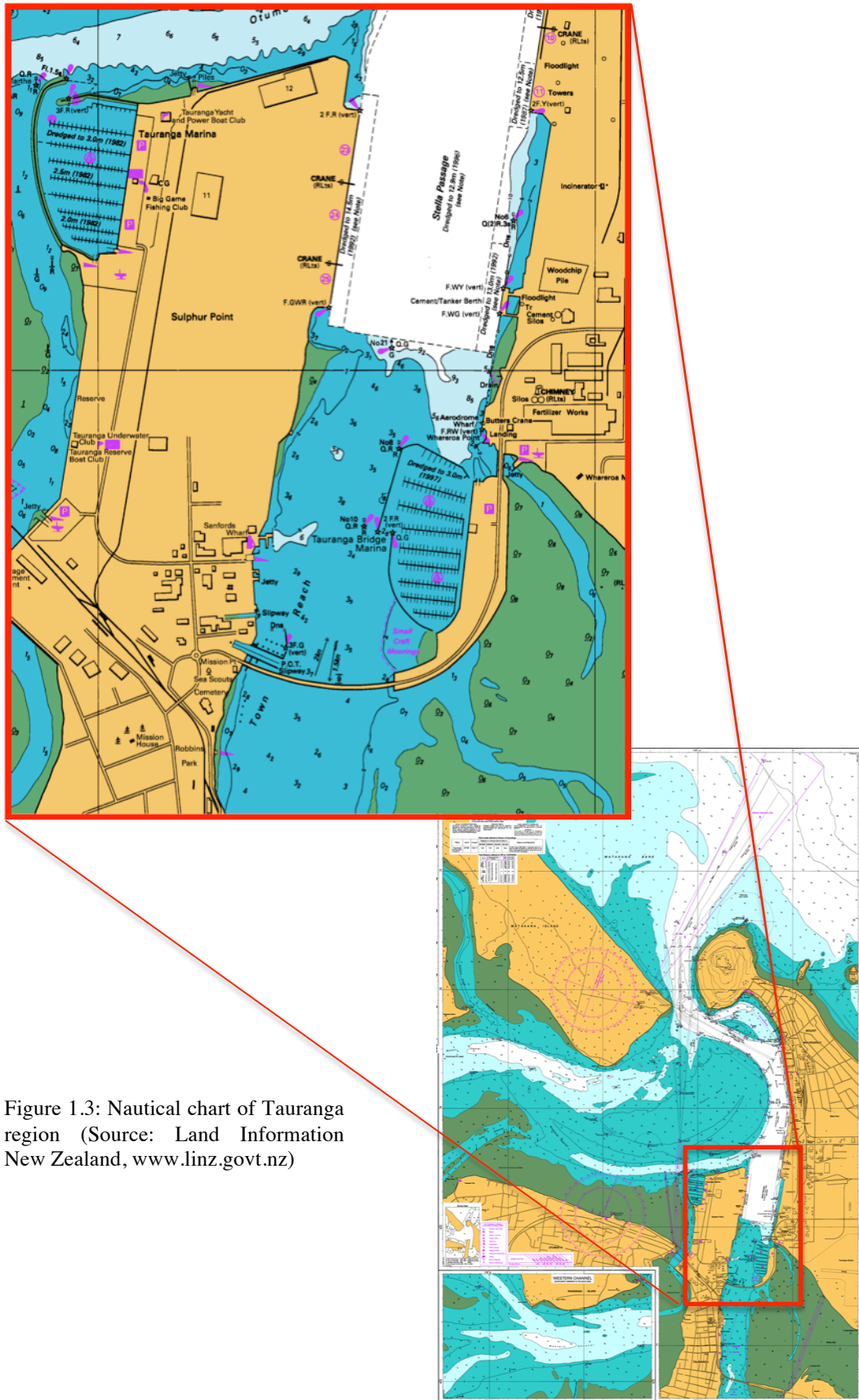


Figure 1.3: Nautical chart of Tauranga region (Source: Land Information New Zealand, www.linz.govt.nz)

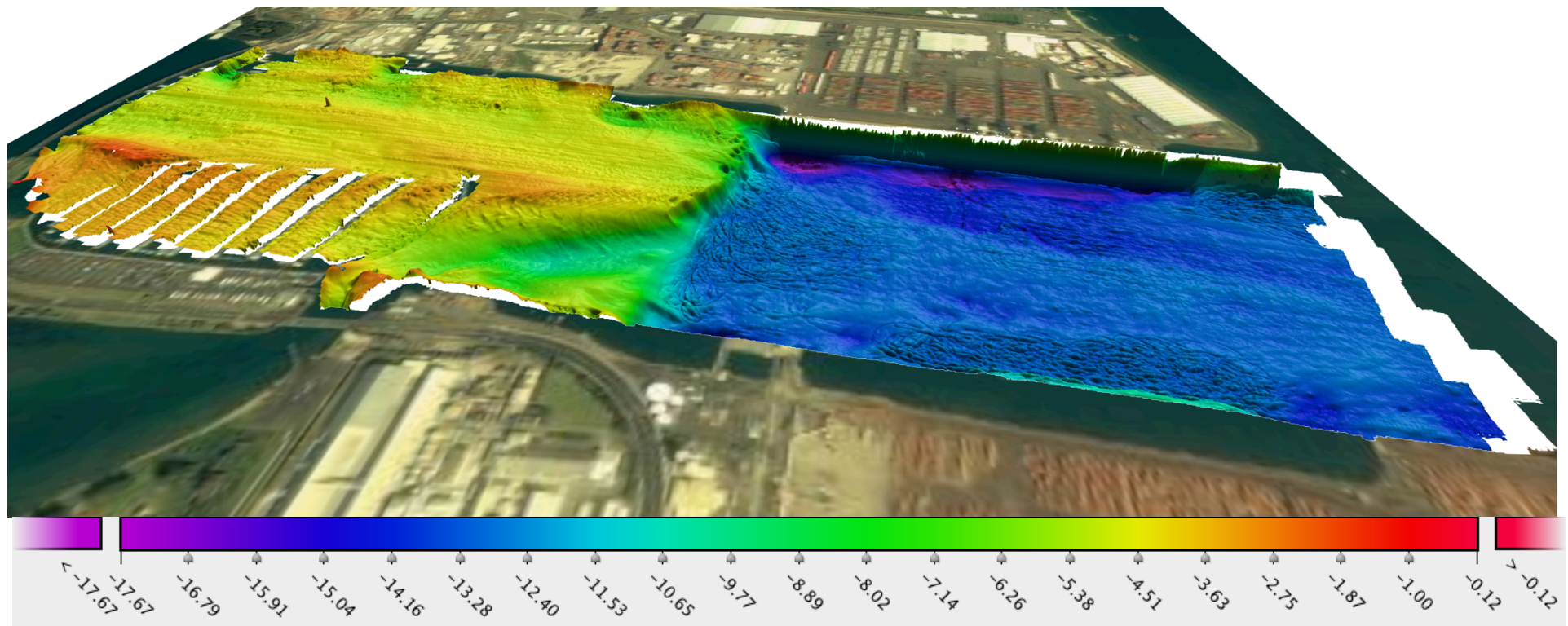


Figure 1.4: 3D view of the Tauranga Stella Passage, Town Reach and Bridge Marina. Image created using the multibeam echosounder survey performed in July 2011 by the University of Waikato. Depths are 6 times vertically exaggerated. This chart clearly shows the current dredged area in the deep (dark blue) part of the Stella Passage. Depths are expressed in meters relative to Mean Sea Level (Moturiki Vertical Datum). (Aerial photo source: Bay of Plenty Regional Council)

1.2. PORT OF TAURANGA: PLANNED MODIFICATIONS

The Port of Tauranga is planning to expand its capacity to accommodate larger container vessels due to constant growth of trade through the port. The three-year program, subject to consent, consists in modifications to the wharves and channels. The Tauranga Container Terminal (west) will be fitted with two additional gantry cranes while the quay will be extended from 600 m to 1155 m. These upgrades, along with the sealing of 21 ha and the enhancement of the Sulphur Point rail sidings, will allow for a ten-fold improvement of the TEU (Twenty-foot Equivalent Unit) handling volume (Port of Tauranga Limited, 2009). The Mount Maunganui Quayside (east) will also see its berthing modified with the construction of an additional 1000 m of quay to the South in order to enhance the handling of bulk and liquid cargoes (Fig 1.5).

The second aspect of the Stella Passage extension program consists of deepening and widening of the navigation channels to accommodate modern larger vessels up to 7000 TEUs with a 14.5 m draught and 347 m overall length. This category of container ships is expected to dominate the shipping business for the next fifteen to twenty years. As part of this program, the channel depths will be increased by an average of 3 m in the Entrance Channel, the Tanea Shelf, the Cutter Channel, the Maunganui Roads Cannel and the Stella Passage. An estimated total volume of 15 Mm³ of material will be removed in stages over the three-year program. Table 1.1 and Figure 1.6 present the planned dredging areas and the expected work to be undertaken.

The dredging plan received the approval from Environment Bay of Plenty in June 2011. The Environment Court also granted its support in December 2011. During the Environment Court Appeal, local iwi raised concerns regarding the impact of the dredging program on “kai moana” (Seafood), especially on the pipi shell beds. As a result, final consent conditions, including a Kaimoana Restoration Plan still have to be drafted and approved by the High Court in 2012 (Bay of Plenty Regional Council, 2010).



Figure 1.5: Planned future expansion of the Container Terminal (Photo Source: Port of Tauranga)

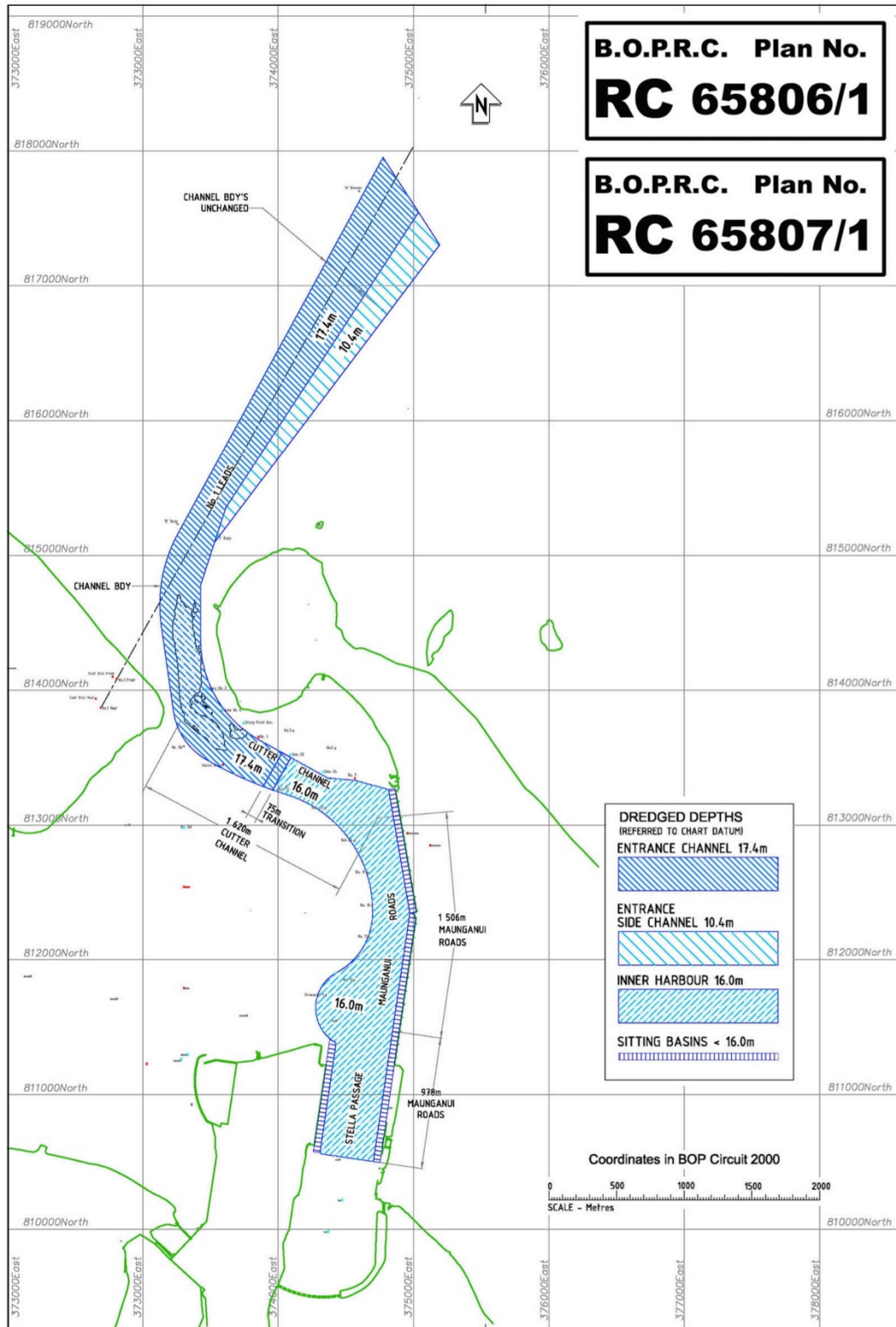


Figure 1.6: Widening and Deepening shipping channels program (Source: Bay of Plenty Regional Council, Resource Consent N°65806)

Table 1.1: Planned quantity of excavation (Source: Bay of Plenty Regional Council, Resource Consent N°65806).

Locality	Works	Approximate volume (million cubic metres)
Entrance Channel	Deepen to 17.4 metres	5.9
Tanea Shelf	Deepen to 17.4 metres and widen to 32 metres	0.4
Cutter Channel	Deepen to 16.0 metres and widen to 115 metres	7.0
Maunganui Roads	Deepen to 16.0 metres and widen to 50 metres Create turning basin 16.0 metres deep and 200 metres by 200 meters	0.4
Stella Passage	Deepen to 16.0 metres	1.3

1.3. TAURANGA BRIDGE MARINA PLANNED MODIFICATIONS

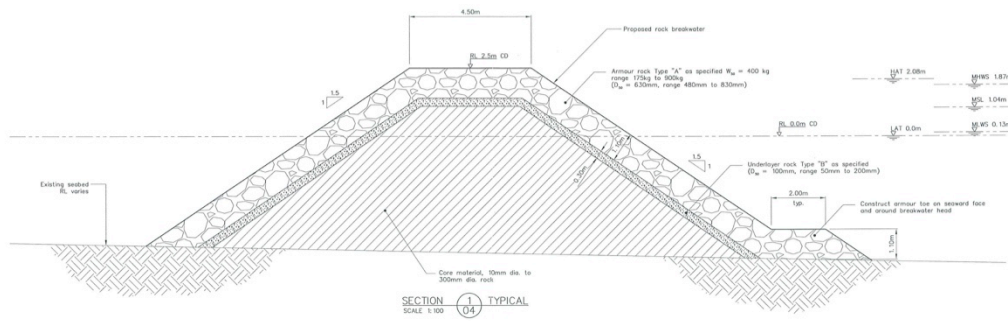
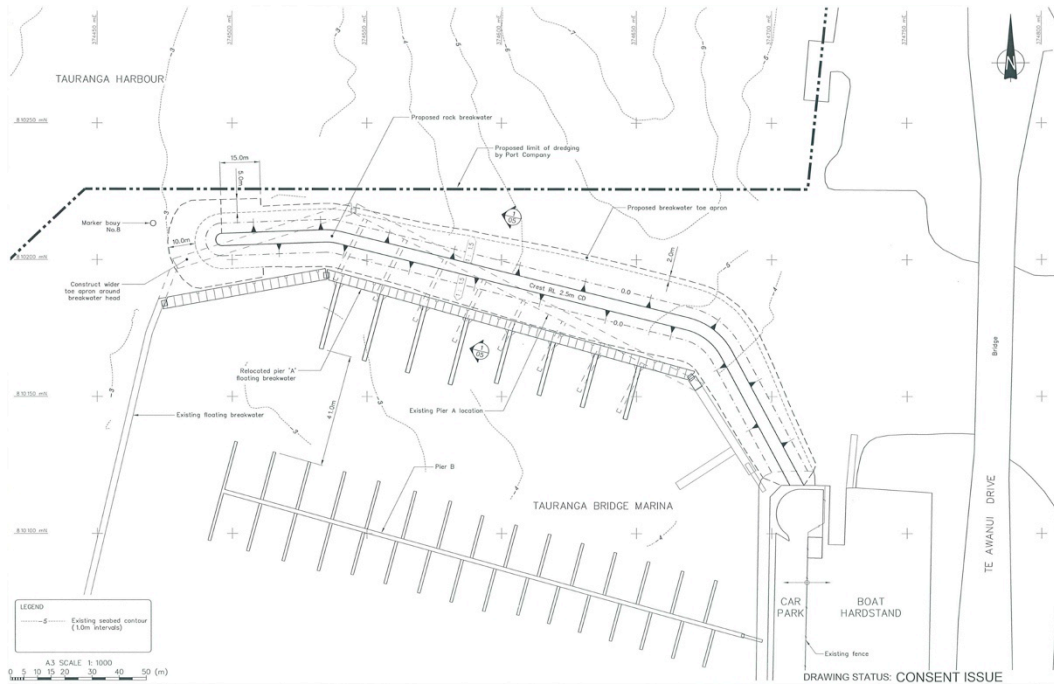
The Tauranga Bridge Marina, as built in 1995, is sheltered from the waves by a 3.6 m wide pontoon extending all around its' berthing (Fig. 1.7). This attenuator was installed to reduce the effects of waves entering the marina, but has proven insufficient to protect the vessels during storm events (Tonkin & Taylor Ltd, 2010). Mooring lines snap and the vessels get damaged in the berths as the pontoons and the links between them also get destroyed. Berthing during strong northerly winds is also considered unsafe because of the currents flowing in the Marina.

The construction of a 245 m long rock breakwater structure is being investigated as a replacement for the existing northern wave attenuator. The proposed design (Fig. 1.8 & 1.9) intends to reduce the effect of northerly storm events on the Marina structures and vessels within the Marina.

The constant traffic of cargo vessels and tugboats associated with the Port of Tauranga can also induce a strong propeller wash flowing into the marina. The construction of a rock wall will help to isolate the Marina from the side effects of the development of the Port. As proposed in the application to the Bay of Plenty Regional Council, the breakwater will be built in the current location of the northern floating pontoon which will be moved 20 m further South in order to keep the pedestrian access to the boats (Tonkin & Taylor Ltd, 2010).



Figure 1.7: Northern floating pontoon of the Tauranga Bridge Marina.



DRAWING STATUS: CONSENT ISSUE

Figures 1.8 & 1.9: Proposed breakwater plan (top) and section (bottom) (Source: Northern Breakwater Assessment of Environmental Effects 2010)

1.4. STUDY AIM AND OBJECTIVES

The general aim of this study is to assess the effects of the Port of Tauranga and Tauranga Bridge Marina modifications on the local geomorphology and surficial sedimentology. To achieve this aim an up-to-date basemap for the future Port expansion program and Bridge Marina breakwater project will be produced.

The specific objectives of this thesis are:

- 1) To investigate and evaluate existing methods of seabed classification based on acoustic data.
- 2) To conduct an extensive hydrographic survey of the Tauranga Stella Passage, Town Reach and Bridge Marina areas, followed by ground-truthing observations.
- 3) To produce bathymetry maps and reflectivity mosaics based on acoustic data from the multibeam echosounder and sidescan sonar.
- 4) To process the different datasets using diverse approaches and to compare their potential for seabed characterization and classification.
- 5) To create a fine-scale surficial sediment map and to compare it to the previous studies.

1.5. THESIS STRUCTURE

Following this introductory chapter, the thesis will be organized as followed:

Chapter 2 reviews the history of environmental studies in the Tauranga Harbour. It will present the methods and results that provided base maps for the past dredging and harbour modification programs.

Chapter 3 develops the theory of habitat mapping and the different methodologies for acoustic characterization and classification. It also introduces the principles of multibeam echosounder and sidescan sonar applied to geomorphology and sediment studies. The concepts of supervised or unsupervised image classifications are also established.

Chapter 4 details the grain-size pattern over the Stella Passage and Bridge Marina areas obtained from the sediment sampling survey. The outputs of this ground-truthing program will be used to train the acoustic classification described in Chapter 5.

Chapter 5 presents the outcomes of the procedures described in Chapter 3 applied to the Tauranga survey dataset. The various types of classification will be investigated, using the results from the sediment sampling and underwater video operations detailed in Chapter 4. Finally, the relationship between the acoustic map products and the ground-truthing observations and their relative significance will be assessed.

Chapter 6 will provide a comparison of the 2011 seabed facies with the previous studies. A critical evaluation of the various classification methods will be developed. Finally, the thesis objectives achievements will be detailed and recommendations for future studies will be drafted.

1.6. REFERENCES

Bay of Plenty Regional Council. (2010). *Decision and recommendations of the hearing panel of the Bay of Plenty Regional Council and the Minister of Conservation.*

Mathew, J. (1997). *Morphologic changes of tidal deltas and an inner shelf dump ground from large scale dredging and dumping, Tauranga, New Zealand.*

Port of Tauranga Limited. (2009). *Port for the future*

Spiers, K. C., Healy, T. R., & Winter, C. (2009). Ebb-Jet Dynamics and Transient Eddy Formation at Tauranga Harbour: Implications for Entrance Channel Shoaling. *Journal of Coastal Research*, 25(1), 234-247. 10.2112/07-0947.1

Tonkin & Taylor Ltd. (2010). *Tauranga Bridge Marina Ltd, Northern Breakwater Assessment of Environmental Effects.*

CHAPTER 2 - PREVIOUS STUDIES OF THE TAURANGA HARBOUR

2.1. INTRODUCTION

Although many studies of the Port of Tauranga have been conducted in the past, they were mostly concentrated on aspects of port development and navigation around the Harbour Entrance. The following chapter reviews previous studies relating to Stella Passage, Town Reach and the Tauranga Bridge Marina areas. The chapter also reviews studies using methods of investigation similar to this project.

2.2. PHYSICAL SETTING

Tauranga Harbour is situated in the southwest of the Bay of Plenty and includes two entrances, the Bowentown entrance in the northwest and the Tauranga entrance in the southeast. It covers an area of 200 km² and consists of two large basins whose water exchanges are limited by wide intertidal flats (Sinner J. et al., 2011). The Harbour mouth is about 500 m wide with an average depth of 30 m (Kruger & Healy, 2006). Tidal currents are the main influence on the sediment transport, with as an estimate of 290 million tonnes of water moving during each tidal cycle through the harbour entrances. Tauranga Harbour sediments have two origins: river inputs, estimated at 120,000 tonnes per year, which tend to be muddy; while the marine sediments entering the harbour through tidal action are mostly sand (Lawrie, 2006). About 42% of the sediment from the catchment is lost to the ocean in the southern harbour basin (Green, 2009).

The Stella Passage is a 450 m wide dredged basin, enclosed by wharves, linking the Harbour Entrance to the Town Reach. The dominant wind direction in the area is southwest. Considering the restricted length of fetch offered by the Stella Passage and Town Reach channel, the waves never exceed a height of 0.7 m in the study area (Beca Carter Hollings and Ferner Ltd, 1985).



Figure 2.1: Aerial photograph of the Tauranga Harbour taken in 1975. (Source: Davies-Colley, 1976)

2.3. A PRELIMINARY ASSESSMENT OF SOME ASPECTS OF THE ECOLOGY OF TAURANGA HARBOUR - 1974

Bioresearches Ltd (Larcombe, Donovan, Bay of Plenty Catchment Commission, & Bioresearches Ltd, 1974) was commissioned by the Bay of Plenty Catchment Commission to undertake a preliminary ecological study of the Tauranga Harbour. The general aims were to provide a preliminary assessment of the range of ecological variation within the Harbour; identify areas with actual or potential ecological problems, and to make recommendations regarding further studies for a better natural resource management of the Harbour. Some more specific objectives were also developed, such as the examination of the edible shellfish populations, study of the Welcome Bay region and the Hereatukahia Estuary where a dairy factory was responsible for a waste discharge. At the time of the study, the intertidal ecology of the Harbour was found to be “natural, healthy and stable”, while the fauna and flora composition of the predominant sandy substrates was mostly dependent on the intertidal level and submergence period.

The investigations on the edible shellfish identified several species available for human consumption:

- *Amphibola crenata* (mud snail)
- *Amphidesma australe* (pipi)
- *Chione stutchburyi* (cockle)
- *Perna canaliculus* (green mussel)
- *Pecten novaeselandiae* (scallop)

Although this report presents some information on the species present in the Harbour in 1974, it does not provide any geographically specific population densities. No data from this report was used in this thesis for the Stella Passage habitat comparison.

2.4. SEDIMENT DYNAMICS OF TAURANGA HARBOUR AND THE TAURANGA INLET - 1976

The first sediment dynamics study of the Tauranga Harbour was undertaken in 1976 by Davies-Colley (1976) as part of a MSc thesis. His thesis focused on the ebb and flood tidal delta near the inlet entrance. A conceptual model of sediment circulation was created, based on tidal streamlines, bedforms, sediment discharge measurements and theoretical calculations (Brannigan, 2009).

The Tauranga Harbour entrance was sampled using a specially designed dredge in order to obtain a sufficient amount of coarse sediment for textural analysis. The sediment texture being the most important characteristic in regards to the depositional environments investigated, along with the composition and mineralogy.

The results of these analysis showed that sands were predominant in the harbour, followed by “shelly gravel and a very small content of mud”. The sands were composed of sodic plagioclase, quartz and volcanic glass, while the gravel fraction comprised “shells, shell fragments and some rhyolite rock and pumice fragments”. Davies-Colley (1976) points out that the coarse sediment, mainly shell gravel, mostly occurs in strong energy areas. This could be explained by the natural occurrence of the pipis in strong current velocity environments and the transport and concentration of their shells as lag deposits.

Although Davies-Colley focused mostly on the Harbour entrance, he provided important results on the sampling and analysis techniques suitable for this environment, and the expected types of sediment to be found in the estuary. He also reported the occurrence of megaripples in the Stella Passage, detected using a single-beam echosounder.



Figure 2.2: Underwater photograph of coarse shelly sediment, Southwest of the Centre Bank. Shells are mainly cockles (*Chione stutchburyi*), pips (*Amphideam australe*) and various gastropods. These shells are the main roughness element on the seabed. (Photo: Wayne Ruegg from Davies-Colley, 1976)



Figure 2.3: Underwater photograph of a relatively fine sandy sediment bed, Northeast of the Central Bank. The sediment bed is deformed by the action of tidal currents into small sinuous and linguoid ripples. (Photo: John White from Davies-Colley, 1976)

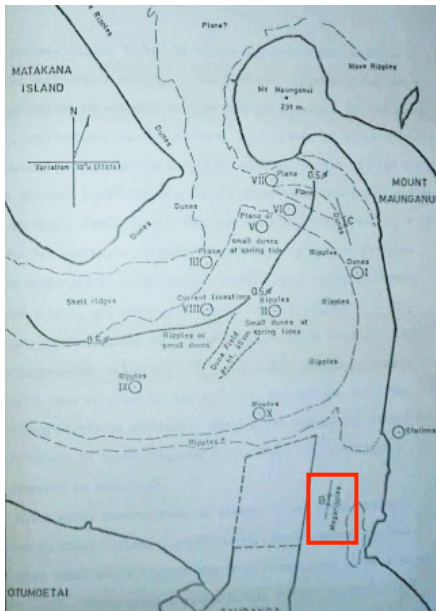
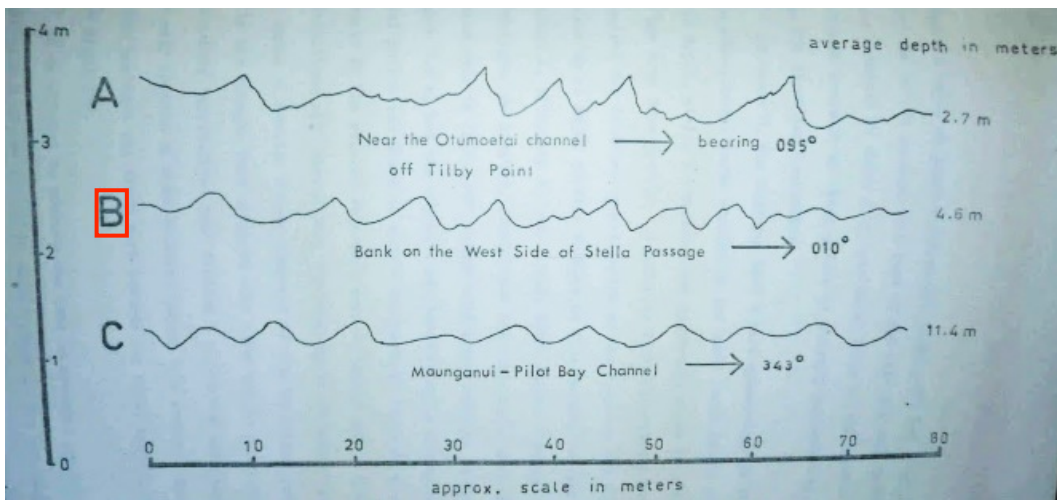


Figure 2.4 (Left): Distribution of the bedforms within Tauranga Harbour. (Source: Davies-Colley, 1976)

Figure 2.5 (Below): Echosounder profiles across sand dunes located within harbour channels. (Source: Davies-Colley, 1976)



2.5. TAURANGA HARBOUR STUDY - 1985

The Tauranga Harbour Study project started in 1983 and served as a baseline map for numerous later studies. It included hydrographic soundings, tide gauge recordings, current monitoring, drogue tracking, sediment sampling, underwater photography, size and settling velocity analysis of the sediments, suspended sediment sampling, side-scan sonar mapping and sub-bottom seismic profiling, aerial photography and wind and rain recordings. This dataset was then used to produce the first hydrodynamic and sediment transport numerical model.

2.5.1. Bathymetry

In 1985, Barnett digitized nautical charts from 1852, 1902, 1927, 1964 and 1970 in order to run the numerical models on historical grids (Barnett, 1985). Plotting and differencing these grids using the software CHECKTOPO obtained the areas of erosion/accretion.

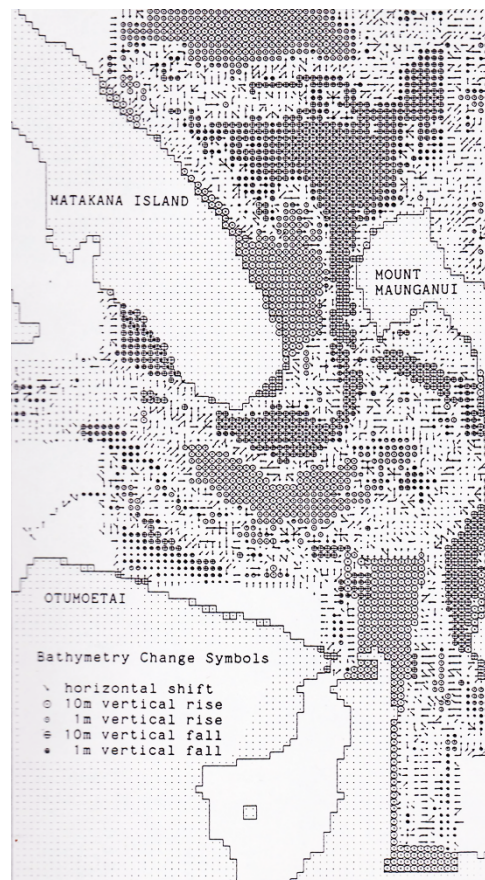
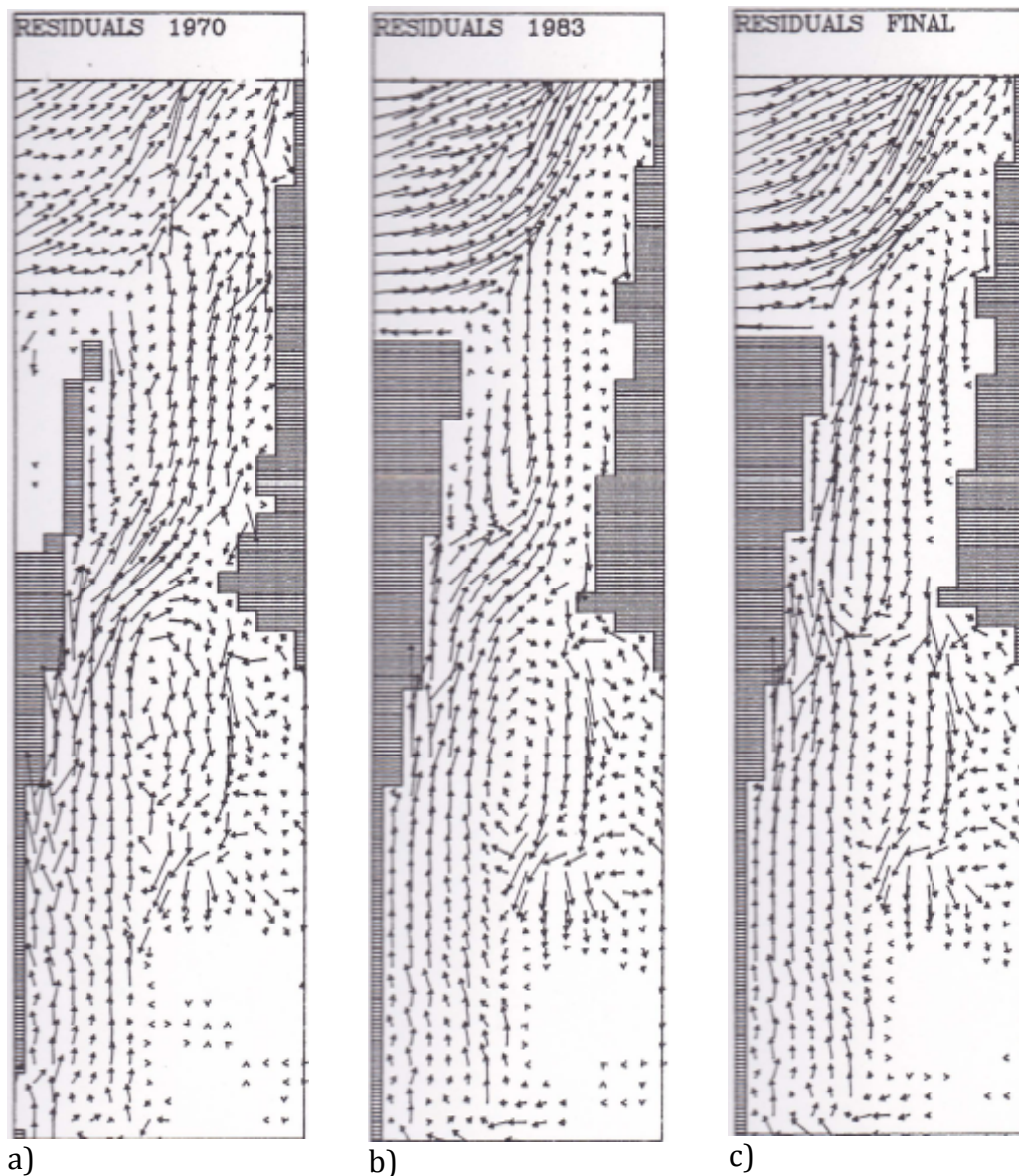


Figure 2.6: Bathymetry changes between 1852 and 1983. Note the deepening of the west side of the Stella Passage and the reclamation on Sulphur Point. (Source: Barnett, 1985)

2.5.2. Hydrodynamic Modelling

An accurate hydrodynamic model was required as a basis for the sediment transport model and for the development of ship handling models (Barnett, 1985). The model would also be used for further studies on the effects of tidal currents on various types of modifications of the harbour due to Port development. The Danish Hydraulic Institute (DHI) System 21 numerical model was chosen and set up on the University of Waikato computer. A coarse 300m square grid was first used to cover the whole estuary, and output boundary tide level conditions used on a finer 75m grid used by the PORT model for the main shipping channels.



Figures 2.7, 2.8 and 2.9: Residual current vectors showing net current circulation averaged over a complete tidal cycle in the Stella Passage in 1970 (a), 1983 (b) and after completion of the dredging programme (c) (Source: Black, 1984)

2.5.3. Sediment Transport Modelling

The sediment transport modelling aspect of the Tauranga Harbour Study was undertaken by Dr Kerry Black using his own 2SS model (Black, 1985). The results of this modelling program show an expected accretion of the Southwest area of the Stella Passage after completion of the dredging programme.

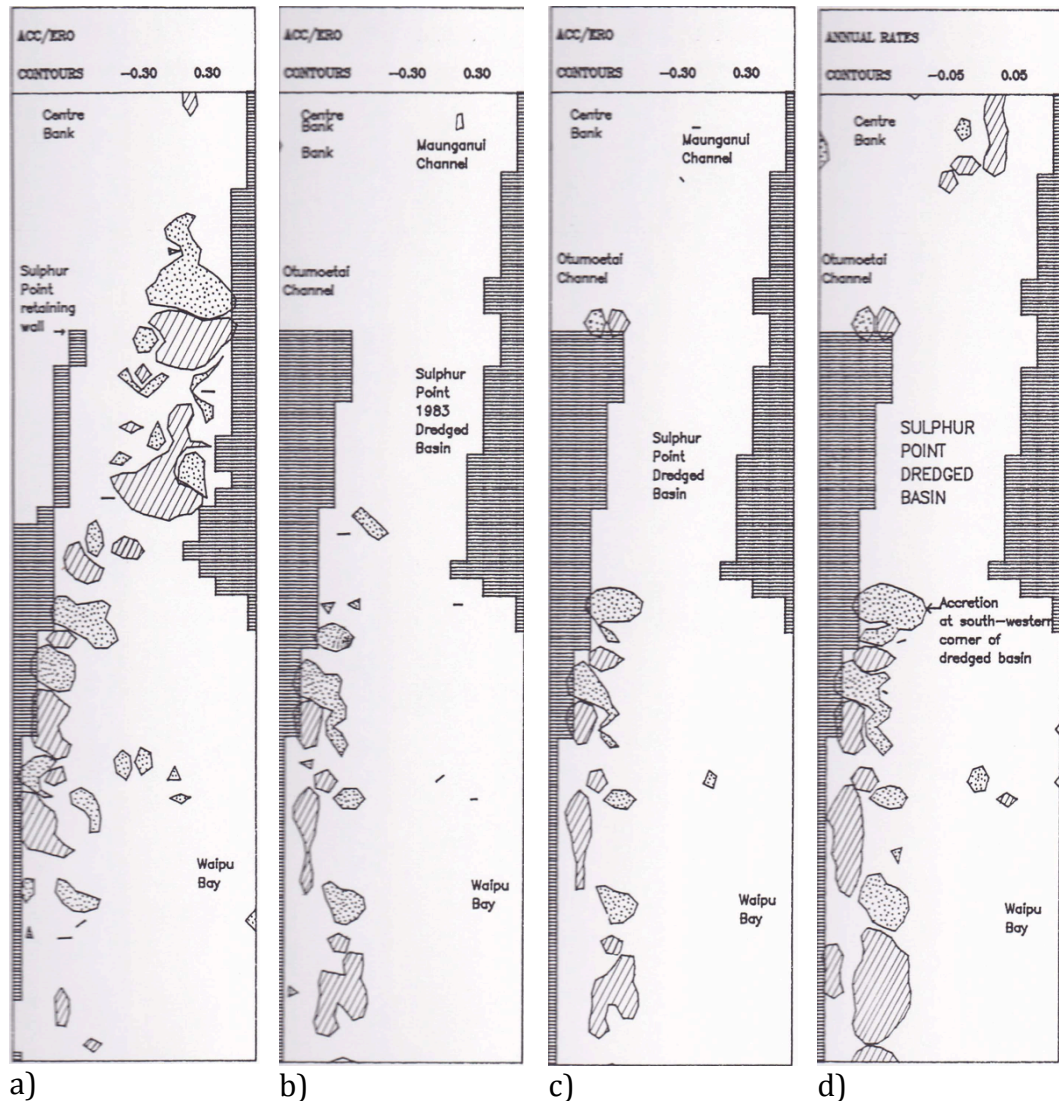


Figure 2.10, 2.11, 2.12 And 2.13: Sedimentation patterns in the Stella Passage in 1970 (a), 1983 (b) and after completion of the dredging programme for a medium sand on a spring tidal range (c) and averaged over a year (d). Erosion is crosshatched; accretion is dotted. (Source: Black, 1984)

2.5.4. Morphological Study

The morphological study of the Port of Tauranga was integrated in the field data collection program in order to help set up and calibrate the hydrodynamic and sediment transport models (Healy, 1985). The aerial photographs (Figs. 2.20 &

2.21) were used to identify shallow bedforms. Divers performed underwater photography and direct observations to describe the sedimentary facies of 290 sites. An extensive sampling of the surficial sediments on the same locations was undertaken for textural analysis by the University of Waikato computerised Rapid Sediment Analysis System. Figure 2.16 presents the locations of the diving and sediment sampling sites.

A sidescan sonar survey was also completed using a Klein 595 sidescan system (Fig. 2.14) in order to help delineate the bottom sediment facies. The range used was 150 m on each side, and the acoustic signal responses were recorded on wet paper, while regular navigation fixes were performed by dual sextant angles pointing at known points around the Harbour. Figure 2.17 presents the sidescan track, while Figure 2.18 provides an example of the data obtained from this system. A single-beam echosounder (Fig. 2.15) was run concurrently with the sidescan sonar in order to confirm the potential bedforms or facies observed on the sidescan swath.

An E.G.&G. Model 230 "Uniboom" high-resolution continuous seismic profiling sub-bottom profiler (Fig. 2.14) was also used to investigate the underlying layers of sediments in the Harbour. The combination of the different datasets and their inter-validation allowed production of a sedimentary facies map of the Tauranga Harbour, as shown in Figure 2.19. Nine dominant units were found: shell lag, very shelly sands, rock outcrop, gravel or boulders, strongly developed mega ripples, poorly developed mega ripples, clean sands; shelly sands and silty sands. The bedforms were found to be representative of active sediment pathways while the shell lags were associated with strong current flows.



Figure 2.14: Klein sidescan sonar system (towfish) and Uniboom Seismic profiler. (Source: de Lange, 2011)



Figure 2.15: Single-beam echosounder recording onboard the BOPHB work vessel "Mahi". (Source: de Lange, 2011)

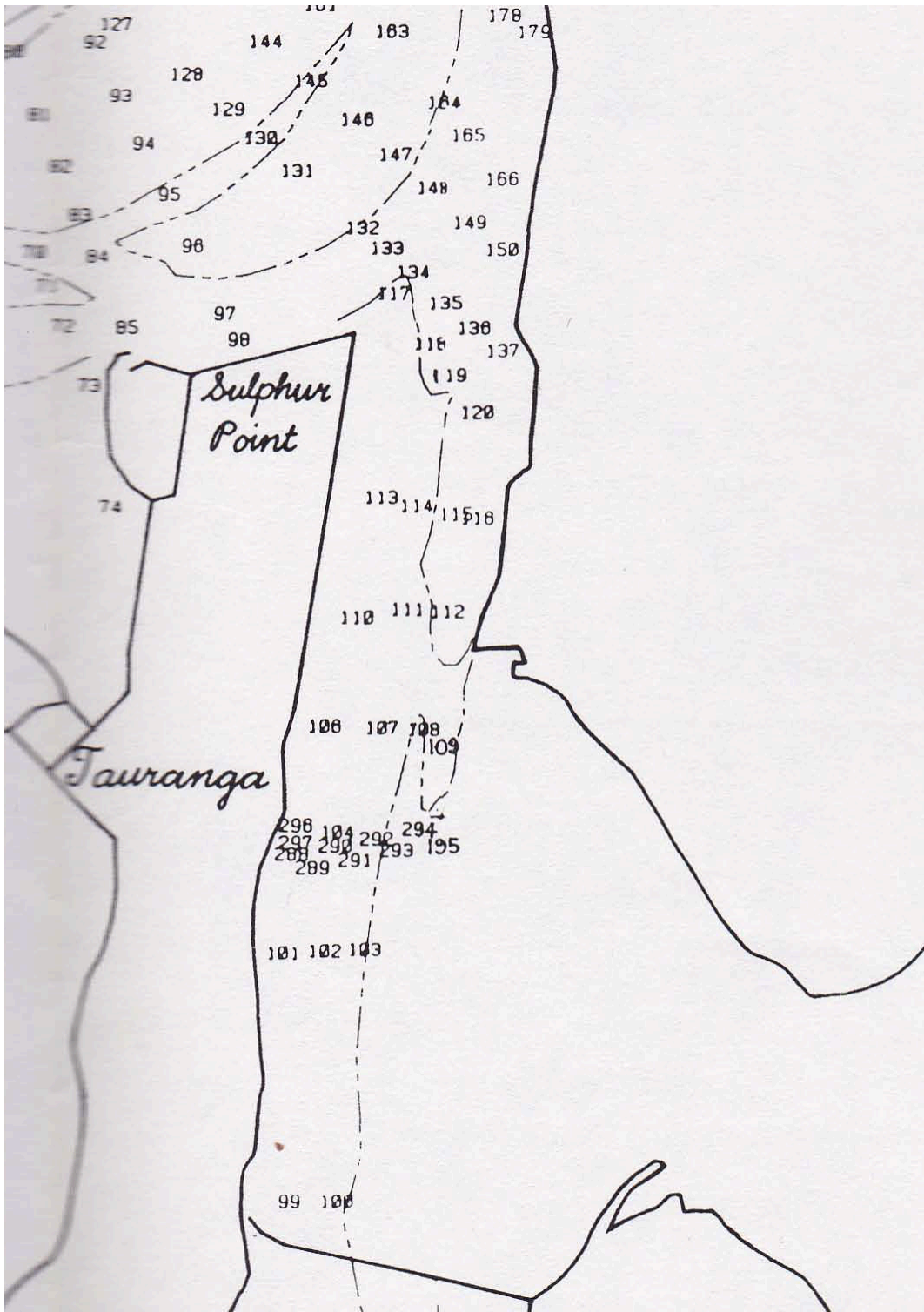


Figure 2.16: Underwater photography and sediment sampling locations. (Source: Healy, 1985)

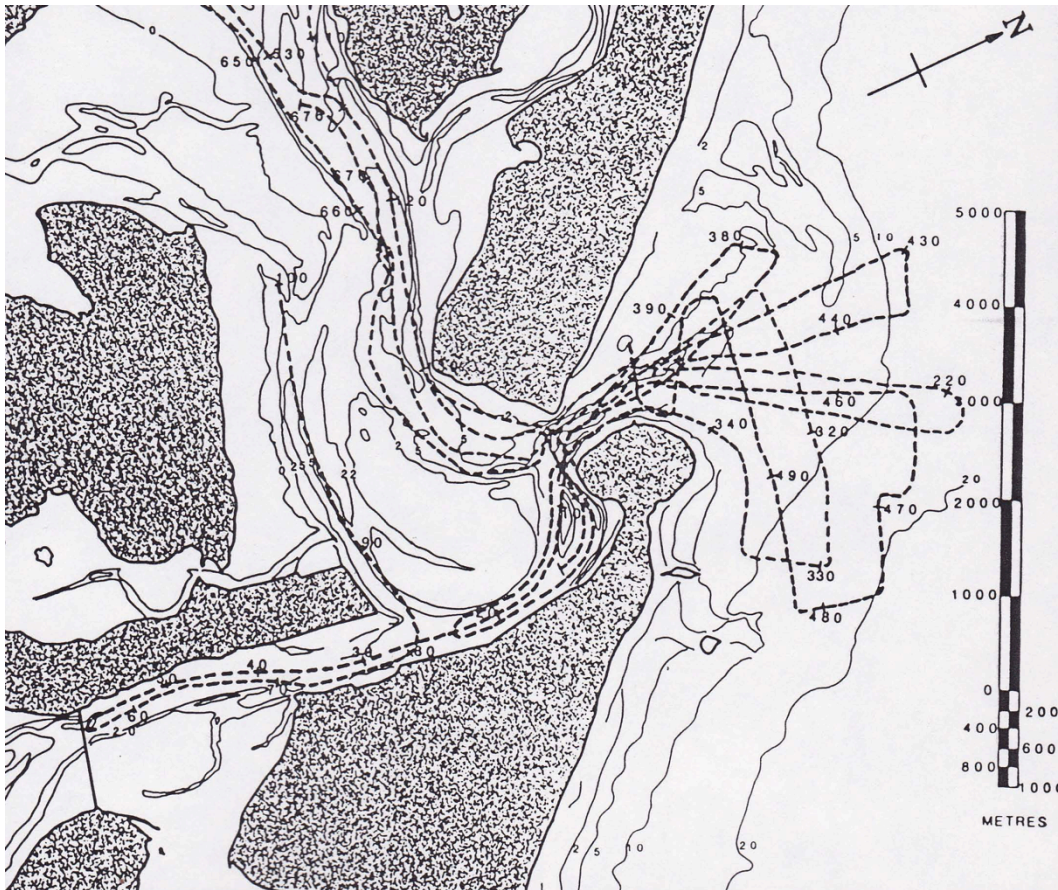


Figure 2.17: Tauranga Harbour sidescan track. (Source: Healy, 1985)

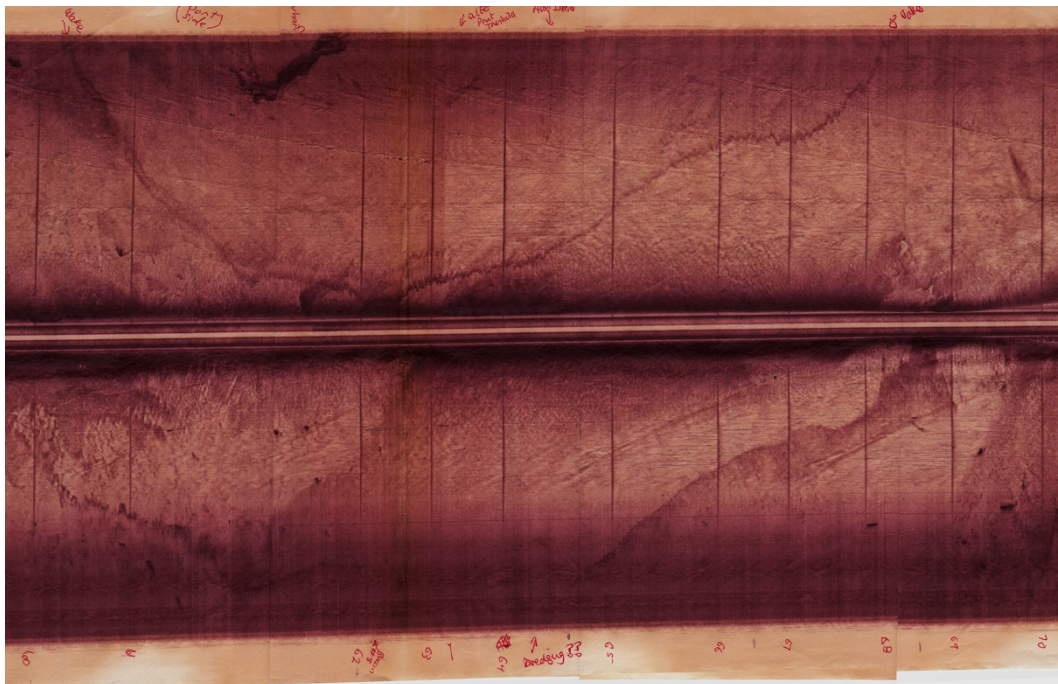


Figure 2.18: Tauranga Harbour sidescan example. The section 60 to 70 from Fig. 2.17 is represented here. (Source: Healy, 1985)

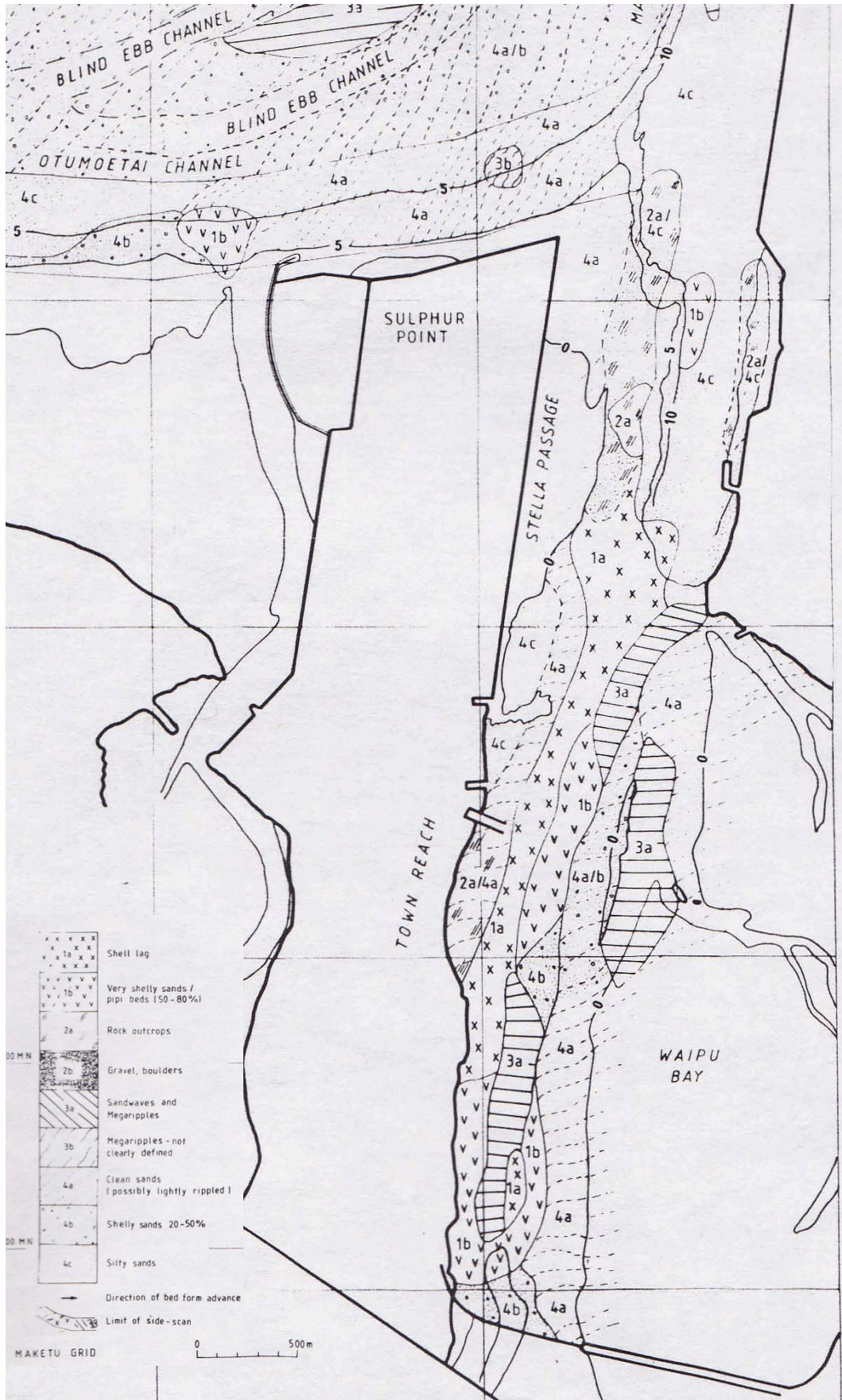


Figure 2.19: Tauranga Harbour bottom sediment facies. (Source: Healy, 1985)



Figure 2.20: Vertical view of the Stella Passage, Town Reach, Sulphur Point and Waipu Bay. (Source: Healy, 1985)



Figure 2.21: Sulphur Point reclamation (looking south-east) during construction of the boat marina in 1981. (Source: Healy, 1985)

2.6. TAURANGA HARBOUR BRIDGE: ENVIRONMENTAL ASSESSMENT - 1985

In 1985, the consulting engineers at Beca Carter Hollings and Ferner Ltd were commissioned by the Tauranga Bridge Committee to provide a technical report indicating the potential impact of the proposed Harbour Bridge on the local environment (Beca Carter Hollings and Ferner Ltd, 1985). Such a project would finally allow the linking of the two complementary areas: the City of Tauranga and the Borough of Mount Maunganui. The objectives of this commission were:

- To provide reasons for the unstable areas of the Harbour and to determine whether they have any affects on the shipping channels,
- To carry out hindcast studies of the historical changes to the harbour bed,
- To study the effects on the Harbour of past and future port development, and
- To study the effects of the proposed Harbour bridge on the harbour.

This study points out that little fishing was being undertaken around the proposed bridge area, except for the people of Whareroa Marae. Only small quantities of edible shellfish would be taken by persons with a knowledge of local resources, while the general public seemed to be unaware of the existence these shellfish in these difficult to access areas. The favourite species gathered were found to be cockles (tuangi), horse mussels (hururoa) and cat's eyes (pupu, *Turbo smaragdus*).

The habitats study was undertaken by Bioresearches Ltd, and focused on areas surrounding the proposed bridge and causeway alignments. As this investigation was also focusing on edible shellfish species, targeted samples of cockles (*Chione stutchburyi*) and wedge shells (*Tellina liliana*) were taken in the area of interest (Fig. 2.22). A few live horse mussels (*Atrina zelandica*) were found at low densities around sampling site 8 (Fig. 2.22). Significant areas of edible shellfish (mainly cockles) were found on sand flats south of the alignment. Figure 2.23 shows that no shell beds were found in the Stella Passage or Town Reach at the time, although they were found shortly before during Tauranga Harbour Study.

In 1983, a sediment transport and hydrodynamic modelling investigation was undertaken as part of the Tauranga Harbour Study (Healy, 1985). Part of this included investigating the effects of the proposed Harbour Bridge on the tidal currents and sediment movements. The ebb tide velocity under the bridge was found to remain identical, while the flood velocity, although lower than the ebb one, would increase slightly after the construction of the bridge. The tidal model predicted the velocities at any distance greater than 100 m from the bridge would remain unchanged. The sediment transport model indicated that little scour would be created under the minor bridge as small quantities of material were involved. The proposed causeway and bridge route was also found to have little effect on the Harbour regime.

The study predicted that marine habitats would be moderately affected by the construction of the Bridge. The area to be filled would only represent a small portion of the widely spread and highly productive intertidal habitats and would have no serious consequence on the local ecosystem. The retaining walls of the causeway were predicted to host colonies of oysters and barnacles, while the bridge piers would support dense populations of small black mussels, rock oysters (in the mid to low tide one) and green-lipped mussels (at low tide level).

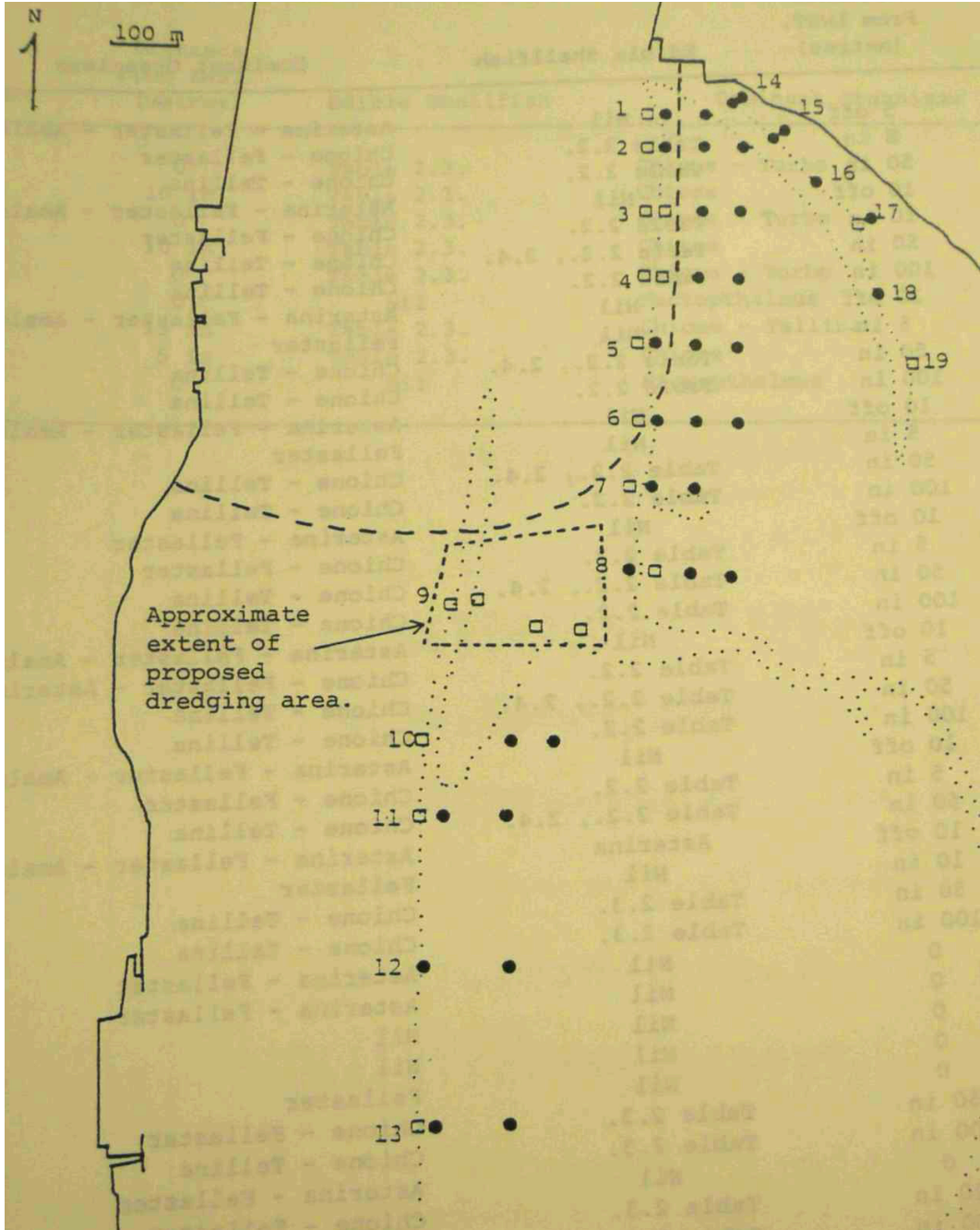


Figure 2.22: Shellfish sampling stations. (Source: Beca Carter Hollings and Ferner Ltd, 1985)

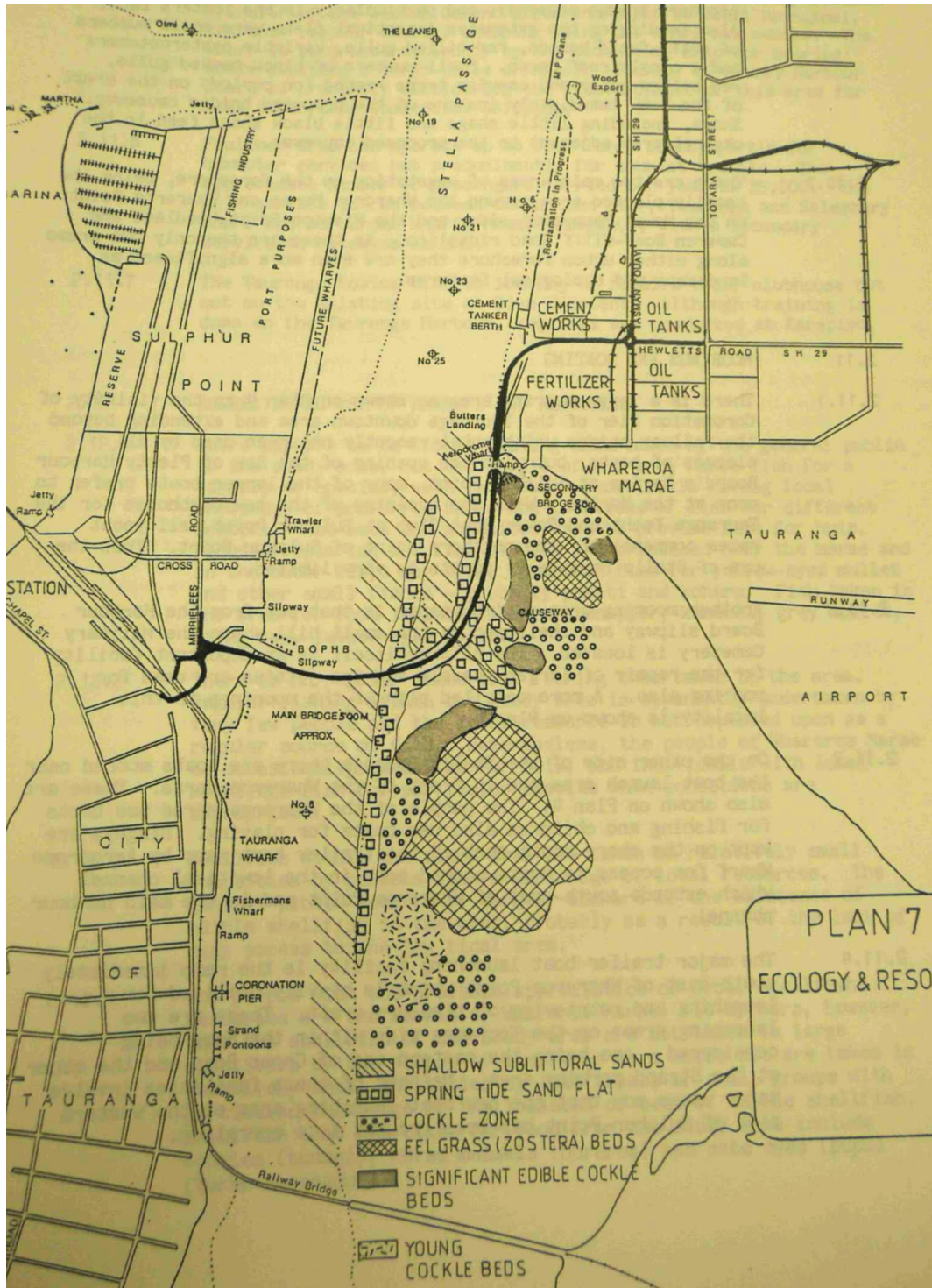


Figure 2.23: Ecology and Resources of the Tauranga Bridge area. (Source: Beca Carter Hollings and Ferner Ltd, 1985)

2.7. WAVE CLIMATE AND SEDIMENT TRANSPORT WITHIN TAURANGA HARBOUR IN THE VICINITY OF PILOT BAY - 1988

The Pilot Bay study was undertaken in 1988 by de Lange as part of a DPhil thesis (1988). The currents were measured in the area of interest and compared with the results from two previous investigations: the Hydraulic Research Station's (HRS, 1963) and the Tauranga Harbour Study hydrodynamic model (Barnett, 1985). De Lange repeated the Pilot Bay and Cutter Channel sediment samples from the 1985 study, using the same analysis protocol with the Rapid Sediment Analyser, and combined the results into a sublittoral sediment facies distribution map (Fig. 2.29). Seven dominant facies were observed:

- Rock outcrop: rocks or boulders cover more than 70% on the seabed.
- Shell lag: shells cover more than 80% of the seabed (Fig. 2.24).
- Very shelly sands: 50-80% of the seabed is covered in shells (Fig. 2.25).
- Shelly sands: 20-50% of the seabed is covered in shell fragments or live shell (Fig. 2.26).
- Clean sands: they contain <20% shell cover and occasional ripples (Fig. 2.28).
- Silty sands: finer sediments (Fig. 2.27).

This thesis, although it does not present any direct material on the Stella Passage, proved very useful in terms of sediment analysis techniques. It also brought valuable information on the examination of underwater videos for shell density and species identification.



Figure 2.24: Shell lag facies made of fresh pipi (*Paphies australis*), turret shell (*Maoricolpus roseus*) and white rock shell (*Thais orbita*). (Source: de Lange, 1988)



Figure 2.25: Very shelly sand facies, pipi and turret shells cover 50-80% of the seabed. (Source: de Lange, 1988)

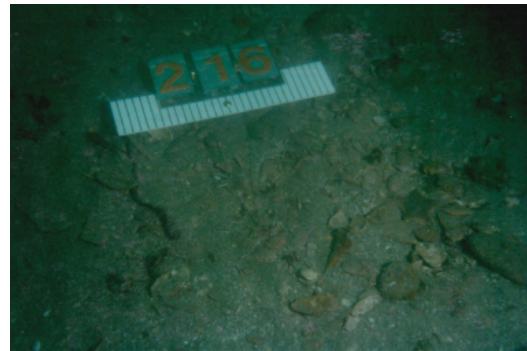


Figure 2.26: Shelly sand facies, shell fragments and occasional live horse mussel and scallop cover 20-50% of the seabed. (Source: de Lange, 1988)



Figure 2.27: Silty sand facies, finer undisturbed sediment with occasional cockles and horse mussels. (Source: de Lange, 1988)

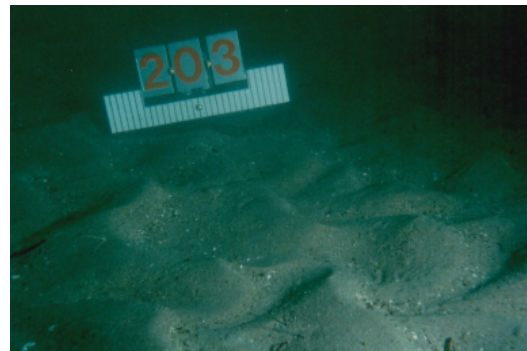


Figure 2.28: Sand waves and megaripples facies. (Source: de Lange, 1988).

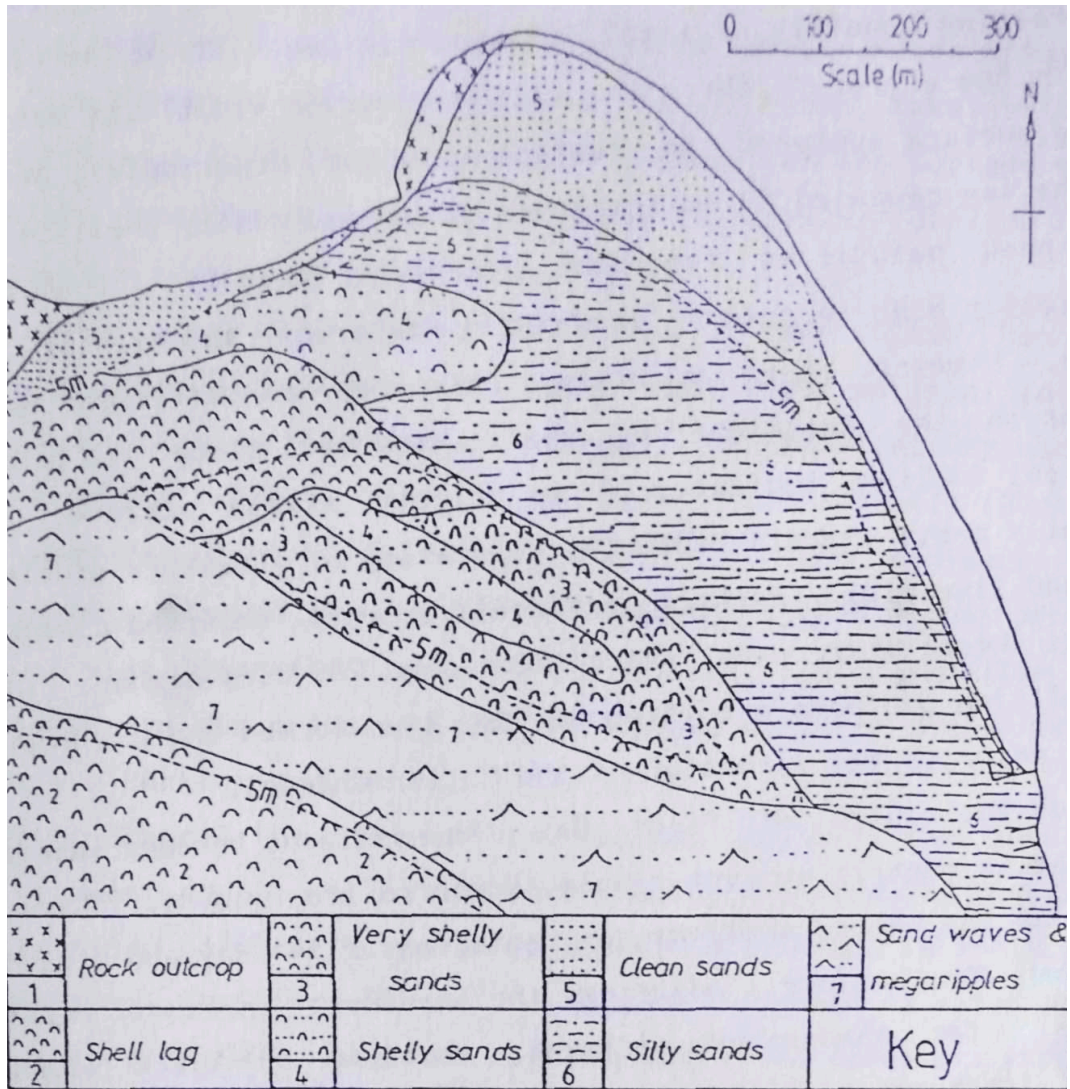


Figure 2.29: Bottom sediment distribution for the Pilot Bay region. (Source: de Lange, 1988)

2.8. PORT OF TAURANGA LTD CHANNEL DEEPENING AND WIDENING DREDGING PROGRAMME: ENVIRONMENTAL ASSESSMENT - 1991

In 1991, an environmental study was commissioned by the Port of Tauranga Limited to investigate the ecological impact of a dredging program intending to deepen and widen the Shipping Channels (Healy, McCabe, Thompson, & Port of Tauranga Limited., 1991). As the annual maintenance dredging would increase from 70,000 m³ to 110,500 m³, an accurate description of the sediments to be removed was necessary.

The Port of Tauranga has been extensively studied since its early developments. This allowed the authors to retrieve 50-60 boreholes (Figure 2.30) from various contractors in order to assess the likely stratigraphy of the sediments to be dredged. No 3-dimensional subsurface stratigraphy was interpolated from the existing boreholes., but a review of these boreholes found the following results:

- Predominance of marine shelly sand and occasional thin silty layers along the Maunganui Roads down to the 12.9 m depth.
- A silty stratum appears to be present around the Stella Passage entrance adjacent to Sulphur Point
- The stratigraphy up channel from there seems to be complex marine sands, although shells were also found by the southern end of the Container Wharf.

Two more representative cores (Fig. 2.34) of the sediment to be dredged were obtained in the Stella Passage (Fig. 2.31). The first core, D76 (Fig. 2.32 and 2.35), presented “tight cohesive grey green silt with shells” which was decided inappropriate for dumping over the chosen sandy substrate ground. The core D75 (Figure 2.33 and 2.36) was constituted of white to pink pumice sand and gravel with occasional silty bands and was also found detrimental to the dumping on the shelf. The Rapid Sediment Analyser from the University of Waikato was used to obtain grain-size distributions for both cores:

- D75: Gravel 0%, Sand 86.44%, Silt 13.56% and Clay 0%.
- D76: Gravel 0.17%, Sand 17.01%, Silt 82.82% and Clay 0%.

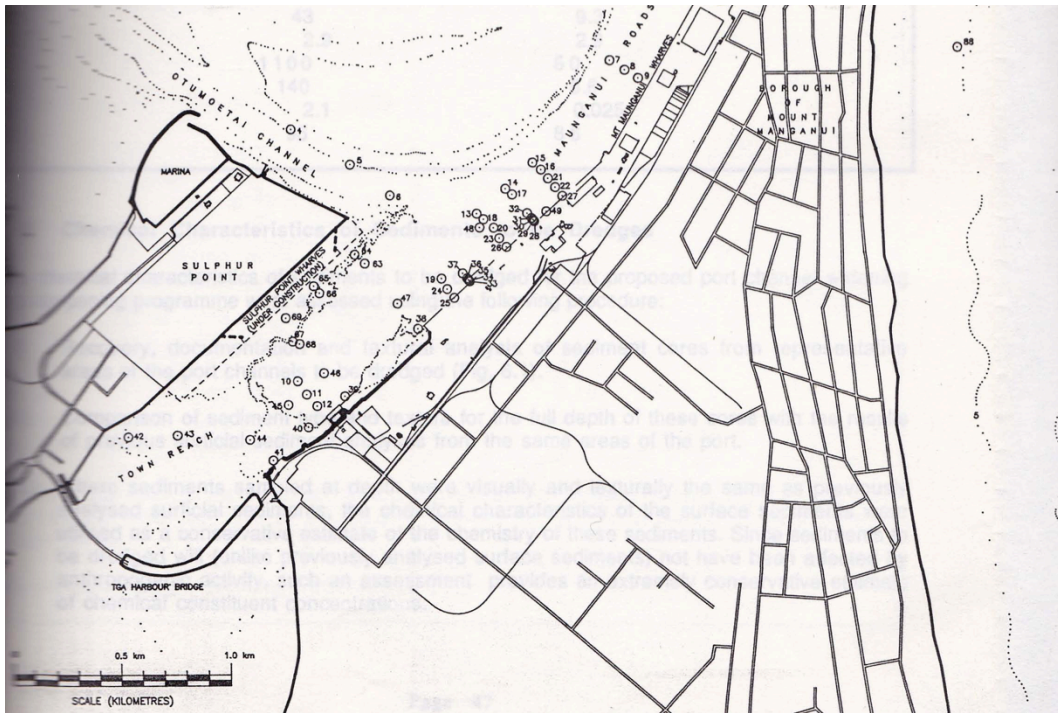


Figure 2.30: Historic sediment sampling site locations (Source: Healy *et al*, 1991)

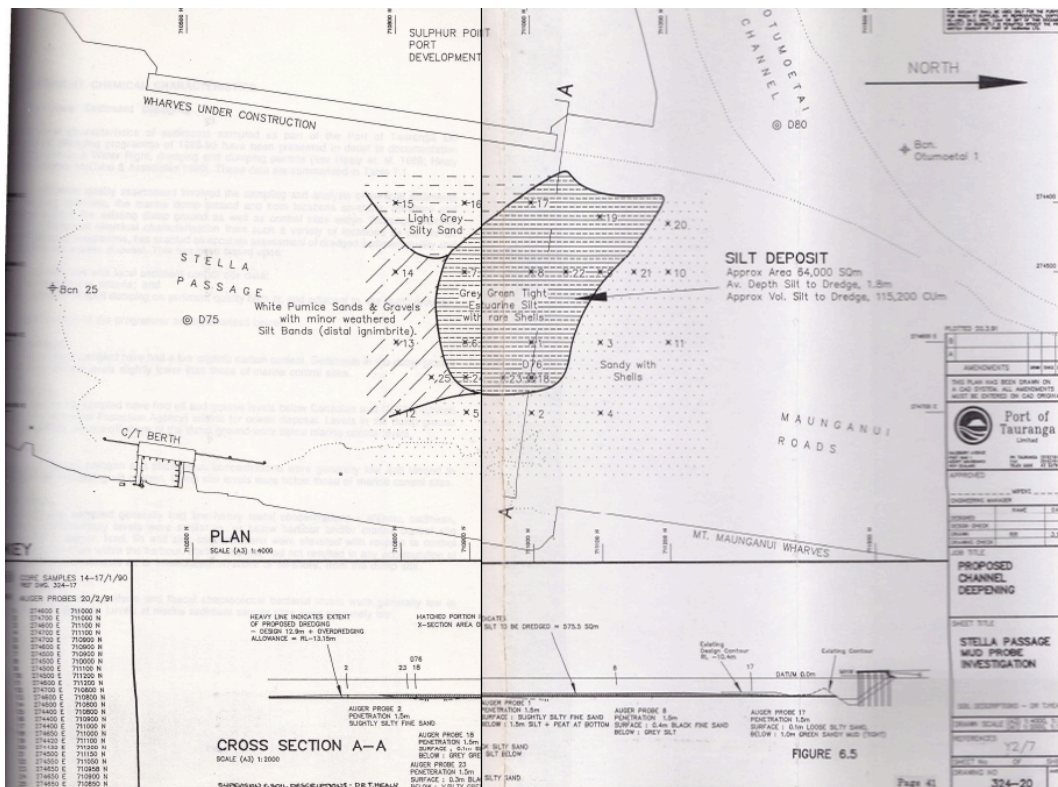


Figure 2.31: Stella Passage mud probe investigations and interpreted sediment types. (Source: Healy *et al*, 1991)

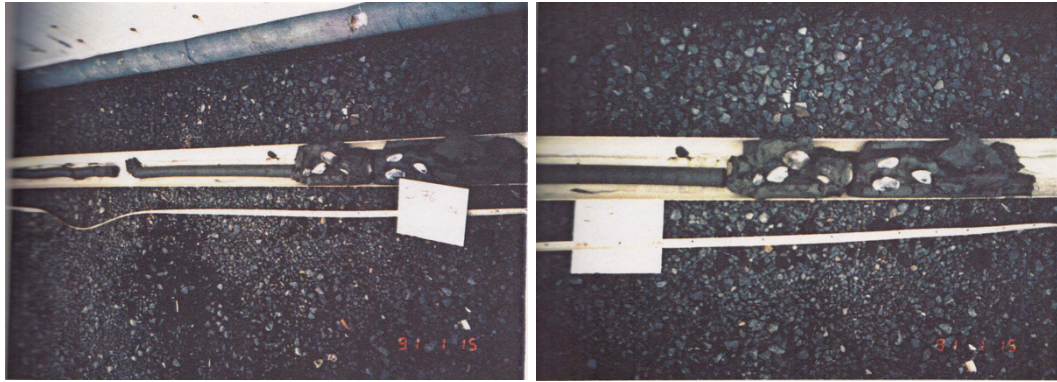


Figure 2.32: Core D76. (Source: Healy *et al*, 1991)

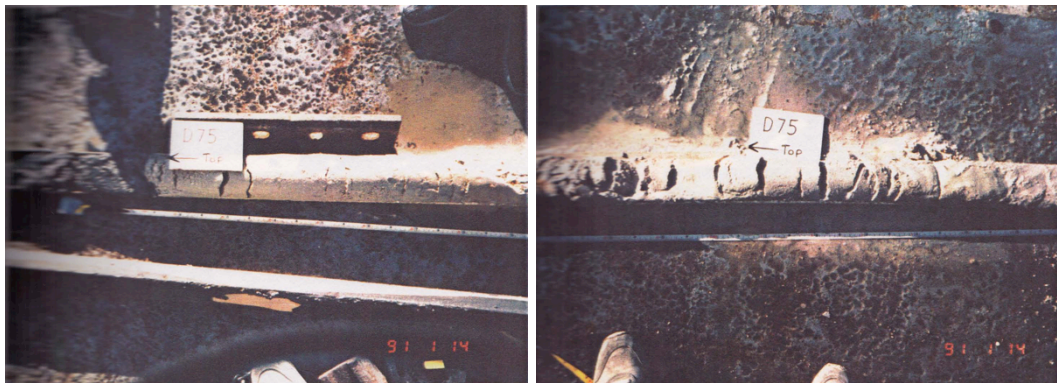
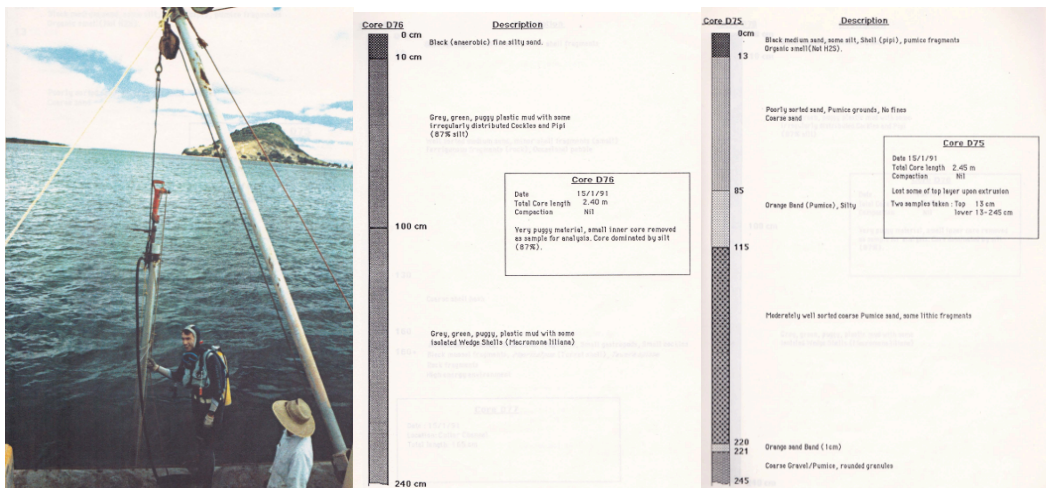


Figure 2.33: Core D75. (Source: Healy *et al*, 1991)



Figures 2.34, 2.35 and 2.36: Vibratory coring device, Core D76 stratigraphy and Core 75 stratigraphy. (Source: Healy *et al*, 1991)

2.9. SEDIMENTATION OF THE ENTRANCE CHANNEL OF THE TAURANGA HARBOUR - 1999

In 1999, Kruger investigated the sediment patterns of the Tauranga Harbour entrance as part of a MSc thesis (1999). A current velocity study was undertaken during a 14-hour survey of the entrance using an Acoustic Doppler Current Profiler (ADCP). As part of the morphological investigation, a sidescan sonar survey was performed using a Klein 595 system (100/500 KHz) (Fig. 2.37) in order to identify the sediment pathways in the area. Five different acoustic units were identified from the sidescan mosaic (Fig. 2.39). A total number of 63 sediment samples were collected and analysed with the Rapid Sediment Analyser to provide ground-truthing for the sonar data. A classification scheme was applied to the complex-texture area sonagraph in order to produce a sediment facies map (Fig. 2.38).

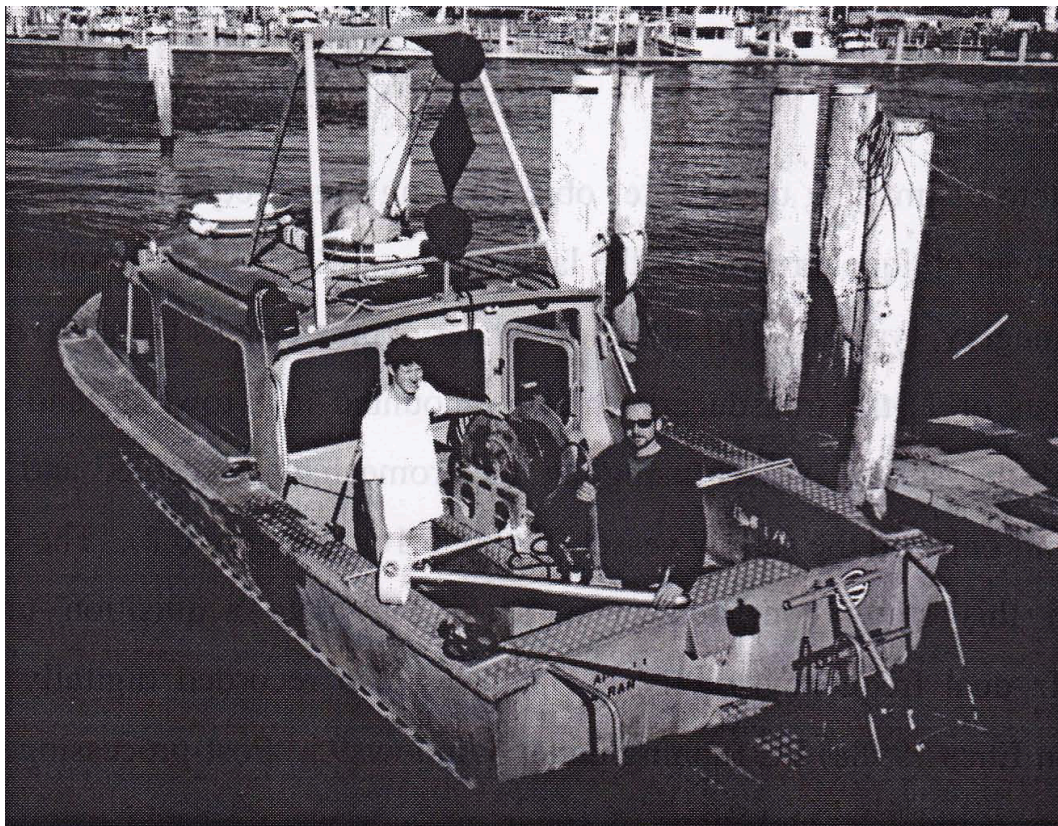


Figure 2.37: The Klein 595 system on board the Port of Tauranga Kairuri IV work vessel. (Source: Kruger, 1999)

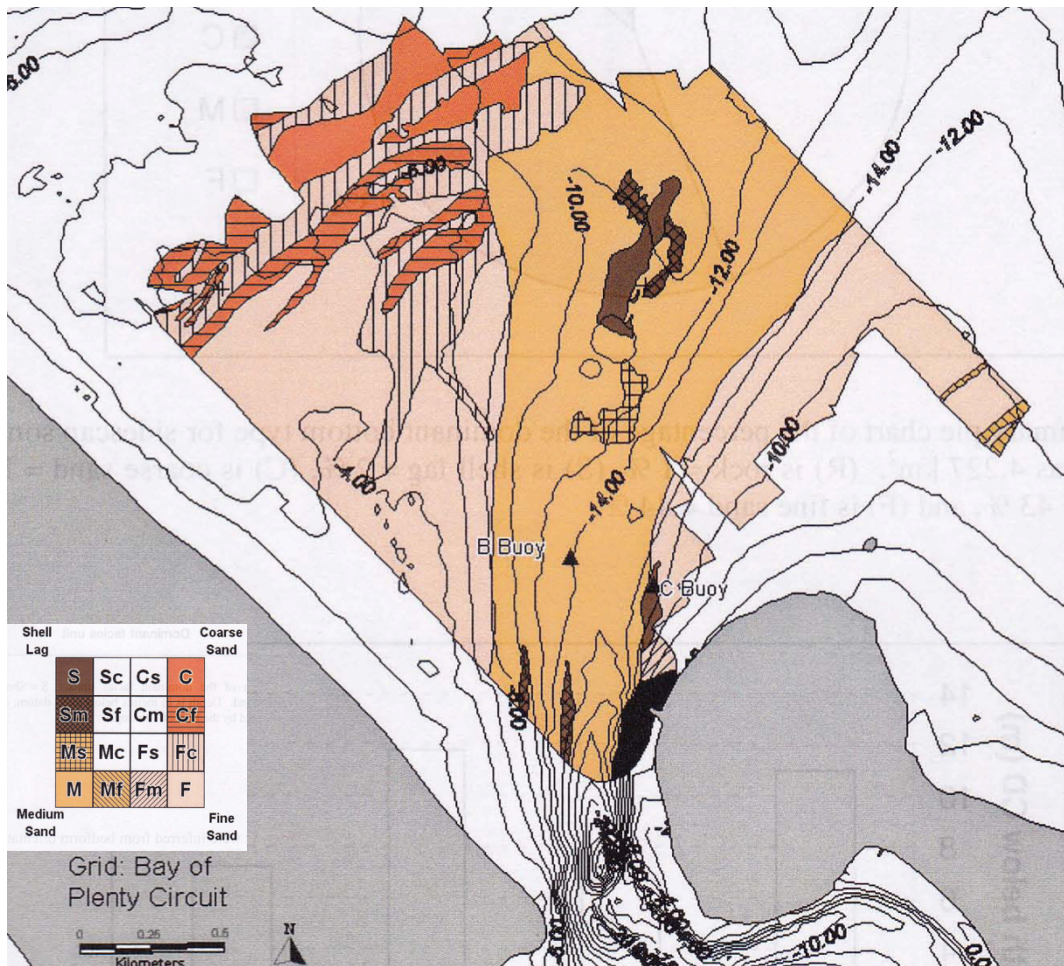


Figure 2.38: Ebb tidal delta bottom sediment facies map. (Source: Kruger, 1999)

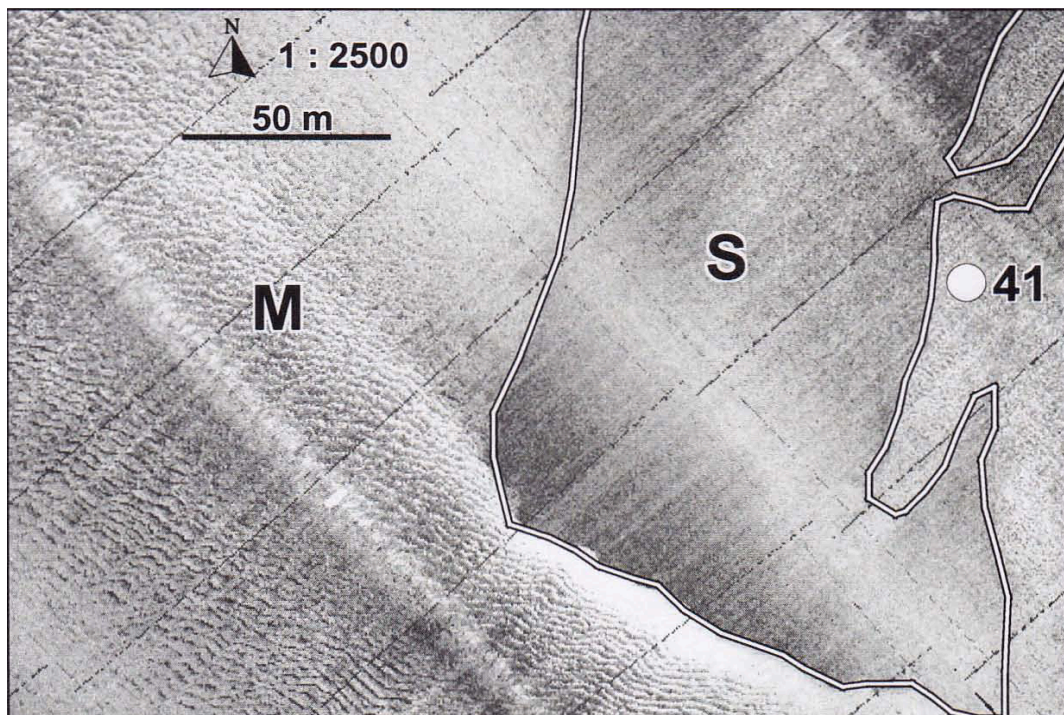


Figure 2.39: Sonograph from the Klein 595 showing medium-sand dunes and a shell lag. (Source: Kruger, 1999)

2.10. EVALUATION OF AN INNER SHELF SITE OFF TAURANGA HARBOUR, NEW ZEALAND, FOR DISPOSAL OF MUDDY SANDY DREDGED SEDIMENTS - 1999

In 1999, the Port of Tauranga was undergoing a capital dredging program around the area of Sulphur Point and the navigation channels. The dredged material mainly constituted of shelly and gravelly sand that were disposed at a dumping ground 4 km off the coast. The planned extension of the southern Sulphur Point would require the removal of sediments with a higher amount of silt and clay, making them inappropriate to be dumped at the existing disposable ground.

A study was undertaken by Michels and Healy (1999) to locate a new disposal ground for the muddy sediments. The dredged area sediments stratigraphy and composition were assessed by the analysis of past studies core samples and the use of a seismic sub-bottom profiler. The results showed that the sediment to be dredged was mainly constituted of shelly and gravelly sand, pumiceous sediments with silty-clayey sands (silt/clay content >80%) and cohesive marine clays (silt/clay content >90%).

The potential disposal grounds were studied through a bathymetric survey, a sidescan sonar survey, sediment samples and current measurements. Four main facies were identified during the sidescan sonar survey: coarse grained ripples; featureless and finely rippled fine to medium sand; irregular dune bedforms; and sand waves (Fig. 2.40). The boundaries between units were then defined as either “sharp” or “transitional”. The sediment samples analysis allowed to confirm the coarse grained and fine-medium sandy facies of the sonar survey.

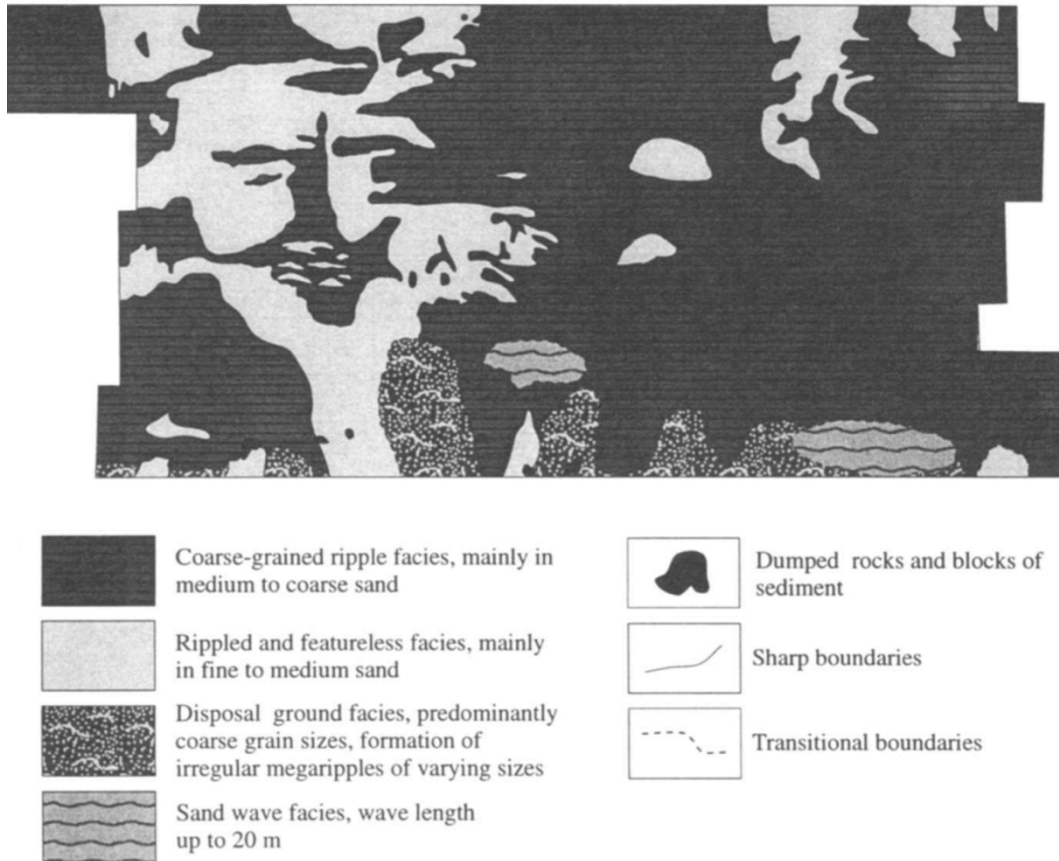


Figure 2.40: Interpretation of the features from the sidescan sonar survey on the proposed disposable ground. (Source: Michels & Healy, 1999)

2.11. BENTHIC COMMUNITIES OF THE STELLA PASSAGE REGION - 1999

The benthic communities of the Stella Passage were investigated by Butler (1999) as part of a Master thesis. His study aimed at describing the spatial and temporal variations of the different species and their immediate response to the maintenance dredging occurring in the area. A total of 18 sites were sampled four times and subsequent analysis identified four distinct community groups (Fig. 2.41 and 2.42):

- Fine black silt sediments/low current velocities: *Nucula liartvigiana*, *Pectinaria australis* and *Helice crassa*.
- Coarse sand/high current velocities: *Tawera spissa* and *Paguridae sp.*
- Shelly seabed: *Paphies australis* and *Micrelenchus huttoni*.
- Macroalgae patches: *Maoricolpus roseus* and *Armandia maculate*.

Over the whole survey, the pipi shells (*P. australis*) accounted for half the individuals collected during the whole survey. They were found to be rarely present in the September and January samples, with a greater abundance in April and June for all sites. Physical and/or biological processes govern the presence and abundance of the communities. Sediment deposition rates can impact the suspension feeding organisms, and the grain structure can alter the deposit feeding species. Butler (1999) pointed out that the benthic communities of the Stella Passage tended to vary in areas with uniform grain size characteristics, indicating that other parameters than the substrate could explain the presence of shells: tidal current strength, water depth or the presence of *Ulva sp.* and intact shell material. He hypothesised that the area next to the Bridge Marina could act as a nursery for juveniles prior to their possible migration to the Tauranga Harbour entrance. However, this idea was judged unlikely, as the area north of the Marina, the deep dredged channel presenting low current velocities, would potentially block this migration.

Butler (1999) then investigated the impact of dredging on the benthic communities of the Stella Passage. A series of surveys showed that the dredging

of the area impacted the shell population and the seabed on different levels. The sediment grain size was decreased, algae mats of *Ulva sp.* disappeared and the water depth was 0.5m greater. The species composition was also altered as the decline of tube building polychaete (*Owenia fusiformis*) allowed for greater species diversity after dredging.

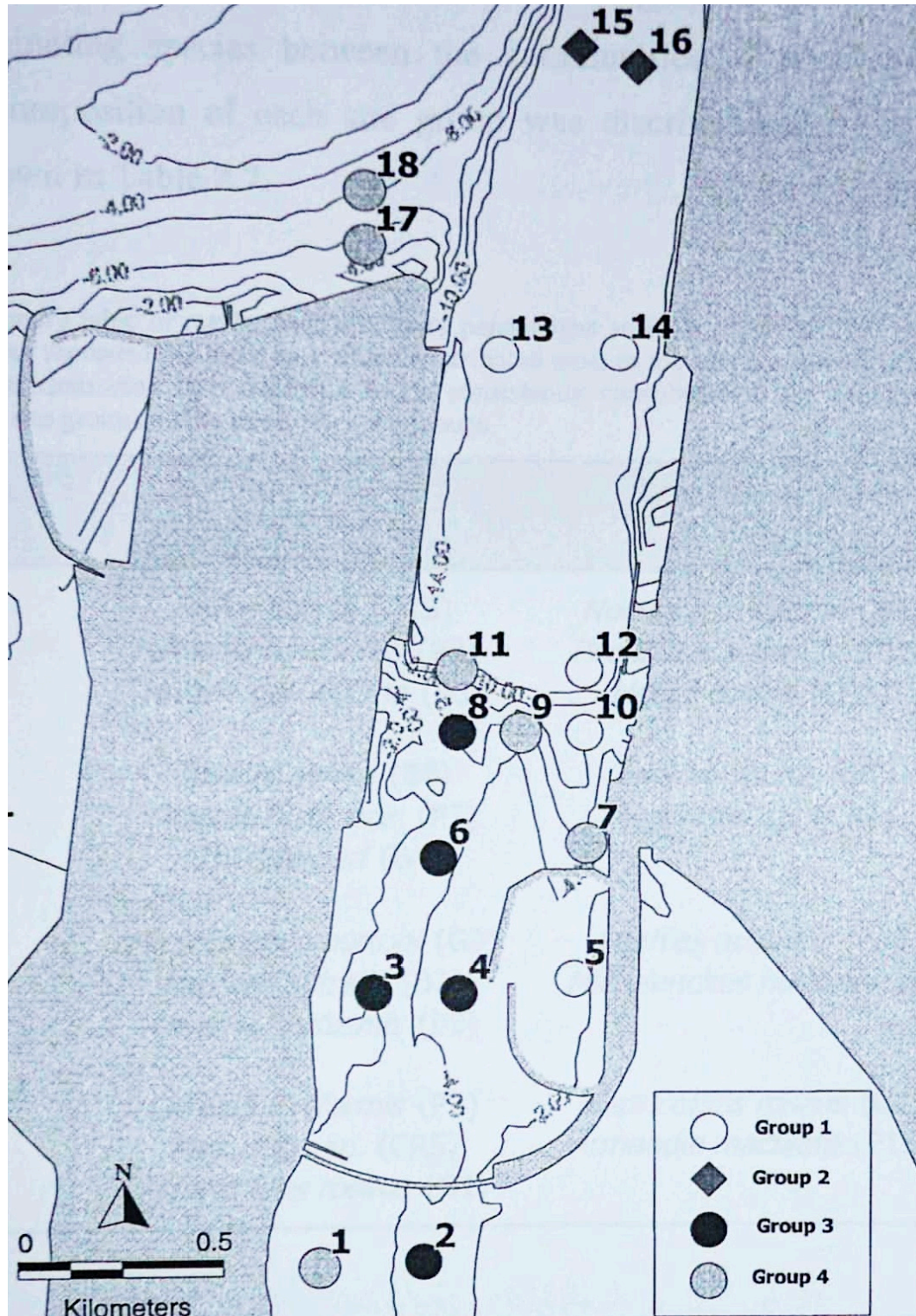


Figure 2.41: Sampling sites and macrofaunal community composition. (Source: Butler, 1999)

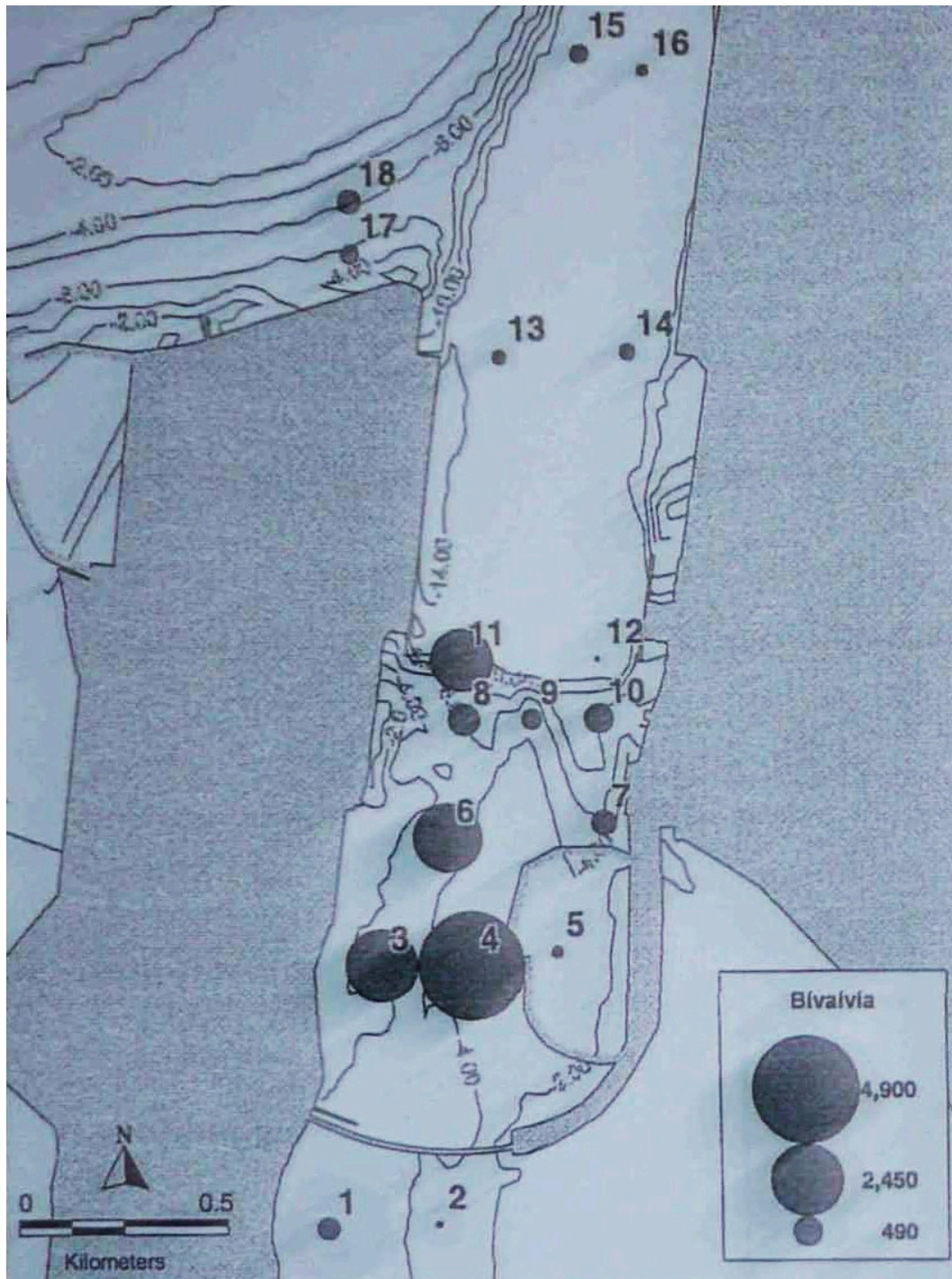


Figure 2.42: Total number of individuals for the Bivalvia taxonomic group. (Source: Butler, 1999)

2.12. THE POPULATION DYNAMICS AND PRODUCTION OF PAPHIES AUSTRALIS (PIPI) IN THE SOUTHERN BASIN, TAURANGA HARBOUR - 2001

In 2001, Gouk studied the population of pipi shells (*Paphies australis*) in three sites of the Tauranga harbour: the Centre bank, the Tilby Channel and the Wairoa River (Gouk, 2001). These sites were chosen as they offered different salinity, temperature and suspended sediment conditions. The individuals' size was found to decrease during winter and increase during spring as a consequence of the variations in salinity and temperature.

The author used Pearson's correlation coefficients (Fig. 2.43) in order to define the correlations between the shell weight and the environment factors: salinity, temperature, sediment characteristics and seston (bioplankton) characteristics. A strong correlation was found between the pipi mass production and the sediment clay and silt content in the sediment. This result seemed unlikely at first, as clay and silt are known to smother the pipi by clogging their gills and mantle. This correlation between the individuals size and clay/silt percentage was explained by calmer weather conditions, during which the particles deposit on the seabed, allowing the shells to feed more efficiently.

Table 3.18 Pearson's correlation coefficients between mean pipi condition index and AFDW production with seston characteristics, salinity, temperature, and sediment characteristics ($\alpha = 0.05$) (top value = Pearson correlation coefficient; bottom value = p -value) at Centre Bank, Tilby Channel, and Wairoa River (significant correlations are indicated by p -values in bold).

	Centre Bank		Tilby Channel		Wairoa River	
	Condition	Production	Condition	Production	Condition	Production
SPM	0.045 0.916	0.315 0.447	0.070 0.838	0.319 0.338	-0.255 0.448	0.018 0.958
% POM	-0.177 0.675	-0.550 0.157	0.103 0.726	-0.552 0.078	0.596 0.053	0.012 0.972
Chlorophyll a	0.436 0.280	0.137 0.746	0.256 0.447	0.256 0.448	0.299 0.371	-0.002 0.996
Pheophytin	0.071 0.867	0.088 0.837	0.220 0.516	0.350 0.291	0.107 0.754	0.194 0.568
Salinity	-0.799 0.017	-0.314 0.449	0.028 0.934	-0.490 0.126	0.208 0.540	-0.168 0.621
Temperature	0.153 0.718	0.039 0.927	0.602 0.049	-0.480 0.135	0.834 0.001	-0.129 0.704
Sediment chlorophyll a	-0.249 0.552	0.205 0.627	-0.062 0.856	-0.682 0.030	0.021 0.955	-0.248 0.490
Sediment pheophytin	0.160 0.705	0.374 0.361	0.082 0.822	0.005 0.989	0.291 0.415	0.304 0.393
Sediment organic	0.015 0.971	0.176 0.677	0.702 0.024	-0.233 0.518	0.034 0.926	0.315 0.376
% clay	0.496 0.211	-0.359 0.382	0.038 0.916	0.056 0.878	0.277 0.438	0.036 0.921
% silt	0.758 0.029	0.392 0.337	0.518 0.125	0.223 0.535	0.409 0.240	0.335 0.343
% sand	0.372 0.364	0.075 0.860	-0.646 0.044	0.145 0.690	-0.613 0.059	-0.480 0.161
% gravel	-0.457 0.255	0.100 0.813	0.550 0.100	-0.199 0.581	0.401 0.251	0.315 0.376
% mud	0.748 0.033	0.251 0.550	0.403 0.248	0.185 0.608	0.414 0.234	0.307 0.387

Figure 2.43: Pearson's correlation coefficients between the pipi descriptors and the environmental conditions. Top value is Pearson's coefficient. Bottom value is p -value. Significant correlations are in bold. (Source: Gouk, 2011)

2.13. CHANGE IN GEOMORPHOLOGY, HYDRODYNAMICS AND SURFICIAL SEDIMENTS OF THE TAURANGA ENTRANCE TIDAL DELTA SYSTEM - 2009

The Tauranga Entrance was investigated by Brannigan (2009) as part of a MSc thesis. This report analyses historical changes of the Tauranga Harbour delta system and presents the results of a numerical modelling study based on these past bathymetries. From 1852 to 1954, the Stella Passage underwent little change. Between 1954 and 2004, this area was subject to two major modifications that altered the local hydrodynamics. Dredging from 5 m to 13 m depth seems to have reduced the current velocity in the deep areas, while the construction of the Harbour Bridge and its' causeway appears to have increased the velocity around the shoal (Fig. 2.44)

A morphological study was undertaken by Brannigan (2009) that comprised a sidescan sonar survey, a sediment-sampling program and underwater video recordings in order to determine the surficial shell coverage to be compared to past studies. A Klein 595 system (500 kHz) was used to perform the sonar survey towed by the University of Waikato survey vessel *Tai Rangahau*. Four distinctive reflectivity units were digitized from the sonograph (Fig. 2.45) and classified using the ground-truthing sediment samples and underwater videos: fine sand, medium sand, shell lag and rock. A surficial sediments and shell coverage map was created (Fig. 2.46) and compared to the 1985 study (Healy, 1985) (Fig. 2.47). The results of this morphological study show that the sediments from the north of Stella Passage were mainly composed of “very fine sand with no shell coverage”.

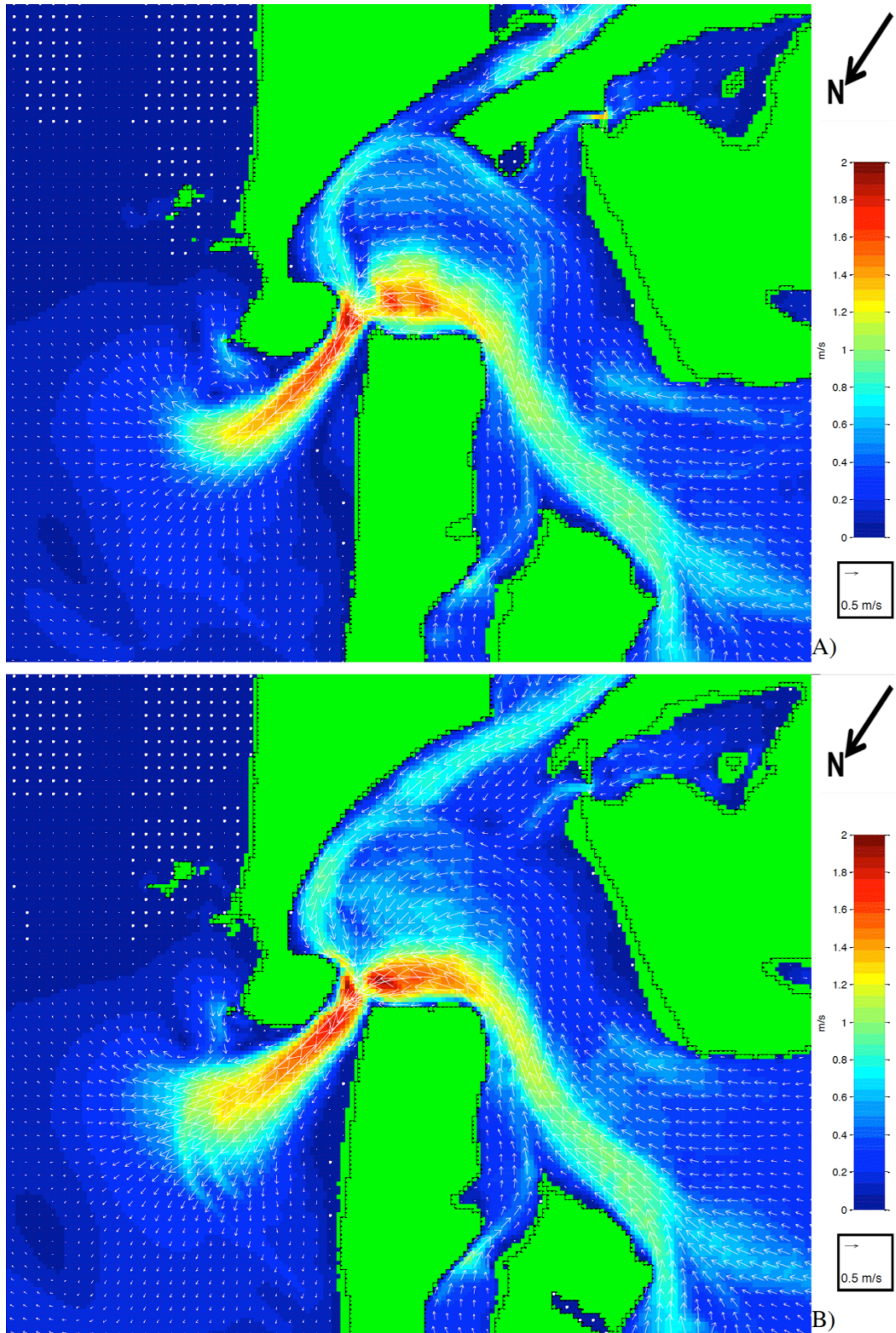


Figure 2.44: Mean spring tide peak flood velocity vector plot for 2006 (top) and 1954 (bottom). (Source: Brannigan, 2009)

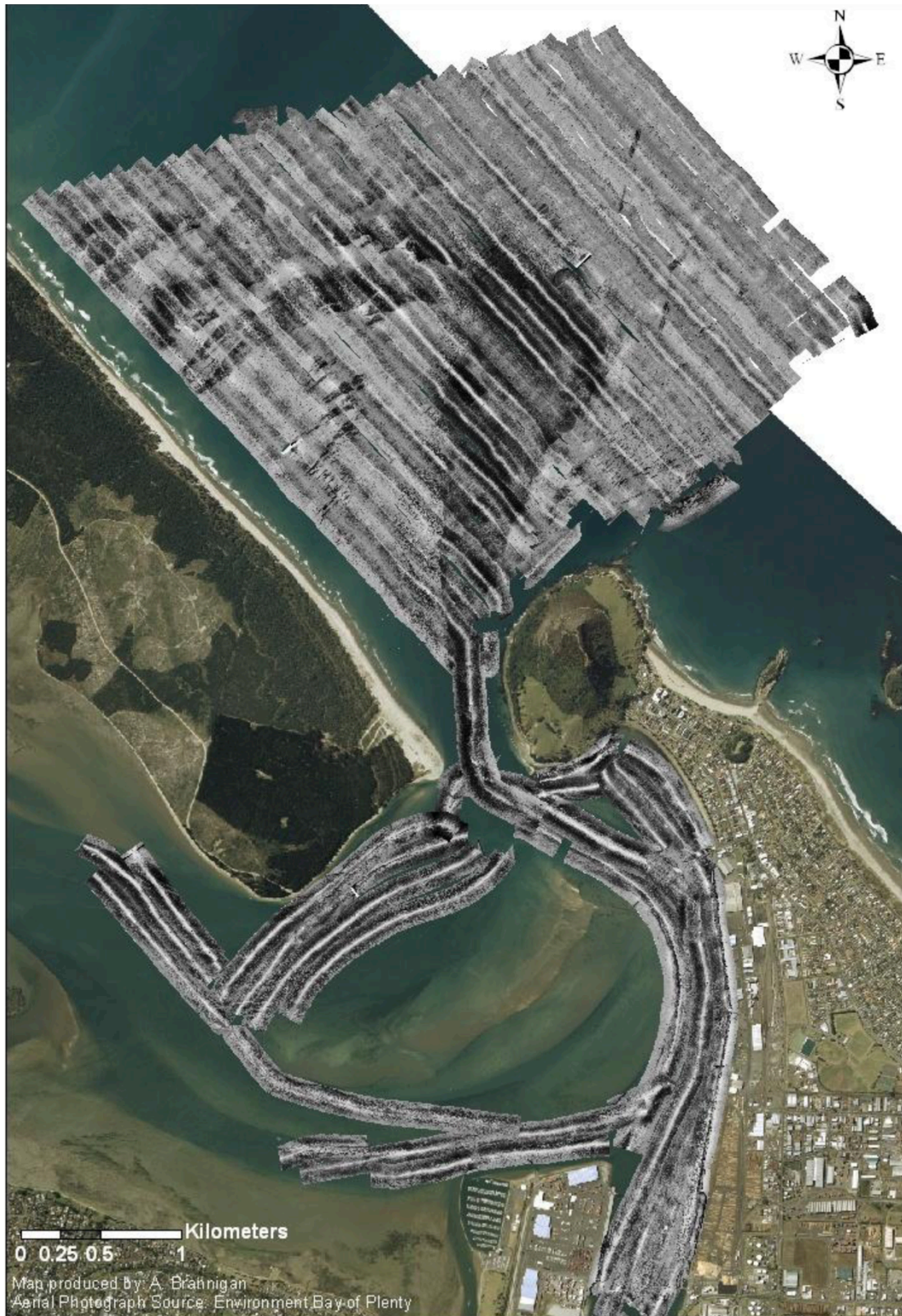


Figure 2.45: Sidescan sonar mosaic of the Tauranga Harbour in 2007. (Source: Brannigan, 2009)

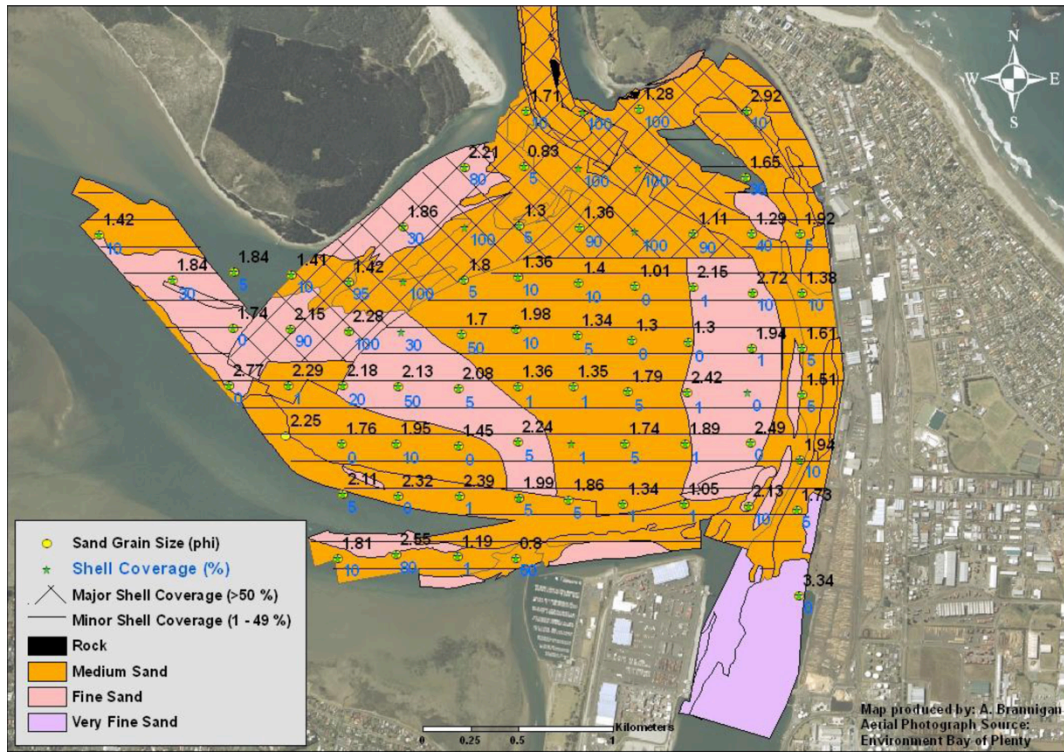


Figure 2.46: Surficial sediment and shell coverage map of the Tauranga Harbour in 2007. (Source: Brannigan, 2009)

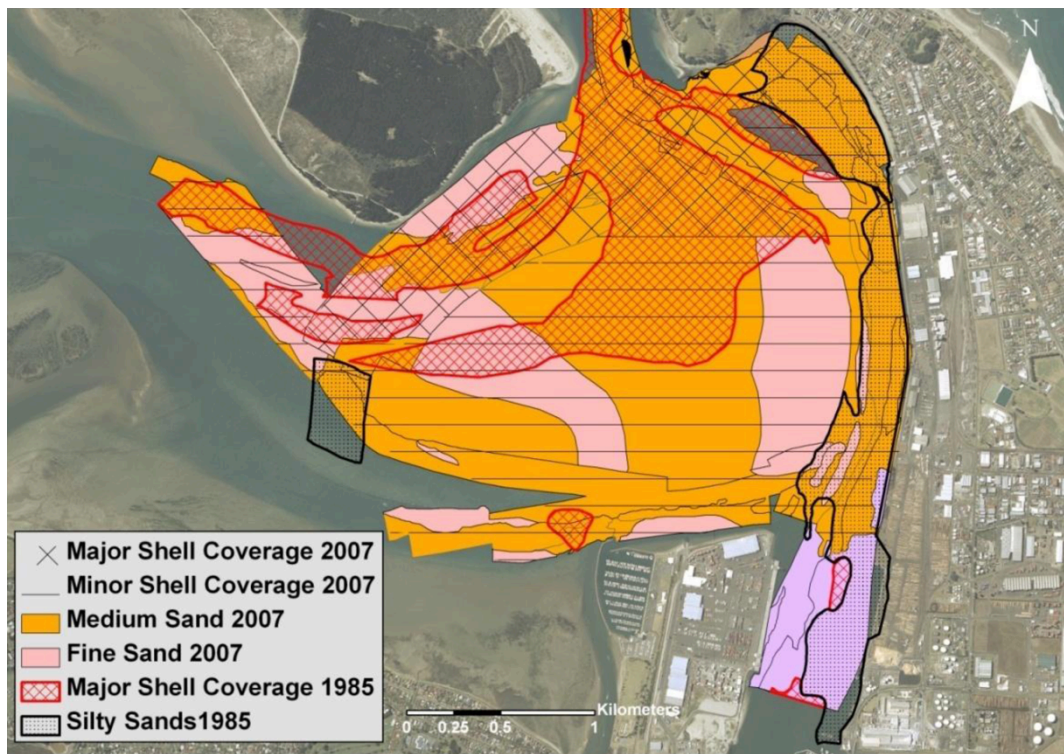


Figure 2.47: Comparison of 2007 and 1983 surficial sediment and shell coverage maps for the Tauranga Harbour. (Source: Brannigan, 2009)

2.14. TAURANGA BRIDGE MARINA: NORTHERN BREAKWATER ASSESSMENT OF ENVIRONMENTAL EFFECTS - 2009

In 2009, Tauranga Bridge Marina Ltd commissioned Tonkin & Taylor Ltd to undertake an Assessment of Environmental Effects as part of an application to construct a rock breakwater at the northern end of the Marina (Tonkin & Taylor Ltd, 2010). A hydrodynamic numerical model was used to study the tidal currents for all the proposed options, and a survey of the benthic invertebrate communities was undertaken.

Six sites were core-sampled along the existing northern breakwater (Fig. 2.48). The local substrates were found to be mainly composed of “marine sands and silts with accumulation of shell hash”. The most abundant bivalves in all samples were *Tawera spissa* and *Nucula hartvigiana* while the dominant gastropods were *Notoacmea subtilis* and *Eatoniella sp.*

The results from the hydrodynamic study show that two effects of the breakwater construction have to be considered: changes to the tidal currents; and the scour effect of the seabed. At present, flood tidal currents are found to flow at 0.1-0.3 m/s in the Stella Passage, 0.5-0.6 m/s on the Town Reach shallow flat area and 0.6-0.9 m/s under the Tauranga Harbour Bridge. The construction of the breakwater would not impact the Stella Passage current velocities, but would deflect the flood flow westwards as it approaches the Marina, where the velocity would be reduced from 0.5 m/s to 0.0-0.1 m/s (Fig. 2.49). The existing ebb tidal currents are around 0.6-0.9 m/s as they pass the Harbour Bridge, 0.7-0.8 m/s within Town Reach, 0.2-0.5 m/s in the Marina and 0.5-0.7 m/s in Stella Passage.

After the construction of the breakwater, the tidal currents in the Marina would be reduced to 0.1-0.3 m/s while they would increase to 0.9-1.1 m/s on the Town Reach and 0.7-0.9 m/s in the Stella Passage, meaning an overall gain of one third in these two areas (Fig. 2.50). The numerical modelling shows that the dredging of the Stella Passage and Town Reach after the construction of the breakwater would reduce the enhanced velocities to the current situation.

A scouring effect of the seabed could be expected following the increase of the tidal current velocities in the vicinity of the Bridge Marina; depending on the seabed material, location in the harbour and current speed. Considering the probability of the Harbour sediments levels fluctuating from storm action, the authors predicted 1.0-1.5 m lowering of the sediment beds in the area, in response to the increase of the current velocities. The impacted area would more likely be restricted to where the Port of Tauranga has already planned to dredge and extend the Sulphur Point berth, limiting the scouring impact of the construction of the Marina breakwater. Under the Whareroa Point Bridge, the tidal currents were modelled to increase only by 15%, and were not expected to cause any significant scour in the area.

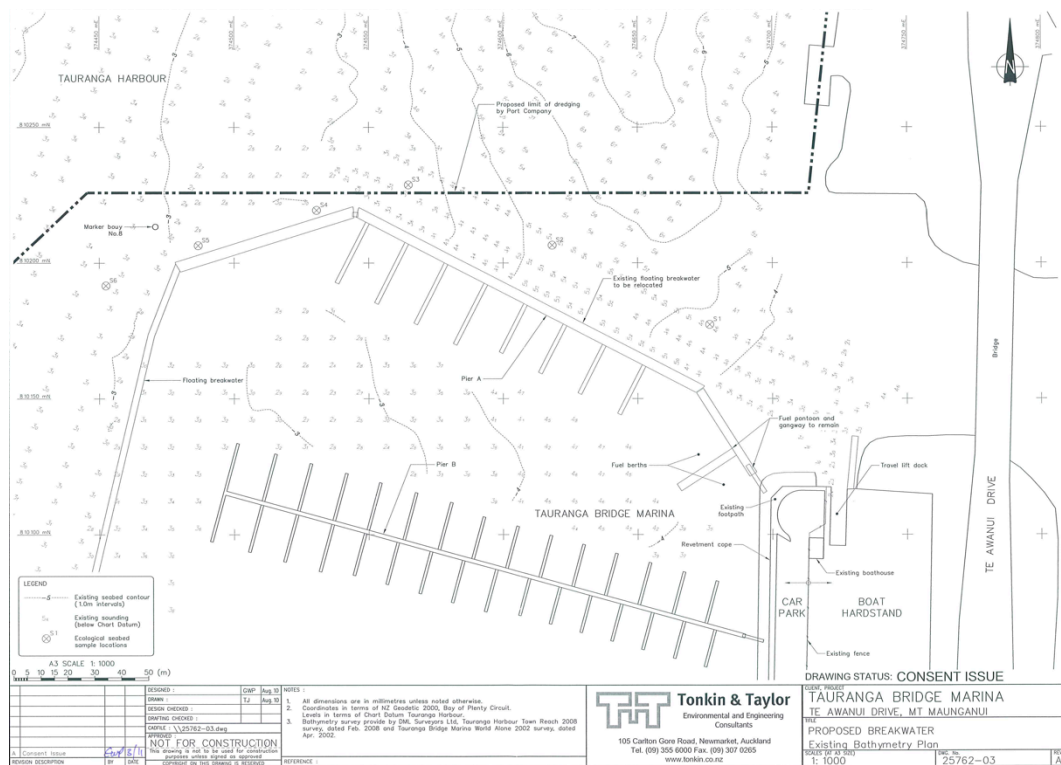


Figure 2.48: Existing bathymetry plan and core samples locations. (Source: Tonkin & Taylor Ltd, 2009)

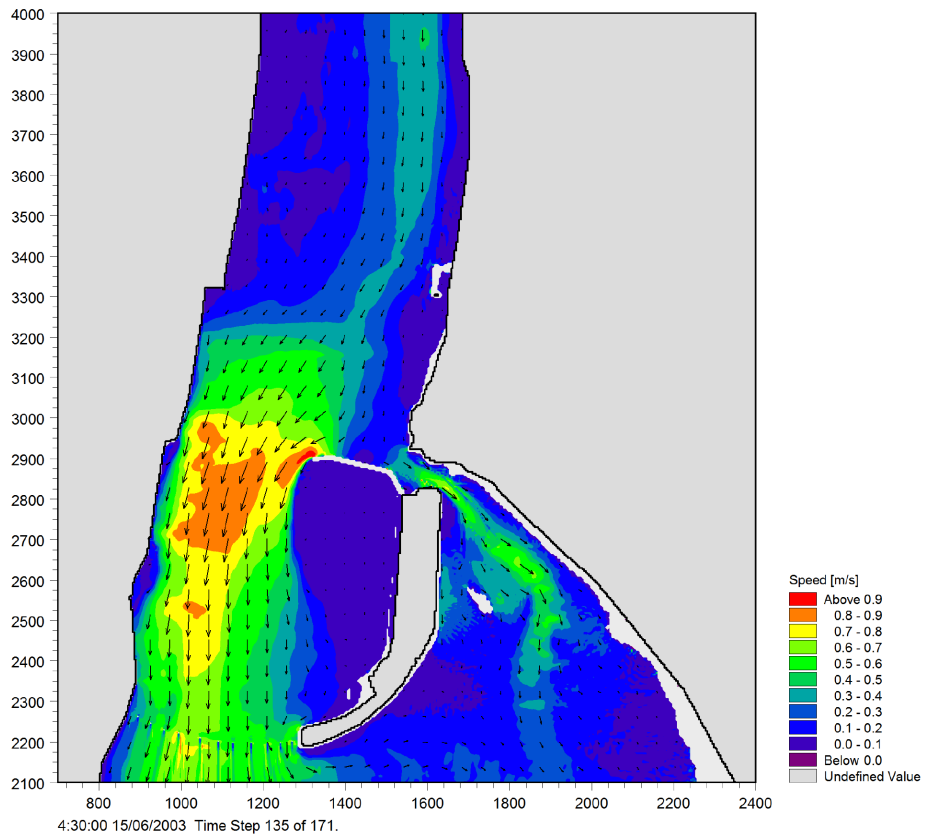


Figure 2.49: Peak flood tide currents after construction of the breakwater. (Source: Tonkin & Taylor Ltd, 2009)

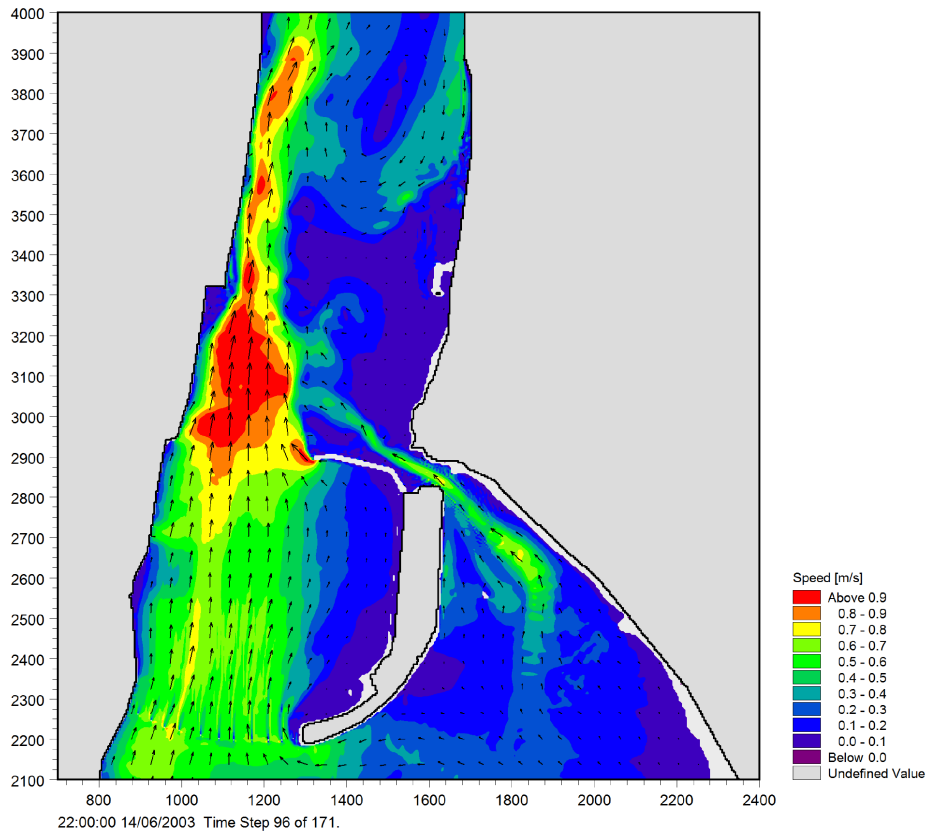


Figure 2.50: Peak ebb tide currents after construction of the breakwater. (Source: Tonkin & Taylor Ltd, 2009)

2.15. CONCLUSION

Based on the previous studies, several features are expected to be found in the Stella Passage, Town Reach and Tauranga Bridge Marina. The previous studies identified large areas of dense shell coverage, especially in high current velocities areas like the Town Reach channel. The pipi and turret shells were predominant in all previous papers and will likely represent the most represented species in this thesis. There was no extensive investigation of the Stella Passage since the last dredging campaign in 1992. As this program is still ongoing in order to maintain an average 13 m depth, the seafloor is expected to present strong differences with previous studies. No morphological study has been undertaken inside the Tauranga Bridge Marina after its construction. This area presented shallow sublittoral sands in the 1985 study. The currents have apparently increased since, hence the need for a solid breakwater, so the seabed is expected to present high velocities areas characteristics such as sand waves and coarser sediment.

2.16. REFERENCES

- Barnett, A. G. (1985). *Tauranga Harbour study, part I Overview, Part III Hydrodynamics*. N.Z.: Bay of Plenty Harbour, New Zealand Ministry of Works Development, Dansk hydraulisk Institut, University of Waikato
- Beca Carter Hollings and Ferner Ltd. (1985). *Tauranga Harbour Bridge: an environmental impact assessment*. Beca Carter Hollings and Ferner Ltd, Tauranga Harbour Bridge Committee, Bioresarches Ltd, Hegley Acoustic Consultants, Boffa Miskell Partners. Retrieved from <http://books.google.co.nz/books?id=I87IMAAACAAJ>
- Black, K. P. (1985). *Tauranga Harbour study, part IV Text, Figures and Tables*. Bay of Plenty Harbour, New Zealand Ministry of Works Development, Dansk hydraulisk Institut, University of Waikato
- Brannigan, A. M. (2009). *Change in geomorphology, hydrodynamics and surficial sediment of the Tauranga entrance tidal delta system, 2009*. Retrieved from <http://hdl.handle.net/10289/2799>
- Butler, R. J. (1999). *Benthic communities of the Stella Passage region, Tauranga Harbour, New Zealand*.
- Davies-Colley, R. J. (1976). *Sediment dynamics of Tauranga Harbour and the Tauranga Inlet*. University of Waikato.
- De Lange, W. P. (1988). *Wave climate and sediment transport within Tauranga Harbour, in the vicinity of Pilot Bay* (D Phil Earth Sciences). University of Waikato.
- Gouk, S. G. (2001). *The population dynamics and production of Paphies australis (Pipi) in the Southern Basin, Tauranga Harbour, New Zealand*.
- Green, M. O. (2009). *Tauranga Harbour Sediment Study: Predictions of Harbour sedimentation under future scenarios*. Hamilton, N.Z.: National Institute of Water and Atmospheric Research (N.Z.),. Retrieved from <http://www.boprc.govt.nz/media/32631/NIWA-100721-THSS-E2-PredictionsofHarbourSedimentationUnderFutureScenariosAmendedMay2010.pdf>
- Healy, T., McCabe, B., Thompson, G. N., & Port of Tauranga Limited. (1991). *Port of Tauranga Ltd channel deepening and widening dredging programme 1991-92 : environmental impact assessment*. [Tauranga, N.Z.: s.n.]
- Healy, T. R. (1985). *Tauranga Harbour study, part II & V Field Data Collection Programme and Morphological Study*. Bay of Plenty Harbour, New Zealand Ministry of Works Development, Dansk hydraulisk Institut, University of Waikato

- HRS. (1963). *Tauranga Harbour Investigation: Report on First Stage*. Hydraulics Research Station, Wallingford, England. Retrieved from http://books.google.co.nz/books?id=M0_dtgAACAAJ
- Krüger, J.-C. (1999). *Sedimentation at the entrance channel of Tauranga Harbour, New Zealand* (M Sc Earth Sciences). University of Waikato.
- Kruger, J. C., & Healy, T. R. (2006). Mapping the morphology of a dredged ebb tidal delta, Tauranga Harbour, New Zealand. *Journal of Coastal Research*, 22(3), 720-727. 10.2112/03-0117.1
- Larcombe, M. F., Donovan, W. F., Bay of Plenty Catchment Commission, & Bioresearches Ltd. (1974). *A preliminary assessment of some aspects of the ecology of Tauranga Harbour*. Auckland: Bioresearches Limited.
- Lawrie, A. L. (2006). *Tauranga Harbour integrated management strategy* (Vol. 2006/09). Whakatane, N.Z.: Bay of Plenty Regional Council.
- Michels, K. H., & Healy, T. R. (1999). Evaluation of an inner shelf site off Tauranga harbour, New Zealand, for disposal of muddy-sandy dredged sediments. *Journal of Coastal Research*, 15(3), 830-838.
- Sinner J., Clark D., Ellis J., Roberts B., Jiang W., Goodwin E., et al. (2011). Health of Te Awanui Tauranga Harbour. Manaaki Taha Moana Research Report No. 1. Cawthron Report No.1969., 131.
- Tonkin & Taylor Ltd. (2010). *Tauranga Bridge Marina Ltd, Northern Breakwater Assessment of Environmental Effects*.

CHAPTER 3 - BENTHIC HABITAT MAPPING AND ACOUSTIC SEABED CLASSIFICATION

3.1. INTRODUCTION

The aim of this chapter is to introduce and give an overview of the various approaches of benthic habitat mapping. The concept of acoustic seabed classification is developed in the first part. This will be followed by a presentation of the different technologies used for seabed characterization. Finally, the third section will provide a description of the existing methods for multibeam echosounder backscatter processing.

3.2. BACKGROUND OF SEABED CHARACTERIZATION

3.2.1. Habitat ecological definition

A benthic habitat is defined alternatively as a place where a population is found, by a particular population inhabiting it, or by a series of environmental variables defining this place (Begon, Harper, & Townsend, 1996; Mitchell, 2005). These variables include but are not limited to depth, seabed type, topography, temperature, salinity, hydrodynamics, and nutrients availability. The scale of the study, the type of species targeted, or the technology being used will define the approach to benthic habitat mapping chosen (Brown, Smith, Lawton, & Anderson, 2011). As a consequence, a comprehensive understanding of the variables defining a particular species habitat and their relative significance has to be achieved. The integration of all possible parameters defining an ecosystem is necessary to avoid the simplistic association of seabed type with benthic habitat (Diaz, Solan, & Valente, 2004).

3.2.2. Acoustic Seabed Classification

In 2007, the International Council for the Exploration of the Sea reviewed acoustic seabed mapping systems and their relevance for habitat mapping (Anderson et al., 2007). This review defined Acoustic Seabed Classification (ASC) as:

“The organization of bottom types into discrete units based on a characteristic acoustic response.”

This definition only takes into account the remote-sensing aspect of habitat mapping, mainly derived from acoustic backscatter data, without considering other biological factors. The biological aspects of the substrate types are only to be used to verify or support the classification process of the acoustic data.

The concept of linking acoustic properties to seabed characteristics was developed in the early stages of marine acoustics (Nafe & Drake, 1963). The development of commercial systems in 1990s drove the interest in acoustic seabed classification systems (Anderson et al., 2007). The first stage included the use of vertical single-beam echosounder. Latter developments of sidescan sonars and multibeam echosounders allowed for the addition of oblique information and wider coverage.

3.2.3. Various approaches to Acoustic Seabed Classification

Seabed identification or segmentation aims at partitioning the seafloor into subsets from a classification scheme depending on the physical characteristics of the surficial sediment and their influence on the acoustic signal (Brown et al., 2011).

The discrimination of acoustic data into identical subsets can follow two distinct approaches: supervised or unsupervised. The supervised classification is used when the classes are known, and a set of ground-truth samples are used to train the partitioning of the acoustic dataset. When the seabed types are unknown prior to segmentation, an unsupervised classification is performed, during which the differentiation is only performed based on the homogeneity of the subsets. In other words, segments consist of clusters of small regions of pixels that have a

similar acoustic response. The *in-situ* data are then integrated in order to identify the created clusters.

The classification process can also be subdivided into manual and automatic. Manual classification, either supervised or unsupervised, requires the input of a human operator and, consequently, the presentation of the acoustic data in a format that the operator can process, usually an image. This technique used to be the most common before the introduction of computer-driven systems, but is still in use, although it requires an experienced operator. Automatic classification designates the process in which the acoustic data is analysed without the need for any human. As previously described it can either be supervised or unsupervised.

The classification methodologies can also be separated between “top-down” and “bottom-up” approaches (Fig. 3.1). The top-down method first clusters the acoustic data into areas of similar patterns, which are then confirmed using ground-truthing datasets (video or samples). The bottom-up methodology gives greater weight to the *in-situ* information as the seabed is first described using direct observations. A statistical relationship between the ground-truthing dataset and the acoustic map is then developed (Rooper & Zimmermann, 2007).

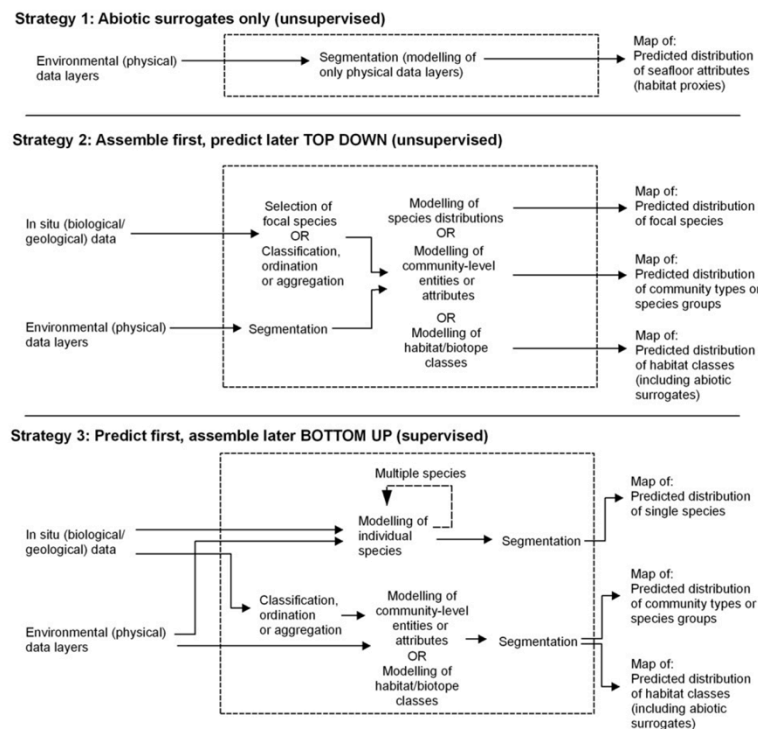


Figure 3.1: Strategies for the production of benthic habitat maps (Source: (Brown et al., 2011))

3.3. ACOUSTIC SEABED MAPPING TECHNIQUES

The most common acoustic devices utilised for seabed mapping can be classified in the following categories: ground-discriminating single-beam echosounders (AGDS), sidescan sonars (SSS), multibeam echosounders (MBES), and sub-bottom profilers (Kenny et al., 2003). Sub-bottom profilers allow for a high-definition of the substrate stratification, but will not be discussed further in this thesis as the research is only focused on surficial sediment.

3.3.1. Introduction to underwater acoustics

A sound wave consists of a vibration or regular motion of an elastic substance transmitted through a solid, liquid or gas. It is considered as a pressure change in the environment and propagates from a source in a given direction. A sound wave can also be represented as mechanical energy in the form of kinetic energy of the particles in motion. A sound wave can be characterized by its frequency, wavelength, period, amplitude, intensity, velocity and direction. Depending on the environment of propagation, the sound velocity will vary from about 340 m/s in air to about 1500 m/s in sea water (Bisquay, 2006).

The propagation of a sound wave in seawater consists of a succession of compressions and rarefactions of the water. Sound velocity in seawater varies from 1450 to 1550 m/s depending on the temperature, salinity and pressure. As the absorption of sound is weak, viscosity represents the main cause of attenuation at frequencies greater than 100 kHz. A boundary between two dissimilar propagation mediums (normally due to density differences) can induce a reflection and refraction of parts of the energy. The sound wave reflection consists in the return of all or part of the initial sound energy as it can either be reflected or dissipated. The sea bottom acts as a sound reflector and will have a varying influence on the acoustic signal depending on numerous parameters inherent to the signal itself (frequency, pulse length, source level, beam pattern), the geometry between the acoustic source and the seabed (incident angle, surface covered) or the geoacoustic properties of the seafloor (roughness, impedance,

heterogeneity) (Schimel, Healy, McComb, & Immenga, 2010). A hard and uniform seabed will induce a better sound reflection than a soft and disorganized facies (Buckingham, 2000). As different materials present different acoustic impedances and reflection coefficients, we can acoustically distinguish between the types of sea bottom (i.e. rock, sand, mud) (Anderson et al., 2007).

3.3.2. Sidescan Sonars

A sidescan sonar is an acoustic device usually installed on a fish towed near the seafloor (Lurton, 2002). The beams are emitted by two side transducers and present a very narrow horizontal (along-track) directivity ($<1^\circ$) and very wide aperture across-track (Fig. 3.2). These characteristics allow for a very good definition of the seabed irregularities due to a greater grazing angle. The backscatter reflected towards the transducer is recorded for each time step as a trace of reflectivity amplitudes. These time-series traces are stacked and allow for the creation of a “scan” of the seabed in the form of a waterfall display. The intensity of the return echo provides information on the nature of the seafloor, while the projected acoustic shadows reflect the actual size of the irregularity on the seabed. The overlapping survey lines are then combined and geo-referenced in the form of a “mosaic”

The sidescan sonar is often used as a complement to multibeam echosounder or sub-bottom profiler systems. Sidescan imagery is often the main source of acoustic seabed classification, although it relies on the interpretation made by experienced geophysicists of the mosaic of acoustic intensity reflecting the nature of the seabed surface (Blondel, Parson, Robigou, & Ieee, 1998). The classification consists of the aggregation of areas of similar acoustic signature corresponding to a type of facies. The sediment type is then usually confirmed by grab samples, although the identification of small-scale features such as sand-waves provides a good clue as to the expected seabed.

Sidescan sonars are limited to a flat-bottom assumption, and have problems with complex rough bathymetry. In fact, they cannot interpret the incident backscatter signal in order to obtain an estimate of the bathymetry. A new generation of

interferometric sonars, which measure the bathymetry, compensates for the limitations due to the lack of bottom topography information.

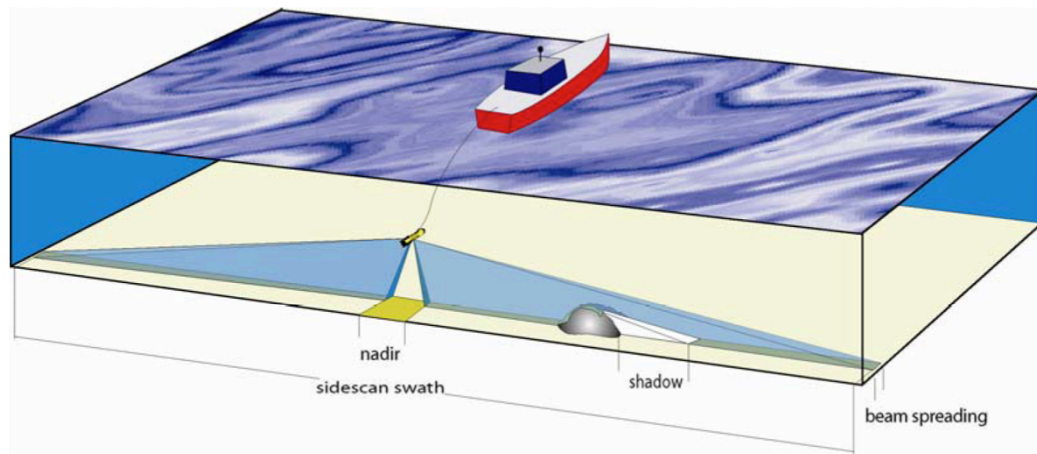


Figure 3.2: Beam pattern of a sidescan sonar (Source: (Penrose et al., 2005))

3.3.3. Single-beam echosounders

Single-beam echosounders (SBES) were the first type of acoustic systems developed in the early 1920s and are still widely used as a primary source to measure water depth (Lurton, 2002). One large pulse of sound is sent downwards at a particular frequency (30-200 kHz), reflects off the seabed and is recorded by the transducer (Penrose et al., 2005). The time of return provides information on the water depth provided the speed of sound is known.

The shape of the reflected acoustic signal or echo provides two types of useful information for bottom classification. The magnitude of the first-order echo trailing portion (E1 in Fig. 3.3) provides an estimate of the roughness of the seabed, which is dependent on the topography, grain size, and seabed attenuation. The second-order echo return (E2 in Fig. 3.3) gives an idea of the hardness, as it is the result of complex scattering of the sound pulse by the sea surface and the seabed (Anderson et al., 2007).

Numerous classification systems exist that rely solely on a broad interpretation of these two parameters only. Other systems, like QTCView, are more focussed as they extract a number of features from the first echo and select the few most

relevant through a statistical test (Principal Component Analysis). This type of system offers the advantages of being an off-the-shelf solution that offers the possibility of a supervised or unsupervised classification at a lower price compared to a multibeam system. However, they offer a poor resolution and a small coverage that requires spatial interpolation to provide a regional coverage (Schimel, Healy, et al., 2010).

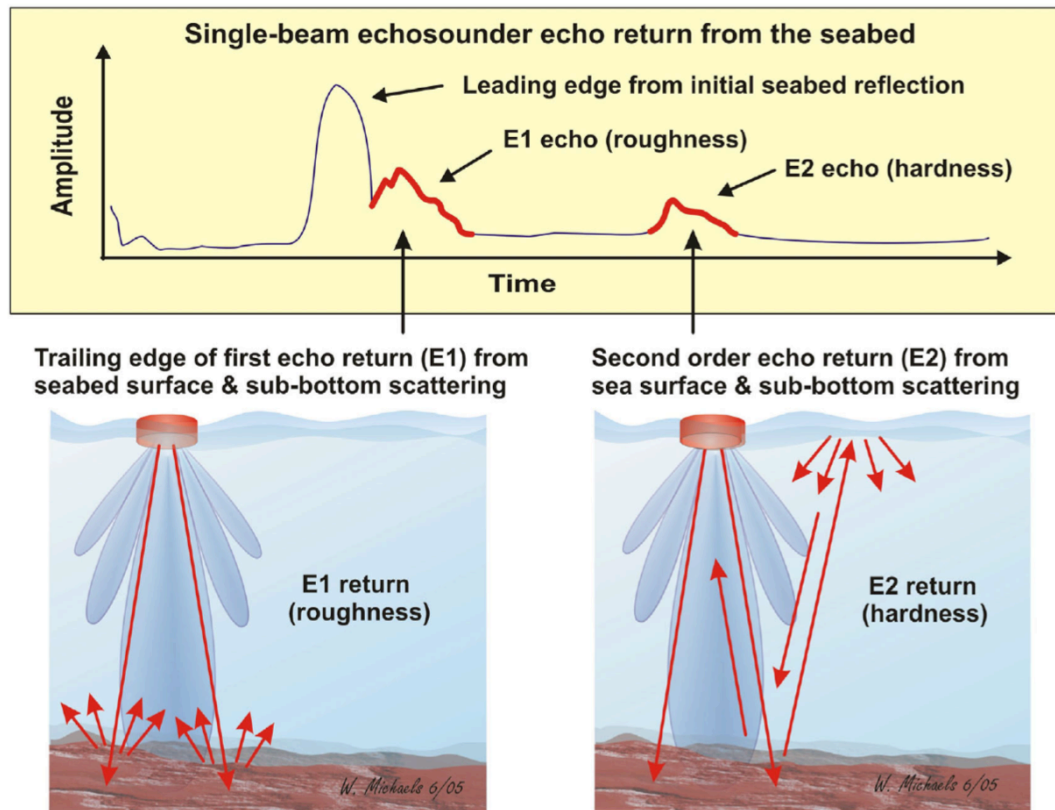


Figure 3.3: Single-beam echosounder for seabed interpretation (Source: (Anderson et al., 2007))

3.3.4. Multibeam echosounders

Since their introduction in 1977, the multibeam echosounders (MBES) have proven to be powerful seabed-modelling tool designed to provide both bathymetric information and backscatter intensity for mapping and classification uses. The MBES are an evolution of the single-beam echosounders, where the single vertical beam is replaced by a wide fan of narrow individual beams ($1-3^\circ$) across the ship's track (Fig. 3.4), providing a large area of ensonification (Lurton, 2002). In the late 1980s, a new generation of digital MBES introduced the possibility to record the reflectivity (intensity of backscattered acoustic energy)

from the seafloor (De Moustier, 1986). The latest developments in computer technology, processing capabilities, data storage and positioning have added the extra possibility to now record data from the water column similar to Acoustic Doppler Current Profilers (ADCPs).

3.3.4.1. Bathymetry measurement by MBES

Even though it is the primary purpose of a multibeam echosounder, the measurement of water depth is of limited interest in the case of a sediment facies study, but it is a strong environmental indicator for studies concerning benthic or pelagic habitats.

A MBES collects bathymetric information using n beams measuring the water depth in n different directions, perpendicular to the vessel track (Fig. 3.4). Multiple transducers are used in order to achieve a suitable pulse frequency and swath coverage (Eve, 2008). A major benefit of using a MBES system is the complete coverage of the area of interest, as it typically ensonifies 8-10 times the water depth. The beam angular opening determining the range of ensonification is usually 120-150° and is defined as:

$$R = P \tan \theta_M \quad (1)$$

With P being the water depth and θ_M the angular opening (Bisquay, 2006).

High resolution is another advantage of the MBES and is governed by the individual aperture of each beam. It allows for the study of small-scale spatial variations and bathymetry derivatives such as slope or roughness that can be implemented in an Acoustic Seabed Classification.

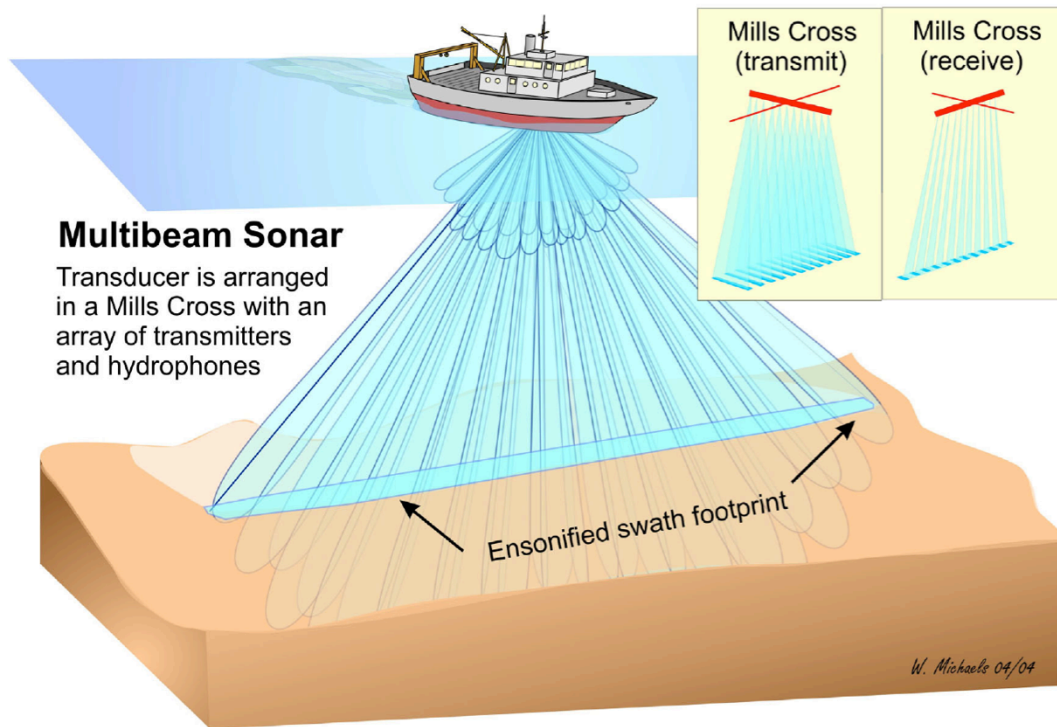


Figure 3.4: Multibeam echosounder principle (Source: (Anderson et al., 2007))

3.3.4.2. Backscatter and mosaic

The seabed sampled by a MBES can be characterized by its geoacoustic properties such as grain size, roughness, sound speed and porosity (Brown & Blondel, 2009). These variables can be determined through indirect measures from the backscatter and their comparison to theoretical models (Fonseca & Mayer, 2007). The backscatter is the result of the scattering of the acoustic pulse from the transducer as it reaches the seabed, which results in a portion of the reflected signal being picked up by the transducer. The reflectivity value, representing the seabed's reflectivity, is obtained by the amplitude of the return signal and covers a wide array of incident angles. It is typically higher on hard substrate, such as rocks, and weaker on a soft sediment such as silt.

The backscatter data can come in three forms: one average backscatter value per beam, one time series of average backscatter around each beam or a time series of intensities for each beam centred on the bottom detect (Beaudoin, Hughes Clarke, Van Den Aemele, & Gardner, 2002). The backscatter strength (BTS) measured in decibels (dB) can be seen in the sonar equation (Lurton, 2002):

$$SN = SL - 2TL - NL + BTS + DI \quad (2)$$

Where SN is the signal to noise ratio, SL the source level, TL the transmission loss, NL the noise level, BTS the bottom target strength (backscatter) and DI the directivity index (all values are expressed in dB).

The echo level EL represents the detected backscatter strength; the part of initial energy that is reflected back to the source. It depends on the source level SL, the transmission loss LS and the bottom target strength BTS:

$$EL = SL - 2TL + BTS \quad (3)$$

A MBES mosaic represents the variations of backscatter strength in the spatial domain. However, a MBES backscatter mosaic differs from a SSS mosaic in various aspects. As the MBES source is not located close to the seabed but on surface, the shadowing effect is very limited and does not allow identification of small-scale morphological features such as sand waves. Also, the nature of the angular response from a MBES induces a strong banding effect on the mosaic (Schimel, Healy, et al., 2010). Finally, the distance of the MBES sonar from the seabed results in a lower image resolution than the SSS mosaic. The impact of the last two differences have recently been reduced as the resolution of the MBES images is in constant enhancement, due to developments such as techniques to reduce the banding effect. The growing interest in MBES imagery is easily explained by the fact that the backscatter is co-registered with the bathymetry, allowing a morphological study to be easily combined with a digital terrain analysis.

3.3.4.3. Angular Response

The alternative to the creation of a MBES backscatter mosaic for texture analysis is to work in the angular response (AR) space that represents the acoustic signature of the various seafloor types through the whole width of incident angles. This method results from the intrinsic influence the angle in incidence on the seafloor has on the backscatter strength, leading to an unfortunate banding effect during the creation of a MBES mosaic (Fig. 3.5). Numerous techniques have been developed that extract several parameters from stacks of consecutive pings and compare them to mathematical models in order to characterize the seabed (Brown

et al., 2011; Fonseca, Brown, Calder, Mayer, & Rzhanov, 2009; Fonseca & Mayer, 2007; J. Hughes Clarke, 1994; Rzhanov, Fonseca, & Mayer, 2012). The methods of analysis of the angular response will be further developed in Section 3.4.3.

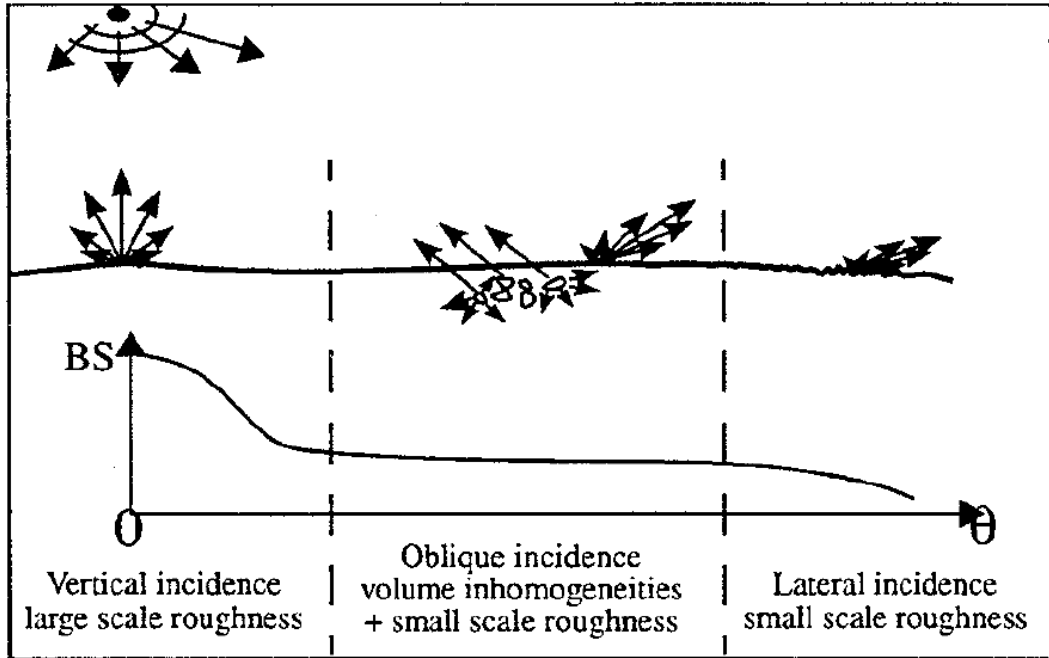


Figure 3.5: Principle of the angular dependence of reflected energy (Source: (Dugelay, Graffigne, & Augustin, 1996))

3.4. CLASSIFICATION METHODS AND ALGORITHMS

3.4.1. Introduction

As previously discussed, acoustic classification methodologies can be separated into two main approaches: image-based analysis; or angular response analysis. The first one involves the compensation of the angular dependency of the backscatter strength, while the second one uses the angular response's dependence on the seafloor geoaoustic properties (Augustin et al., 1996; Fonseca et al., 2009; Hughes Clarke, Danforth, & Valentine, 1997; McGonigle, Brown, Quinn, & Grabowski, 2009; Parnum, 2007; Preston, 2009). The physical parameters governing the interaction between an acoustic signal and the scattering surface are well known. The grey scale patterns of sonar mosaics have allowed successful identifications of the seabed characteristics, but the process of mosaicking acoustic data also induces a resolution problem. Indeed, simplifying the mosaic grey levels and their association to individual sediment classes means ignoring the other parameters affecting the acoustic response of the seabed such as: acoustic impedance, slope and roughness (Anderson et al., 2007; Fonseca et al., 2009). Therefore, two types of methods have been developed that aim for a better use of the backscatter data. The texture analysis of sonar data focuses on the extraction of statistical properties of the pixel in the mosaic. The second methodology works on the acoustic signal itself, and particularly on the angular signature of the seabed, dependent on the type of homogeneous seafloor.

3.4.2. Image-based and Texture Analysis

Textural analysis of MBES mosaics has been largely developed in the past as it is very similar to the techniques used for the sidescan sonar data processing. This method requires compensating for the angular dependence of the backscatter before the implementation of statistical tools on the mosaic image. This type of image-based processing can be assimilated by other remote-sensing imagery techniques involving texture analysis and clustering, mainly derived from either roughness or contrast. As for signal-based methods, various approaches exist for the seabed characterization based on the MBES mosaic.

The most common method to classify sonar imagery is the evaluation of the mosaic based on Grey Level Co-occurrence Matrices (GLCMs) (Blondel & Gomez Sichi, 2009; Blondel et al., 1998). This technique summarizes the textural statistics between each pixel and its neighbours and represents the backscatter amplitude variation over a selected distance and direction within a chosen image patch (Anderson et al., 2007).

Other types of methodologies used for mosaic classification include neural network (Marsh & Brown, 2009; Stewart, Jiang, & Marra, 1994), fractal analysis (Carmichael, Linnett, Clarke, & Calder, 1996), wavelet analysis (Atallah, Smith, & Bates, 2002) or Fourier transforms (Pace & Gao, 1988). These various methods have in common that they attempt to recreate the principles involved in image recognition by the human eye.

3.4.3. Angular Response Analysis

As previously discussed, the backscatter intensity is dependent on the grazing angle, as defined by the Angular Response (AR) of the seabed to an acoustic pulse. The seabed characterization procedures based on the AR can either describe its shape through empirical parameters (J. Hughes Clarke, 1994), or compare it to a geoacoustic model (Fonseca et al., 2009). The empirical approach focuses on the relative difference in the angular response for various seafloor types. Hughes Clark (1994) managed to extract 10 of these features (mean, slope...) from the

angular response curves that were relevant for seabed characterization. The advantage of the empirical approach is that the clustering does not require any information on the seabed characteristics as the areas of similar angular response are compared to each other. However, ground-truthing data is necessary after the segmentation process in order to characterize the classes obtained.

The second approach compares the average AR to a mathematical model based on the theoretical geoacoustic properties of the seafloor, in order to characterize the seabed (Fonseca et al., 2009). The model-based method requires minimal ground-truthing information, as an inversion of the model is usually performed that trains the model predictions with *in-situ* data. In practice, the existing high frequency scattering models do not cover the whole range of possible seabed types, making the empirical method more preferable (Hamilton & Parnum, 2010). Also, the model-based method requires compensating for the beam-pattern, supposedly calibrated by the sonar manufacturers and built in the sonar itself (Díaz, 2000). This compensation is achieved by finding a uniformly hard seabed that will present a clean Lambertian response (ie. follows Lambert's Law), calculating the difference between the obtained angular response and the model, and then applying this corrected beam-pattern to the rest of the dataset.

3.4.4. Geocoder

Geocoder is a tool developed to produce and visualize perfect backscatter mosaics and to provide seabed characterization based on multibeam echosounder acoustic signal. It was developed by Luciano Fonseca from the University of New Hampshire (Fonseca & Calder, 2005) and is now incorporated in various survey or multibeam processing software packages (Caris, Hypack and IVS Fledermaus). The Angular Range Analysis (ARA) allows for sediment characterization without the need for ground-truth data, while the mosaic creation requires a certain number of corrections to be made on the backscatter signal.

3.4.4.1. Mosaic Creation and Acoustic Signal Corrections

In order to produce a “pretty” and accurate mosaic of the seafloor to be used for

target detection or texture analysis, several corrections have to be performed on the backscatter data. Various geometric and radiometric corrections aim at compensating for distortions between data acquired close to the sonar and data from the outer range. The slant-range correction consists of the removal of the water column emission-reception time for re-referencing of backscatter data in the horizontal range instead of the time space where it is recorded. The speckle noise created during MBES data acquisition is removed by applying a median filter with a percentile threshold that reduces the backscatter values to a common scale between the different acquisition lines (Fonseca & Calder, 2005). The aliasing effect due to the low resolution of the mosaic compared to the high resolution of the sonar sampling is resolved in Geocoder by applying an anti-aliasing filter. The data redundancy created by overlapping survey lines is solved by smoothing the seam artefact between two lines in a method called “feathering” that compares the redundant pixels’ respective quality factors (Rzhanov, Linnett, & Forbes, 2000).

3.4.4.2. Angular Range Analysis and model inversion

As previously developed, Angular Range Analysis offers the possibility to characterize the seafloor depending on the AR of the backscatter signal. Geocoder works on the acoustic return (angle and variation of the backscatter strength) to compare it to a geoacoustic model based on the Biot equations, the Lambert’s Law or the Hamilton Relations describing the sediment acoustic behaviour (Fonseca & Mayer, 2007).

The AR curves from each side of the track are averaged over stacks of consecutive pings, creating “seafloor patches”(Fonseca & Calder, 2005). The benefit of this process is to remove the noise from the time angular series although it reduces the ARA spatial resolution accordingly. The Angular Range Analysis divides the AR into grazing angle ranges called near, far and outer ranges (Fig. 3.6). The near range of the angular signature is processed first with the computing of “ARA parameters” which are the slope (representative of the roughness) and the intercept (representative of the impedance).

A model based on interface and volume scattering (Ivakin, 1998) is compared to

the AR after the correction for geometric and radiometric biases have been performed. Interface scattering happens when the water-sediment interface acts as a reflector and scatterer of the acoustic pulse, while volume scattering is the result of a fraction of the source pulse penetrating inside the seafloor and scattering through the heterogeneities in the structure (Fonseca & Mayer, 2007). The Geocoder model uses several parameters such as: sound speed ratio, density ratio, loss parameter, porosity, permeability, tortuosity (complexity), exponent of bottom relief and volume scattering parameter (Fonseca & Mayer, 2007). However, Fonseca and Mayer (2007) acknowledge that the most important controlling the model are the acoustic impedance, the seafloor roughness and the volume heterogeneities (Fonseca, Mayer, Orange, & Driscoll, 2002).

The inversion phase is the ultimate goal for Angular Range Analysis as it provides an estimate of acoustic impedance, roughness and mean grain-size for the whole ensonified area based on the comparison between the ARA model (Fig. 3.7) and the ground-truthing data. It is done by adjusting the near-slope, near-intercept, far-intercept, far-slope and orthogonal distance between the model and the observations (*in-situ* data) (Fonseca et al., 2009).

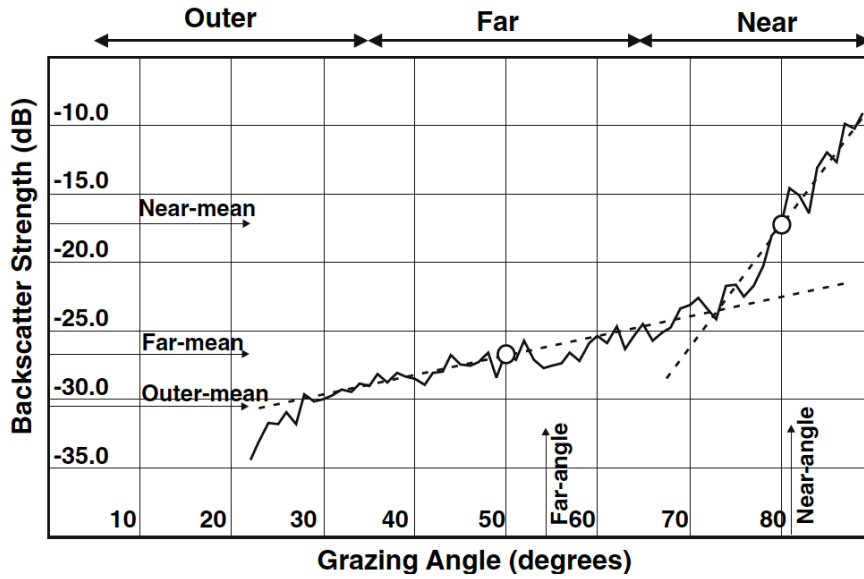


Figure 3.6: Stacked backscatter angular response ranges from one side of an EM3000 multibeam sonar. The dashed lines represent the slope and the white circle the intercept. (Source: (Fonseca & Mayer, 2007))

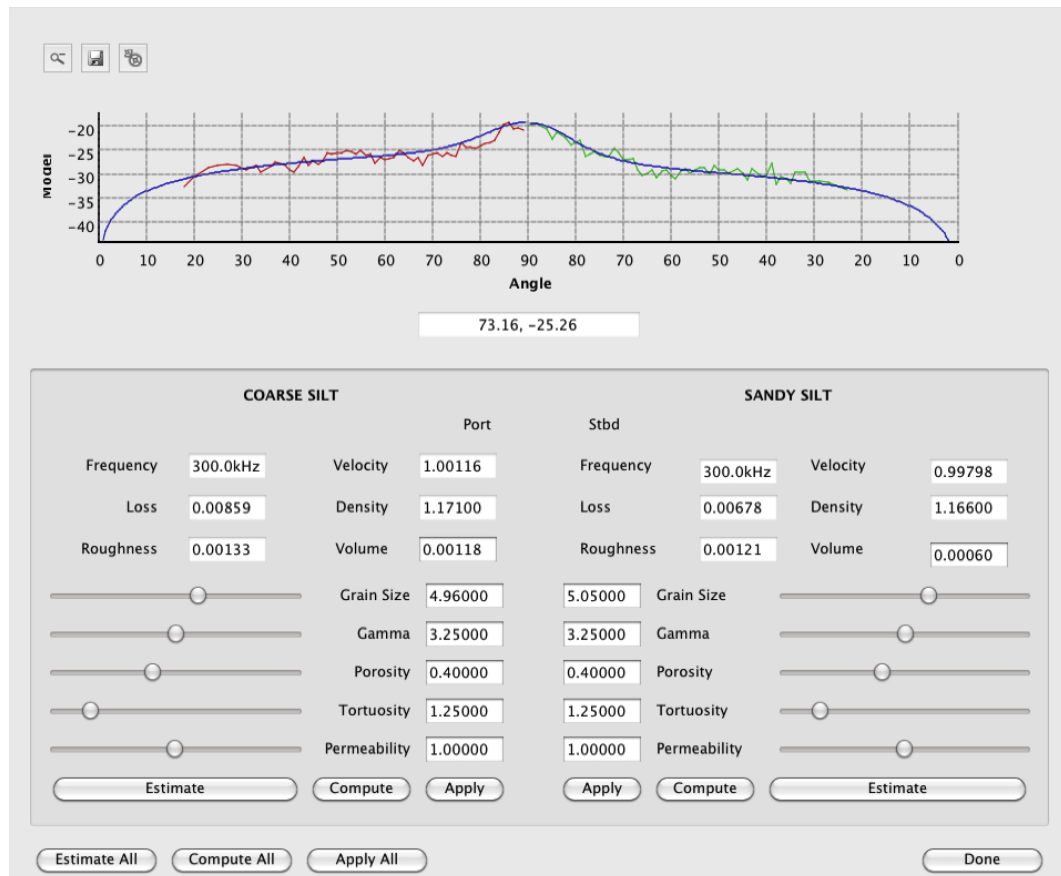


Figure 3.7: Example of model fitting (blue) on the raw time series angular response on portside (red) and starboard (blue) in a version of Geocoder implemented in IVS Fledermaus. The manual modifications of the ARA parameters with ground-truthing data allow the model inversion.

3.4.5. Combined approach

As previously described, two main approaches exist for MBES backscatter analysis, the image-based processing and the angular response methods. They have both been widely judged as valid descriptors of the seabed's physical properties (Hughes Clarke, Mayer, & Wells, 1996). Therefore, as they can show similar results (Brown & Blondel, 2009), the possibility of a combined approach was investigated (Augustin, Dugelay, Lurton, Voisset, & Ieee, 1997). One of these studies introduced the notion of "acoustic themes", which represents a homogeneous manually delineated area of the mosaic for which the average AR would be exported for further Automatic Seabed Classification similar to the Geocoder's patch method. The drawback of this technique is the reliance on a human operator to digitize subjective areas based solely on the grey scale from the mosaic.

Recent work by Rzhанov (2012) introduced a new methodology for combining the spatial and angular variations in an unsupervised segmentation of MBES data. The first stage is the segmentation of the mosaic in areas of homogeneous acoustic aspect. These segments are then compared and aggregated based on their spatial proximity and respective angular response's similarity to facies resulting from a previous coarse segmentation of the mosaic (Fig. 3.8). This approach allows for the creation of larger uniform themes exempt from mosaic artefacts (Schimel, Rzhанov, et al., 2010).

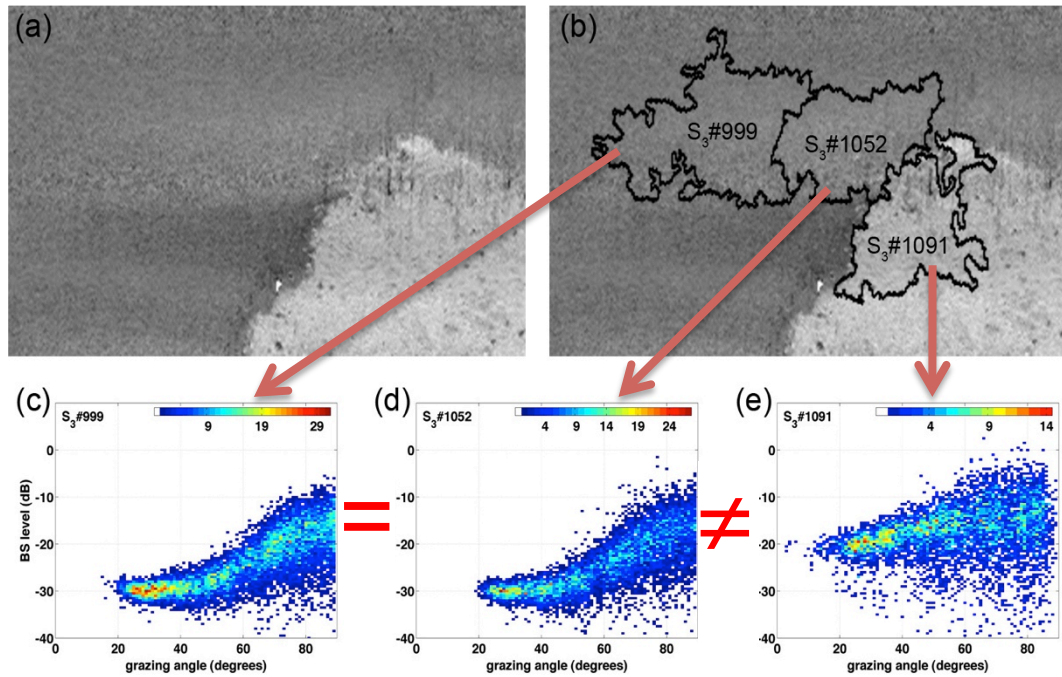


Figure 3.8: Second stage of the unsupervised segmentation based on the angular response, here presented as a histogram instead of a curve. Following this stage, the two segments on the left will be aggregated. Source: (Schimel et al., in preparation)

3.5. CONCLUSION

This study will investigate the combined use of a multibeam echosounder system (Kongsberg-Simrad EM3000) and a sidescan sonar (Starfish 452F). The Chapter 5 will introduce the hydrographic survey undertaken in the Port of Tauranga. The MBES backscatter data will be processed using both angular response based techniques and image-based methods. The SSS reflectivity data will be processed following image-based methodologies in the form of a gray-scale mosaic for comparison. Both supervised, using the ground-truthing results from Chapter 5, and unsupervised classifications techniques will be investigated.

3.6. REFERENCES

- Anderson, J. T., Holliday, D. V., Kloser, R., Reid, D., Simard, Y., Brown, C. J., et al. (2007). *Acoustic seabed classification of marine physical and biological landscapes*: International Council for the Exploration of the Sea.
- Atallah, L., Smith, P. J. P., & Bates, C. R. (2002). Wavelet analysis of bathymetric sidescan sonar data for the classification of seafloor sediments in Hopvagen Bay - Norway. *Marine Geophysical Researches*, 23(5-6), 431-442. 10.1023/b:mari.0000018239.07561.76
- Augustin, J. M., Dugelay, S., Lurton, X., Voisset, M., & Ieee. (1997). *Applications of an image segmentation technique to multibeam echo-sounder data*. New York: I E E E.
- Augustin, J. M., Suave, R., Lurton, X., Voisset, M., Dugelay, S., & Satra, C. (1996). Contribution of the multibeam acoustic imagery to the exploration of the sea-bottom. *Marine Geophysical Research*, 18(2), 459-486. 10.1007/bf00286090
- Beaudoin, J. D., Hughes Clarke, J. E., Van Den Ameele, E. J., & Gardner, J. V. (2002). Geometric and radiometric correction of multibeam backscatter derived from Reson 8101 systems. *Canadian Hydrographic Conference, Toronto, Canada* (pp. 1-22): Canadian Hydrographic Association.
- Begon, M., Harper, J. L., & Townsend, C. R. (1996). *Ecology: Individuals, Populations and Communities*: Blackwell Science.
- Bisquay, H. (2006). Course material for Multibeam Course - Intechmer (
- Blondel, P., & Gomez Sichi, O. (2009). Textural analyses of multibeam sonar imagery from Stanton Banks, Northern Ireland continental shelf. *Applied Acoustics*, 70(10), 1288-1297.
- Blondel, P., Parson, L. M., Robigou, V., & Ieee. (1998). *TexAn: Textural analysis of sidescan sonar imagery and generic seafloor characterisation*. New York: Ieee.
- Brown, C. J., & Blondel, P. (2009). Developments in the application of multibeam sonar backscatter for seafloor habitat mapping. *Applied Acoustics*, 70(10), 1242-1247.
- Brown, C. J., Smith, S. J., Lawton, P., & Anderson, J. T. (2011). Benthic habitat mapping: A review of progress towards improved understanding of the spatial ecology of the seafloor using acoustic techniques. *Estuarine, Coastal and Shelf Science, In Press, Corrected Proof*
- Buckingham, M. J. (2000). Wave propagation, stress relaxation, and grain-to-grain shearing in saturated, unconsolidated marine sediments. *The Journal of the Acoustical Society of America*, 108(6), 2796-2815.

- Carmichael, D. R., Linnett, L. M., Clarke, S. J., & Calder, B. R. (1996). Seabed classification through multifractal analysis of sidescan sonar imagery. *IEE Proceedings: Radar, Sonar and Navigation*, 143(3), 140-147.
- De Moustier, C. (1986). Beyond bathymetry: mapping acoustic backscattering from the deep seafloor with Sea Beam. *Journal - Acoustical Society of America*, 79(2), 316-331.
- Díaz, J. V. M. (2000). *Analysis of Multibeam Sonar Data for the Characterization of Seafloor Habitats*. The University of New Brunswick.
- Diaz, R. J., Solan, M., & Valente, R. M. (2004). A review of approaches for classifying benthic habitats and evaluating habitat quality. *Journal of Environmental Management*, 73(3), 165-181. 10.1016/j.jenvman.2004.06.004
- Dugelay, S., Graffigne, C., & Augustin, J. (1996). *Segmentation of Multibeam Acoustic Imagery in the Exploration of the Deep Sea-Bottom*. Paper presented at the Proceedings of the 13th International Conference on Pattern Recognition - Volume 2,
- Eve, D. (2008). *Comparison of the Simrad EM3002 backscatter data processed in Geocoder with grab sample data from Plymouth Sound and data processed in QTC Multiview*. University of Plymouth.
- Fonseca, L., Brown, C., Calder, B., Mayer, L., & Rzhano, Y. (2009). Angular range analysis of acoustic themes from Stanton Banks Ireland: A link between visual interpretation and multibeam echosounder angular signatures. *Applied Acoustics*, 70(10), 1298-1304.
- Fonseca, L., & Calder, B. R. (2005). Geocoder: An Efficient Backscatter Map Constructor *U.S. Hydrographic Conference* (San Diego, CA.:
- Fonseca, L., & Mayer, L. (2007). Remote estimation of surficial seafloor properties through the application Angular Range Analysis to multibeam sonar data. *Marine Geophysical Researches*, 28(2), 119-126. 10.1007/s11001-007-9019-4
- Fonseca, L., Mayer, L., Orange, D., & Driscoll, N. (2002). The high-frequency backscattering angular response of gassy sediments: Model/data comparison from the Eel River Margin, California. *Journal of the Acoustical Society of America*, 111(6), 2621-2631. 10.1121/1.1471911
- Hamilton, L. J., & Parnum, I. (2010). Acoustic seabed segmentation from direct statistical clustering of entire multibeam sonar backscatter curves. *Continental Shelf Research*, 31(2), 138-148.
- Hughes Clarke, J. (1994). Toward remote seafloor classification using the angular response of acoustic backscattering, a case study from multiple overlapping Gloria data. *Ieee Journal of Oceanic Engineering*, 19(1), 112-127.
- Hughes Clarke, J. (1994). Toward remote seafloor classification using the angular response of acoustic backscattering: a case study from multiple overlapping GLORIA data. *IEEE Journal of Oceanic Engineering*, 19(1), 112-127.

- Hughes Clarke, J., Mayer, L. A., & Wells, D. E. (1996). Shallow-water imaging multibeam sonars: A new tool for investigating seafloor processes in the coastal zone and on the continental shelf. *Marine Geophysical Researches*, 18(6), 607-629.
- Hughes Clarke, J. E., Danforth, B. W., & Valentine, P. (1997). Areal Seabed Classification using Backscatter Angular Response at 95kHz. In N. S. U. R. Centre (Ed.), *High Frequency Acoustics in Shallow Water* (p. 9). Lerici, Italy:
- Ivakin, A. N. (1998). A unified approach to volume and roughness scattering. *The Journal of the Acoustical Society of America*, 103(2), 827-837.
- Kenny, A. J., Cato, I., Desprez, M., Fader, G., Schuttenhelm, R. T. E., & Side, J. (2003). An overview of seabed-mapping technologies in the context of marine habitat classification. *Ices Journal of Marine Science*, 60(2), 411-418. 10.1016/s1054-3139(03)00006-7
- Lurton, X. (2002). *An Introduction to Underwater Acoustics: Principles and Applications*: Springer.
- Marsh, I., & Brown, C. (2009). Neural network classification of multibeam backscatter and bathymetry data from Stanton Bank. - 70(- 10), - 1276.
- McGonigle, C., Brown, C., Quinn, R., & Grabowski, J. (2009). Evaluation of image-based multibeam sonar backscatter classification for benthic habitat discrimination and mapping at Stanton Banks, UK. *Estuarine, Coastal and Shelf Science*, 81(3), 423-437.
- Mitchell, S. C. (2005). How useful is the concept of habitat? a critique. *Oikos*, 110(3), 634-638. 10.1111/j.0030-1299.2005.13810.x
- Nafe, J. E., & Drake, C. L. (1963). *Physical properties of marine sediments* (Vol. 3)
- Pace, N. G., & Gao, H. (1988). Swath Seabed Classification. *Ieee Journal of Oceanic Engineering*, 13(3), 83-90.
- Parnum, I. M. (2007). *Benthic Habitat Mapping using Multibeam Sonar Systems*. Curtin University of Technology.
- Penrose, J. D., Siwabessy, P. J. W., Gavrilov, A., Parnum, I., Hamilton, L. J., Brooke, B., et al. (2005). *Acoustic Techniques For Seabed Classification*.
- Preston, J. (2009). Automated acoustic seabed classification of multibeam images of Stanton Banks. *Applied Acoustics*, 70(10), 1277-1287.
- Rooper, C. N., & Zimmermann, M. (2007). A bottom-up methodology for integrating underwater video and acoustic mapping for seafloor substrate classification. *Continental Shelf Research*, 27(7), 947-957.
- Rzhanov, Y., Fonseca, L., & Mayer, L. (2012). Construction of seafloor thematic maps from multibeam acoustic backscatter angular response data. *Computers & Geosciences*, 41(0), 181-187. 10.1016/j.cageo.2011.09.001

- Rzhanov, Y., Linnett, L. M., & Forbes, R. (2000). Underwater video mosaicing for seabed mapping (pp. 224-227):
- Schimel, A. C. G., Healy, T. R., McComb, P., & Immenga, D. (2010). Comparison of a Self-Processed EM3000 Multibeam Echosounder Dataset with a QTC View Habitat Mapping and a Sidescan Sonar Imagery, Tamaki Strait, New Zealand. *Journal of Coastal Research*, 26(4), 714-725. 10.2112/08-1132.1
- Schimel, A. C. G., Rzhanov, Y., Fonseca, L., Mayer, L., Healy, T. R., & Immenga, D. (2010). Automated delineation of acoustic themes from Multibeam backscatter data for seafloor characterization, Tapuae Marine Reserve, NZ *Geohab* (Wellington, NZ):
- Schimel, A. C. G., Rzhanov, Y., Fonseca, L., Mayer, L., Healy, T. R., & Immenga, D. (in preparation). Unsupervised acoustic seabed classification using both angular and spatial information from multibeam backscatter data.
- Stewart, W. K., Jiang, M., & Marra, M. (1994). A neural-network approach to classification of sidescan sonar imagery from a mid-ocean ridge area. *Ieee Journal of Oceanic Engineering*, 19(2), 214-224. 10.1109/48.286644

CHAPTER 4 - SURFICIAL SEDIMENT AND SHELL COVERAGE FOR GROUND-TRUTHING

4.1. INTRODUCTION

As previously discussed, the creation of benthic maps requires the input of observations or ground-truthing data in order to train a data processing model or confirm the unsupervised classification (Anderson et al., 2007). This chapter presents the results of sediment sampling and underwater video surveys undertaken on the 4th and 5th of September 2011. These outputs were then used to help for the classification of the sidescan sonar and multibeam echosounder surveys of the Tauranga Stella Passage, Town Reach and Bridge Marina areas detailed in Chapter 5. At each station, a sediment sample and underwater video footage were obtained to characterize the main sediment type and to assess the shell coverage.

4.2. SEDIMENT SAMPLING

4.2.1. Method

A total of 42 locations (Fig. 4.1), based on a predefined grid with a regular spacing of 150 m, were sampled with a “Petite Ponar” grab with the positioning obtained from a RTK-GPS (accuracy < 0.5 m). The coordinates of the sediment sampling sites are provided in Appendix III. The 14 kg stainless steel grab sampler is designed to obtain a volume of 2.4 l of sediment over an area of 0.15 × 0.15 m² (Wildco, 2012). The grab was light enough to be operated off the Department of Earth and Ocean Sciences survey vessel *Tai Rangahau* by a single person at the stern platform supervising the launching and retrieving, along with a capstan operator (Fig 4.2). All locations were sampled (Appendix IV), although some re-runs had to be performed, as shells would sometimes jam the grab and prevent the jaws closing tight. The sediment textural results are expressed using the Udden-Wentworth sediment classification scale (Table 4.1) in order to allow

comparisons with the results from previous investigations and the grain sizes derived from the Angular Range Analysis in Geocoder. Figures 4.3, 4.4, 4.5 and 4.6 show typical examples of different types of sediment collected during this campaign.



Figure 4.1: Sediment sampling and underwater video locations. (Aerial photo source: Bay of Plenty Regional Council)



Figure 4.2: Sediment sampling setup on the University of Waikato's survey vessel *Tai Rangahau*. The capstan hauling the Ponar grab sampler through the pulley on the davit (visible on top) is located on the left behind the operator.



Figures 4.3, 4.4, 4.5 and 4.6: Examples of sediment samples from the Port of Tauranga. Sites 14 (left) and 23 (right) are shown on the top; 21 (left) and 37 (right) are displayed on the bottom line.

4.2.2. Grain Size Analysis

Before the sediment texture and grain-size were investigated, the samples were treated with at 10% solution of hydrogen peroxide (H_2O_2) to “digest” and remove the organic matter from the sediment. A combination of sieving for the coarse part (sand and gravel) and laser sizing for the finer (mud) part, was chosen in order to describe the full spectrum of grain-sizes found in the work area. For each sample, the volume percentage of clay, silt, sand and gravel was computed, along with the mean grain size. The Rapid Sediment Analyser (RSA) from the University of Waikato, although widely used in numerous studies of the Port of Tauranga (De Lange, 1988; DeLange, Healy, & Darlan, 1997; Healy, 1985), was not chosen as this study is focussed on the presence and density of the shell coverage in the surficial sediment, and the RSA is not suitable for shell-rich samples.

Table 4.1: Udden-Wentworth sediment classification scale in terms of phi units and mm.

Phi Units	Size	Wentworth Size Class	Sediment Name
-8	256 mm	Boulders	GRAVEL
		Cobbles	
-6	64 mm	Pebbles	
-2	4 mm	Granules	
-1	2 mm	Very Coarse Sand	
0	1 mm	Coarse Sand	
1	0.5 mm	Medium Sand	
2	0.250 mm	Fine Sand	
3	0.125 mm	Very Fine Sand	
4	0.062 mm	Silt	MUD
8	0.004 mm	Clay	

4.2.2.1. Dry Sieving

Following the “digestion” procedure, the sediment samples were dried and weighted before being processed using a “Octagon” vibrating column and sieves matching the major divisions of the Udden-Wentworth scale: 2 mm, 1 mm, 500 μm , 250 μm , 125 μm and 63 μm . The mud fraction (<63 μm) was not sieved, as the laser-sizer would investigate this fraction more accurately. However, the fraction <63 μm was recorded, to provide the relative proportions of gravel (i.e. shells), sand and mud.



Figure 4.7: “Octagon” sieve shaker fitted with the 6 different grain sizes sieves.

4.2.2.2. Laser Diffraction

A laser-sizer was used to obtain a better description of the muddy fraction (< 63 μm) of the sediment present in the Tauranga Harbour. A subset of the sediment samples, <2 mm in size due to the requirements of the equipment, was examined with the University of Waikato’s Malvern Mastersizer-S 300RF. This equipment utilizes the scattering (diffraction) of light from a laser and provides the results as “equivalent spherical volumes”. It is important to remember that this analysis did

not account for the presence of gravels in the samples (i.e. shells), but only analysed the sand and mud fractions.

4.2.3. Results and Spatial Variation

The sediment grain size distributions were obtained from both dry sieving ($> 63 \mu\text{m}$) and laser sizing ($< 2\text{mm}$) as previously described. Both sets of results are presented independently, as the sieves provide a measurement of intermediate axis of the grains, while the laser-diffraction method used by the Malvern report the light scattering behaviour of equivalent spherical particles (Nathier-Dufour, Bougeard, Devaux, Bertrand, & Le Deschault de Monredon, 1993).

4.2.3.1. Laser Diffraction

The laser diffraction data (Appendix I) presents the results in terms of sand, silt and clay proportions of the sampled volume. The distribution diagram shows a narrow peak between 0 and 4 Phi units (Fig. 4.8), indicating the sediments were predominantly sand-sized. Although the laser-sizer provided data for the fine fraction composition, these results are unfortunately considered unreliable as further analysis of the results, and discussions with the equipment manufacturer, indicated that the pumping/flushing system of the Malvern MasterSizer was clogged by coarser debris during the investigation. Hence, the results from the laser diffraction analysis were then only used to confirm those provided by dry sieving.

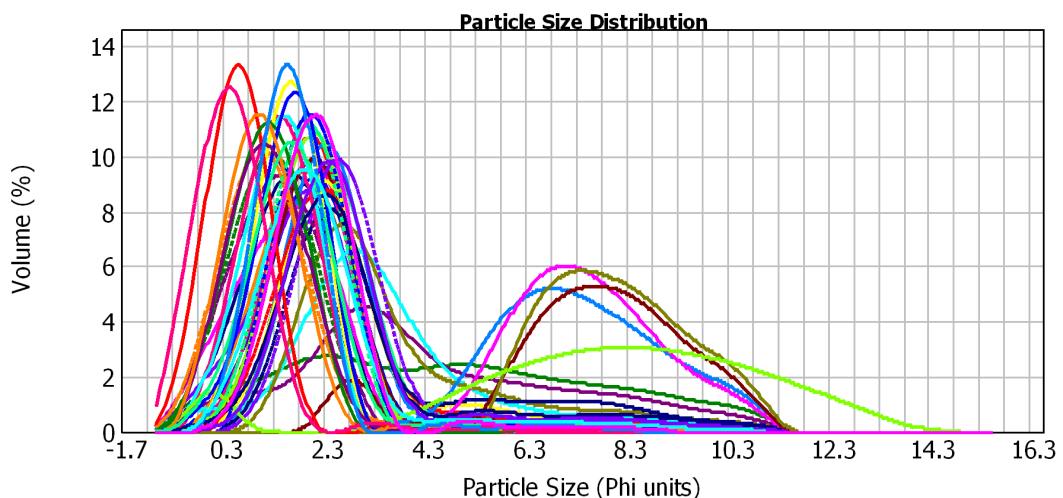


Figure 4.8: Overall laser diffraction particle size distribution of the Tauranga Harbour sediment samples. We can notice the clear dominance of the sand class (Phi values between -1 and 4).

4.2.3.2. Dry Sieving

The goal of this particular investigation was to describe the sand fraction (2-0.063 mm) in size; as the coarser fraction - the shells we are interested in - would be further studied using the video survey. For this reason, the 2mm sieve recorded weights were not accounted for in the description of the samples.

The statistics from the dry sieving were processed using the GRADISTAT software routine written for MS Excel (Blott & Pye, 2001). This package allows for the interpretation of sieve weights and the calculation of mean size, sorting, skewness and various statistics based on the Folk and Ward method. Figure 4.9 below shows the dominance of the fine sand class, followed by medium sand and coarse sand. The silty fine sand and silty very fine sand classes occur twice and once respectively. The frequency distribution (Fig. 4.10) and cumulative frequency (Fig. 4.11) graphs also show the predominance of the fine sand class in the dataset. The spatial distribution of the sediment textural data is presented in Figure 4.12, while the detailed statistical results are summarised in Appendix II.

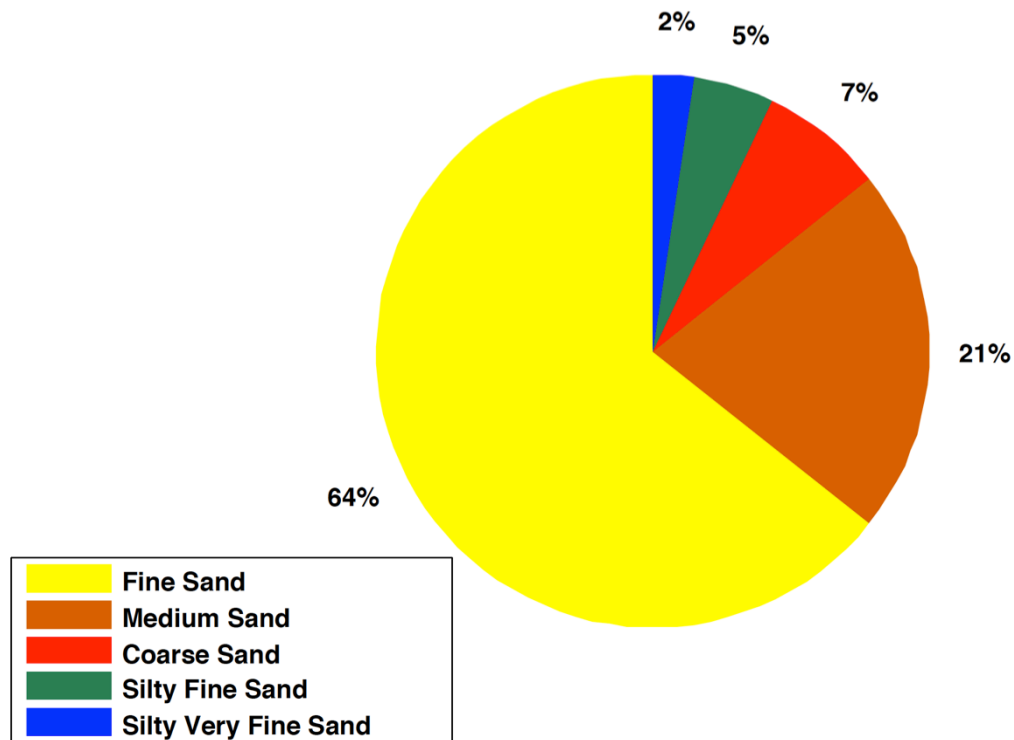


Figure 4.9: Percentage of each sediment class in the combined Tauranga samples.

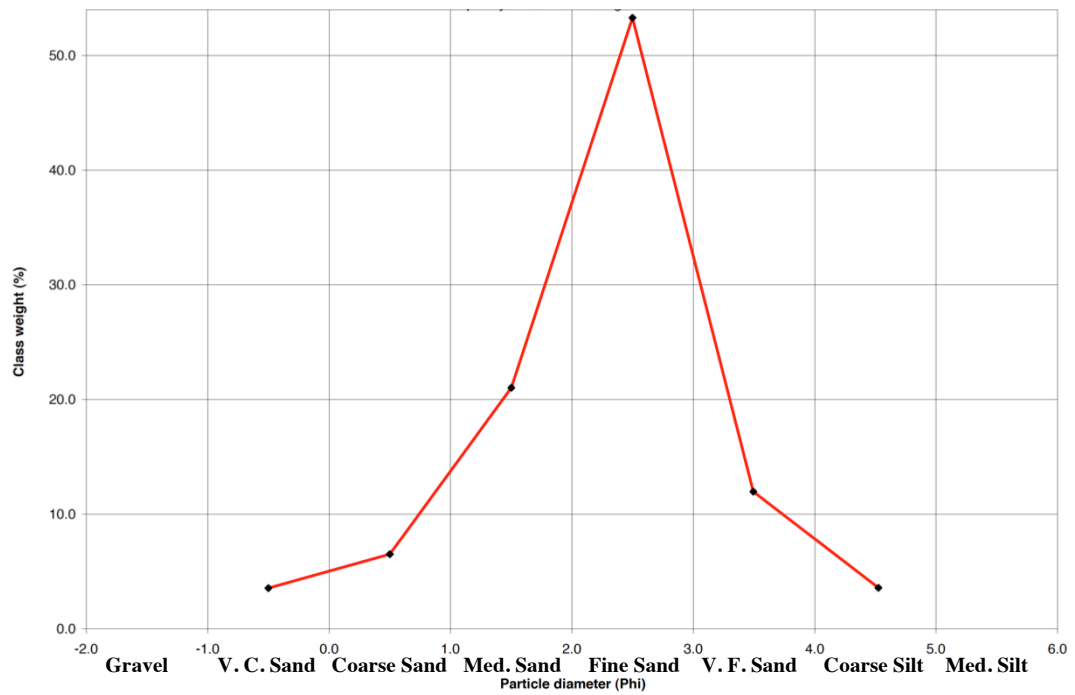


Figure 4.10: Overall frequency distribution histogram of the Tauranga sediment samples obtained from dry sieving, not including the gravel fraction. Note the importance of the fine sand class. (Phi 2 to 3). Graph produced with Gradistat.

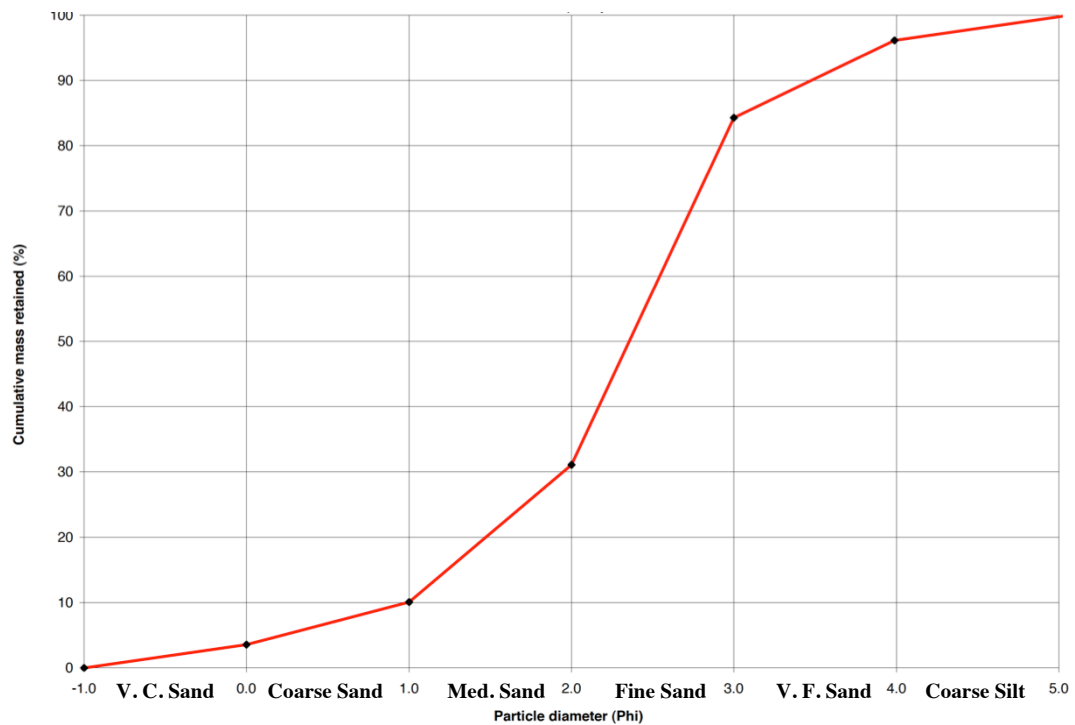


Figure 4.11: Overall cumulative frequency of the Tauranga sediment samples obtained from dry sieving, not including the gravel fraction (> 2 mm). Graph produced with Gradistat.

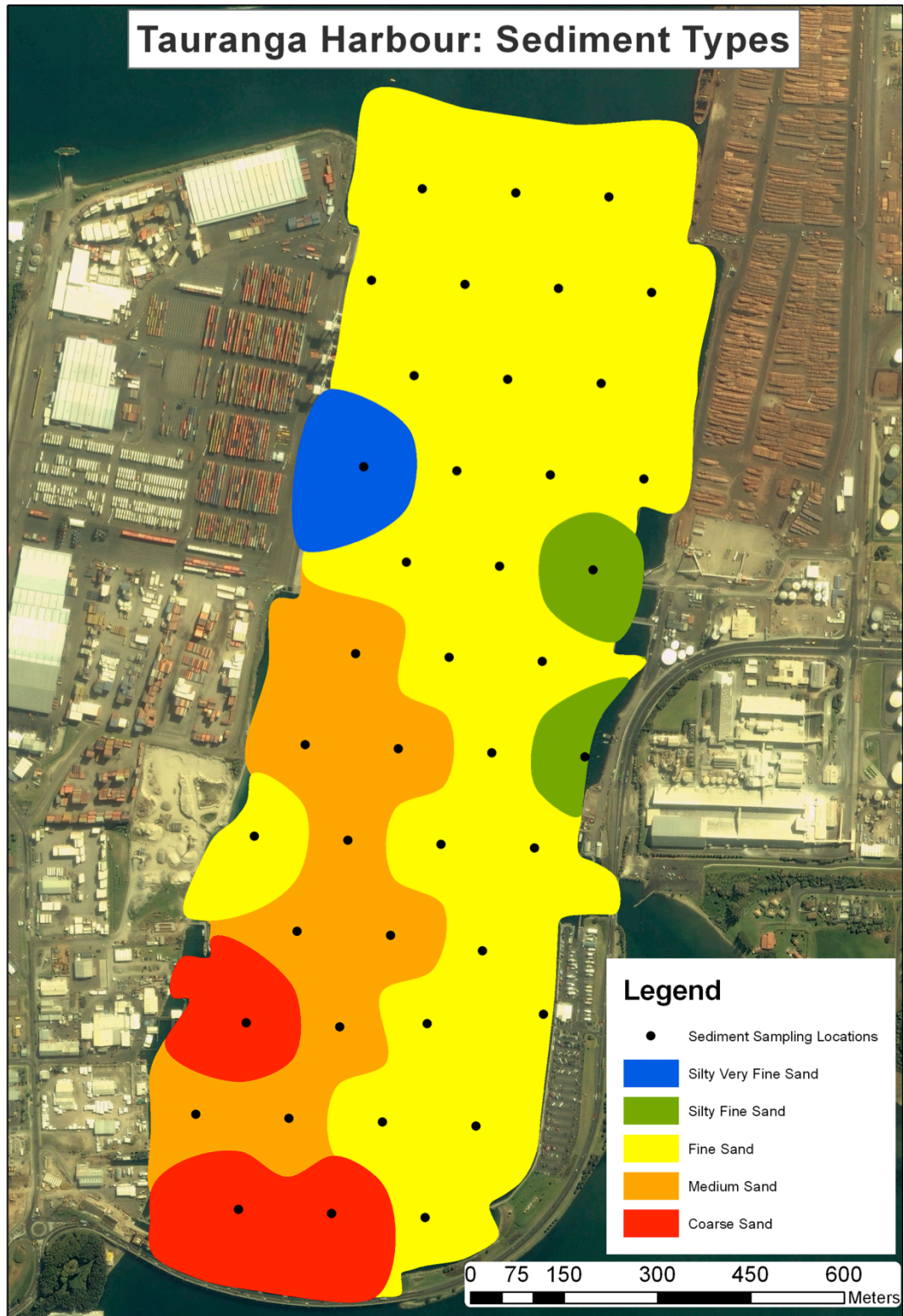


Figure 4.12: Surficial sediment map of the Stella Passage, Town Reach and Bridge Marina areas of Tauranga Harbour derived from grab samples. The colour-coded clusters group similar sampling sites and do not mean to represent the actual sediment class boundaries of the area.

4.3. UNDERWATER VIDEO SURVEY

4.3.1. Method

The surficial shell coverage was determined using underwater video imagery. The waterproof camera was attached to a weighted 50 cm × 50 cm frame and dropped on the same 42 locations as the sediment samples. Positioning was provided by RTK GPS and the video was recorded on surface on a standard video camera. The camera is fitted on the frame, about 70 cm high from the seafloor and looking straight downward. This technique proved very efficient, as the height of the camera above the seabed was ideal to estimate the shell coverage over a representative area.



Figure 4.13: Underwater video camera fitted on the weighted frame (about 50 cm × 50 cm), sitting on the back deck of the University of Waikato survey vessel *Tai Rangahau*.

4.3.2. Shell Coverage

The video footage was examined in order to determine the shell coverage. The coverage values were obtained comparing snapshots of the video with the “charts for estimating mineral grain percentage composition of rocks and Sediments” (Compton, 1962). Four density classes (Fig. 4.14 to 4.17) were chosen in order to be consistent with the studies by Healy (1985) and de Lange (1988):

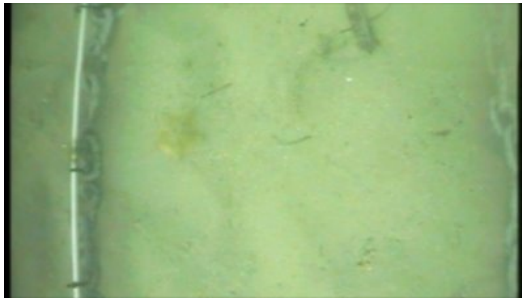


Figure 4.14: Sand: very little or no shells (<20%) at Site 1.

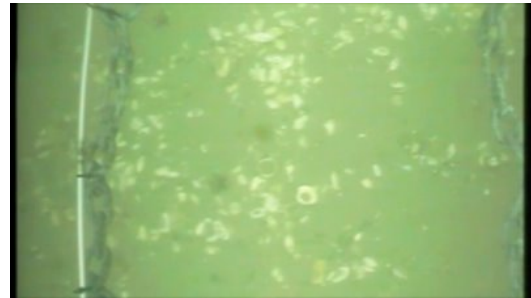


Figure 4.15: Shelly sand (20-50%) at Site 4.



Figure 4.16: Very Shelly Sand (50-80%) at Site 21.



Figure 4.17: Shell Lag (>80%) at Site 40.

The results of this video analysis are displayed in Figure 4.18 and Table 4.3; snapshots are available in Appendix V. The sand facies appears to be dominant in the Stella Passage and Bridge Marina areas, while the shallow Town Reach channel shows a dense shell coverage on its entire length. A large area of shelly sand is also present on the central north Stella Passage.

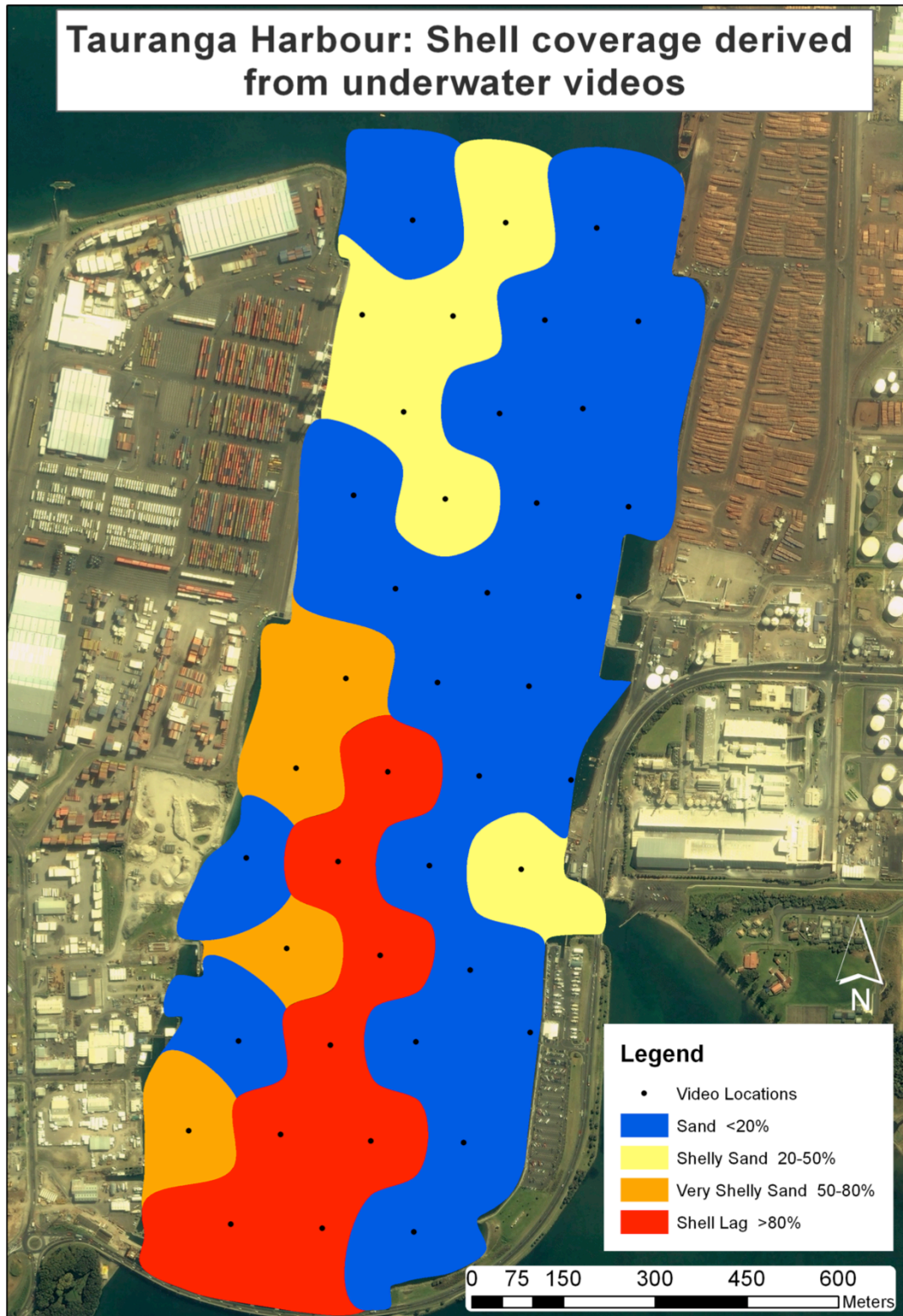


Fig 4.18: Surficial shell coverage derived from underwater video analysis in the Tauranga Harbour. The colour-coded clusters group similar sampling sites and do not represent the actual shell coverage boundaries of the area.

4.3.3. Species identified

The benthic fauna assessment using both videos and sediment samples identified 4 major groups:

- Pipis (*Paphies australis*)
- Turret Shells (*Maoricolpus roseus*)
- Cockles (*Austrovenus stuchburyi*)
- Various starfish species (mainly *Patiriella regularis* and *Astrostole scabra*)

The Table 4.2 provides the details of the results plotted in Figures 4.19 to 4.22. Pipis, the dominant species found by this study, were located in two main areas, the shallow Town Reach Channel and the north-western Stella Passage, and make for the greatest density of the shell lag facies. Pipis equally favour the fine and medium sand substrates. Turret shells were the second most common species, and were generally found in the same areas as the pipis, mostly on a fine sand or medium sand seabed. The cockle's spatial distribution did not show any significant pattern, and they were found both on fine and medium sand areas, but never in large abundance. The various starfish species were mostly encountered on fine sand facies, particularly around the Town Reach steep drop-off to the Stella Passage or around the Bridge Marina, Starfish were always found in large quantities and almost always in areas with no other benthic species.

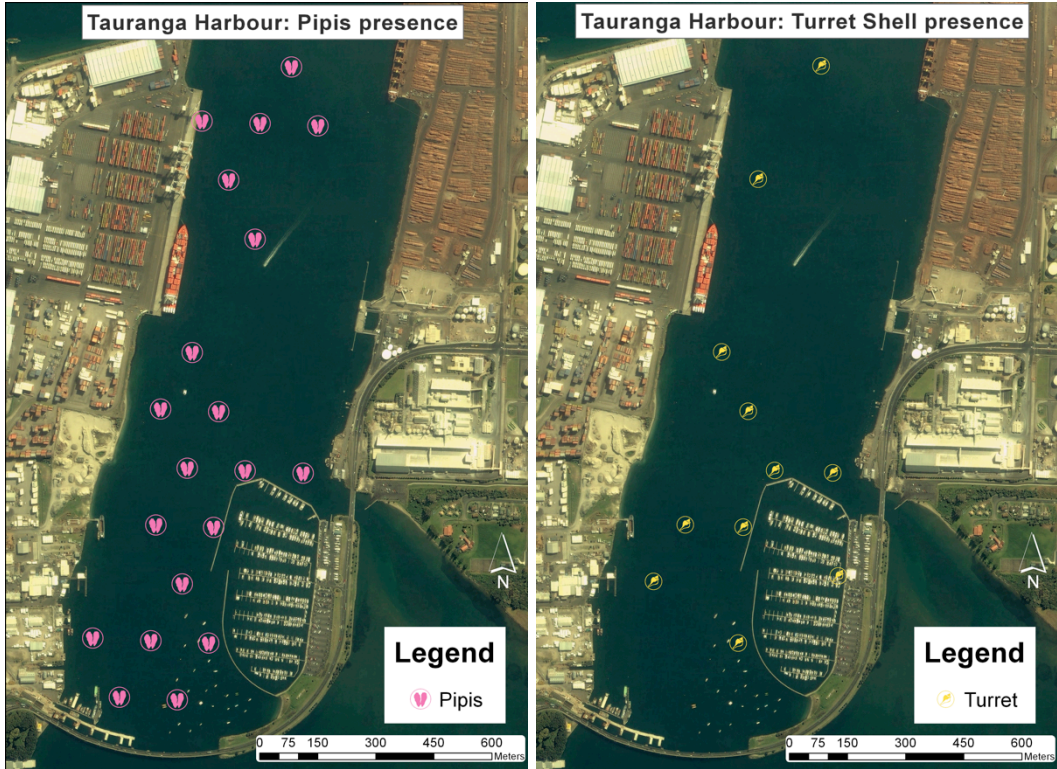


Figure 4.19 & 4.20: Pippi (Left) and turret shell (right) spatial distributions.

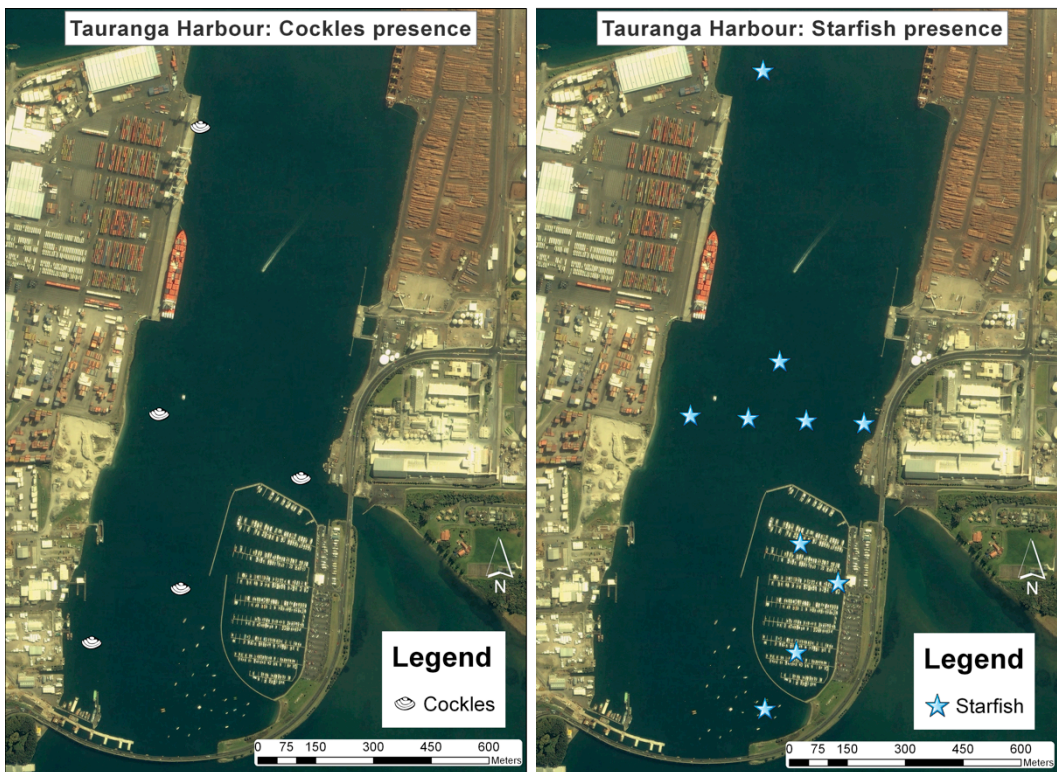


Figure 4.21 & 4.22: Cockle (Left) and starfish (right) spatial distributions.

Table 4.2: Summary of species found in the sediment samples and underwater videos of the Port of Tauranga.

Site	X (NZTM)	Y (NZTM)	Water Depth (m)	Sediment Class	Pipi	Turret Shell	Cockle	Starfish
1	1880197.937	5827259.754	12.91	Fine Sand				X
2	1880347.936	5827253.349	13.39	Fine Sand	X	X		
3	1880497.935	5827246.943	12.93	Fine Sand				
4	1880116.533	5827112.958	14.32	Fine Sand	X		X	
5	1880266.531	5827106.552	13.96	Fine Sand	X			
6	1880416.53	5827100.147	13.10	Fine Sand	X			
7	1880566.529	5827093.742	11.62	Fine Sand				
8	1880185.127	5826959.756	13.79	Fine Sand	X	X		
9	1880335.125	5826953.351	13.08	Fine Sand				
10	1880485.124	5826946.945	13.01	Fine Sand				
11	1880103.722	5826812.961	15.18	Very Fine Sand				
12	1880253.72	5826806.555	13.19	Fine Sand	X			
13	1880403.719	5826800.149	13.40	Fine Sand				
14	1880553.718	5826793.743	8.92	Fine Sand				
15	1880172.315	5826659.759	13.00	Fine Sand				
16	1880322.314	5826653.353	12.94	Fine Sand				
17	1880472.313	5826646.947	13.30	Fine Sand				
18	1880090.91	5826512.964	5.95	Medium Sand	X	X		
19	1880240.908	5826506.557	9.03	Fine Sand				X
20	1880390.907	5826500.151	12.41	Fine Sand				
21	1880009.504	5826366.168	7.08	Medium Sand	X		X	X
22	1880159.503	5826359.762	4.32	Medium Sand	X	X		X
23	1880309.501	5826353.356	5.95	Fine Sand				X
24	1880459.5	5826346.949	4.89	Fine Sand				X
25	1879928.099	5826219.373	4.92	Fine Sand				
26	1880078.097	5826212.967	4.44	Medium Sand	X			
27	1880228.096	5826206.56	2.99	Fine Sand	X	X		
28	1880378.094	5826200.154	6.39	Fine Sand	X	X	X	
29	1879996.691	5826066.172	4.66	Medium Sand	X	X		
30	1880146.69	5826059.765	3.34	Medium Sand	X	X		
31	1880294.572	5826035.366	3.17	Fine Sand				X
32	1879915.285	5825919.377	5.68	Coarse Sand		X		
33	1880065.284	5825912.97	3.84	Medium Sand	X		X	
34	1880205.757	5825918.204	3.04	Fine Sand				
35	1880392.401	5825933.229	3.70	Fine Sand		X		X
36	1879833.879	5825772.582	3.88	Medium Sand	X		X	
37	1879983.877	5825766.175	3.86	Medium Sand	X			
38	1880133.876	5825759.768	3.53	Fine Sand	X	X		
39	1880283.874	5825753.361	2.64	Fine Sand				X
40	1879902.471	5825619.38	5.43	Coarse Sand	X			
41	1880052.469	5825612.973	4.99	Coarse Sand	X			
42	1880202.468	5825606.566	2.52	Fine Sand				X

4.4. SUMMARY

In order to compare the shell coverage results between the underwater videos and the grab samples, both datasets were classified using three density indexes: 0 for no shell or very little; 1 for an equal volume of sand and shell; and 2 for a very dense and shell dominated seabed/sample. A shell density agreement factor was calculated, by subtracting the two density indexes from each other (grab sample index minus video index) for every sample in order to determine the degree of confidence in the results (Table 4.3). A mean result of 0 would mean a full agreement between the video and the grab sample. A mean result of 1 means a light disagreement between both datasets.

A few samples showed a result of 2, meaning a complete disagreement. This can be the result of slight positioning errors, a current drift during the descent of the camera or the grab sampler or the presence of shells below the surface, hidden from the camera. When looking at the locations of the conflicting sites, it appeared that most of them were situated in areas of mixed backscatter reflectivity (Fig. 4.23), which could explain that a positioning bias could have occurred between the sediment sampling and the underwater video. It was decided that the sites with an agreement factor of 2 would not be used for ground-truthing the multibeam echosounder backscatter data. For locations with a factor of 1, the underwater video density would be chosen in preference over the shell coverage from the grab samples as the surficial coverage is the main focus of this study.

This ground-truthing study provided discrete descriptions of both the sediment composition and the surficial shell coverage. The habitat mapping study using sidescan sonar and multibeam echosounder data will interpolate these seabed characteristics between the sampling sites.

Table 4.3: Summary of shell densities and sediment types obtained from both sediment samples and underwater video, expressed on a scale from 0 (no shell) to 2 (dense coverage). The agreement factor is the difference between both indexes and represents the repeatability of the results between both datasets. The shell coverage class column provides a final finer definition of the type of shell density similar to the 1985 study by Healy (1985) and de Lange (1988).

	Video: Shell coverage	Grab Sample: shell presence	Agreement factor	Shell Coverage Class	Sediment Class
1	0	0	0	Rippled Sand	Fine Sand
2	1	2	1	Shelly Sand	Fine Sand
3	0	0	0	Sand	Fine Sand
4	1	1	0	Shelly Sand	Fine Sand
5	1	1	0	Shelly Sand	Fine Sand
6	0	2	2	Sand	Fine Sand
7	0	0	0	Sand	Fine Sand
8	1	1	0	Shelly Sand	Fine Sand
9	0	1	1	Sand	Fine Sand
10	0	0	0	Sand	Fine Sand
11	0	0	0	Sand	Very Fine Sand
12	1	1	0	Shelly Sand	Fine Sand
13	0	0	0	Sand	Fine Sand
14	0	0	0	Sand	Fine Sand
15	0	1	1	Sand	Fine Sand
16	0	0	0	Sand	Fine Sand
17	0	0	0	Sand	Fine Sand
18	2	2	0	Very Shelly Sand	Medium Sand
19	0	0	0	Sand	Fine Sand
20	0	0	0	Sand	Fine Sand
21	2	2	0	Very Shelly Sand	Medium Sand
22	2	2	0	Shell Lag	Medium Sand
23	0	0	0	Sand	Fine Sand
24	0	0	0	Sand	Fine Sand
25	0	0	0	Rippled Sand	Fine Sand
26	2	2	0	Shell Lag	Medium Sand
27	0	2	2	Rippled Sand	Fine Sand
28	1	2	1	Shelly Sand	Fine Sand
29	2	2	0	Very Shelly Sand	Medium Sand
30	2	2	0	Shell Lag	Medium Sand
31	0	0	0	Rippled Sand	Fine Sand
32	0	1	1	Sand	Coarse Sand
33	2	2	0	Shell Lag	Medium Sand
34	0	1	1	Rippled Sand	Fine Sand
35	0	1	1	Sand	Fine Sand
36	1	2	1	Very Shelly Sand	Medium Sand
37	2	2	0	Shell Lag	Medium Sand
38	2	2	0	Shell Lag	Fine Sand
39	0	0	0	Sand	Fine Sand
40	2	2	0	Shell Lag	Coarse Sand
41	2	2	0	Shell Lag	Coarse Sand
42	0	0	0	Sand	Fine Sand

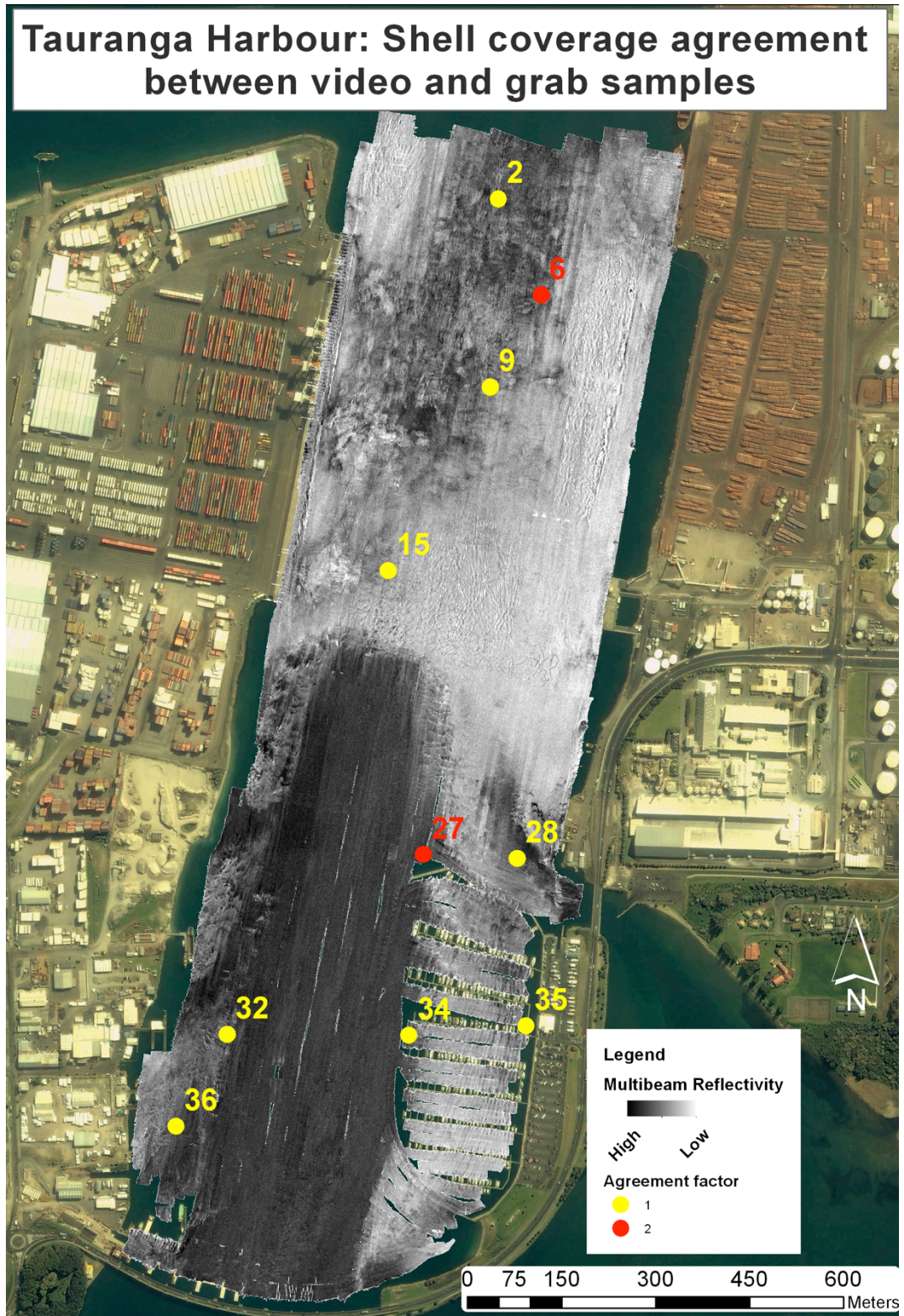


Figure 4.23: Locations of the shell coverage disagreements between the sediment samples and underwater videos. The numbers are the sample location number (Fig. 4.1), and the colours indicate the level of disagreement.

4.5. REFERENCES

- Anderson, J. T., Holliday, D. V., Kloser, R., Reid, D., Simard, Y., Brown, C. J., et al. (2007). *Acoustic seabed classification of marine physical and biological landscapes*: International Council for the Exploration of the Sea.
- Blott, S. J., & Pye, K. (2001). GRADISTAT: A grain size distribution and statistics package for the analysis of unconsolidated sediments. *Earth Surface Processes and Landforms*, 26(11), 1237-1248. 10.1002/esp.261
- Compton, R. R. (1962). *Manual of field geology*: Wiley.
- De Lange, W. P. (1988). *Wave climate and sediment transport within Tauranga Harbour, in the vicinity of Pilot Bay* (D Phil Earth Sciences). University of Waikato.
- DeLange, W. P., Healy, T. R., & Darlan, Y. (1997). Reproducibility of Sieve and Settling Tube Textural Determinations for Sand-sized Beach Sediment. *Journal of Coastal Research*, 13(1), 73-80.
- Healy, T. R. (1985). *Tauranga Harbour study, part II & V Field Data Collection Programme and Morphological Study*. Bay of Plenty Harbour, New Zealand Ministry of Works Development, Dansk hydraulisk Institut, University of Waikato
- Nathier-Dufour, N., Bougeard, L., Devaux, M.-F. o., Bertrand, D., & Le Deschault de Monredon, F. (1993). Comparison of sieving and laser diffraction for the particle sizemeasurements of raw materials used in foodstuff. *Powder Technology*, 76(2), 191-200. 10.1016/s0032-5910(05)80027-0
- Wildco. (2012). *Environmental Sampling Equipment*. Retrieved from <http://www.wildco.com/Petite-Ponar-Grab-Stainless-Steel-Scoops-Plated-Steel-Arms.html>

CHAPTER 5 - BENTHIC HABITAT MAPPING AND ACOUSTIC SEABED CLASSIFICATION

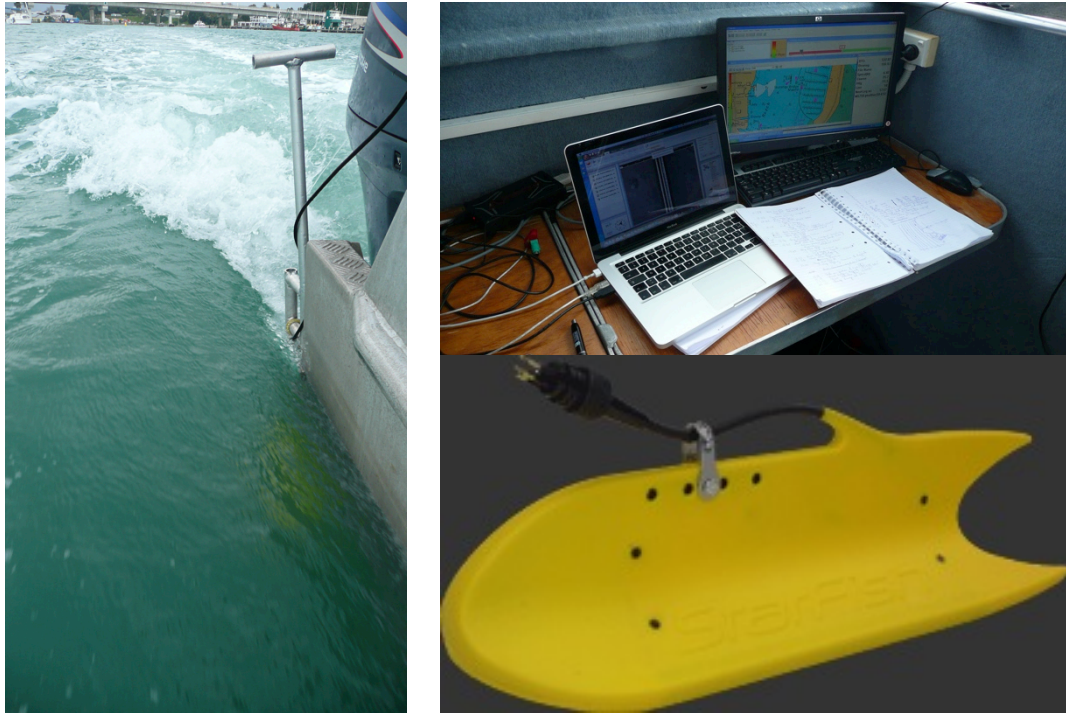
5.1. INTRODUCTION

This chapter details the hydrographic survey undertaken in the Port of Tauranga in July/August 2011 and the processing methodology that followed. A sidescan sonar and multibeam echosounder investigation were performed prior to the ground-truthing operations described in chapter 4. The various habitat mapping techniques described in chapter 3 are here applied to the Tauranga datasets in order to produce surficial sediment maps for comparison with previous studies. Two classification softwares trial versions were also tested. Triton Perspective uses a supervised classification method based on the training of neural nets. QTC Swathview utilizes a multivariate statistical processing technique (Principal Components Analysis) to classify sidescan sonar and multibeam sonar raw data. Unfortunately, due to the lack of time and available scientific literature, the results of these two methods were not judged of sufficient relevance and quality to be presented in this report.

5.2. SIDESCAN SONAR SURVEY

5.2.1. Method

The first step of the planned fieldwork was a sidescan sonar survey undertaken between the 4th and 7th of July 2011. A Starfish 452F sonar (450kHz) was pole-mounted on the University of Waikato survey vessel *Tai Rangahau* (Fig. 5.1 to 5.3). The positioning was provided by RTK-GPS. The sonar imagery datagrams were recorded on the Triton Scanline software (Starfish - Seabed Imaging Systems, 2012), which runs on a laptop and allows for the control of range, contrast and gains (Fig. 5.4). The log files were then exported as XTF (eXtended Triton Format – Triton Imaging Inc.) for post-processing. A total length of 50.2 km of transects was recorded as a range of 50m on each side was used (Fig. 5.5).



Figures 5.1, 5.2 & 5.3: Installation of the Starfish 452F (bottom right) sidescan sonar on the hull of the University of Waikato survey vessel *Tai Rangahau* (left). The top-right photo presents the simple survey station required to operate this equipment on the survey vessel.

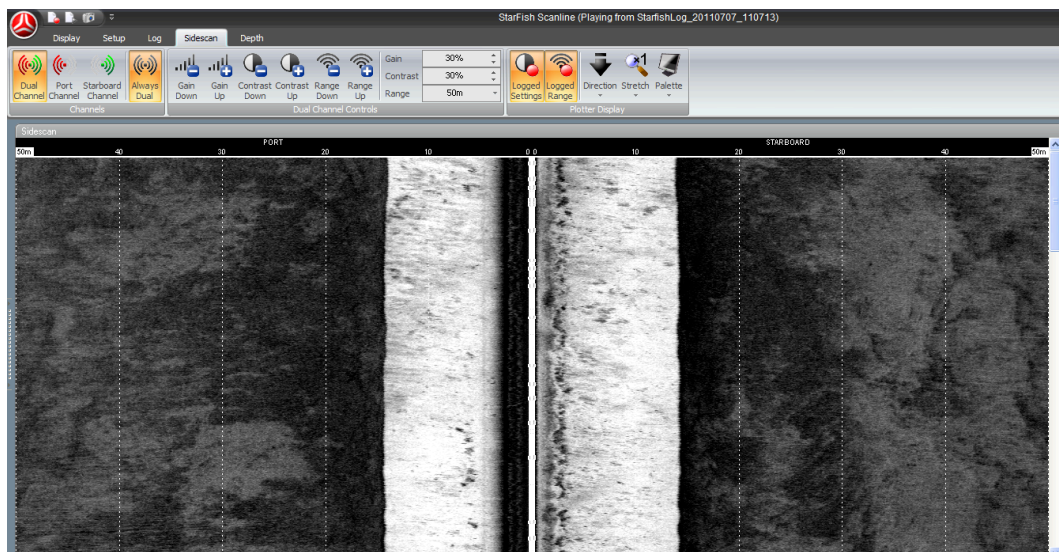


Figure 5.4: Screenshot of the Starfish Scanline acquisition software.



Figure 5.5: Sidescan sonar survey coverage of Stella Passage and Town Reach, Tauranga Harbour, based on the navigation recording (July 2011).

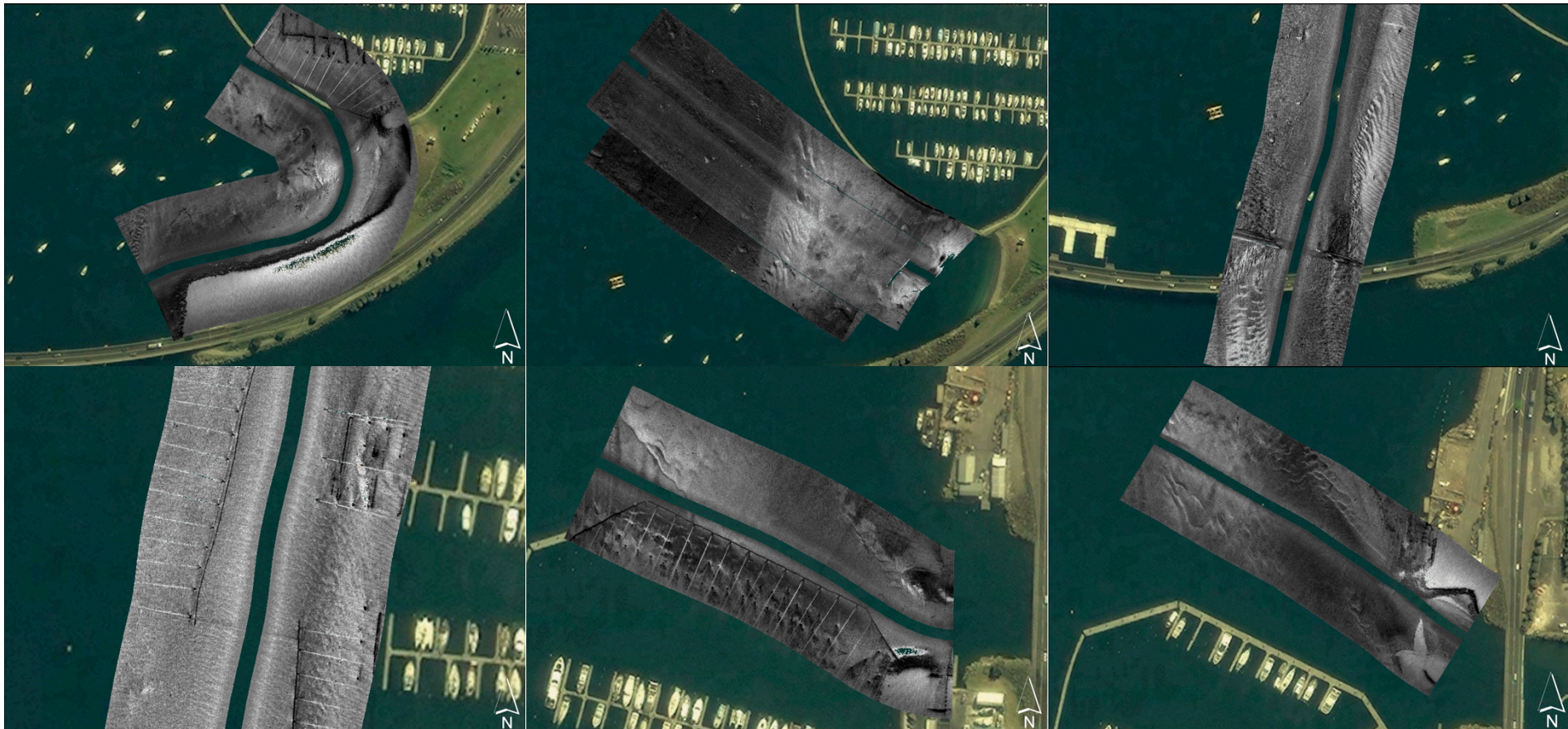
5.2.2. Mosaic Creation

The post-processing and mosaicking of the sonar datagrams was performed using both Triton ISIS and Perspective software. All transects were individually bottom-tracked before geometric and radiometric corrections, including a Time Varying Gain (TVG) correction, were applied. A mosaic image was created, reflecting the strength of the acoustic signal over the whole work area. The sidescan sonar provides slant-range measurements that require an assumption of a flat, horizontal bottom (Anderson et al., 2007). As the Starfish was hull-mounted and not towed following the seabed slopes, the contrasts of reflectivity are different between the deep and shallow areas.

One of advantages of the sidescan sonars over the multibeam echo sounder systems is the greater coverage that can be achieved (Pohner, Bakke, Nilsen, Kjaer, & Fonseca, 2007). This sidescan dataset provided high-resolution images of the various features on the seabed of the Tauranga Harbour. The raw recordings (Fig. 5.7 to 5.12) proved to offer a better definition of the fine details than the high-resolution (20cm) mosaic produced (Fig. 5.6). However, the mosaic created showed less noise than expected, and image-based interpretations could be performed in order to confirm the facies areas found using the MBES backscatter data.



Figure 5.6: Sidescan sonar reflectivity mosaic of the Port of Tauranga (July 2011).



Figures 5.7 to 5.12: Preview of identifiable facies based on sidescan sonar reflectivity. The top row shows the area around the Tauranga Harbour Bridge's east end. The left image shows the rock wall of the artificial bank and several mooring concrete blocks and chains (dark spots). The centre and right pictures show the sand waves and sediment type clear delineation just north of the Bridge gap. The bottom line presents seabed images around the Bridge Marina. The left image is the Marina entrance showing clear reflections on the piles. The centre and right image present the northern breakwater and the sediment patches and sand waves aligned with the Whareroa inlet.

5.3. MULTIBEAM ECHOSOUNDER SURVEY

5.3.1. Method

A multibeam echosounder survey was conducted in the Port of Tauranga on the 22nd, 23rd and 24th of August 2011. The Kongsberg-Simrad EM3000 sonar was operated from the University of Waikato survey vessel *Tai Rangahau* (Fig. 5.13 & 5.14). The positioning was provided by a Trimble MS750 RTK-GPS system while a TSS MAHRS motion sensor measured the vessel attitude. The speed was maintained at a constant 7 knots during the whole survey. An Applied Microsystems Ltd SVPlus was operated to obtain regular sound velocity casts used by the EM3000 PU (Processing Unit) computer to compensate for any ray-bending due to sound velocity variations. The tide levels were provided by the Port of Tauranga from tide gauges located at Sulphur Point and the Tug Berth.

A total of 1.1 km² over 126 transect lines were insonified during this survey (Fig. 5.15). The average line spacing during the operations was around 3.5 times the water depth, in order to obtain the best possible overlap for the use of backscatter data. The EM3000 produces an acoustic pulse at 300 kHz with a ping rate of up to 25 Hz, a pulse length of 150 μ s on a 130° (across track) by 1.5° (along track) swath made up by the 127 beams per swath (Kongsberg Maritime, 2001). The optimal depth accuracy offered by this system is less than 10cm RMS. The acoustic data were recorded using the Hypack/Hysweep 2010 software in both .ALL raw Kongsberg format and .HSX Hypack format.



Figures 5.13 & 5.14: University of Waikato survey vessel *Tai Rangahau* (left) showing the Kongsberg EM3000 fitted on a bow pole (right).

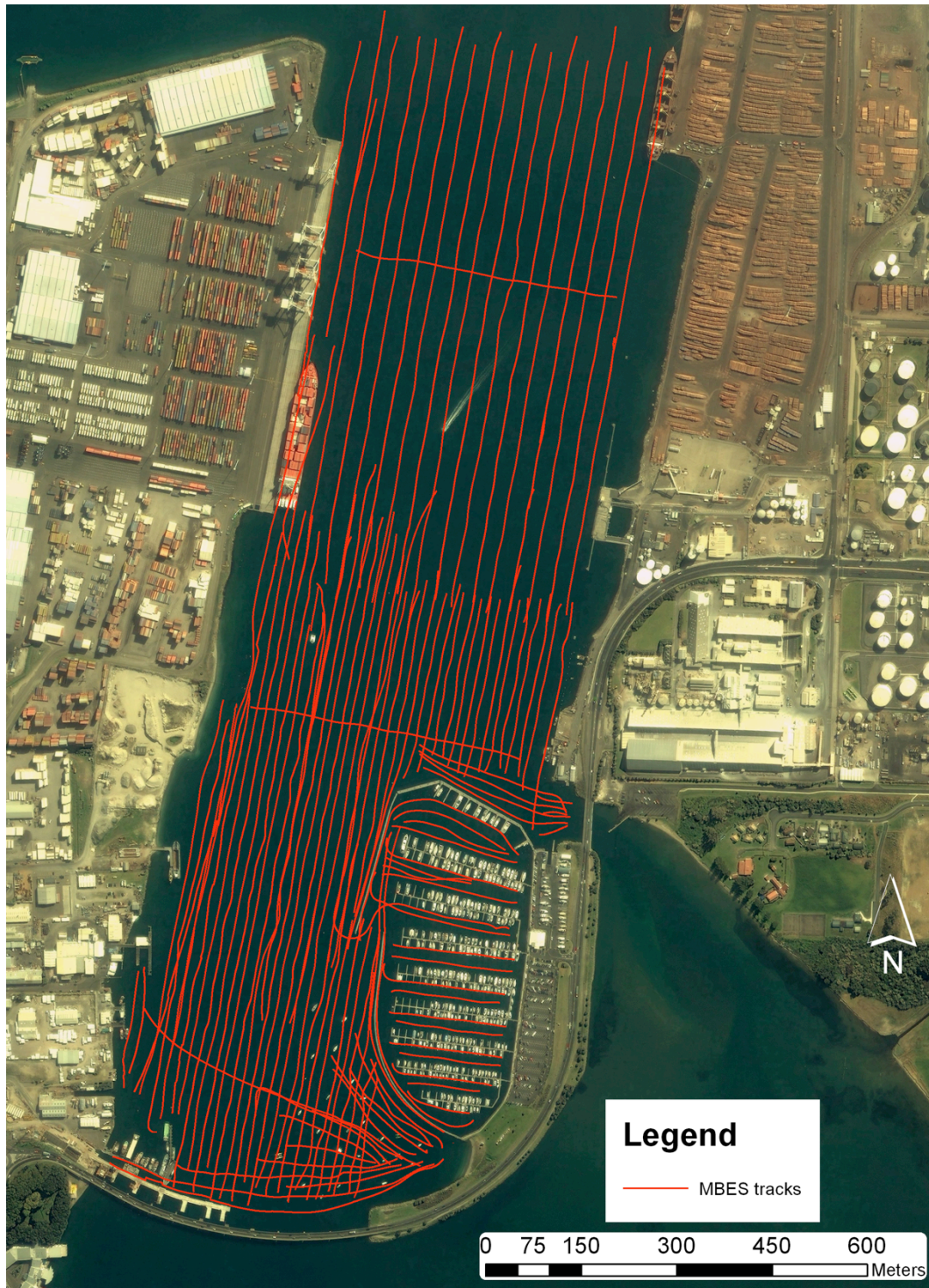


Figure 5.15: Multibeam echosounder (Kongsberg-Simrad EM3000) survey coverage of the Port of Tauranga (August 2011).

5.3.2. Bathymetry processing

The bathymetry was processed from the .HSX files using the Hypack MBMAX multibeam data processing suite. A “patch test” was performed in order to compute the exact mounting angles of the sonar head and obtain the roll, pitch and yaw offsets, along with the precise GPS latency. The navigation processing included the removal of outliers and the correction for the latency calculated from the patch test. The bathymetry processing comprised the correction of the sounding positions with the offsets from the patch test, the integration of tide levels in the depth measurements and the individual inspection and filtering of all the individual survey lines to remove any depth outliers. The coverage was sufficient to not require any interpolation between the lines. A 0.5 m fine mesh bathymetry chart (Fig. 5.16) was produced using the New Zealand Transverse Mercator projection and the Moturiki Chart Datum. Spatial derivatives of the bathymetry were produced in IVS Fledermaus that included slope and rugosity.

The results of the bathymetry survey show the features expected from the nautical chart. The Stella Passage appears with an average depth of 13 m, with a few very clear deeper areas: along the Sulphur Point Container Wharf on the west side; and at the Tanker Berth and the Maunganui Wharves on the east side. All these patches of deeper seabed (pink areas on Fig. 5.17 & 5.18) correspond to berthing areas for large ships and could be the result of propeller wash from either the vessel’s thrusters (Fig. 20) or the Tug Boats (Fig. 21). The Stella Passage also clearly shows 3 distinct dredging areas, noticeable by the dredge head scar marks left on the seabed. The very steep drop creating by the 1992 dredging program is also distinctly defined. The Town Reach Channel is represented by a relatively flat seabed with an average depth around 4 m. Around Whareroa Point (east) the outgoing tidal currents identified in previous studies have created a trough leading to the Stella Passage. The Bridge Marina has an average depth of 2.5 m over an irregular seabed created by the numerous scours behind the pontoon piles. The mooring area east of the Town Reach occurs as a narrow shallow ridge (red area on Fig. 5.16) aligned with the eastern side of Tauranga Bridge access to the south bay.

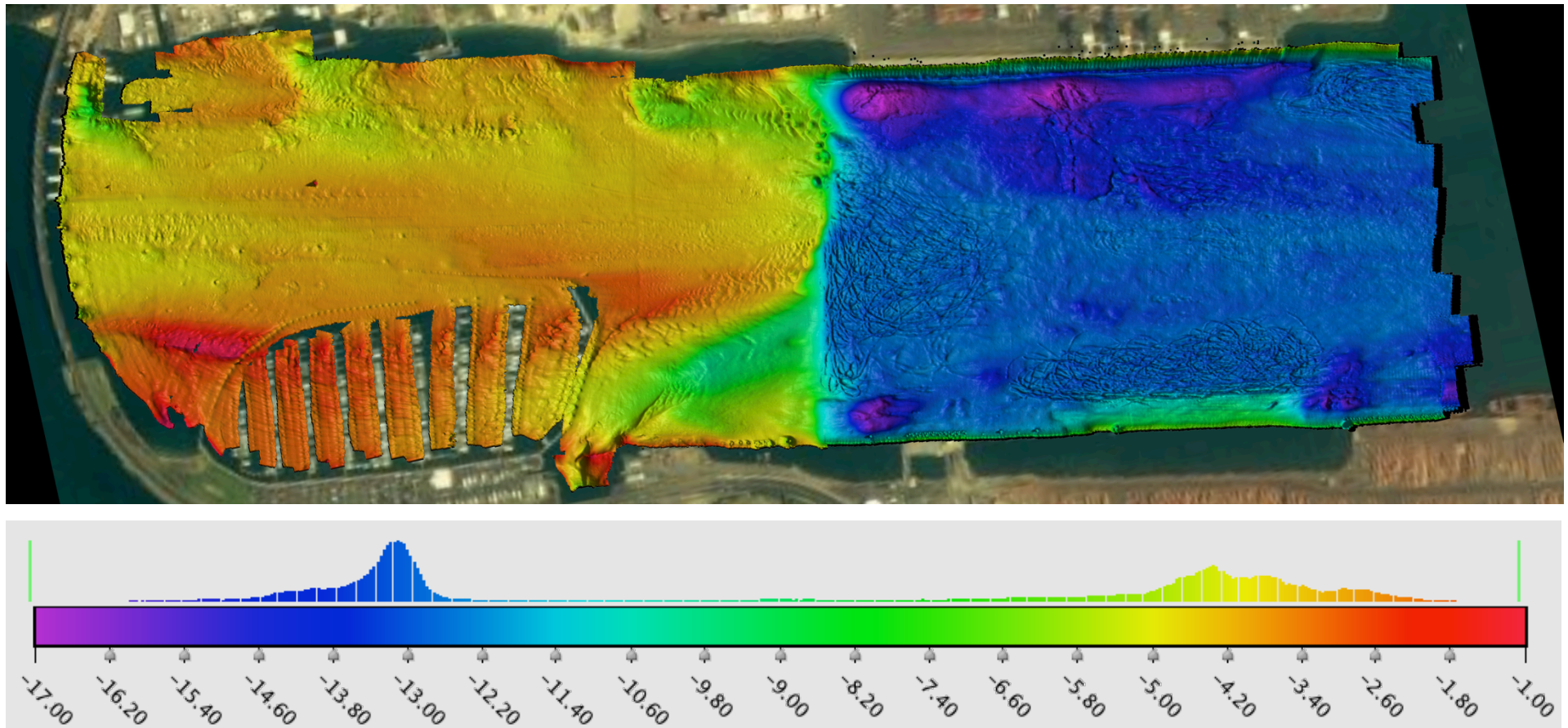
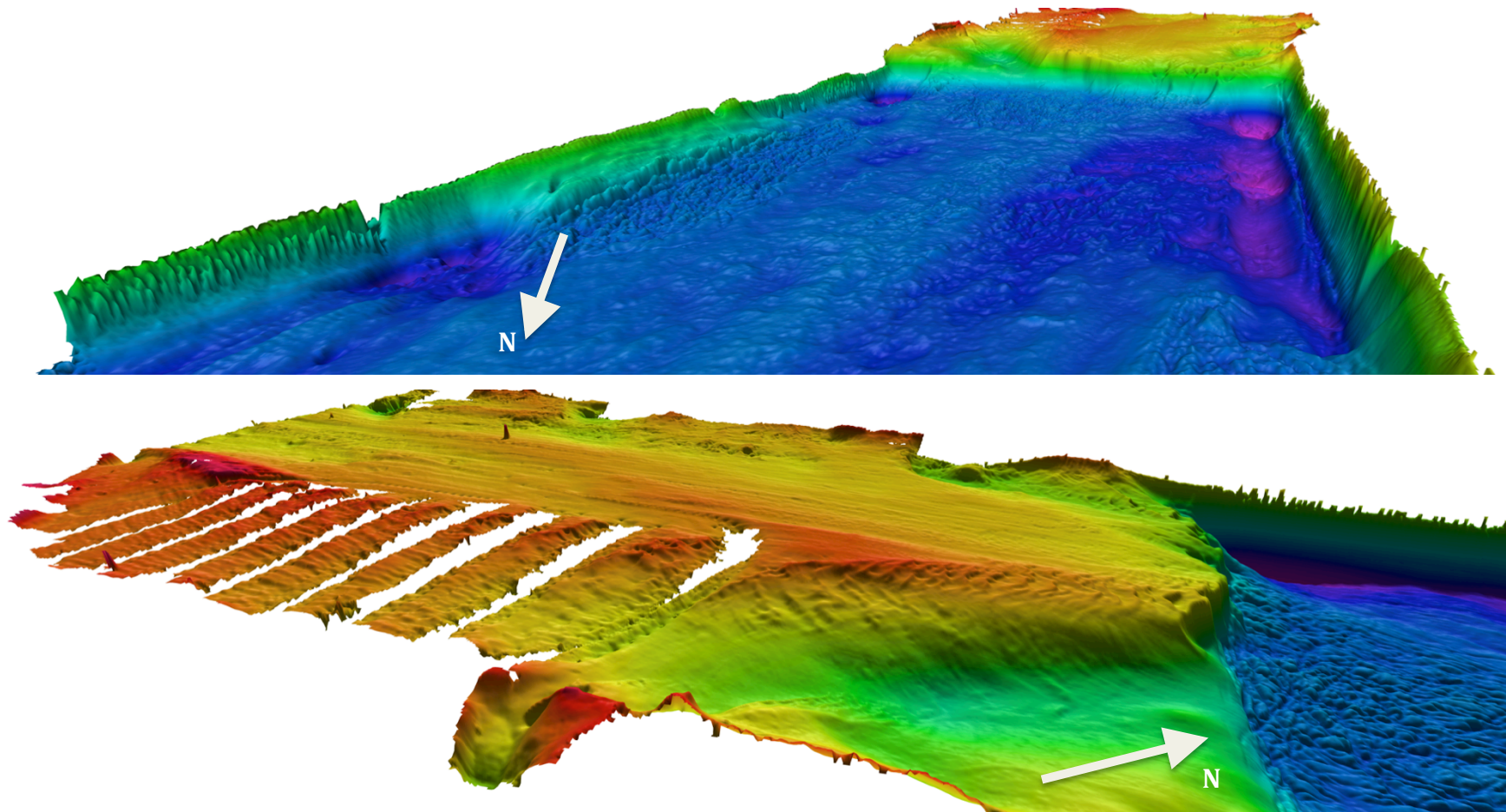


Figure 5.16: Bathymetry of the Port of Tauranga based on the multibeam echosounder survey performed in August 2011 (water depth based on Moturiki Chart Datum).



Figures 5.17 & 5.18: 3D side views of the Tauranga Harbour bathymetry survey (August 2011), with a 6 times vertical exaggeration. The dredging marks, the deep areas (purple) and the uneven seafloor of the Marina are here clearly visible.



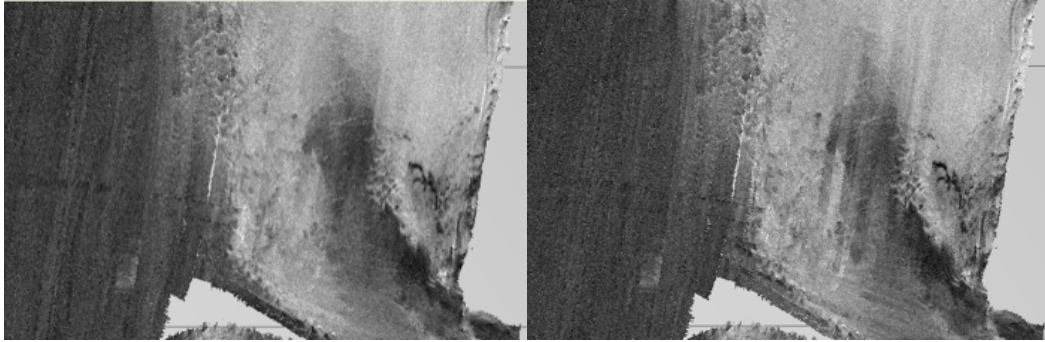
Figure 5.19: Slope factor derived from the bathymetry.



Figures 5.20 & 5.21: Photos of the Port of Tauranga in August 2011 showing the propeller wash from the ship's bow thrusters (top) or the tugboats (bottom). These could explain the deep areas adjacent to the wharves.

5.3.3. Mosaic creation

The raw reflectivity data recorded in the .ALL Kongsberg files (Kongsberg Maritime, 2001) was processed in FMGT (Fledermaus Geocoder Toolbox) version 7.1 in order to produce a grey-scale mosaic. This step was necessary to exploit the spatial variation of the backscatter over the whole area and starts by correcting the geometric and radiometric distortions. The first phase was to compensate for the angular dependence of the backscatter levels by applying a “trend” AVG (Angle Varying Gain) filter to the dataset over a window of pings; 30 pings in this case. The “trend” AVG filter was chosen over the “flat” or “adaptive” ones as it proved to clean the artefacts more efficiently (Fig. 5.21 and 5.22). The slant range was corrected by using the bathymetry stored in the raw datagrams. The mosaicking technique that aims to merge overlapping survey lines was based on feathering techniques developed by Rzhhanov (2000) that reduce the seam between the lines based on a quality factor stored in every cell (Fonseca & Calder, 2005). The backscatter data for the Port of Tauranga was found to range from -35 dB to -12 dB (Fig. 5.23). An adjusted geo-referenced backscatter data mosaic could be created with resolution of 15 cm on a New Zealand Transverse Mercator spatial projection (Fig. 5.24).



Figures 5.22 & 5.23: Multibeam echosounder backscatter mosaics using “trend” (left) and “flat” (right) AVG filters. The “trend” method clearly shows fewer artefacts.

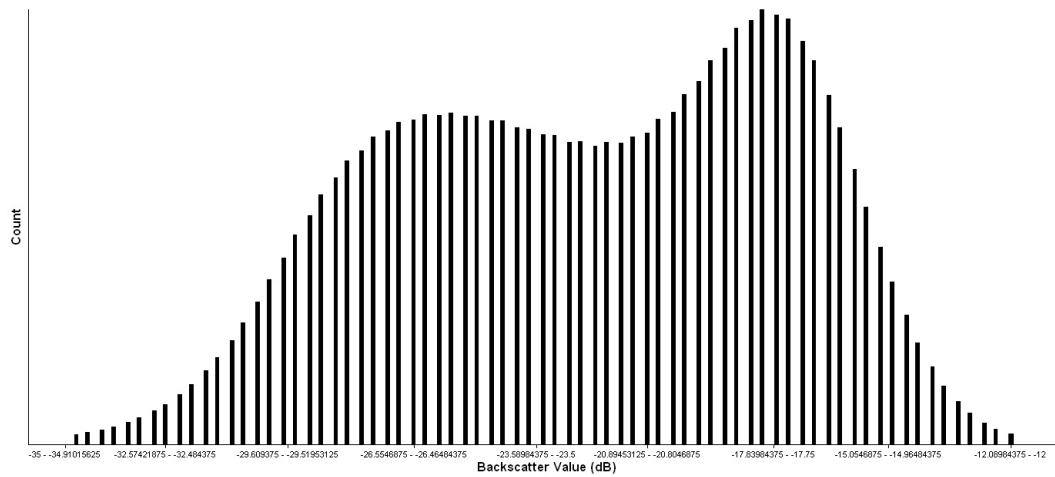


Figure 5.24: Multibeam echosounder backscatter distribution in the Tauranga Harbour (August 2011).



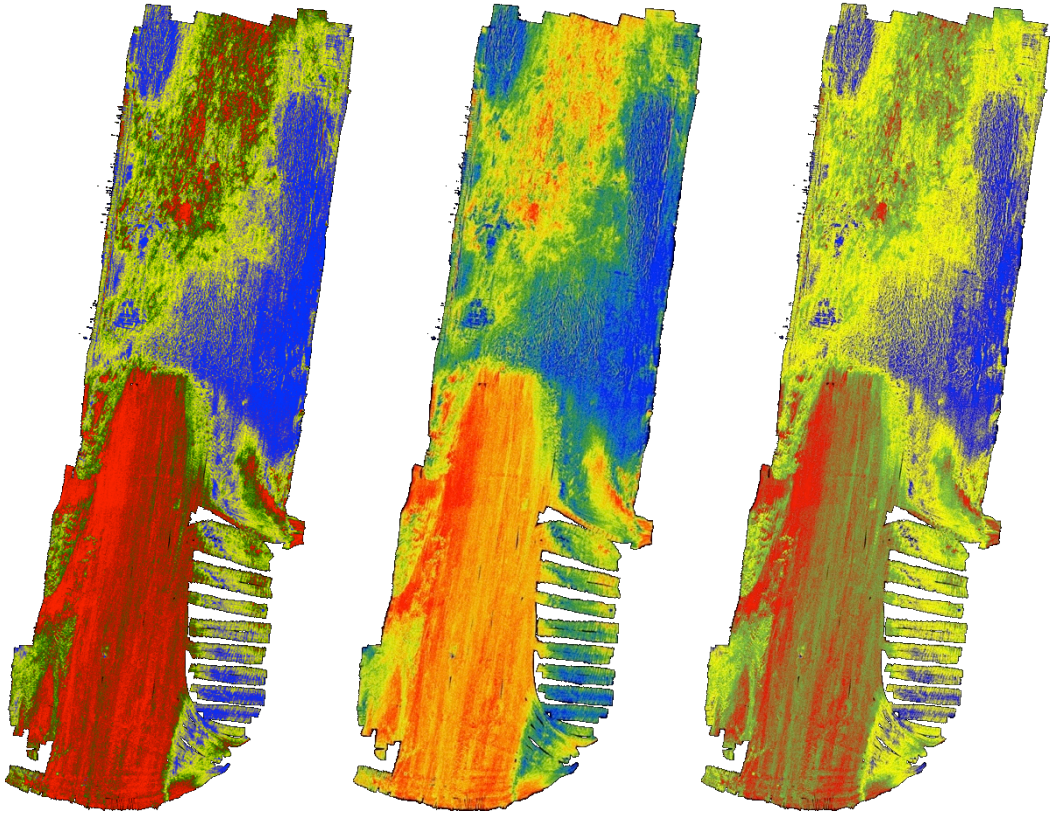
Figure 5.25: Multibeam echosounder backscatter mosaic of the Tauranga Harbour, based on the survey performed in August 2011.

5.4. IMAGE-BASED CLASSIFICATION

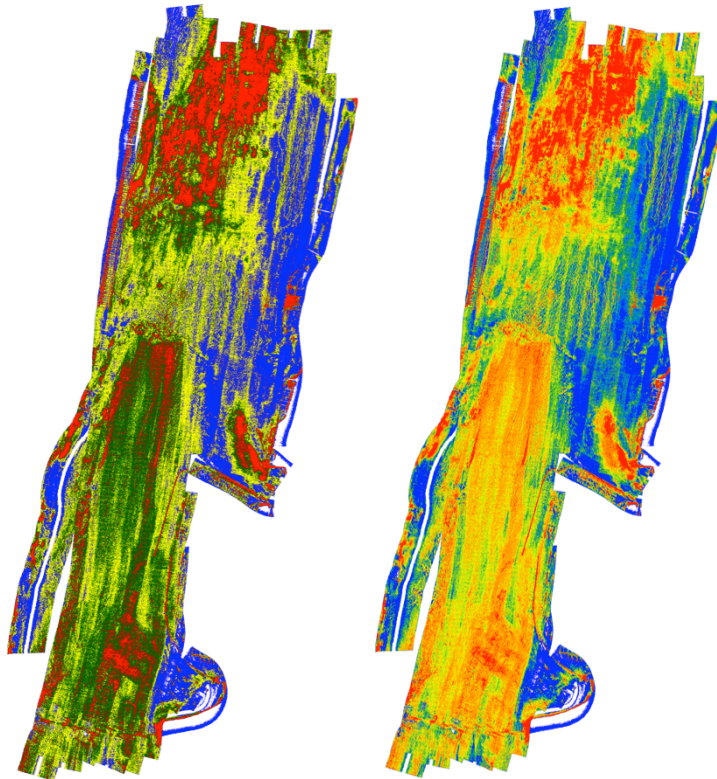
Classification is the process of using pattern-recognition techniques to extract spatial information from geo-referenced images and create thematic maps. The human brain can distinguish between certain textures and colours but computer-assisted recognition allows working in the fine-scale and statistics domain (Geographic Imaging by ERDAS, 2009). The level of interaction between the analyst and the processing computer defines two types of classifications: supervised and unsupervised. The supervised classification, closely controlled by the operator, utilizes the statistics and signatures from representative training samples chosen for each class determined by the ground truthing operations. Unsupervised classification determines the classes based on the spectral distinctions within the image. Two different software types are here compared: a Geographic Information System (GIS) and a Remote Sensing program.

5.4.1. Erdas Imagine

The remote-sensing software Erdas Imagine v.9.1 provides various tools for photo-interpretation. These classification tools are usually applied to satellite or aerial imagery to obtain land cover types, but they were here used on the grey-scale mosaics created for both the MBES and the SSS. The segmentation, comprising both classification and delineation, was achieved with unsupervised and supervised techniques. The supervised classification using the Maximum Likelihood algorithm was only undertaken on the MBES mosaic (Fig. 5.27) by training the model with the 4 shell coverage classes (sand, shelly sand, very shelly sand, shell lag) resulting from the underwater video ground-truthing operations. The high resolution of the SSS mosaic combined with the numerous acoustic artefacts made the training samples creation and supervised classification difficult and the results unreliable. Unsupervised classifications for the MBES and SSS were also performed using either 4 classes (Fig. 5.25 & 5.28) like the shell coverage, or 11 classes (Fig. 5.26 & 5.29), like the Angular Response Analysis later discussed.



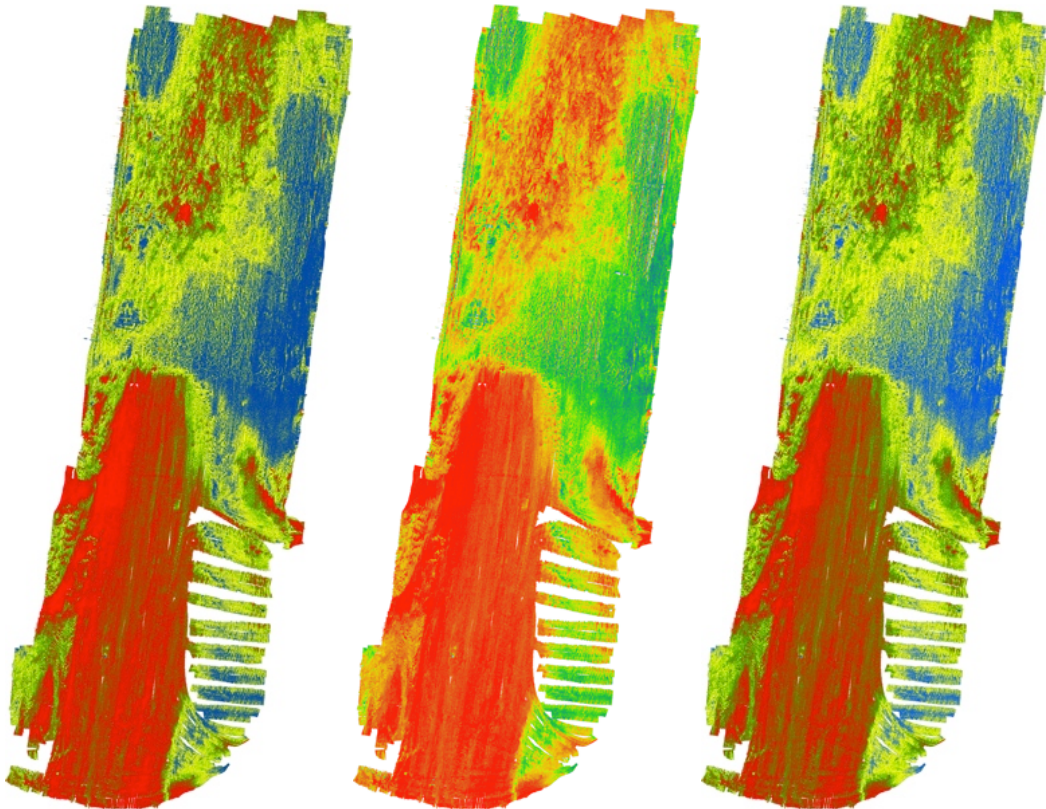
Figures 5.26, 5.27 & 5.28: Results of the various classification methods of the MBES backscatter on ERDAS Imagine: unsupervised classification with 4 classes (left), unsupervised classification with 11 classes (centre) and supervised classification with 4 classes (right).



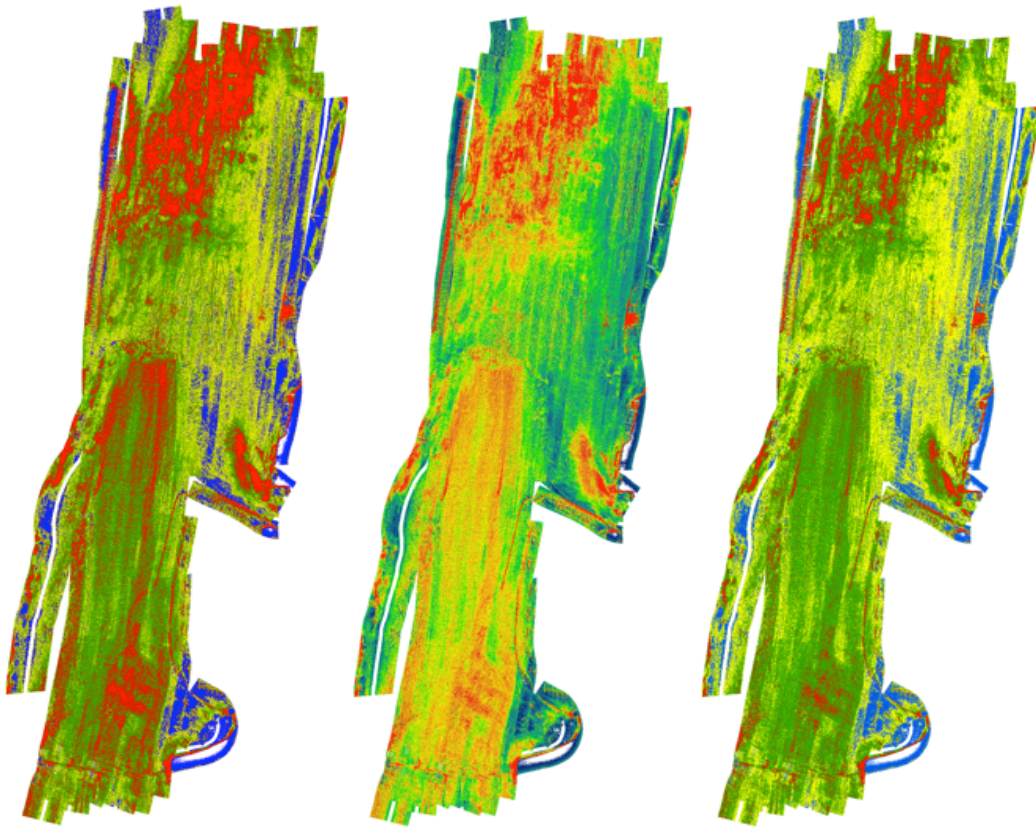
Figures 5.29 & 5.30: Results of the various classification methods of the SSS reflectivity on ERDAS Imagine: unsupervised classification with 4 classes (left) and unsupervised classification with 11 classes (right).

5.4.2. ArcGis Spatial Analyst

The Spatial Analyst extension in ArcGis offers an image classification toolbar that converts multi- or single-band imagery into a raster with a number of classes to be used for thematic maps (ESRI ArcGis, 2010). This toolbar allows the creation of training samples in the form of polygons that can be evaluated before the supervised classification (Maximum Likelihood). An unsupervised Iso-cluster classification is also available. Both types of classifications were performed for both the MBES and the SSS mosaics. The unsupervised method was run with 4 classes (Fig. 5.30 & 5.33) to fit the shell coverage scheme, or with 11 classes (Fig. 5.31 & 5.34) for a comparison with the later results from the Angular Response Analysis. The supervised classification with 4 training areas was this time successful on both the MBES (Fig. 5.32) and SSS (Fig. 5.35) mosaics.



Figures 5.31, 5.32 & 5.33: Results of the various classification methods of the MBES backscatter on ArcGis Spatial Analyst: unsupervised classification with 4 classes (left), unsupervised classification with 11 classes (centre) and supervised classification with 4 classes (right).

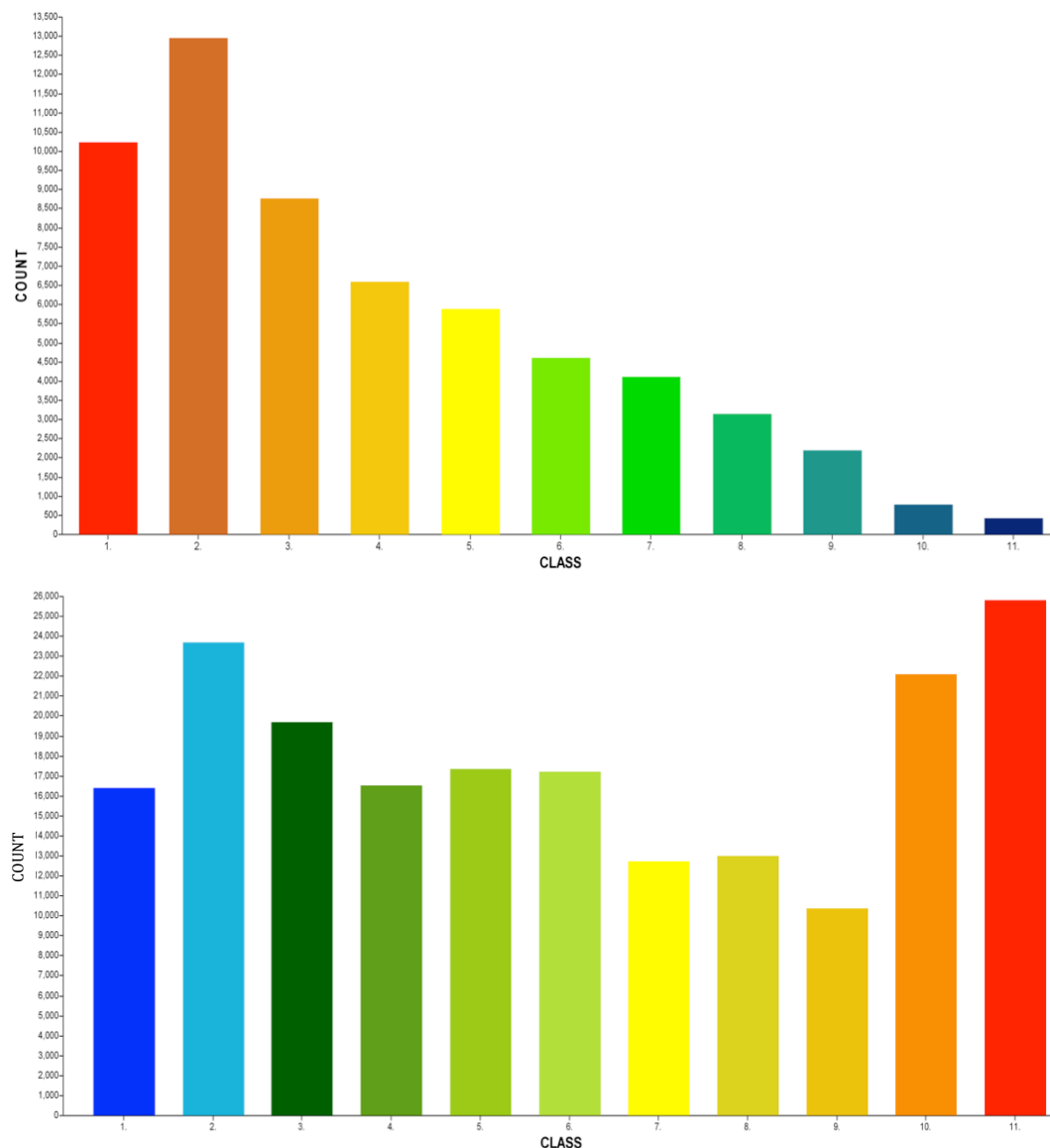


Figures 5.34, 5.35 & 5.36: Results of the various classification methods of the SSS reflectivity on ArcGis Spatial Analyst: unsupervised classification with 4 classes (left), unsupervised classification with 11 classes (centre) and supervised classification with 4 classes (right).

5.4.3. Image Based Analysis Results

The unsupervised classifications of the MBES backscatter using either Erdas Imagine or ArcGis Spatial Analyst showed great results for the delineation of identifiable areas in the Tauranga Harbour. When used with four classes, the various high reflectivity areas tended to be classified as one unique type. The use of 11 classes allowed resolving this simplification by offering more contrast spectrum and enhancing the gradual transitions between distinctive regions. ERDAS Imagine appeared to pick up a contrast change on the high reflectivity area of the Town Reach's shallow shelf western side (dense red patch on Fig. 5.27), probably indicating a change in surface shell coverage not clearly visible with the human eye. Spatial Analyst also indicates this class change, but not as clearly. This example demonstrates the processing dissimilarities of these two softwares. The histograms (Fig. 5.37 & 5.38) of the resulting classes show the differences in distribution between the two techniques. ArcGIS uses an Iso-cluster

method while Erdas Imagine uses the ISODATA algorithm (Iterative Self-Organizing Data Analysis Technique) based on the calculations of the minimum spectral distance formula to form clusters (Leica Geosystems, 2006). The combination of the 4 and 11 classes supervisions also permitted definition of the mixed sediment areas in the north Stella Passage. The results of these image-based analyses did not mean to provide a definitive segmentation of the work area's seabed, but were only intended to serve as a fine-resolution support and confirmation tool for the Angular Response Analysis described hereafter.



Figures 5.37 & 5.38: Classes distribution resulting of the Unsupervised Classification of the MBES backscatter on Erdas Imagine (top) and ArcGis Spatial Analyst (bottom). Both methods were performed on the grey-scale mosaic of the MBES data obtained from the Port of Tauranga in July 2011.

5.5. ANGULAR RESPONSE ANALYSIS

The Angular Response Analysis (ARA) was developed at the Center for Coastal and Ocean Mapping (CCOM) from the University of New Hampshire. It is based on the backscatter dependence to the grazing angle in order to determine the seafloor properties. For this study, the IVS Fledermaus Geocoder Toolbox (FMGT v7.3.2) was used. It consists of one of the various implementations of the Geocoder algorithm developed by Luciano Fonseca (Fonseca & Calder, 2005; Fonseca & Mayer, 2007) in either survey or data processing software suites and utilizes the raw .ALL Kongsberg MBES files (Fig. 39).

The first stages of the ARA processing are common with mosaic creation, and consist of the compensation for geometric and radiometric distortions. The ARA itself is then performed over patches made of consecutive pings. An average Angular Response is obtained for both port and starboard side before comparison to the model. A preliminary seabed class map is then created that still needs to be corrected for the sonar beam pattern.

The beam pattern of a given echosounder is the radiometric distortion of the reflectivity as a result of anomalies in the transmit power and can be assimilated to the sonar's signature on the backscatter (Maddock, 2010). It is known to be different from one sonar model to the other, but also between sonar heads of the same model. In order to study the pure backscatter signal necessary to calculate the bottom sediment type, this beam pattern needs to be compensated for. It is determined by running the Angular Response Analysis over an area of known bottom type. By correcting the observed response to make the model fit the expected seabed class, we can extract the beam pattern as a residual of both signals. For this study, the beam pattern was extracted over a uniform sandy area with no surficial shell coverage in the southeast of the Stella Passage (Fig. 5.40).

After the beam pattern was extracted and applied to the dataset, another ARA was executed that would only be based on the pure backscatter signal. The inversion was then performed over the results of this previous ARA by adjusting the model

to the results of the ground truthing operations. The Figures 5.41 to 5.43 show the particular acoustic signatures of various seabed classes found in the work area. The resulting map is a 5 m resolution chart (Fig. 5.44) presenting the spatial distribution of 11 sediment classes ranging from Gravel ($\Phi \leq -1$) to Clay ($\Phi \geq 8$). The Figure 5.45 shows the overall resulting classes distribution. The sandy classes appear clearly dominant over the study area while very few regions of finer (silt and clay) sediments were found. The gravel class, mostly on the Town Reach shallow shelf, represents about 1 % of the seabed coverage encountered here.

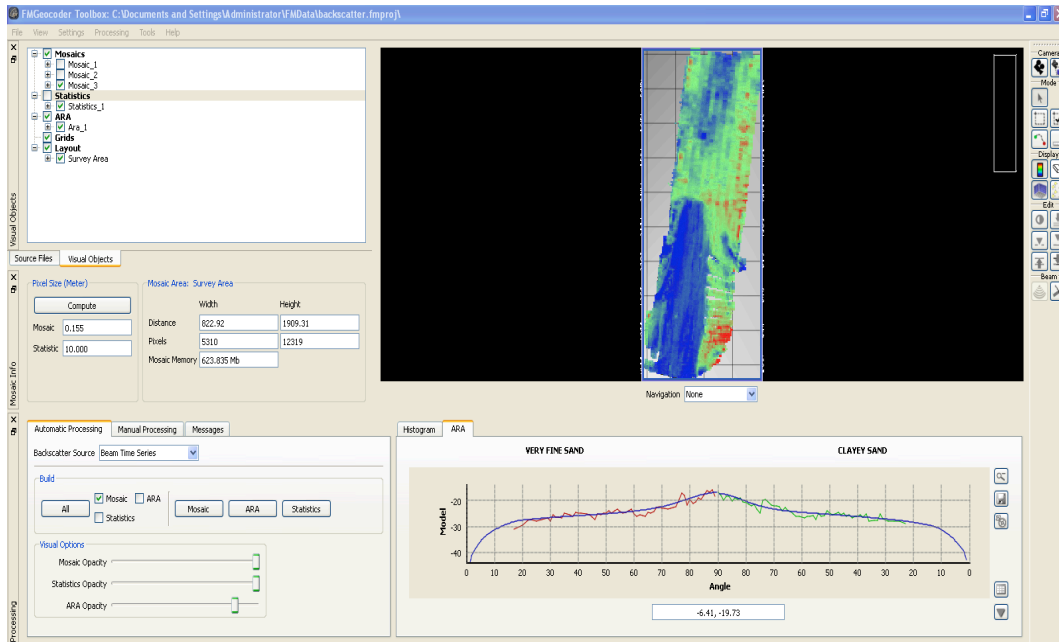


Figure 5.39: Screenshot of the Fledermaus Geocoder Toolbox.

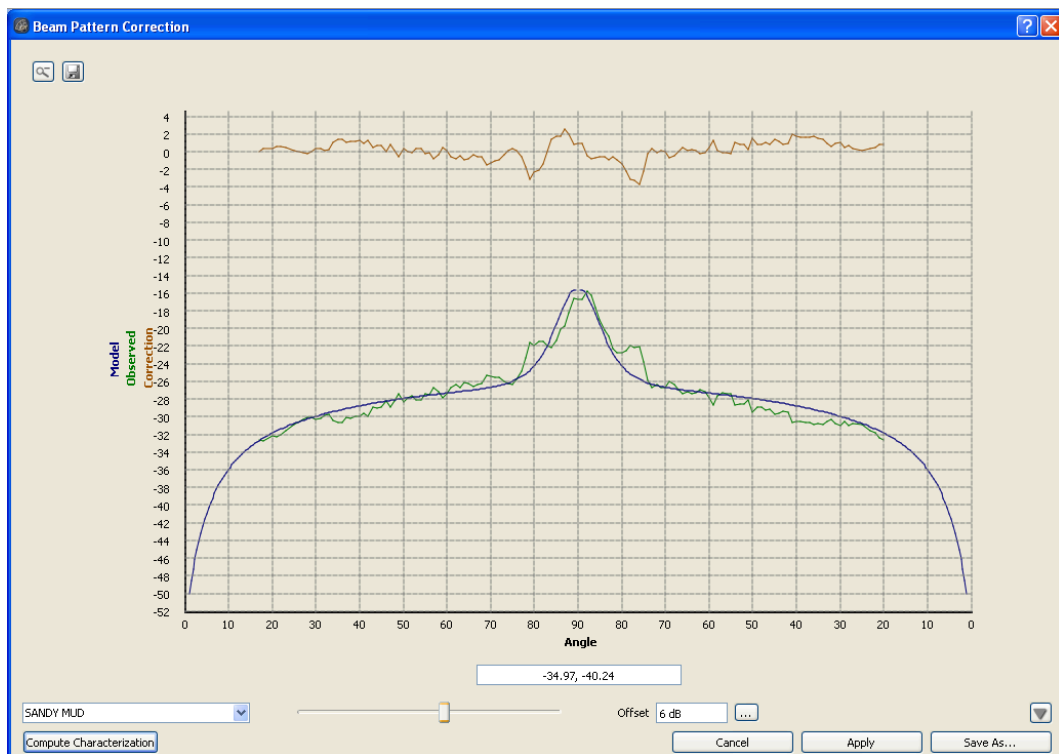
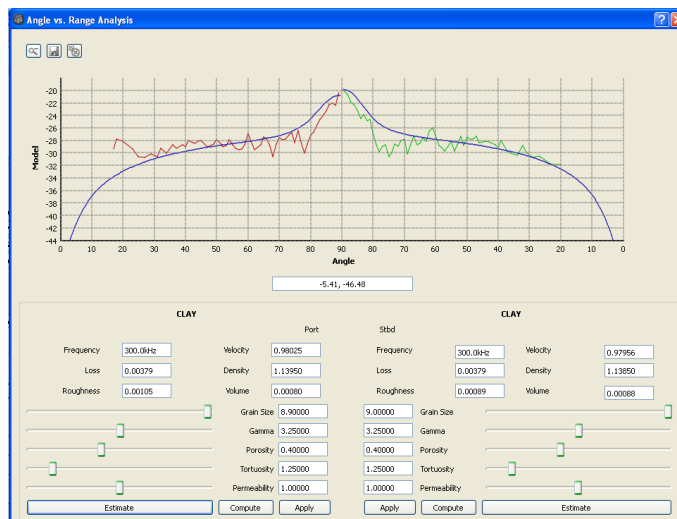
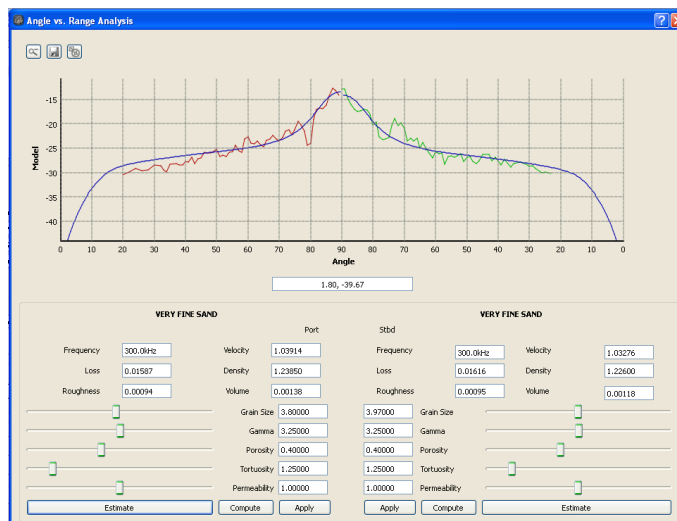
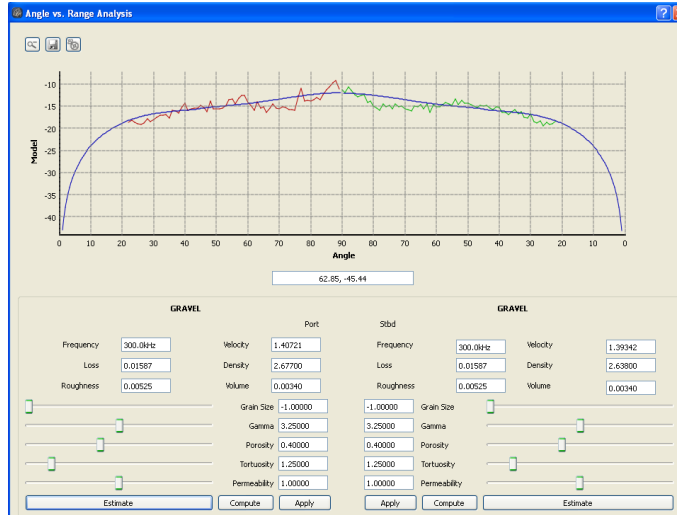


Figure 5.40: Beam pattern extraction in FMGT. The observed signal (backscatter measurement) in green is compared to the model in blue chosen according to the ground-truthing results. The residual beam pattern signal in brown can then be extracted for latter compensation.



Figures 5.41, 5.42 & 5.43: Angular Response signatures in the Tauranga Harbour for gravel (top), very fine sand (centre) and clay (bottom). The near, far and outer ranges show very distinct shapes depending on the seabed type.

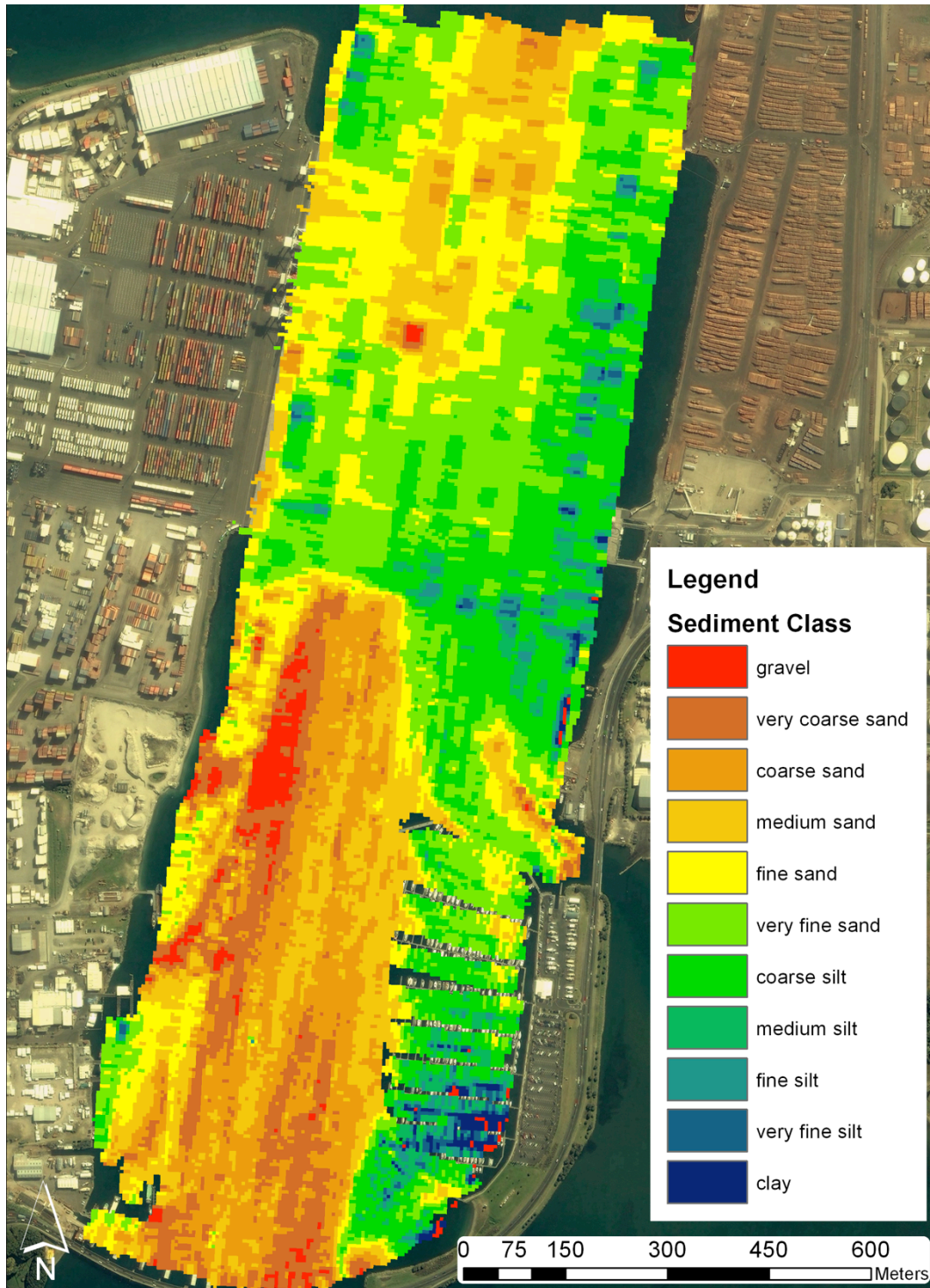


Figure 5.44: Angular Response Analysis results and their spatial distribution in the Tauranga Harbour based on Kongsberg-Simrad EM3000 multibeam echosounder backscatter data.

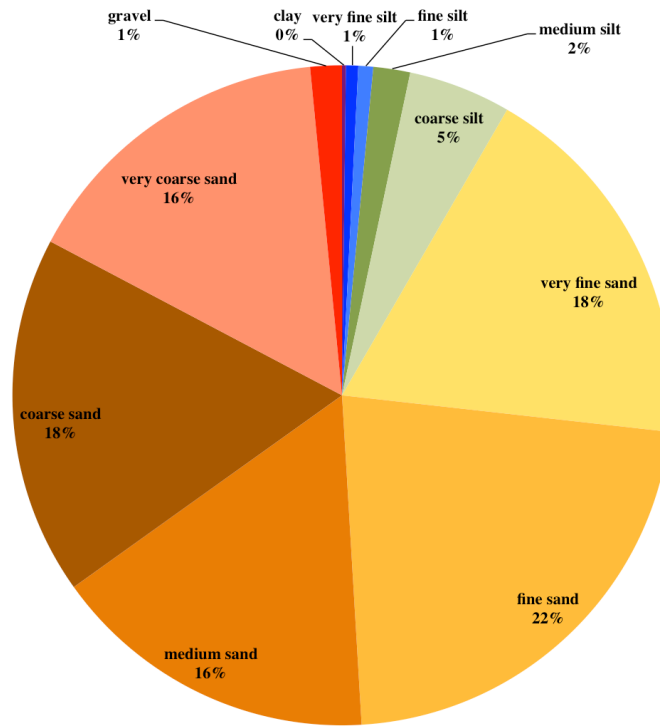


Figure 5.45: Distribution of the 11 sediment classes resulting from the Angular Response Analysis of the MBES backscatter in the Port of Tauranga. The sandy classes are here clearly dominant.

Station	Phi	Station	Phi
1	3.660634	22	0.718039
2	0.71224	23	4.076296
3	3.865108	24	7.42204
4	2.473464	25	0.725974
5	0.684469	26	0.324961
6	2.700674	27	1.258827
7	4.544145	28	2.142643
8	1.746665	29	-0.534287
9	2.586992	30	1.084566
10	6.129428	31	3.890438
11	3.060945	32	1.9606
12	3.031037	33	0.945554
13	3.053926	34	1.925046
14	4.1825	35	4.599999
15	3.085207	36	1.438734
16	3.802697	37	1.283547
17	6.656025	38	0.846369
18	0.227454	39	8.99649
19	5.598101	40	-0.395275
20	5.13132	41	-0.205755
21	1.566911	42	4.429395

Figure 5.46: Phi results of the Angular Response Analysis for every ground-truthing station.

5.6. CORRELATION OF THE VARIOUS DATASETS

The dependence of acoustic backscatter on sediment grain size distributions and other environment variables was investigated through statistical analysis. The various data were extracted from a 5 m radius area around each sampling location, except for the conflicting sites identified in the Chapter 4, in order to investigate their relative relationships and relevance. This sampling area size was chosen according to the navigation uncertainties and the resolution of the various data processing result layers. Using each area's mean value allowed cleaning of potential noise from the data, especially on the SSS mosaic.

Some variables were expected to contribute to the backscatter intensity, such as the sediment grain size or surficial shell coverage. A scatter plot matrix (Fig. 5.46) was first created in order to visualize the relationships between the variables. It appeared from this figure that some variable relationships seemed to form clusters of identical phi value represented in colour code. A Pearson's linear correlation table (Fig. 5.47) was then produced, expressing "r" values or linear dependences in order to find the predictors for the MBES backscatter in the area.

The SSS reflectivity, although sampled over a 5 m radius area in order to remove potential speckle noise, did not show any significant correlation with either the shell coverage or the sediment type as was originally expected. This result can be explained by the data alterations inherent to this particular mosaic processing. In fact, the SSS data that was compared to the other datasets was no longer expressed in reflectivity values (dB) but in pixel value (0 to 256), as a result of the mosaicking phase.

The MBES backscatter values were found to be strongly correlated (r 0.91) to the ARA Phi results (Fig. 5.50), which was expected since the same FMGT software produces them both. The grain size obtained from dry sieving also had a strong correlation with the backscatter (r 0.8) and the ARA Phi (r 0.78). On the Figure 5.49, the ARA Phi and dry sieving Phi seem to follow a similar trend even though the first one always gives a much greater result than the dry sediment analysis

result. Their relationship (Fig. 5.52) can probably be explained by the model inversion by which the ARA model was trained with the ground truthing results. The correlation between the dry sieving Phi and the pure backscatter signal (Fig. 5.51) is a good sign for the use of MBES reflectivity data for seabed type prediction.

The shell coverage obtained from both underwater video and grab samples showed a strong relationship with the grain size from dry sieving (r 0.75). This can be explained by the tendency of densely covered areas to contain coarser sediment. A strong correlation was also found with the ARA Phi (r 0.69) and the backscatter (r 0.73). As the ARA Phi is basically a derivative of the backscatter data, this is not surprising. The limitation of this result is that the Geocoder algorithm does not process grain sizes over the very coarse class and it does not differentiate between gravels and shell coverage. Therefore, the backscatter processed with Geocoder can be a good predictor of the presence of shells on the seabed surface but ground truthing observations will always be necessary in order to confirm that the surface is made of shells or solid gravel.

The water depth and its slope derivative did not show any significant correlation with any other variable. The grain size obtained from laser sizing was also found to be uncorrelated to the rest of the dataset. The problems encountered during the Malvern analysis, as described in the part “4.2.3.1. Laser Diffraction”, could be the cause of this lack of relationship between the laser-sizing outputs with the rest of the dataset.

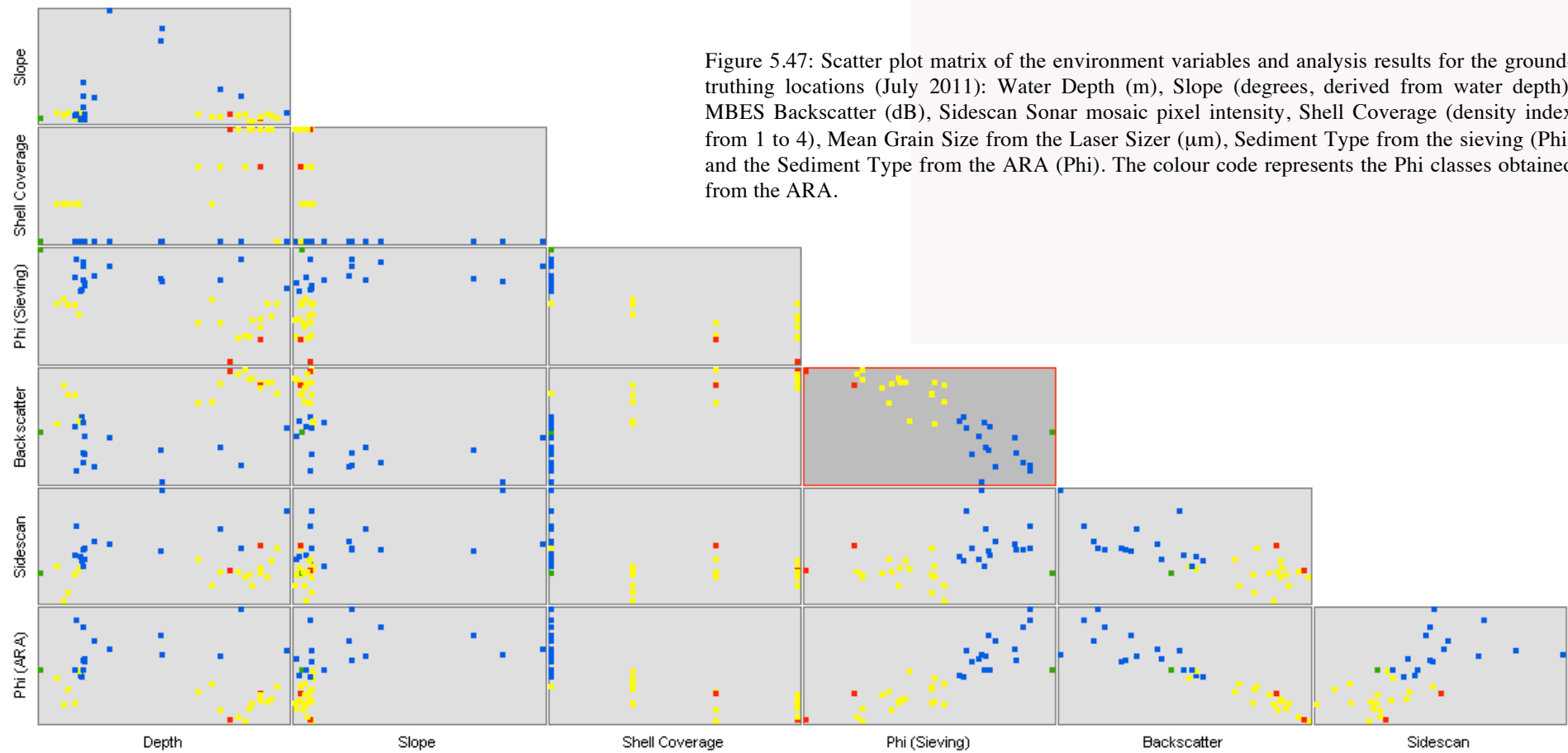


Figure 5.47: Scatter plot matrix of the environment variables and analysis results for the ground-truthing locations (July 2011): Water Depth (m), Slope (degrees, derived from water depth), MBES Backscatter (dB), Sidescan Sonar mosaic pixel intensity, Shell Coverage (density index from 1 to 4), Mean Grain Size from the Laser Sizer (μm), Sediment Type from the sieving (Phi) and the Sediment Type from the ARA (Phi). The colour code represents the Phi classes obtained from the ARA.

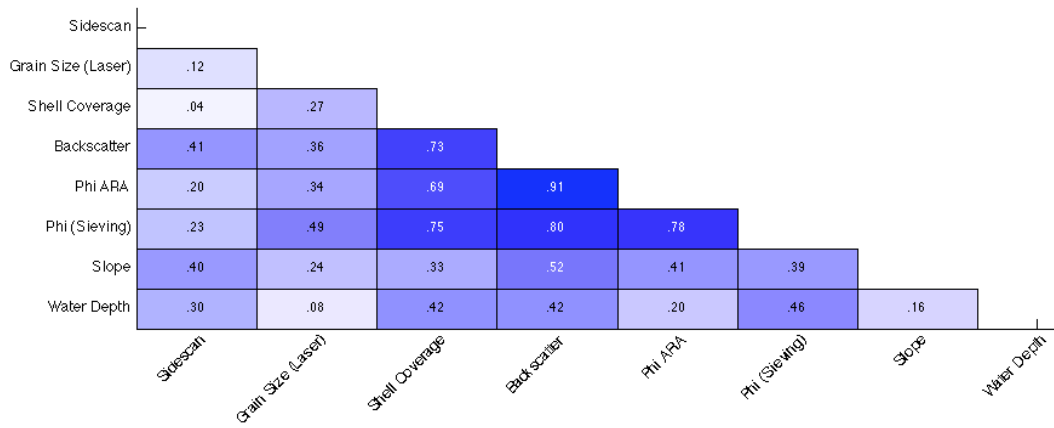


Figure 5.48: Pearson’s linear correlation table of the variables extracted for every ground-truthing station of the Tauranga Harbour (2011). The shading increases according to the correlation values.

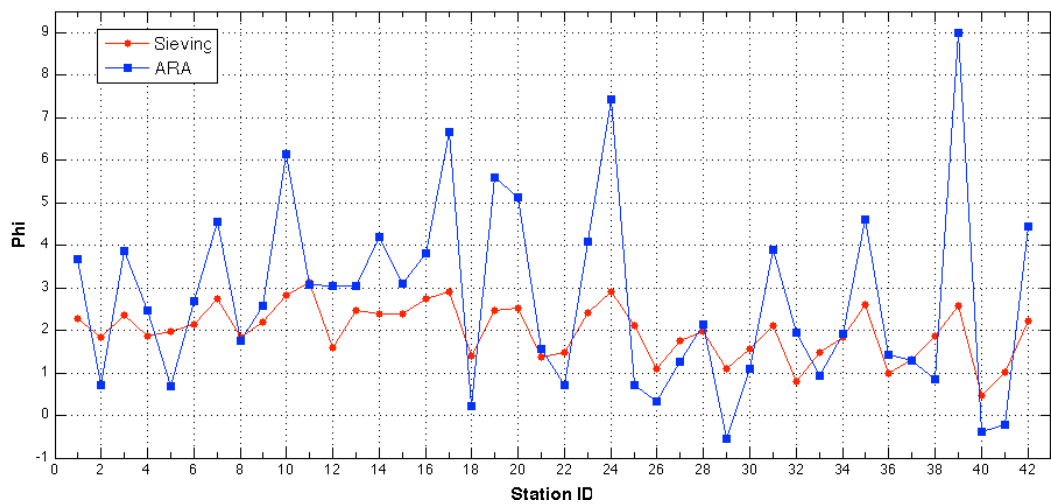


Figure 5.49: Comparison of the grain size results from the Angular Response Analysis and the dry sieving of the sediment samples of the Tauranga Harbour (July 2011).

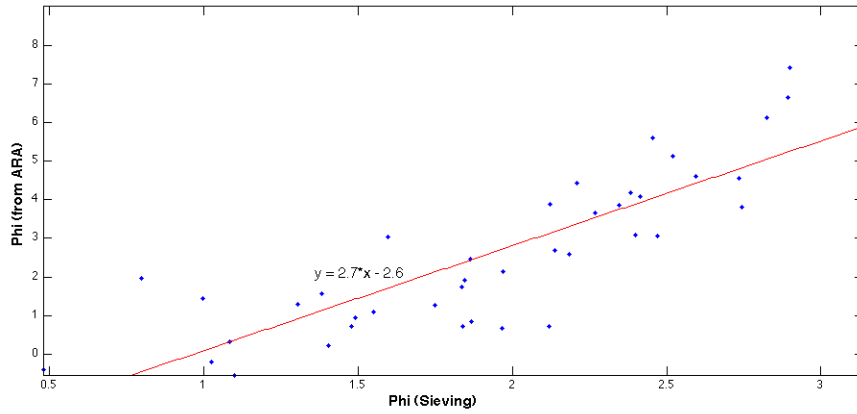


Figure 5.50: Scatter plot and linear regression of the dry sieving results against the ARA Phi for the Port of Tauranga (July 2011).

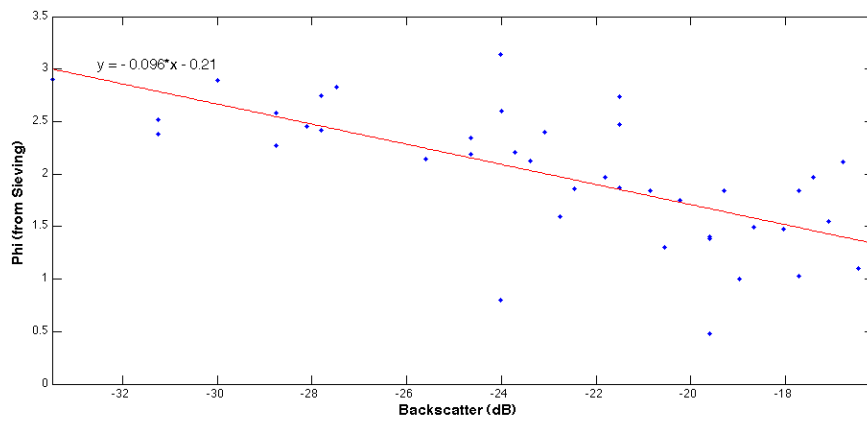


Figure 5.51: Scatter plot and linear regression of the dry sieving results against the backscatter values for the Port of Tauranga (July 2011).

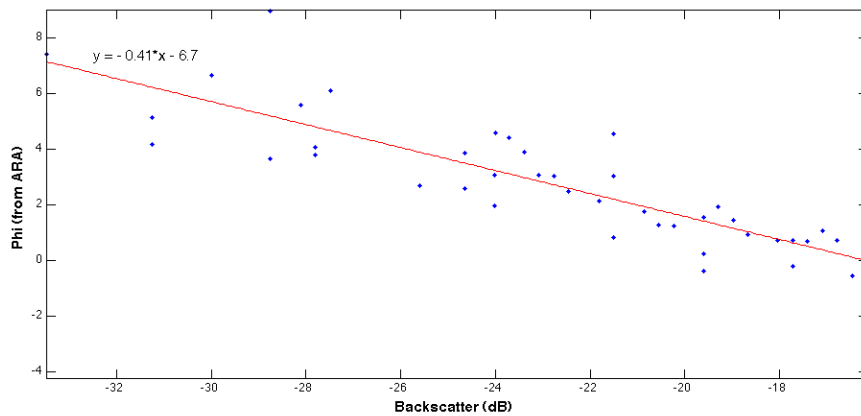


Figure 5.52: Scatter plot and linear regression of the ARA phi results against the backscatter values for the Port of Tauranga (July 2011).

5.7. BENTHIC HABITAT MAP CREATION

A benthic sediment map was created using a combination of the various classification methods and ground-truthing information. Since both ARA and image-based classification results were raster images, basic simplification and segmentation were undertaken in order to produce the sediment classes map. A series of generalization tools were applied to all the raster datasets on ArcGis Desktop 10 in order to create polygons of similar facies. The various maps were then compared, while the ground truthing dataset was consulted for confirmation at every stage of the process, and a final benthic habitat map (Fig. 5.53) was produced that represents the various seabed types and features of the Tauranga Harbour in July 2011.

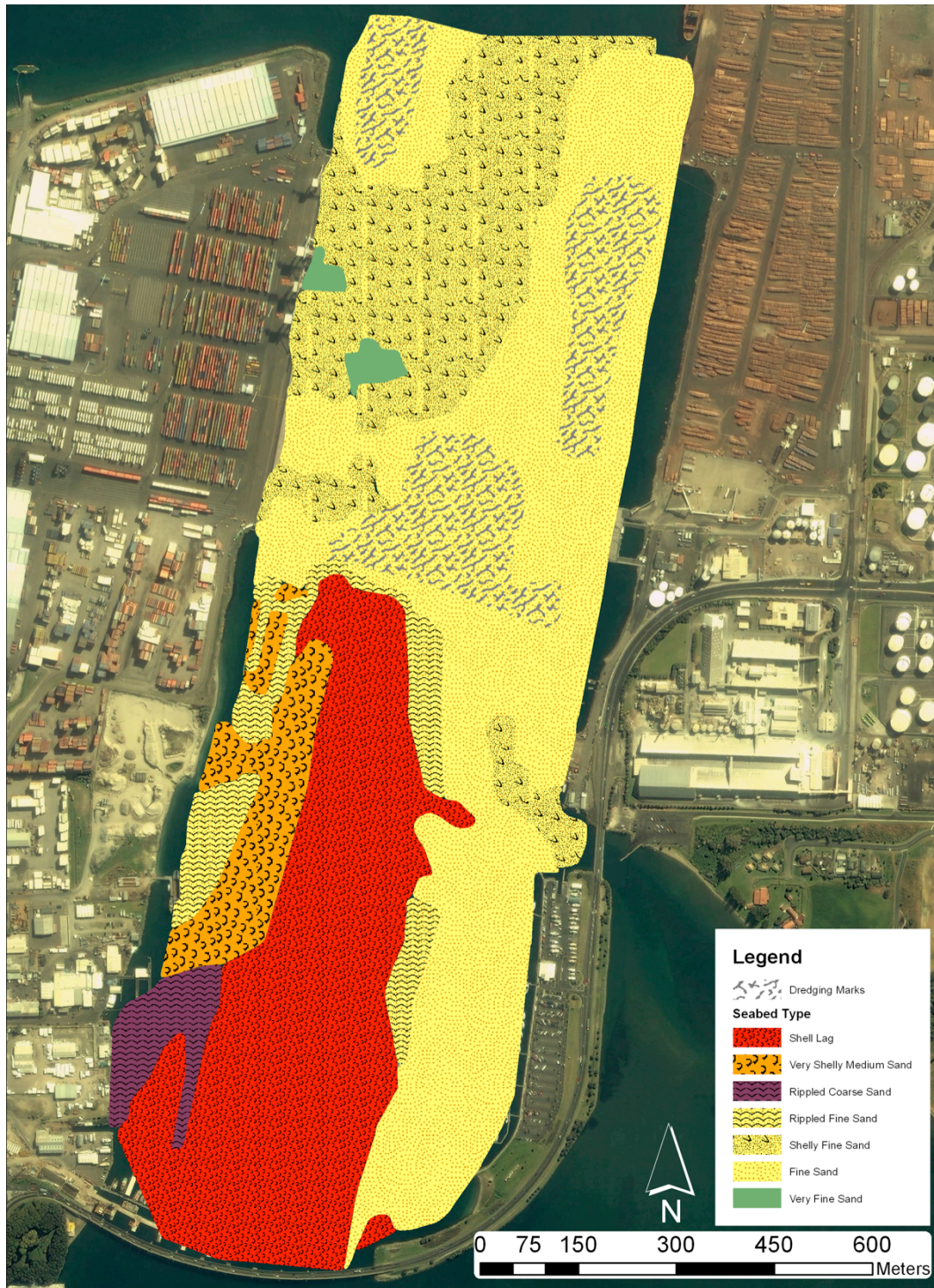


Figure 5.53: Final benthic habitat map of the Tauranga Harbour (July 2011).

5.8. CONCLUSIONS

This chapter presented the acoustic mapping of the Port of Tauranga and the data processing that followed. The mosaicking techniques for multibeam echosounder backscatter data and sidescan sonar reflectivity were developed prior to the two main types of classification: image-based and angular response analysis.

Image based analysis was proven an efficient technique to confirm the areas found by the Angular Response Analysis (ARA) method, even though the high resolution of this survey made the classification complicated. Mixed areas like the central north Stella Passage could be better defined using a combination of 4 and 11 classes unsupervised classifications. Except for this mixed area, all image-based classifications presented a general agreement on the areas delineation.

The ARA generally agreed with the image-based segmentation. The biggest advantage of this technique was that it worked on the raw acoustic data at a lower level than the image based methods that required a mosaicking/simplification phase. However, the resulting seabed classification was only calculated and presented with a coarser resolution (5 m in this study) than what the mosaics offered (0.2 m for MBES and SSS). The grain size provided by the ARA was found to correlate strongly with both the grain size from the sediment sampling and the shell coverage from the ground truthing operations, making the ARA a strong tool to predict the seabed characteristics. However, the ARA only supports sediment classes from clay ($\Phi > 8$) to gravel ($\Phi = -1$). In this study the sediment class results from the ARA were not objectively used as such, but allowed for a relative classification of the various facies encountered in the area. For example, the gravel areas provided by the ARA turned out to be shell lags or very coarse sand with a high shell density.

The other problem encountered with the ARA was the intrinsic nature of the result presentation. As the acoustic signatures were calculated over a stack of consecutive pings for each side of the vessel track, only a low-resolution sediment

type map could be created. This posed a problem when a transition in sediment type was encountered inside a patch, leading to an uncharacteristic angular response.

Other classification techniques were also investigated without success. The Triton Perspective SeaClass (Triton Imaging) module is based on a supervised method based on a neural net training set. This software was tried on both the SSS and the MBES mosaics. The final map resolution is dependent upon the training set chosen grid size. QTC Swathview (Qeuster Tangent) utilizes multivariate statistical processing (Principal Components Analysis) to classify both MBES and SSS data without the need of the mosaic processing. Both these softwares were tested on the Tauranga Harbour dataset but unfortunately the results were not proven efficient, due to mostly a lack of time to get fully familiar with these programs.

Overall, the complexity of the local sedimentation and environment caused difficulties for producing a seabed characterization chart. The depth gradient, the acoustic data fine resolution, the shell coverage variability, the relative uniformity of the sediment grain size and the influence of the diverse constructions made the reflectivity segmentation and interpretation more complicated than the relatively flat areas where the backscatter analysis procedures are mostly used to discriminate between high contrast sandy and rocky areas. Consequently, techniques commonly used to discriminate high-variability/low resolution regions were here adapted to a mostly sandy/high resolution area.

5.9. REFERENCES:

- Anderson, J. T., Holliday, D. V., Kloser, R., Reid, D., Simard, Y., Brown, C. J., et al. (2007). *Acoustic seabed classification of marine physical and biological landscapes*: International Council for the Exploration of the Sea.
- ESRI ArcGis. (2010). *Image Classification toolbar introduced at ArcGIS 10*. Retrieved from <http://blogs.esri.com/esri/arcgis/2010/08/09/image-classification-toolbar-introduced-at-arcgis-10/>
- Fonseca, L., & Calder, B. R. (2005). Geocoder: An Efficient Backscatter Map Constructor *U.S. Hydrographic Conference* (San Diego, CA.:
- Fonseca, L., & Mayer, L. (2007). Remote estimation of surficial seafloor properties through the application Angular Range Analysis to multibeam sonar data. *Marine Geophysical Researches*, 28(2), 119-126. 10.1007/s11001-007-9019-4
- Geographic Imaging by ERDAS. (2009). *Image Analysis for ArcGIS*. 260
- Kongsberg Maritime. (2001). *EM3000 Multibeam echo sounder, Operator Manual, Base Version* (160615/I).
- Leica Geosystems. (2006). *ERDAS Imagine 9.1 Help*.
- Maddock, D. (2010). *Beam Patterns in GEOCODER*: Hypack Inc.,
- Pohner, F., Bakke, J., Nilsen, O., Kjaer, T., & Fonseca, L. (2007). Integrating imagery from hull mounted sidescan sonars with multibeam bathymetry *U.S. Hydrographic Conference* (Norfolk, VA, USA:
- Quester Tangent. *QTC Swathview Seabed Classification*. Retrieved from <http://www.questertangent.com/seabed-classification/seabed-classification-products/qtc-swathview-seabed-classification/>
- Rzhanov, Y., Linnett, L. M., & Forbes, R. (2000). Underwater video mosaicing for seabed mapping (pp. 224-227):
- Starfish - Seabed Imaging Systems. (2012) Retrieved from <http://www.starfishsonar.com>
- Triton Imaging. *Triton SeaClass, Advanced Seabed Classification*. Retrieved from <http://www.tritonimaginginc.com/site/content/products/modules/seaclass/>

CHAPTER 6 - DISCUSSION AND CONCLUSIONS

6.1. OVERVIEW

This chapter discusses the results and findings of this study, and summarises how the original objectives were reached. It starts with a comparison of the benthic mapping programme undertaken for this study, with the previous studies of the Tauranga Harbour discussed in the Chapter 2. This will be followed by a critical evaluation of the processing methods. The chapter ends with a summary of the achievements of this study in relation to the objectives, and recommendations for further research.

6.2. COMPARISON TO PREVIOUS STUDIES

A total of 1.1 km² has been mapped at high resolution within the Tauranga Harbour Stella Passage and Town Reach channels, and within the Tauranga Bridge Marina using modern hydrographic equipment in conjunction with an extensive ground-truthing program. This program consisted of the most advanced and complete survey undertaken in this area, even though it has been extensively investigated since the early Harbour developments in the late 1970s. These developments have included capital and more numerous maintenance dredging campaigns.

Based on previous studies, seven substrate classes were identified in the work area, namely: shell lag, very shelly medium sand, rippled coarse sand, rippled fine sand, shelly fine sand, fine sand and very fine sand. Overall, the work area shows a clear domination of the fine sand class followed by the shell lag facies (Fig. 6.1). The results from the previous studies (all scanned from paper reports) were geo-referenced and digitized in ArcGis Desktop 10 for comparison with this thesis. Figure 6.3 summarises the surficial sediment distribution derived from the results of the Tauranga Harbour Study by Healy (1985). This distribution is based on the

paper sidescan sonograms (Fig. 6.2), which were scanned and geo-referenced to produce the interpreted sediment facies map.

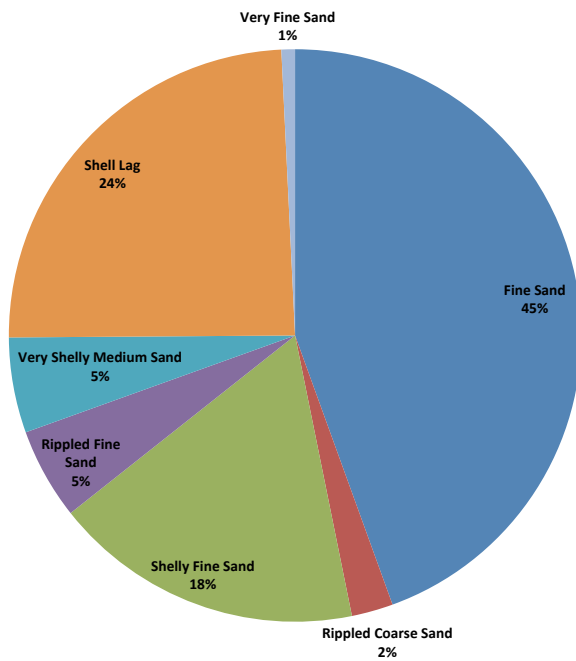


Figure 6.1: Final distribution of the 7 seabed classes of the benthic habitat map of the Tauranga Harbour, July-August 2011.



Figure 6.2: Sidescan sonar paper recordings of the Tauranga Harbour Study (Healy, 1985)

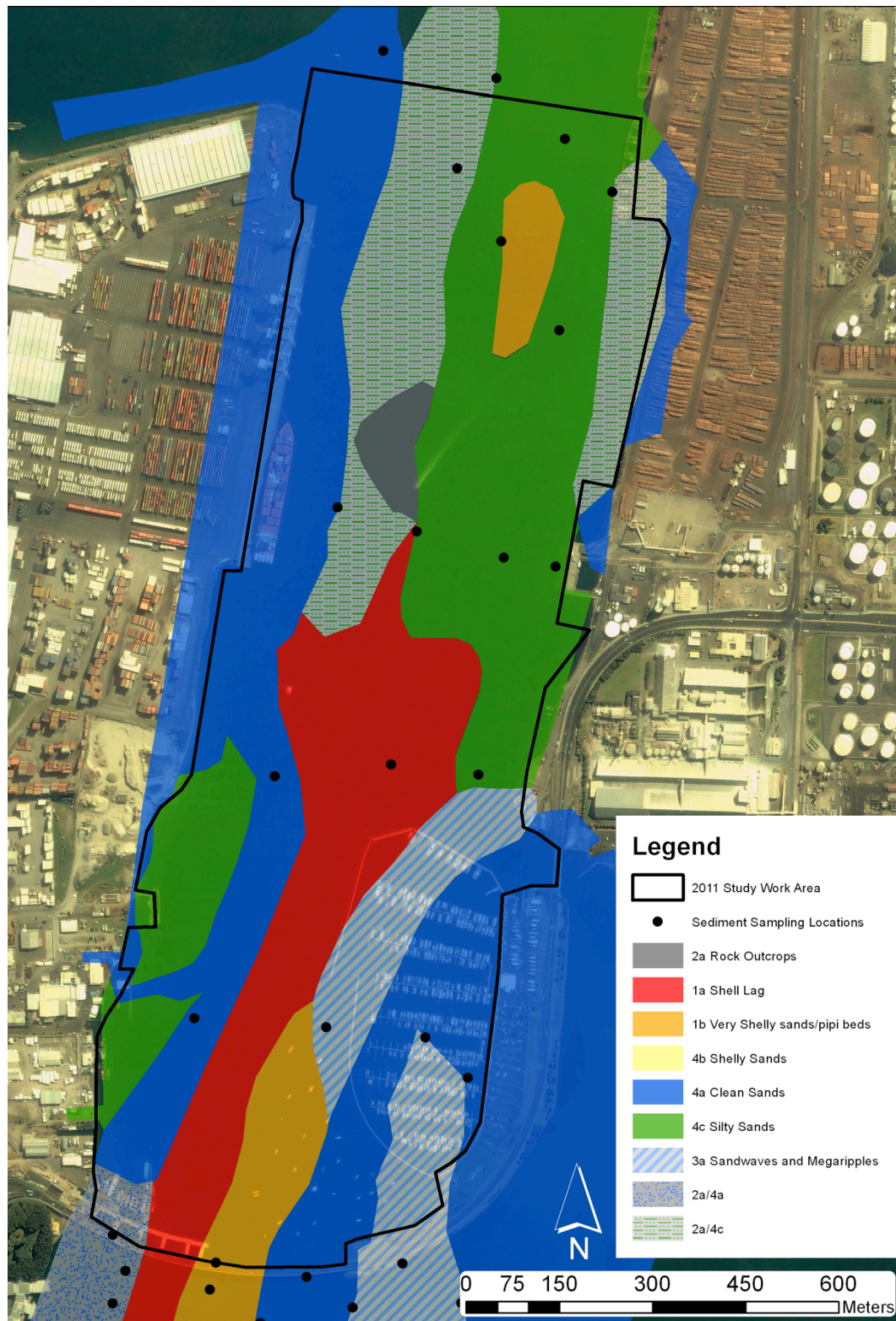


Figure 6.3: Tauranga Harbour Study (Healy, 1985) sediment facies map derived from a sidescan sonar survey and sediment sampling.

6.2.1. Stella Passage

The Stella Passage was highly dominated by fine sand-sized sediment with the exception of two small areas of very fine sand next to the Container Terminal. These two patches of finer sediment also represent deeper areas clearly visible on the bathymetry. A reason for the presence of these two areas was discussed in section “5.3.2 Bathymetry Processing”, where the final hypothesis is that they result from the impact of the propeller wash from either container ships or tugboats during docking operations.

Stella Passage also features a large area of shelly fine sand that was easily identified during both the ground-truthing operations and the hydrographic survey. However, the SSS and MBES mosaics showed this area as a region of mixed reflectivity. This shelly fine sand region could actually be more patchy or diverse than the ground-truthing operations could identify. Finally, there are three main areas of dredging characterised by the clear dredge scars on both MBES and SSS mosaics. The whole Stella Passage area is subject to an on-going dredging maintenance program, so these regions probably represent the most recent work in August 2011.

The study by Davies Colley (1976) had identified sand dunes on the 4.6 m deep west bank of the Stella Passage. These sand waves are no longer present as the 1992 dredging program increased the water depth and reduced the local current velocity.

The Tauranga Harbour Study (Barnett, 1985; Black, 1985; Healy, 1985) was undertaken during the development of the Sulphur Point reclamation and before the 1992 capital dredging program. Figure 6.3 presents the result of the sediment facies study during the Tauranga Harbour Study. The most noticeable feature is the grey rock outcrop in the central Stella Passage. A close inspection at the MBES and SSS reflectivity mosaics does not bring any evidence that this rock area is still present. In 1985, the west side of the Stella Passage was dominated with fine sand and mixed silty sands-rock outcrops. The east side featured a large

bank of silty sand included a smaller area of very shelly sand and another patch of mixed rock outcrop-silty sand. None of these layers are present anymore. As with the sand dunes found during the 1976 study, these surface facies have probably been removed during the 1992 dredging program.

The Channel Widening and Deepening Program (Healy, McCabe, Thompson, & Port of Tauranga Limited., 1991) was preceded by a study of a set of historic boreholes and additional sediment cores in the Stella Passage. Sample D76, in the central north Stella Passage in front of the Sulphur Point, showed black fine silty sands on surface. Sample D75, in the centre of the Stella Passage in front of the Tanker Berth featured surficial black medium sands with pipi shells. The interpreted sediment facies map showed a wide area of silt deposit in the central northern Stella Passage and a large area of shelly sand immediately north of it. This silty patch was removed during the capital dredging, and can no longer be found in the 2011 study. Since this area was originally located between two shelly sand areas, it appears that these two regions connected after the dredging program was complete to form the large shelly sand region that is now forming the majority of the northern Stella Passage.

The study by Brannigan (2009) included a large sidescan sonar survey, with an extensive sediment sampling campaign. The southernmost limit of the investigated area included the Stella Passage, where the surficial facies was found to be a uniform “very fine sand with no shell coverage” covering the whole area. However, the 2011 study located areas of partial shell coverage in the north Stella Passage. This result can only be explained by the fact that the 2009 study only covered the Stella Passage with a sidescan sonar survey, while no sediment sample or underwater video was performed in the area. Also, the sidescan sonar used at the time had a lower resolution than the system used for the 2011 project. Therefore, the mixed acoustic signal areas picked up by the MBES and SSS might not have been identified as shell covered facies.

6.2.2. Town Reach and Tauranga Bridge Marina

This study identified a Town Reach region largely dominated by a shell lag facies on the shallow shelf between the Tauranga Bridge and the dredged Stella Passage. A smaller very shelly medium sand area is also present, located on the western side of this shell lag. Rippled fine and medium sands surround these densely covered areas. Fine sands dominate seabed under the Bridge Marina, while the Mareroa Point channel features a shelly fine sand bank.

The Tauranga Harbour Study (Barnett, 1985; Black, 1985; Healy, 1985) also investigated the Town Reach before the construction of the Tauranga Harbour Bridge (1988) and Bridge Marina (1995). Figure 6.3 shows that a shell lag was already present, generally around the same location as found during the 2011 study. A long clean sand bank linked the southwestern corner of the Town Reach to the Stella Passage and Sulphur Point. Alternate silty sand patches were also present along the western side. Sandwaves and megaripples were found where the Bridge Marina is now. There is still some evidence of sandwaves inside the Marina but they seem to be aligned with the pontoon piles and could be the result of pier scouring effect in a high velocity environment, rather than relics of the pre-causeway situation. However, the 2011 SSS survey also identified clear sandwaves to the north of the Tauranga Bridge's eastern end (Fig.5.9).

Overall, the situation around Town Reach and Bridge Marina seems to have undergone little change since the 1985 study. The construction of the Bridge and its artificial causeway may have increased the current velocities on the flat shelf, leading to an overall increase in grain size and shell density. Further, the construction of the Marina may have sheltered the eastern side from the ebb tidal currents responsible for the now disappeared megaripples where the Marina stands. The creation of the artificial causeway for the Bridge eastern landing, and the resulting funnelling of the ebb-tide currents around Whareroa Point, may have increased the velocities locally, leading to the formation of the narrow shelly sand bank now visible. The slight difference of location of the various facies can be attributed to the low precision of the data acquisition system (analogue sidescan

sonar) and positioning devices (dual sextant) used in 1982-85.

The effect of the Tauranga Bridge construction was the subject of a consulting report (Beca Carter Hollings and Ferner Ltd, 1985). The local benthic species were studied in a series of samples around the proposed artificial bank, and the results of the 1985 Tauranga Harbour Study's hydrodynamic model were used to predict the influence of the Bridge construction on the local current regimes. The flood current was predicted to increase, while the ebb velocity would remain unchanged. The model did not predict any velocity change under the minor bridge by Whareroa Point, or over the whole area as a consequence of the artificial causeway. A shallow sublittoral sand bank was originally located north of the Bridge's eastern junction with the artificial causeway. In terms of benthic habitats, the consultants predicted little change to the local communities.

The 2011 study, as detailed before, found an increase in the shell coverage on the Town Reach shelf and within the Whareroa channel. A shallow ridge is still present north of the eastern side of the Bridge within the mooring area next to the Bridge Marina, and could represent what is left of the sublittoral bank identified in 1985.

Butler (Butler, 1999) studied the benthic communities of the Stella Passage. A total of 18 sites were sampled four times and he identified four distinct community groups (Fig. 2.41 and 2.42). This 2011 study confirmed these results, and found that a greater density of pipi shells occurs on the Town Reach shelf. A comparison with a hydrodynamic model found a correlation between dense shell communities and high current velocities. In the Stella Passage, Butler (1999) identified fine black silt sediment with low current velocities, this facies being also present in the Bridge Marina. Once again, the 2011 study results are similar. Butler's group 4, comprising the turret shell (*Maoricolpus roseus*), was also found in areas very similar to the 2011 study. Overall, the 2011 ground truthing operations were consistent with Butler (1999) and confirmed the established relationship between current velocity and shell density.

An environmental assessment of a proposed modification to the Bridge Marina's

northern breakwater included a hydrodynamic model study and benthic invertebrate investigation (Tonkin & Taylor Ltd, 2010). In the six samples collected north of the Marina, the sediment was found to be mainly “marine sands and silts with an accumulation of shell hash”. None of the bivalves and gastropods identified in their consulting report were found during the 2011 ground-truthing operations.

6.2.3. Summary

The sediment and benthic community maps resulting from the 2011 hydrographic survey and ground-truthing were compared to several previous studies that either focused only on the Stella Passage, the Town Reach/Bridge Marina area or both. Several changes that occurred between the studies can be recognised:

- The 1992 dredging campaign removed most of the surficial sediment facies identified between 1982 and 1985, including rock outcrops and mixed rock/sand areas. Another consequence of the dredging was the reduction of the current velocities in the Stella Passage.
- The dense shell coverage on the Town Reach shelf was present before the first investigations of the Port of Tauranga were performed. Most likely, the rippled sand areas surrounding it were also present. However, it seems to have increased in size since the 1985 study. If the shell coverage is positively correlated with the current velocity, this expansion of the shell lag could be a consequence of the construction of the Tauranga Harbour Bridge and the narrowing of the channel under it by the causeway.
- The sandwaves identified in the 1985 Tauranga Harbour Study in the Bridge Marina area have disappeared, as a consequence of either the Bridge or Marina construction. Only a very small area of rippled mixed sediment is still present north of the Bridge’s more eastern piles.
- A shelly fine sand patch has been created in the Whareroa Channel that was not identified in any of the earlier studies presented here. This could be the result of an increase in the current velocity as a consequence of the Bridge causeway construction.

Further, there are some obvious relationships between the shells present and hydrodynamics and dominant sediment type:

- The tidal current velocities have a direct impact on the shell coverage density, with stronger currents being associated with a denser coverage.
- The sediment type influences the shell coverage species composition. Fine and medium sands mostly host pipi, while turret shells favour finer sediments, such as silty sands. The diverse starfish species seem to be found mostly in fine sand areas, with no other obvious surficial shell coverage.

6.3. GEOCODER

FM Geocoder is an innovative tool for the analysis of multibeam echosounder backscatter data. The software is user-friendly, well documented and time saving. It is in constant improvement and the support is excellent, whether from regular webinar trainings, or direct communication with the software developers. It utilizes raw MBES recordings, allowing the operator to keep a complete control on how the data is modified or sampled. The creation of an accurate backscatter mosaic can be very quick, and beam pattern correction is also very simple, even for new operators. The Angular Response Analysis is a straightforward process and provides all necessary results in an understandable way.

The Fledermaus suite, in which the Fledermaus Geocoder Toolbox (FMGT) is included, is fully integrated with ESRI ArcGis Desktop, making the results of multibeam data processing easily available for mapping and comparison to other datasets. FMGT has proven efficient for automatic seabed texture determination, but the final results have to be carefully checked before final interpretation.

6.3.1. Angular Response Analysis versus ground-truthing

As described earlier, the Angular Response Analysis was found to give comparable results to the ground-truthing outputs. The grain size “tendency” (coarse or fine) was right, but the absolute classification provided by the ARA was usually slightly different from the one given by the sediment sample analysis.

The initial cause of the observed discrepancies was considered to be a potential inaccuracy in the positioning of the grab samples or the underwater videos. Even though a Differential GPS system was used, the boat could drift during the time required for the dredge/camera to descend and be recovered. However, the difference between the ARA and the observed data was consistent over the whole work area, indicating that it was a systematic error.

The sediment sampling technique could also be a factor. Classification from the

ARA included large regions of very fine sand and silty material. These facies did not appear during the ground-truthing analysis. The Ponar dredge used during this study could lose the very fine material during its recovery. Often, some shells would stop the dredge from closing completely, allowing finer sediment to be washed out as the dredge was recovered. The sampling was repeated when this problem was apparent. However, even coarse sediment could create a space sufficient enough between the “claws” of the dredge for the fine sediment to be lost. Using divers for the sediment sampling operations could solve this problem.

The intrinsic design of Geocoder did not allow sub-classification of the shell coverage. The results only covered the range from clay ($\Phi < 8$) to the sand/gravel limit ($\Phi - 1$), as this algorithm was designed to classify sand and mud sedimentary facies. Therefore, this classification technique needed to be adapted for the facies discovered during the ground-truthing operations in the Port of Tauranga. The ARA results could not be used as the only source of sediment type for the final classification, but had to be combined with image-based segmentation and ground-truthing data to produce a final surficial seabed map.

6.3.2. Limitations of Geocoder

The Angular Response Analysis works well on homogeneous areas. However, regions presenting a variable morphology or sediment type will often be misclassified due to an inherent limitation in the design of the Geocoder algorithm. The ARA process assumes a homogenous seabed for each of the starboard and port side beams, and each angular response curve is averaged over a patch representing a stack of consecutive pings. Consequently, heterogeneous areas are simplified in both across and along-track dimensions. The resulting ARA class is then actually a combination of individual sediment types, and does not represent the true seabed characteristics. Geocoder is based on the measure of backscatter strength across the grazing angle range. This technique requires an accurate calibration of the MBES system. This can be performed using the “Beam Pattern Correction” tool built in FMGT, but requires knowledge of the exact sediment type of a homogenous surveyed area, making ground-truthing operations mandatory for the seabed characterisation.

6.4. SUMMARY OF THE VARIOUS CLASSIFICATION METHODS

The major difference between the ARA and the segmentation of reflectivity mosaics is that the first provides a grain size estimation based on acoustic characteristics of the seabed, while the second divides the area into homogeneous regions but does not label them (Preston, 2012). They will, however, both need a set of ground-truth data that will be used to label the clusters for image classification and for calibration of the sonar for the ARA.

Both automatic and manual methodologies for classification have advantages and disadvantages (Table 6.1). The choice between them requires the consideration of time, cost, skill, data quality and calculation capacities. The automatic technique can provide a good outline of the seabed types encountered in the area, which can then be refined using an image-based segmentation that preserves the complex geometries of the seafloor. Methods that incorporate a combination of both automatic and manual classifications are being developed in order to keep the best of each technique.

Table 6.1: Summary of the advantages and disadvantages for manual and automatic classifications of acoustic seabed data.

	AUTOMATIC CLASSIFICATION	MANUAL CLASSIFICATION
STRENGTHS	<ul style="list-style-type: none"> - Time saving - Keeps the gradual changes in sediment type - Produces a statistical report 	<ul style="list-style-type: none"> - Good integration of the various datasets (bathymetry, backscatter,...) - Data manipulation and combination (hillshade...) allows for a better recognition of features
WEAKNESSES	<ul style="list-style-type: none"> - Also classifies artifacts - Poor resolution (data processed over patches of seabed) 	<ul style="list-style-type: none"> - Requires more time - Subjective - Requires an experienced operator to recognize patterns and features - Requires a good mosaicking procedure

6.5. ACHIEVEMENTS OF THE STUDY

All the specified objectives for this study were achieved.

1) To investigate the existing methods of seabed classification based on acoustic data.

This objective was achieved through the study of the most researched classification techniques. The automatic acoustic-based techniques were compared to image-based segmentations. The supervised and unsupervised methods of image-based classification were also compared.

2) To conduct an extensive hydrographic survey of the Tauranga Stella Passage, Town Reach and Bridge Marina areas, followed by ground-truthing operations.

This objective was achieved by conducting the most complete, high-resolution and extensive survey using modern hydrographic survey techniques in the area. A dense grid of 42 sediment samples and underwater videos formed the ground truthing dataset to be compared to the acoustic data processing outputs.

3) To produce bathymetry maps and reflectivity mosaics based on acoustic data from the multibeam echosounder and sidescan sonar.

A 0.5 m resolution bathymetry chart was created using the multibeam echosounder in the Tauranga Stella Passage, Town Reach and Bridge Marina. Seabed reflectivity mosaics based on the MBES backscatter (0.15 m resolution) and sidescan sonar (0.20 m resolution) were produced that covered the same area. The two acoustic seabed-mapping techniques, MBES and SSS, proved to be very complementary for this study. The MBES also provided co-registered backscatter and bathymetry.

4) To process the different datasets using diverse approaches and to compare their potential for seabed characterization and classification.

Both MBES and SSS mosaics were classified using supervised and unsupervised image-based classifications. The sidescan sonar data was proven to be inefficient at a mosaic scale, as the reflectivity contrast was made unreliable by the water

depth variations on this hull-mounted system. However, a close inspection of single SSS transects permitted a better definition of some mixed seabed areas. The MBES backscatter mosaic was the main source of information for the classification process. The automatic Angular Response Analysis was used to outline the grain size variations in the area while the image-based segmentation was used to provide a fine resolution segmentation of the various seabed types.

5) To create a fine-scale surficial sediment map and to compare it to the previous studies.

A combined use of the outputs from the ground truthing results, the Angular Response Analysis and the image-based segmentation of both MBES and SSS mosaics, led to the production of the benthic habitat map presented in the Figure 5.53. The seabed facies discovered during this study were compared with the results of various past studies to assess the influence of the consecutive dredging campaigns and the construction of the Tauranga Bridge and Bridge Marina.

6.6. RECOMMENDATIONS FOR FUTURE RESEARCH

This study was the most recent of a sequence of investigations undertaken at the Port of Tauranga. The general method followed was basically the same as during the Tauranga Harbour Study in the early 1980s, except that it used modern equipment and processing techniques. The first obvious recommendation for further research would be to keep studying the area and update to the constantly evolving hydrographic survey and classification techniques. There will be a need to assess the impact of the Bridge Marina's solid breakwater on the local sedimentation and the effects of the Stella Passage planned modifications on the benthic communities.

An issue remains regarding the almost complete disappearance of the very fine sand and silty seabed regions that were always present in previous studies. The sediment sampling technique used for ground-truthing seems to have been a problem. The Ponar grab sample that was used may have lost the fine part of the surficial sediment during its recovery. Getting divers to collect the samples in watertight containers could solve this issue.

Unfortunately, not enough time was left to investigate multivariate analysis techniques of multibeam echosounder for seabed classification in this study. Software packages exist for this type of analysis that have been proven effective by numerous researchers, but the trial version of QTC Swathview that was obtained a month before the end of this thesis was insufficient to fully investigate the potential of such methodology. A complete comparison of Geocoder and QTC Swathview using the Tauranga dataset, with its shell coverage details, would present a challenging research topic.

6.7. REFERENCES

- Barnett, A. G. (1985). *Tauranga Harbour study, part I Overview, Part III Hydrodynamics*. N.Z.: Bay of Plenty Harbour, New Zealand Ministry of Works Development, Dansk hydraulisk Institut, University of Waikato
- Beca Carter Hollings and Ferner Ltd. (1985). *Tauranga Harbour Bridge: an environmental impact assessment*. Beca Carter Hollings and Ferner Ltd, Tauranga Harbour Bridge Committee, Bioresarches Ltd, Hegley Acoustic Consultants, Boffa Miskell Partners. Retrieved from <http://books.google.co.nz/books?id=I87IMAAACAAJ>
- Black, K. P. (1985). *Tauranga Harbour study, part IV Text, Figures and Tables*. Bay of Plenty Harbour, New Zealand Ministry of Works Development, Dansk hydraulisk Institut, University of Waikato
- Brannigan, A. M. (2009). *Change in geomorphology, hydrodynamics and surficial sediment of the Tauranga entrance tidal delta system, 2009*. Retrieved from <http://hdl.handle.net/10289/2799>
- Butler, R. J. (1999). *Benthic communities of the Stella Passage region, Tauranga Harbour, New Zealand*.
- Davies-Colley, R. J. (1976). *Sediment dynamics of Tauranga Harbour and the Tauranga Inlet*. University of Waikato.
- Healy, T., McCabe, B., Thompson, G. N., & Port of Tauranga Limited. (1991). *Port of Tauranga Ltd channel deepening and widening dredging programme 1991-92 : environmental impact assessment*. [Tauranga, N.Z.: s.n.]
- Healy, T. R. (1985). *Tauranga Harbour study, part II & V Field Data Collection Programme and Morphological Study*. Bay of Plenty Harbour, New Zealand Ministry of Works Development, Dansk hydraulisk Institut, University of Waikato
- Preston, J. (2012). *Theoretical and Practical Limitations of GeoCoder* (Quester Tangent Corporation).
- Tonkin & Taylor Ltd. (2010). *Tauranga Bridge Marina Ltd, Northern Breakwater Assessment of Environmental Effects*.

Grain Size Analysis, Laser Diffraction



Department of Earth & Ocean Sciences
School of Science and Engineering
The University of Waikato
Private Bag 3105
Hamilton, New Zealand



Department of Earth & Ocean Sciences
School of Science and Engineering
The University of Waikato
Private Bag 3105
Hamilton, New Zealand

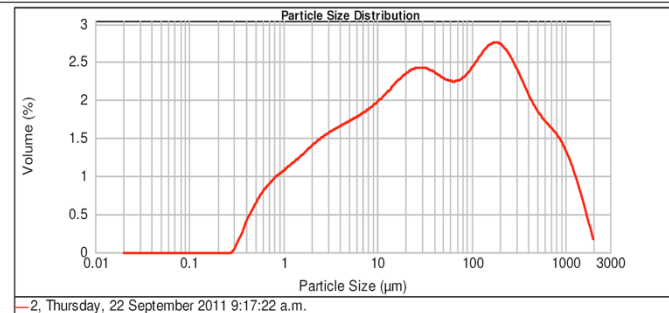
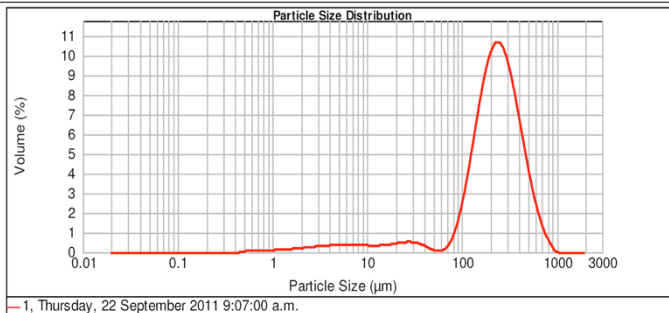
Result Analysis Report

Sample Name: 1	SOP Name: Marine Sediment	Measured: Thursday, 22 September 2011 9:07:00 a.m.
Sample Source & type:	Measured by: sobc1	Analysed: Thursday, 22 September 2011 9:07:01 a.m.
Sample bulk lot ref: 36	Result Source: Measurement	
Particle Name: Marine Sediment	Accessory Name: None	Analysis model: General purpose
Particle RI: 1.500	Absorption: 0.2	Size range: 0.020 to 2000.000 μm
Dispersant Name: Water	Dispersant RI: 1.330	Weighted Residual: 0.524 %
		Sensitivity: Enhanced
		Obscuration: 13.31 %
		Result Emulation: Off
Concentration: 0.0754 %Vol	Span : 1.631	Uniformity: 0.509
Specific Surface Area: 0.155 m^2/g	Surface Weighted Mean D[3,2]: 38.693 μm	Vol. Weighted Mean D[4,3]: 248.264 μm

Result Analysis Report

Sample Name: 2	SOP Name: Marine Sediment	Measured: Thursday, 22 September 2011 9:17:22 a.m.
Sample Source & type:	Measured by: sobc1	Analysed: Thursday, 22 September 2011 9:17:23 a.m.
Sample bulk lot ref: 37	Result Source: Measurement	
Particle Name: Marine Sediment	Accessory Name: None	Analysis model: General purpose
Particle RI: 1.500	Absorption: 0.2	Size range: 0.020 to 2000.000 μm
Dispersant Name: Water	Dispersant RI: 1.330	Weighted Residual: 0.774 %
		Sensitivity: Enhanced
		Obscuration: 14.81 %
		Result Emulation: Off
Concentration: 0.0133 %Vol	Span : 12.826	Uniformity: 3.91
Specific Surface Area: 1.08 m^2/g	Surface Weighted Mean D[3,2]: 5.531 μm	Vol. Weighted Mean D[4,3]: 176.554 μm

d(0.1): 84.294 μm d(0.5): 223.954 μm d(0.9): 449.463 μm d(0.1): 1.842 μm d(0.5): 42.163 μm d(0.9): 542.631 μm

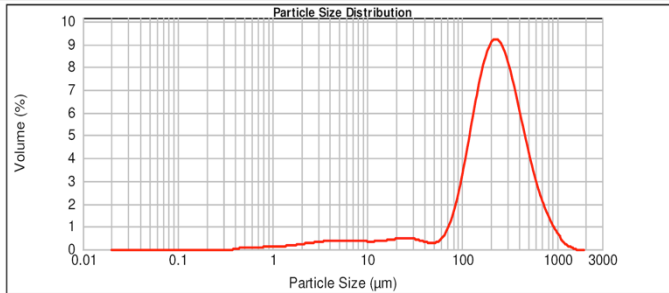


Result Analysis Report

Sample Name: 3
SOP Name: Marine Sediment
Measured: Thursday, 22 September 2011 9:25:59 a.m.
Sample Source & type: Measured by: socb1
Analysed: Thursday, 22 September 2011 9:26:01 a.m.
Sample bulk lot ref: 38
Result Source: Measurement

Particle Name: Marine Sediment	Accessory Name: None	Analysis model: General purpose	Sensitivity: Enhanced
Particle RI: 1.500	Absorption: 0.2	Size range: 0.020 to 2000.000 um	Obscuration: 15.86 %
Dispersant Name: Water	Dispersant RI: 1.330	Weighted Residual: 0.493 %	Result Emulation: Off
Concentration: 0.0855 %Vol	Span : 2.034	Uniformity: 0.633	Result units: Volume
Specific Surface Area: 0.169 m ² /g	Surface Weighted Mean D[3,2]: 35.585 um	Vol. Weighted Mean D[4,3]: 262.948 um	

d(0.1): 66.638 um d(0.5): 218.472 um d(0.9): 510.910 um



3, Thursday, 22 September 2011 9:25:59 a.m.

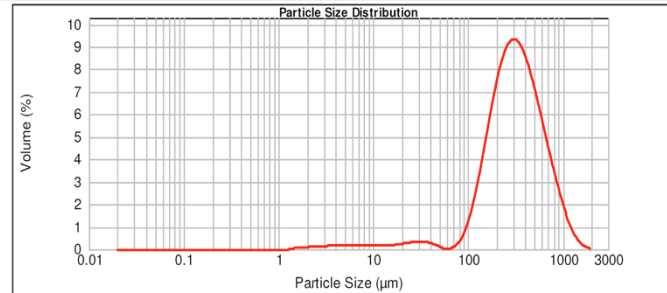
Size (µm)	Volume In %	Size (µm)	Volume In %	Size (µm)	Volume In %	Size (µm)	Volume In %	Size (µm)	Volume In %
0.050	2.59	3.900	7.17	63.000	90.24	2000.000			
3.900		63.000		2000.000					

Result Analysis Report

Sample Name: 4
SOP Name: Marine Sediment
Measured: Thursday, 22 September 2011 9:31:15 a.m.
Sample Source & type: Measured by: socb1
Analysed: Thursday, 22 September 2011 9:31:16 a.m.
Sample bulk lot ref: 39
Result Source: Measurement

Particle Name: Marine Sediment	Accessory Name: None	Analysis model: General purpose	Sensitivity: Enhanced
Particle RI: 1.500	Absorption: 0.2	Size range: 0.020 to 2000.000 um	Obscuration: 14.73 %
Dispersant Name: Water	Dispersant RI: 1.330	Weighted Residual: 0.744 %	Result Emulation: Off
Concentration: 0.2078 %Vol	Span : 1.873	Uniformity: 0.593	Result units: Volume
Specific Surface Area: 0.0591 m ² /g	Surface Weighted Mean D[3,2]: 101.534 um	Vol. Weighted Mean D[4,3]: 371.718 um	

d(0.1): 131.552 um d(0.5): 307.675 um d(0.9): 707.934 um



4, Thursday, 22 September 2011 9:31:15 a.m.

Size (µm)	Volume In %	Size (µm)	Volume In %	Size (µm)	Volume In %	Size (µm)	Volume In %	Size (µm)	Volume In %
0.050	0.79	3.900	3.81	63.000	95.40	2000.000			
3.900		63.000		2000.000					

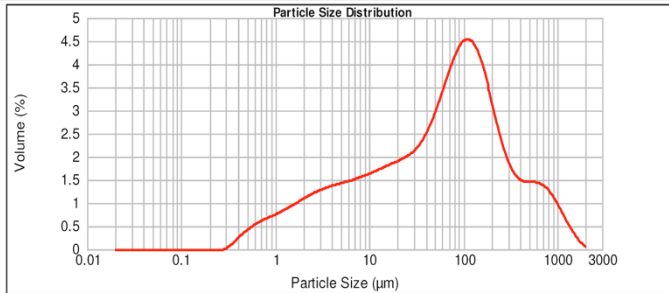
Result Analysis Report

Sample Name: 5
SOP Name: Marine Sediment
Measured: Thursday, 22 September 2011 9:37:04 a.m.
Sample Source & type: Measured by: socb1
Analysed: Thursday, 22 September 2011 9:37:05 a.m.
Sample bulk lot ref: 40
Result Source: Measurement

Particle Name: Marine Sediment
Accessory Name: None
Analysis model: General purpose
Sensitivity: Enhanced
Particle RI: 1.500
Absorption: 0.2
Size range: 0.020 to 2000.000 μm
Obscuration: 19.07 %
Dispersant Name: Water
Dispersant RI: 1.330
Weighted Residual: 0.597 %
Result Emulation: Off

Concentration: 0.0232 %Vol
Span : 6.125
Uniformity: 1.97
Result units: Volume
Specific Surface Area: 0.807 m^2/g
Surface Weighted Mean D[3,2]: 7.438 μm
Vol. Weighted Mean D[4,3]: 151.521 μm

d(0.1): 2.726 μm d(0.5): 66.409 μm d(0.9): 409.461 μm



5, Thursday, 22 September 2011 9:37:04 a.m.

Size (μm)	Volume In %	Size (μm)	Volume In %	Size (μm)	Volume In %	Size (μm)	Volume In %	Size (μm)	Volume In %
0.050	13.07	3.900	35.58	63.000	51.25	2000.000			
3.900		63.000		2000.000					

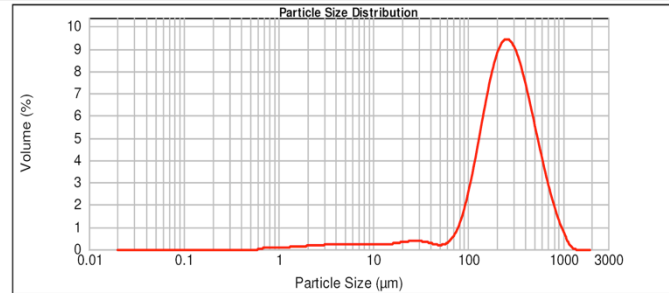
Result Analysis Report

Sample Name: 6
SOP Name: Marine Sediment
Measured: Thursday, 22 September 2011 9:43:01 a.m.
Sample Source & type: Measured by: socb1
Analysed: Thursday, 22 September 2011 9:43:02 a.m.
Sample bulk lot ref: 41
Result Source: Measurement

Particle Name: Marine Sediment
Accessory Name: None
Analysis model: General purpose
Sensitivity: Enhanced
Particle RI: 1.500
Absorption: 0.2
Size range: 0.020 to 2000.000 μm
Obscuration: 14.37 %
Dispersant Name: Water
Dispersant RI: 1.330
Weighted Residual: 0.649 %
Result Emulation: Off

Concentration: 0.1192 %Vol
Span : 1.837
Uniformity: 0.578
Result units: Volume
Specific Surface Area: 0.103 m^2/g
Surface Weighted Mean D[3,2]: 58.132 μm
Vol. Weighted Mean D[4,3]: 294.013 μm

d(0.1): 99.376 μm d(0.5): 249.770 μm d(0.9): 558.255 μm



6, Thursday, 22 September 2011 9:43:01 a.m.

Size (μm)	Volume In %	Size (μm)	Volume In %	Size (μm)	Volume In %	Size (μm)	Volume In %	Size (μm)	Volume In %
0.050	1.59	3.900	4.85	63.000	93.56	2000.000			
3.900		63.000		2000.000					



Department of Earth & Ocean Sciences
 School of Science and Engineering
 The University of Waikato
 Private Bag 3105
 Hamilton, New Zealand



Department of Earth & Ocean Sciences
 School of Science and Engineering
 The University of Waikato
 Private Bag 3105
 Hamilton, New Zealand

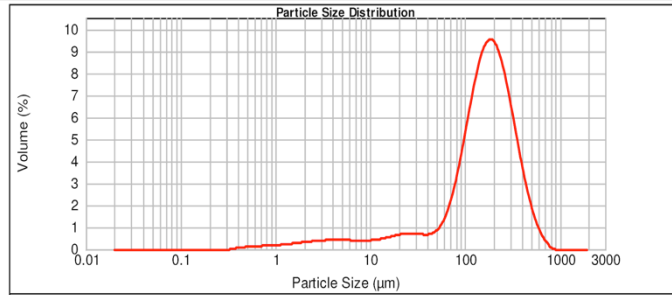
Result Analysis Report

Sample Name: 7
SOP Name: Marine Sediment
Measured: Thursday, 22 September 2011 9:47:48 a.m.
Sample Source & type: Measured by: socb1
Analysed: Thursday, 22 September 2011 9:47:49 a.m.
Sample bulk lot ref: 42
Result Source: Measurement

Particle Name: Marine Sediment
Accessory Name: None
Analysis model: General purpose
Sensitivity: Enhanced
Particle RI: 1.500
Absorption: 0.2
Size range: 0.020 to 2000.000 um
Obscuration: 16.56 %
Dispersant Name: Water
Dispersant RI: 1.330
Weighted Residual: 0.531 %
Result Emulation: Off

Concentration: 0.0630 %Vol
Span : 1.971
Uniformity: 0.576
Result units: Volume
Specific Surface Area: 0.247 m²/g
Surface Weighted Mean D[3,2]: 24.255 um
Vol. Weighted Mean D[4,3]: 184.773 um

d(0.1): 26.145 um d(0.5): 164.826 um d(0.9): 350.988 um



7, Thursday, 22 September 2011 9:47:48 a.m.

Size (µm)	Volume In %	Size (µm)	Volume In %	Size (µm)	Volume In %	Size (µm)	Volume In %	Size (µm)	Volume In %
0.050	3.76	3.900	11.07	63.000	85.17	2000.000			
3.900		63.000		2000.000					

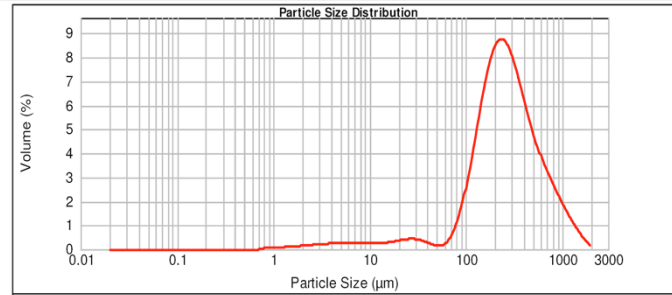
Result Analysis Report

Sample Name: 8
SOP Name: Marine Sediment
Measured: Thursday, 22 September 2011 9:54:25 a.m.
Sample Source & type: Measured by: socb1
Analysed: Thursday, 22 September 2011 9:54:27 a.m.
Sample bulk lot ref: 43
Result Source: Measurement

Particle Name: Marine Sediment
Accessory Name: None
Analysis model: General purpose
Sensitivity: Enhanced
Particle RI: 1.500
Absorption: 0.2
Size range: 0.020 to 2000.000 um
Obscuration: 14.61 %
Dispersant Name: Water
Dispersant RI: 1.330
Weighted Residual: 0.718 %
Result Emulation: Off

Concentration: 0.1273 %Vol
Span : 2.391
Uniformity: 0.747
Result units: Volume
Specific Surface Area: 0.0969 m²/g
Surface Weighted Mean D[3,2]: 61.894 um
Vol. Weighted Mean D[4,3]: 337.874 um

d(0.1): 98.584 um d(0.5): 252.641 um d(0.9): 702.700 um



8, Thursday, 22 September 2011 9:54:25 a.m.

Size (µm)	Volume In %	Size (µm)	Volume In %	Size (µm)	Volume In %	Size (µm)	Volume In %	Size (µm)	Volume In %
0.050	1.49	3.900	5.24	63.000	93.27	2000.000			
3.900		63.000		2000.000					

Result Analysis Report

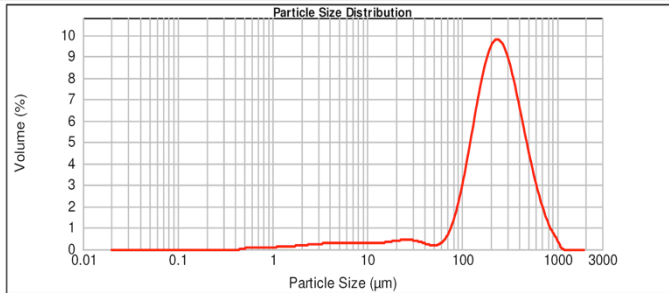
Sample Name: 9
SOP Name: Marine Sediment
Measured: Thursday, 22 September 2011 9:59:13 a.m.
Sample Source & type: Measured by: socb1
Analysed: Thursday, 22 September 2011 9:59:14 a.m.
Sample bulk lot ref: 44
Result Source: Measurement

Particle Name: Marine Sediment	Accessory Name: None	Analysis model: General purpose	Sensitivity: Enhanced
Particle RI: 1.500	Absorption: 0.2	Size range: 0.020 to 2000.000 um	Obscuration: 16.90 %
Dispersant Name: Water	Dispersant RI: 1.330	Weighted Residual: 0.717 %	Result Emulation: Off
Concentration: 0.1106 %Vol	Span : 1.791	Uniformity: 0.562	Result units: Volume
Specific Surface Area: 0.137 m ² /g	Surface Weighted Mean D[3,2]: 43.653 um	Vol. Weighted Mean D[4,3]: 262.047 um	

d(0.1): 86.815 um

d(0.5): 226.219 um

d(0.9): 491.873 um



9, Thursday, 22 September 2011 9:59:13 a.m.

Size (µm)	Volume In %	Size (µm)	Volume In %	Size (µm)	Volume In %	Size (µm)	Volume In %	Size (µm)	Volume In %
0.050	2.07	3.900	5.86	63.000	92.07	2000.000			
3.900		63.000		2000.000					

Result Analysis Report

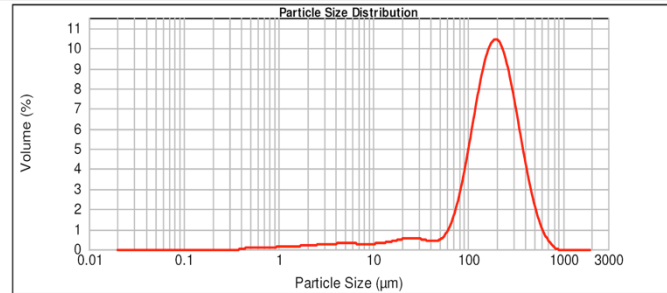
Sample Name: 10
SOP Name: Marine Sediment
Measured: Thursday, 22 September 2011 10:04:07 a.m.
Sample Source & type: Measured by: socb1
Analysed: Thursday, 22 September 2011 10:04:08 a.m.
Sample bulk lot ref: 45
Result Source: Measurement

Particle Name: Marine Sediment	Accessory Name: None	Analysis model: General purpose	Sensitivity: Enhanced
Particle RI: 1.500	Absorption: 0.2	Size range: 0.020 to 2000.000 um	Obscuration: 17.91 %
Dispersant Name: Water	Dispersant RI: 1.330	Weighted Residual: 0.446 %	Result Emulation: Off
Concentration: 0.1022 %Vol	Span : 1.667	Uniformity: 0.52	Result units: Volume
Specific Surface Area: 0.163 m ² /g	Surface Weighted Mean D[3,2]: 36.810 um	Vol. Weighted Mean D[4,3]: 201.295 um	

d(0.1): 64.482 um

d(0.5): 180.660 um

d(0.9): 365.631 um



10, Thursday, 22 September 2011 10:04:07 a.m.

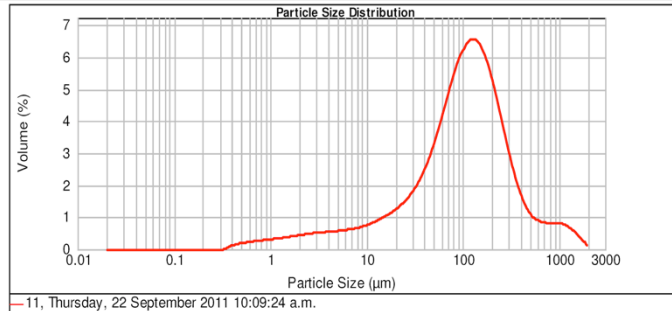
Size (µm)	Volume In %	Size (µm)	Volume In %	Size (µm)	Volume In %	Size (µm)	Volume In %	Size (µm)	Volume In %
0.050	2.27	3.900	7.55	63.000	90.18	2000.000			
3.900		63.000		2000.000					

Result Analysis Report

Sample Name: 11
SOP Name: Marine Sediment
Measured: Thursday, 22 September 2011 10:09:24 a.m.
Sample Source & type: Measured by: socb1
Analysed: Thursday, 22 September 2011 10:09:25 a.m.
Sample bulk lot ref: 46
Result Source: Measurement

Particle Name: Marine Sediment
Accessory Name: None
Analysis model: General purpose
Sensitivity: Enhanced
Particle RI: 1.500
Absorption: 0.2
Size range: 0.020 to 2000.000 um
Obscuration: 16.02 %
Dispersant Name: Water
Dispersant RI: 1.330
Weighted Residual: 0.369 %
Result Emulation: Off
Concentration: 0.0408 %Vol
Span : 3.240
Uniformity: 1.19
Result units: Volume
Specific Surface Area: 0.373 m²/g
Surface Weighted Mean D[3,2]: 16.077 um
Vol. Weighted Mean D[4,3]: 174.307 um

d(0.1): 11.662 um d(0.5): 105.904 um d(0.9): 354.783 um



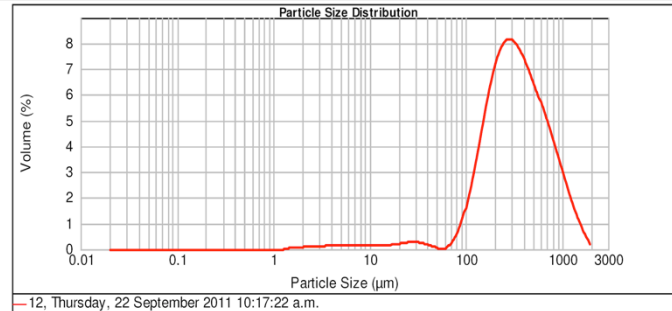
11, Thursday, 22 September 2011 10:09:24 a.m.

Result Analysis Report

Sample Name: 12
SOP Name: Marine Sediment
Measured: Thursday, 22 September 2011 10:17:22 a.m.
Sample Source & type: Measured by: socb1
Analysed: Thursday, 22 September 2011 10:17:24 a.m.
Sample bulk lot ref: 47
Result Source: Measurement

Particle Name: Marine Sediment
Accessory Name: None
Analysis model: General purpose
Sensitivity: Enhanced
Particle RI: 1.500
Absorption: 0.2
Size range: 0.020 to 2000.000 um
Obscuration: 14.75 %
Dispersant Name: Water
Dispersant RI: 1.330
Weighted Residual: 0.917 %
Result Emulation: Off
Concentration: 0.2326 %Vol
Span : 2.269
Uniformity: 0.705
Result units: Volume
Specific Surface Area: 0.053 m²/g
Surface Weighted Mean D[3,2]: 113.254 um
Vol. Weighted Mean D[4,3]: 416.536 um

d(0.1): 129.184 um d(0.5): 319.862 um d(0.9): 855.015 um



12, Thursday, 22 September 2011 10:17:22 a.m.

Result Analysis Report

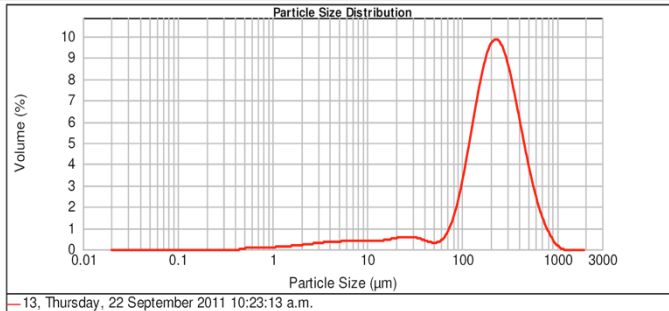
Sample Name: 13
Sample Source & type: Marine Sediment
Sample bulk lot ref: 48

SOP Name: Marine Sediment
Measured by: socb1
Result Source: Measurement

Measured: Thursday, 22 September 2011 10:23:13 a.m.
Analysed: Thursday, 22 September 2011 10:23:14 a.m.

Particle Name: Marine Sediment	Accessory Name: None	Analysis model: General purpose	Sensitivity: Enhanced
Particle RI: 1.500	Absorption: 0.2	Size range: 0.020 to 2000.000 um	Obscuration: 17.08 %
Dispersant Name: Water	Dispersant RI: 1.330	Weighted Residual: 0.395 %	Result Emulation: Off
Concentration: 0.1006 %Vol	Span : 1.860	Uniformity: 0.564	Result units: Volume
Specific Surface Area: 0.152 m ² /g	Surface Weighted Mean D[3,2]: 39.554 um	Vol. Weighted Mean D[4,3]: 242.625 um	

d(0.1): 59.280 um d(0.5): 212.797 um d(0.9): 455.052 um



13, Thursday, 22 September 2011 10:23:13 a.m.

Result Analysis Report

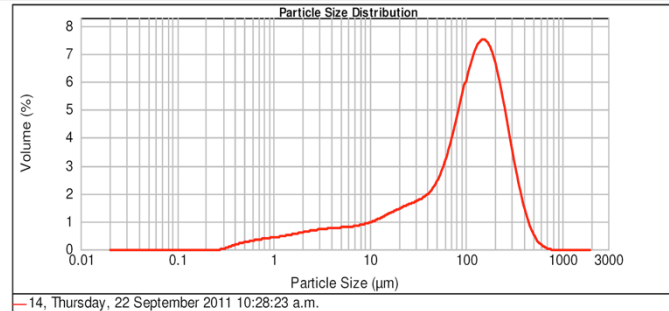
Sample Name: 14
Sample Source & type: Marine Sediment
Sample bulk lot ref: 49

SOP Name: Marine Sediment
Measured by: socb1
Result Source: Measurement

Measured: Thursday, 22 September 2011 10:28:23 a.m.
Analysed: Thursday, 22 September 2011 10:28:24 a.m.

Particle Name: Marine Sediment	Accessory Name: None	Analysis model: General purpose	Sensitivity: Enhanced
Particle RI: 1.500	Absorption: 0.2	Size range: 0.020 to 2000.000 um	Obscuration: 18.59 %
Dispersant Name: Water	Dispersant RI: 1.330	Weighted Residual: 0.426 %	Result Emulation: Off
Concentration: 0.0370 %Vol	Span : 2.415	Uniformity: 0.756	Result units: Volume
Specific Surface Area: 0.493 m ² /g	Surface Weighted Mean D[3,2]: 12.163 um	Vol. Weighted Mean D[4,3]: 125.067 um	

d(0.1): 6.445 um d(0.5): 107.537 um d(0.9): 266.141 um



14, Thursday, 22 September 2011 10:28:23 a.m.

Result Analysis Report

Sample Name: 15
Sample Source & type:
Sample bulk lot ref: 50

SOP Name: Marine Sediment
Measured by: socb1
Result Source: Measurement

Measured: Thursday, 22 September 2011 10:33:24 a.m.
Analysed: Thursday, 22 September 2011 10:33:25 a.m.

Particle Name: Marine Sediment	Accessory Name: None	Analysis model: General purpose	Sensitivity: Enhanced
Particle RI: 1.500	Absorption: 0.2	Size range: 0.020 to 2000.000 um	Obscuration: 16.36 %
Dispersant Name: Water	Dispersant RI: 1.330	Weighted Residual: 0.622 %	Result Emulation: Off
Concentration: 0.2167 %Vol	Span : 1.608	Uniformity: 0.521	Result units: Volume
Specific Surface Area: 0.0639 m ² /g	Surface Weighted Mean D[3,2]: 93.938 um	Vol. Weighted Mean D[4,3]: 261.978 um	

Result Analysis Report

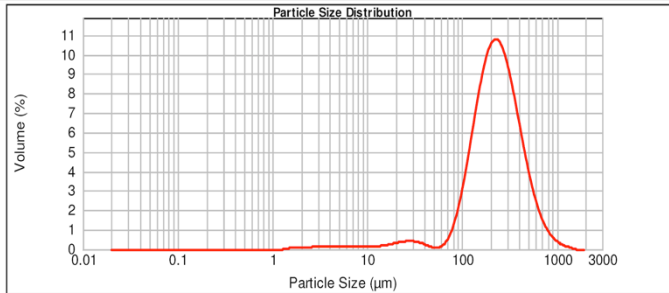
Sample Name: 16
Sample Source & type:
Sample bulk lot ref: 51

SOP Name: Marine Sediment
Measured by: socb1
Result Source: Measurement

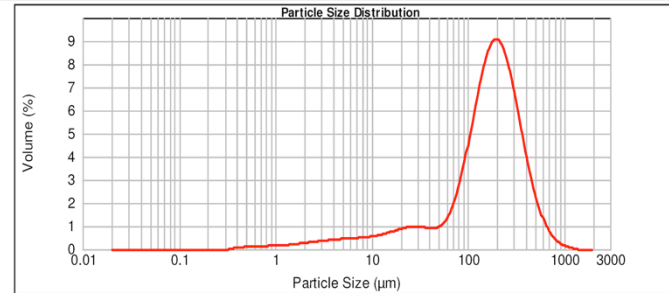
Measured: Thursday, 22 September 2011 10:40:04 a.m.
Analysed: Thursday, 22 September 2011 10:40:05 a.m.

Particle Name: Marine Sediment	Accessory Name: None	Analysis model: General purpose	Sensitivity: Enhanced
Particle RI: 1.500	Absorption: 0.2	Size range: 0.020 to 2000.000 um	Obscuration: 17.98 %
Dispersant Name: Water	Dispersant RI: 1.330	Weighted Residual: 0.417 %	Result Emulation: Off
Concentration: 0.0732 %Vol	Span : 2.106	Uniformity: 0.635	Result units: Volume
Specific Surface Area: 0.233 m ² /g	Surface Weighted Mean D[3,2]: 25.743 um	Vol. Weighted Mean D[4,3]: 198.575 um	

d(0.1): 105.323 um d(0.5): 224.706 um d(0.9): 466.621 um d(0.1): 22.081 um d(0.5): 172.679 um d(0.9): 385.711 um



Size (µm)	Volume In %	Size (µm)	Volume In %	Size (µm)	Volume In %	Size (µm)	Volume In %
0.050	0.79	3.900	4.09	63.000	95.18	2000.000	
3.900		63.000		2000.000			



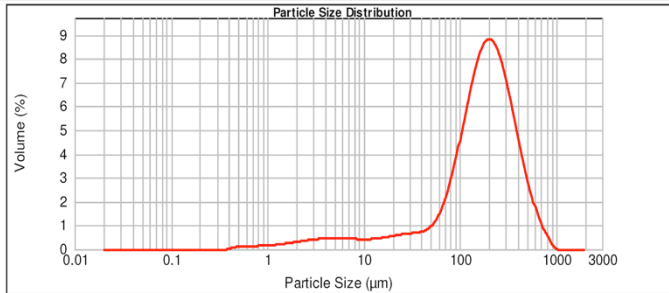
Size (µm)	Volume In %	Size (µm)	Volume In %	Size (µm)	Volume In %	Size (µm)	Volume In %
0.050	3.28	3.900	13.57	63.000	83.17	2000.000	
3.900		63.000		2000.000			

Result Analysis Report

Sample Name: 17
Sample Source & type:
Sample bulk lot ref: 52
SOP Name: Marine Sediment
Measured by: socb1
Result Source: Measurement
Measured: Thursday, 22 September 2011 10:44:50 a.m.
Analysed: Thursday, 22 September 2011 10:44:51 a.m.

Particle Name: Marine Sediment	Accessory Name: None	Analysis model: General purpose	Sensitivity: Enhanced
Particle RI: 1.500	Absorption: 0.2	Size range: 0.020 to 2000.000 um	Obscuration: 15.46 %
Dispersant Name: Water	Dispersant RI: 1.330	Weighted Residual: 0.464 %	Result Emulation: Off
Concentration: 0.0637 %Vol	Span : 2.119	Uniformity: 0.63	Result units: Volume
Specific Surface Area: 0.221 m ² /g	Surface Weighted Mean D[3,2]: 27.101 um	Vol. Weighted Mean D[4,3]: 209.224 um	

d(0.1): 29.394 um d(0.5): 180.309 um d(0.9): 411.479 um



17, Thursday, 22 September 2011 10:44:50 a.m.

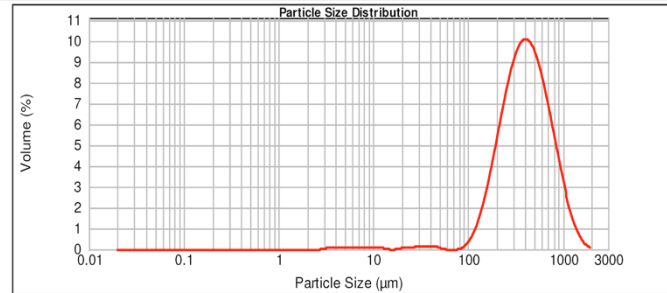
Size (µm)	Volume In %	Size (µm)	Volume In %	Size (µm)	Volume In %	Size (µm)	Volume In %
0.050	3.48	3.900	10.97	63.000	85.55	2000.000	
3.900		63.000		2000.000			

Result Analysis Report

Sample Name: 18
Sample Source & type:
Sample bulk lot ref: 53
SOP Name: Marine Sediment
Measured by: socb1
Result Source: Measurement
Measured: Thursday, 22 September 2011 10:50:59 a.m.
Analysed: Thursday, 22 September 2011 10:51:00 a.m.

Particle Name: Marine Sediment	Accessory Name: None	Analysis model: General purpose	Sensitivity: Enhanced
Particle RI: 1.500	Absorption: 0.2	Size range: 0.020 to 2000.000 um	Obscuration: 15.55 %
Dispersant Name: Water	Dispersant RI: 1.330	Weighted Residual: 1.161 %	Result Emulation: Off
Concentration: 0.4996 %Vol	Span : 1.648	Uniformity: 0.518	Result units: Volume
Specific Surface Area: 0.0266 m ² /g	Surface Weighted Mean D[3,2]: 225.752 um	Vol. Weighted Mean D[4,3]: 463.947 um	

d(0.1): 184.929 um d(0.5): 397.107 um d(0.9): 839.532 um



18, Thursday, 22 September 2011 10:50:59 a.m.

Size (µm)	Volume In %	Size (µm)	Volume In %	Size (µm)	Volume In %	Size (µm)	Volume In %
0.050	0.12	3.900	1.41	63.000	98.46	2000.000	
3.900		63.000		2000.000			

Result Analysis Report

Sample Name: 19
Sample Source & type:
Sample bulk lot ref: 54

SOP Name: Marine Sediment
Measured by: socb1
Result Source: Measurement

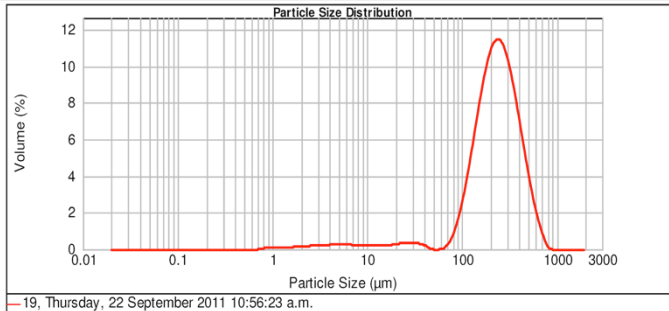
Measured: Thursday, 22 September 2011 10:56:23 a.m.
Analysed: Thursday, 22 September 2011 10:56:25 a.m.

Particle Name: Marine Sediment	Accessory Name: None	Analysis model: General purpose	Sensitivity: Enhanced
Particle RI: 1.500	Absorption: 0.2	Size range: 0.020 to 2000.000 um	Obscuration: 15.44 %
Dispersant Name: Water	Dispersant RI: 1.330	Weighted Residual: 0.613 %	Result Emulation: Off
Concentration: 0.1339 %Vol	Span : 1.426	Uniformity: 0.453	Result units: Volume
Specific Surface Area: 0.0979 m ² /g	Surface Weighted Mean D[3,2]: 61.280 um	Vol. Weighted Mean D[4,3]: 248.744 um	

d(0.1): 107.254 um

d(0.5): 227.239 um

d(0.9): 431.306 um



19, Thursday, 22 September 2011 10:56:23 a.m.

Result Analysis Report

Sample Name: 20
Sample Source & type:
Sample bulk lot ref: 55

SOP Name: Marine Sediment
Measured by: socb1
Result Source: Measurement

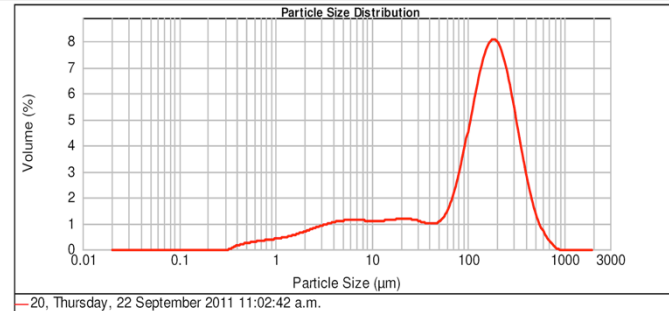
Measured: Thursday, 22 September 2011 11:02:42 a.m.
Analysed: Thursday, 22 September 2011 11:02:43 a.m.

Particle Name: Marine Sediment	Accessory Name: None	Analysis model: General purpose	Sensitivity: Enhanced
Particle RI: 1.500	Absorption: 0.2	Size range: 0.020 to 2000.000 um	Obscuration: 15.57 %
Dispersant Name: Water	Dispersant RI: 1.330	Weighted Residual: 0.532 %	Result Emulation: Off
Concentration: 0.0299 %Vol	Span : 2.314	Uniformity: 0.725	Result units: Volume
Specific Surface Area: 0.489 m ² /g	Surface Weighted Mean D[3,2]: 12.262 um	Vol. Weighted Mean D[4,3]: 156.267 um	

d(0.1): 5.151 um

d(0.5): 139.824 um

d(0.9): 328.715 um



20, Thursday, 22 September 2011 11:02:42 a.m.

Result Analysis Report

Sample Name: 21
Sample Source & type:
Sample bulk lot ref: 56

SOP Name: Marine Sediment
Measured by: socb1
Result Source: Measurement

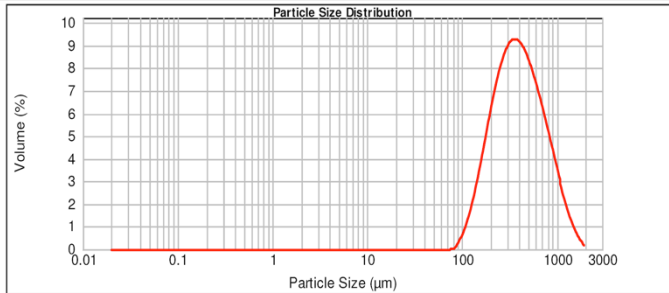
Measured: Thursday, 22 September 2011 11:09:54 a.m.
Analysed: Thursday, 22 September 2011 11:09:55 a.m.

Particle Name: Marine Sediment	Accessory Name: None	Analysis model: General purpose	Sensitivity: Enhanced
Particle RI: 1.500	Absorption: 0.2	Size range: 0.020 to 2000.000 um	Obscuration: 12.62 %
Dispersant Name: Water	Dispersant RI: 1.330	Weighted Residual: 1.532 %	Result Emulation: Off
Concentration: 0.5859 %Vol	Span : 1.854	Uniformity: 0.576	Result units: Volume
Specific Surface Area: 0.0184 m ² /g	Surface Weighted Mean D[3,2]: 325.356 um	Vol. Weighted Mean D[4,3]: 467.993 um	

d(0.1): 176.476 um

d(0.5): 381.658 um

d(0.9): 884.074 um



21, Thursday, 22 September 2011 11:09:54 a.m.

Size (µm)	Volume In %	Size (µm)	Volume In %	Size (µm)	Volume In %	Size (µm)	Volume In %
0.050	0.00	3.900	0.00	63.000	100.00	2000.000	
3.900		63.000		2000.000			

Result Analysis Report

Sample Name: 22
Sample Source & type:
Sample bulk lot ref: 57

SOP Name: Marine Sediment
Measured by: socb1
Result Source: Measurement

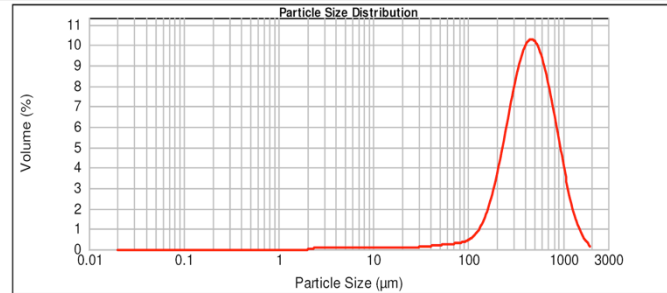
Measured: Thursday, 22 September 2011 11:17:01 a.m.
Analysed: Thursday, 22 September 2011 11:17:02 a.m.

Particle Name: Marine Sediment	Accessory Name: None	Analysis model: General purpose	Sensitivity: Enhanced
Particle RI: 1.500	Absorption: 0.2	Size range: 0.020 to 2000.000 um	Obscuration: 17.01 %
Dispersant Name: Water	Dispersant RI: 1.330	Weighted Residual: 1.329 %	Result Emulation: Off
Concentration: 0.4796 %Vol	Span : 1.621	Uniformity: 0.511	Result units: Volume
Specific Surface Area: 0.0303 m ² /g	Surface Weighted Mean D[3,2]: 197.942 um	Vol. Weighted Mean D[4,3]: 507.704 um	

d(0.1): 194.899 um

d(0.5): 443.780 um

d(0.9): 914.464 um



22, Thursday, 22 September 2011 11:17:01 a.m.

Size (µm)	Volume In %	Size (µm)	Volume In %	Size (µm)	Volume In %	Size (µm)	Volume In %
0.050	0.28	3.900	2.17	63.000	97.57	2000.000	
3.900		63.000		2000.000			



Department of Earth & Ocean Sciences
 School of Science and Engineering
 The University of Waikato
 Private Bag 3105
 Hamilton, New Zealand



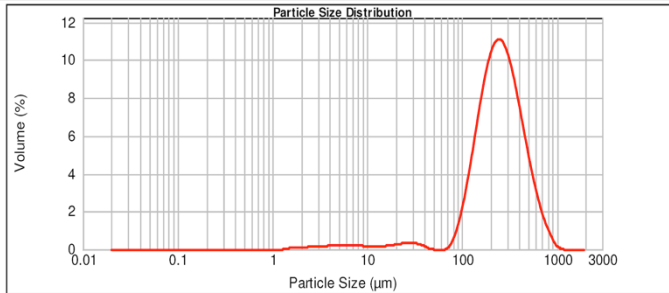
Department of Earth & Ocean Sciences
 School of Science and Engineering
 The University of Waikato
 Private Bag 3105
 Hamilton, New Zealand

Result Analysis Report

Sample Name: 23
Sample Source & type:
Sample bulk lot ref: 58
SOP Name: Marine Sediment
Measured by: socb1
Result Source: Measurement
Measured: Thursday, 22 September 2011 11:22:14 a.m.
Analysed: Thursday, 22 September 2011 11:22:15 a.m.

Particle Name: Marine Sediment	Accessory Name: None	Analysis model: General purpose	Sensitivity: Enhanced
Particle RI: 1.500	Absorption: 0.2	Size range: 0.020 to 2000.000 um	Obscuration: 14.27 %
Dispersant Name: Water	Dispersant RI: 1.330	Weighted Residual: 0.798 %	Result Emulation: Off
Concentration: 0.1839 %Vol	Span : 1.514	Uniformity: 0.483	Result units: Volume
Specific Surface Area: 0.0647 m ² /g	Surface Weighted Mean D[3,2]: 92.782 um	Vol. Weighted Mean D[4,3]: 275.405 um	

d(0.1): 118.503 um d(0.5): 242.852 um d(0.9): 486.270 um



23, Thursday, 22 September 2011 11:22:14 a.m.

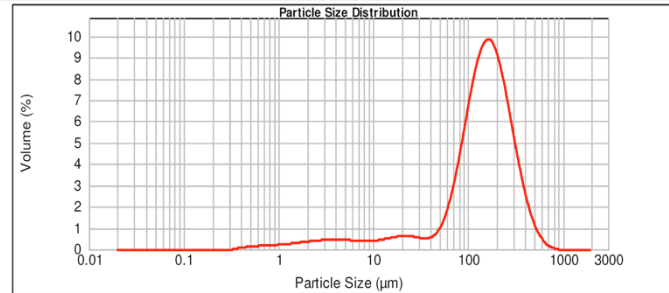
Size (µm)	Volume In %	Size (µm)	Volume In %	Size (µm)	Volume In %	Size (µm)	Volume In %
0.050	0.83	3.900	3.51	63.000	95.67	2000.000	
3.900		63.000		2000.000			

Result Analysis Report

Sample Name: 24
Sample Source & type:
Sample bulk lot ref: 59
SOP Name: Marine Sediment
Measured by: socb1
Result Source: Measurement
Measured: Thursday, 22 September 2011 11:27:00 a.m.
Analysed: Thursday, 22 September 2011 11:27:01 a.m.

Particle Name: Marine Sediment	Accessory Name: None	Analysis model: General purpose	Sensitivity: Enhanced
Particle RI: 1.500	Absorption: 0.2	Size range: 0.020 to 2000.000 um	Obscuration: 16.40 %
Dispersant Name: Water	Dispersant RI: 1.330	Weighted Residual: 0.497 %	Result Emulation: Off
Concentration: 0.0570 %Vol	Span : 1.933	Uniformity: 0.566	Result units: Volume
Specific Surface Area: 0.272 m ² /g	Surface Weighted Mean D[3,2]: 22.063 um	Vol. Weighted Mean D[4,3]: 165.174 um	

d(0.1): 24.604 um d(0.5): 147.416 um d(0.9): 309.515 um



24, Thursday, 22 September 2011 11:27:00 a.m.

Size (µm)	Volume In %	Size (µm)	Volume In %	Size (µm)	Volume In %	Size (µm)	Volume In %
0.050	4.19	3.900	10.93	63.000	84.88	2000.000	
3.900		63.000		2000.000			

Result Analysis Report

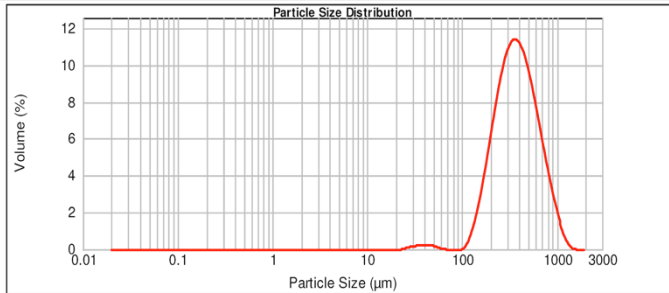
Sample Name: 25
Sample Source & type:
Sample bulk lot ref: 60

SOP Name: Marine Sediment
Measured by: socb1
Result Source: Measurement

Measured: Thursday, 22 September 2011 11:34:13 a.m.
Analysed: Thursday, 22 September 2011 11:34:14 a.m.

Particle Name: Marine Sediment	Accessory Name: None	Analysis model: General purpose	Sensitivity: Enhanced
Particle RI: 1.500	Absorption: 0.2	Size range: 0.020 to 2000.000 um	Obscuration: 15.31 %
Dispersant Name: Water	Dispersant RI: 1.330	Weighted Residual: 1.201 %	Result Emulation: Off
Concentration: 0.6787 %Vol	Span : 1.438	Uniformity: 0.449	Result units: Volume
Specific Surface Area: 0.0196 m ² /g	Surface Weighted Mean D[3,2]: 306.516 um	Vol. Weighted Mean D[4,3]: 415.460 um	

d(0.1): 190.701 um d(0.5): 365.318 um d(0.9): 715.885 um



25, Thursday, 22 September 2011 11:34:13 a.m.

Size (µm)	Volume In %	Size (µm)	Volume In %	Size (µm)	Volume In %	Size (µm)	Volume In %
0.050	0.00	3.900	1.00	63.000	99.00	2000.000	
3.900		63.000		2000.000			

Result Analysis Report

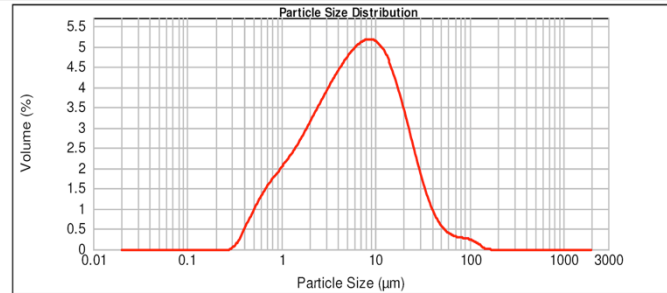
Sample Name: 26
Sample Source & type:
Sample bulk lot ref: 61

SOP Name: Marine Sediment
Measured by: socb1
Result Source: Measurement

Measured: Thursday, 22 September 2011 11:41:40 a.m.
Analysed: Thursday, 22 September 2011 11:41:41 a.m.

Particle Name: Marine Sediment	Accessory Name: None	Analysis model: General purpose	Sensitivity: Enhanced
Particle RI: 1.500	Absorption: 0.2	Size range: 0.020 to 2000.000 um	Obscuration: 19.03 %
Dispersant Name: Water	Dispersant RI: 1.330	Weighted Residual: 1.257 %	Result Emulation: Off
Concentration: 0.0090 %Vol	Span : 3.588	Uniformity: 1.23	Result units: Volume
Specific Surface Area: 2.04 m ² /g	Surface Weighted Mean D[3,2]: 2.946 um	Vol. Weighted Mean D[4,3]: 10.291 um	

d(0.1): 1.121 um d(0.5): 6.113 um d(0.9): 23.056 um



26, Thursday, 22 September 2011 11:41:40 a.m.

Size (µm)	Volume In %	Size (µm)	Volume In %	Size (µm)	Volume In %	Size (µm)	Volume In %
0.050	36.21	3.900	62.52	63.000	1.27	2000.000	
3.900		63.000		2000.000			

Result Analysis Report

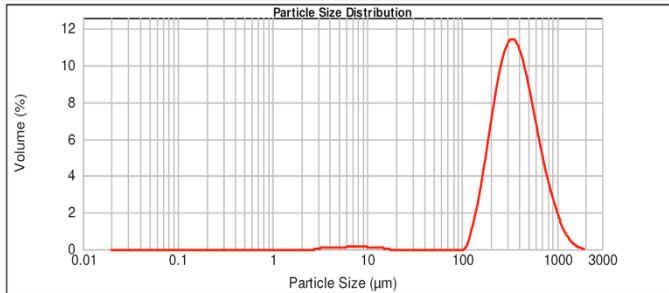
Sample Name: 27
Sample Source & type:
Sample bulk lot ref: 62

SOP Name: Marine Sediment
Measured by: socb1
Result Source: Measurement

Measured: Thursday, 22 September 2011 11:47:01 a.m.
Analysed: Thursday, 22 September 2011 11:47:02 a.m.

Particle Name: Marine Sediment	Accessory Name: None	Analysis model: General purpose	Sensitivity: Enhanced
Particle RI: 1.500	Absorption: 0.2	Size range: 0.020 to 2000.000 um	Obscuration: 15.21 %
Dispersant Name: Water	Dispersant RI: 1.330	Weighted Residual: 1.104 %	Result Emulation: Off
Concentration: 0.4405 %Vol	Span : 1.514	Uniformity: 0.476	Result units: Volume
Specific Surface Area: 0.0294 m ² /g	Surface Weighted Mean D[3,2]: 204.186 um	Vol. Weighted Mean D[4,3]: 409.794 um	

d(0.1): 185.218 um d(0.5): 350.541 um d(0.9): 715.920 um



— 27, Thursday, 22 September 2011 11:47:01 a.m.

Size (µm)	Volume In %	Size (µm)	Volume In %	Size (µm)	Volume In %	Size (µm)	Volume In %
0.050	0.13	3.900	1.02	63.000	98.85	2000.000	
3.900		63.000		2000.000			

Result Analysis Report

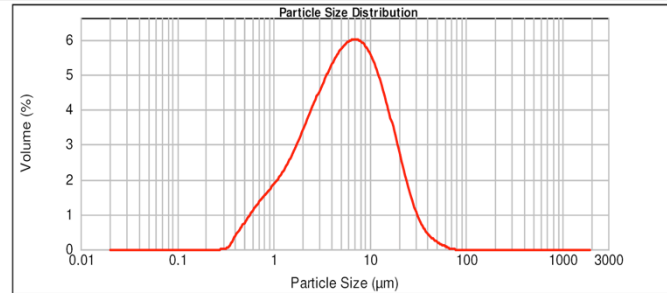
Sample Name: 28
Sample Source & type:
Sample bulk lot ref: 63

SOP Name: Marine Sediment
Measured by: socb1
Result Source: Measurement

Measured: Thursday, 22 September 2011 11:54:14 a.m.
Analysed: Thursday, 22 September 2011 11:54:15 a.m.

Particle Name: Marine Sediment	Accessory Name: None	Analysis model: General purpose	Sensitivity: Enhanced
Particle RI: 1.500	Absorption: 0.2	Size range: 0.020 to 2000.000 um	Obscuration: 9.99 %
Dispersant Name: Water	Dispersant RI: 1.330	Weighted Residual: 1.921 %	Result Emulation: Off
Concentration: 0.0045 %Vol	Span : 2.920	Uniformity: 0.932	Result units: Volume
Specific Surface Area: 1.98 m ² /g	Surface Weighted Mean D[3,2]: 3.027 um	Vol. Weighted Mean D[4,3]: 7.863 um	

d(0.1): 1.246 um d(0.5): 5.520 um d(0.9): 17.364 um



— 28, Thursday, 22 September 2011 11:54:14 a.m.

Size (µm)	Volume In %	Size (µm)	Volume In %	Size (µm)	Volume In %	Size (µm)	Volume In %
0.050	37.33	3.900	62.65	63.000	0.02	2000.000	
3.900		63.000		2000.000			

Result Analysis Report

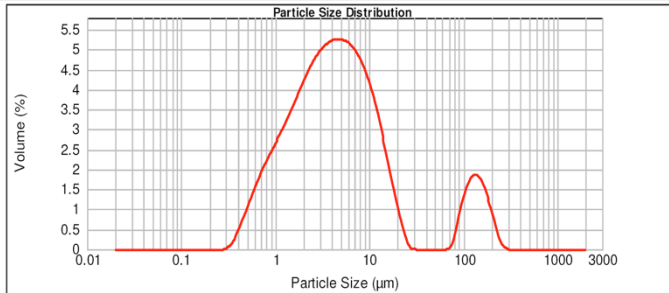
Sample Name: 29
Sample Source & type: Marine Sediment
Sample bulk lot ref: 64

SOP Name: Marine Sediment
Measured by: socb1
Result Source: Measurement

Measured: Thursday, 22 September 2011 12:00:41 p.m.
Analysed: Thursday, 22 September 2011 12:00:42 p.m.

Particle Name: Marine Sediment	Accessory Name: None	Analysis model: General purpose	Sensitivity: Enhanced
Particle RI: 1.500	Absorption: 0.2	Size range: 0.020 to 2000.000 um	Obscuration: 14.70 %
Dispersant Name: Water	Dispersant RI: 1.330	Weighted Residual: 1.622 %	Result Emulation: Off
Concentration: 0.0057 %Vol	Span : 4.872	Uniformity: 3.76	Result units: Volume
Specific Surface Area: 2.39 m ² /g	Surface Weighted Mean D[3,2]: 2.507 um	Vol. Weighted Mean D[4,3]: 18.357 um	

d(0.1): 0.994 um d(0.5): 4.323 um d(0.9): 22.056 um



29, Thursday, 22 September 2011 12:00:41 p.m.

Size (µm)	Volume In %	Size (µm)	Volume In %	Size (µm)	Volume In %	Size (µm)	Volume In %
0.050	46.47	3.900	43.38	63.000	9.55	2000.000	
3.900		63.000		2000.000			

Result Analysis Report

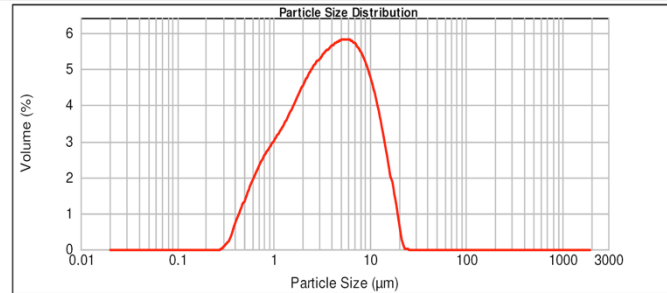
Sample Name: 30
Sample Source & type: Marine Sediment
Sample bulk lot ref: 65

SOP Name: Marine Sediment
Measured by: socb1
Result Source: Measurement

Measured: Thursday, 22 September 2011 12:50:51 p.m.
Analysed: Thursday, 22 September 2011 12:50:53 p.m.

Particle Name: Marine Sediment	Accessory Name: None	Analysis model: General purpose	Sensitivity: Enhanced
Particle RI: 1.500	Absorption: 0.2	Size range: 0.020 to 2000.000 um	Obscuration: 11.46 %
Dispersant Name: Water	Dispersant RI: 1.330	Weighted Residual: 4.235 %	Result Emulation: Off
Concentration: 0.0039 %Vol	Span : 2.803	Uniformity: 0.859	Result units: Volume
Specific Surface Area: 2.75 m ² /g	Surface Weighted Mean D[3,2]: 2.183 um	Vol. Weighted Mean D[4,3]: 5.058 um	

d(0.1): 0.884 um d(0.5): 3.739 um d(0.9): 11.365 um



30, Thursday, 22 September 2011 12:50:51 p.m.

Size (µm)	Volume In %	Size (µm)	Volume In %	Size (µm)	Volume In %	Size (µm)	Volume In %
0.050	51.54	3.900	48.46	63.000	0.00	2000.000	
3.900		63.000		2000.000			

Result Analysis Report

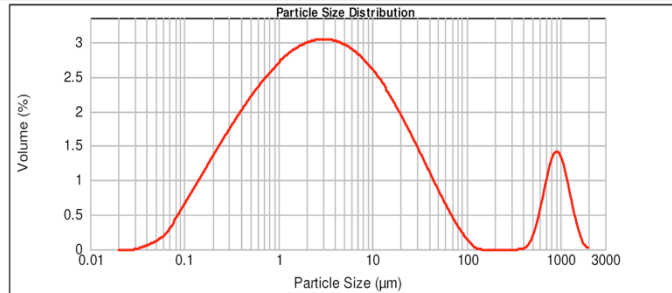
Sample Name: 31
Sample Source & type: Marine Sediment
Sample bulk lot ref: 66

SOP Name: Marine Sediment
Measured by: socb1
Result Source: Measurement

Measured: Thursday, 22 September 2011 12:58:48 p.m.
Analysed: Thursday, 22 September 2011 12:58:49 p.m.

Particle Name: Marine Sediment	Accessory Name: None	Analysis model: General purpose	Sensitivity: Enhanced
Particle RI: 1.500	Absorption: 0.2	Size range: 0.020 to 2000.000 um	Obscuration: 0.00 %
Dispersant Name: Water	Dispersant RI: 1.330	Weighted Residual: 54.676 %	Result Emulation: Off
Concentration: 0.0000 %Vol	Span : 13.754	Uniformity: 22.6	Result units: Volume
Specific Surface Area: 7.48 m ² /g	Surface Weighted Mean D[3,2]: 0.802 um	Vol. Weighted Mean D[4,3]: 72.074 um	

d(0.1): 0.293 um d(0.5): 3.147 um d(0.9): 43.582 um d(0.1): 341.621 um d(0.5): 625.641 um d(0.9): 1105.147 um



31, Thursday, 22 September 2011 12:58:48 p.m.

Size (µm)	Volume In %	Size (µm)	Volume In %	Size (µm)	Volume In %	Size (µm)	Volume In %
0.050	54.08	3.900	37.71	63.000	8.04	2000.000	
3.900		63.000		2000.000			

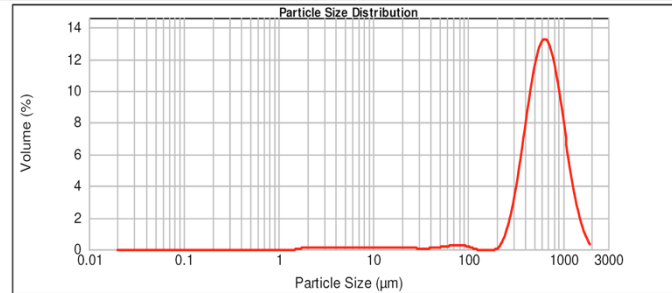
Result Analysis Report

Sample Name: 32
Sample Source & type: Marine Sediment
Sample bulk lot ref: 67

SOP Name: Marine Sediment
Measured by: socb1
Result Source: Measurement

Measured: Thursday, 22 September 2011 1:17:31 p.m.
Analysed: Thursday, 22 September 2011 1:17:32 p.m.

Particle Name: Marine Sediment	Accessory Name: None	Analysis model: General purpose	Sensitivity: Enhanced
Particle RI: 1.500	Absorption: 0.2	Size range: 0.020 to 2000.000 um	Obscuration: 16.52 %
Dispersant Name: Water	Dispersant RI: 1.330	Weighted Residual: 3.037 %	Result Emulation: Off
Concentration: 0.4101 %Vol	Span : 1.220	Uniformity: 0.39	Result units: Volume
Specific Surface Area: 0.0338 m ² /g	Surface Weighted Mean D[3,2]: 177.623 um	Vol. Weighted Mean D[4,3]: 676.625 um	



32, Thursday, 22 September 2011 1:17:31 p.m.

Size (µm)	Volume In %	Size (µm)	Volume In %	Size (µm)	Volume In %	Size (µm)	Volume In %
0.050	0.53	3.900	2.02	63.000	97.44	2000.000	
3.900		63.000		2000.000			



Department of Earth & Ocean Sciences
 School of Science and Engineering
 The University of Waikato
 Private Bag 3105
 Hamilton, New Zealand



Department of Earth & Ocean Sciences
 School of Science and Engineering
 The University of Waikato
 Private Bag 3105
 Hamilton, New Zealand

Result Analysis Report

Sample Name: 33
Sample Source & type:
Sample bulk lot ref: 68
SOP Name: Marine Sediment
Measured by: socb1
Result Source: Measurement
Measured: Thursday, 22 September 2011 1:23:41 p.m.
Analysed: Thursday, 22 September 2011 1:23:43 p.m.

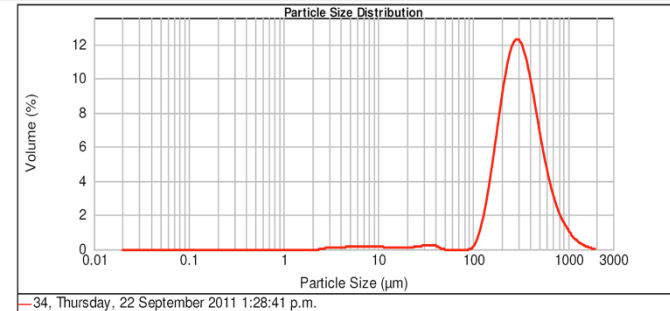
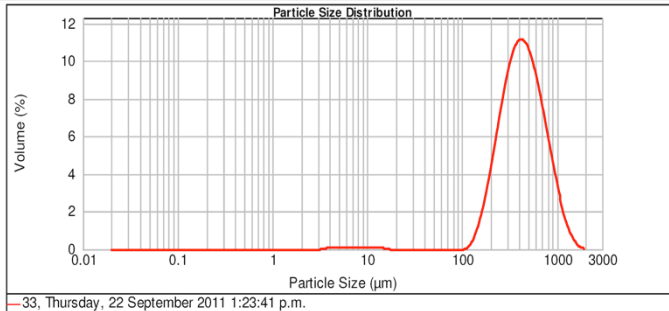
Particle Name: Marine Sediment	Accessory Name: None	Analysis model: General purpose	Sensitivity: Enhanced
Particle RI: 1.500	Absorption: 0.2	Size range: 0.020 to 2000.000 um	Obscuration: 13.73 %
Dispersant Name: Water	Dispersant RI: 1.330	Weighted Residual: 1.644 %	Result Emulation: Off
Concentration: 0.5129 %Vol	Span : 1.474	Uniformity: 0.462	Result units: Volume
Specific Surface Area: 0.0227 m ² /g	Surface Weighted Mean D[3,2]: 264.532 um	Vol. Weighted Mean D[4,3]: 485.138 um	

Result Analysis Report

Sample Name: 34
Sample Source & type:
Sample bulk lot ref: 69
SOP Name: Marine Sediment
Measured by: socb1
Result Source: Measurement
Measured: Thursday, 22 September 2011 1:28:41 p.m.
Analysed: Thursday, 22 September 2011 1:28:43 p.m.

Particle Name: Marine Sediment	Accessory Name: None	Analysis model: General purpose	Sensitivity: Enhanced
Particle RI: 1.500	Absorption: 0.2	Size range: 0.020 to 2000.000 um	Obscuration: 15.40 %
Dispersant Name: Water	Dispersant RI: 1.330	Weighted Residual: 1.082 %	Result Emulation: Off
Concentration: 0.3370 %Vol	Span : 1.456	Uniformity: 0.473	Result units: Volume
Specific Surface Area: 0.0388 m ² /g	Surface Weighted Mean D[3,2]: 154.822 um	Vol. Weighted Mean D[4,3]: 351.017 um	

d(0.1): 217.472 um d(0.5): 423.598 um d(0.9): 841.695 um d(0.1): 163.152 um d(0.5): 300.890 um d(0.9): 601.131 um



Result Analysis Report

Sample Name: 35
Sample Source & type: Marine Sediment
Sample bulk lot ref: 70
SOP Name: Marine Sediment
Measured by: socb1
Result Source: Measurement
Measured: Thursday, 22 September 2011 1:33:56 p.m.
Analysed: Thursday, 22 September 2011 1:33:57 p.m.

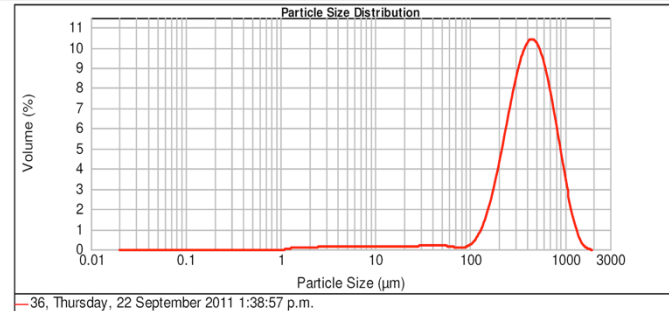
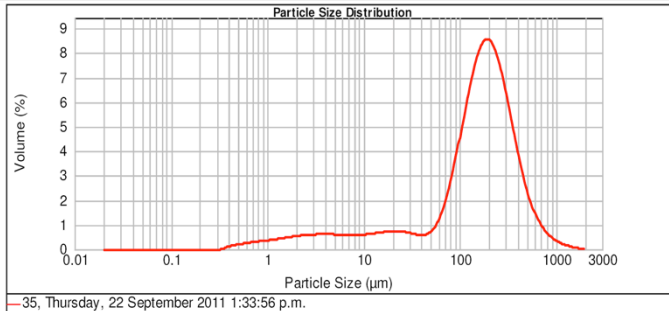
Particle Name: Marine Sediment	Accessory Name: None	Analysis model: General purpose	Sensitivity: Enhanced
Particle RI: 1.500	Absorption: 0.2	Size range: 0.020 to 2000.000 um	Obscuration: 16.22 %
Dispersant Name: Water	Dispersant RI: 1.330	Weighted Residual: 0.610 %	Result Emulation: Off
Concentration: 0.0401 %Vol	Span : 2.322	Uniformity: 0.713	Result units: Volume
Specific Surface Area: 0.387 m ² /g	Surface Weighted Mean D[3,2]: 15.514 um	Vol. Weighted Mean D[4,3]: 202.031 um	

Result Analysis Report

Sample Name: 36
Sample Source & type: Marine Sediment
Sample bulk lot ref: 71
SOP Name: Marine Sediment
Measured by: socb1
Result Source: Measurement
Measured: Thursday, 22 September 2011 1:38:57 p.m.
Analysed: Thursday, 22 September 2011 1:38:59 p.m.

Particle Name: Marine Sediment	Accessory Name: None	Analysis model: General purpose	Sensitivity: Enhanced
Particle RI: 1.500	Absorption: 0.2	Size range: 0.020 to 2000.000 um	Obscuration: 16.53 %
Dispersant Name: Water	Dispersant RI: 1.330	Weighted Residual: 1.842 %	Result Emulation: Off
Concentration: 0.2708 %Vol	Span : 1.555	Uniformity: 0.489	Result units: Volume
Specific Surface Area: 0.0513 m ² /g	Surface Weighted Mean D[3,2]: 116.887 um	Vol. Weighted Mean D[4,3]: 469.157 um	

d(0.1): 9.952 um d(0.5): 168.435 um d(0.9): 401.036 um d(0.1): 185.452 um d(0.5): 418.824 um d(0.9): 836.546 um

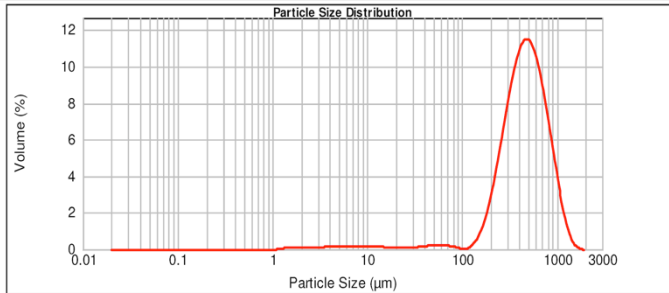


Result Analysis Report

Sample Name: 37
Sample Source & type:
Sample bulk lot ref: 72
SOP Name: Marine Sediment
Measured by: socb1
Result Source: Measurement
Measured: Thursday, 22 September 2011 1:43:58 p.m.
Analysed: Thursday, 22 September 2011 1:43:59 p.m.

Particle Name: Marine Sediment	Accessory Name: None	Analysis model: General purpose	Sensitivity: Enhanced
Particle RI: 1.500	Absorption: 0.2	Size range: 0.020 to 2000.000 um	Obscuration: 14.23 %
Dispersant Name: Water	Dispersant RI: 1.330	Weighted Residual: 1.738 %	Result Emulation: Off
Concentration: 0.2495 %Vol	Span : 1.401	Uniformity: 0.444	Result units: Volume
Specific Surface Area: 0.0473 m ² /g	Surface Weighted Mean D[3,2]: 126.838 um	Vol. Weighted Mean D[4,3]: 502.028 um	

d(0.1): 221.543 um d(0.5): 456.643 um d(0.9): 861.469 um



37, Thursday, 22 September 2011 1:43:58 p.m.

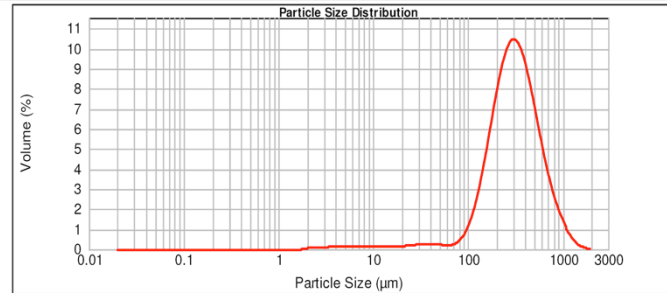
Size (µm)	Volume In %	Size (µm)	Volume In %	Size (µm)	Volume In %	Size (µm)	Volume In %
0.050	0.75	3.900	2.58	63.000	96.68	2000.000	
3.900		63.000		2000.000			

Result Analysis Report

Sample Name: 38
Sample Source & type:
Sample bulk lot ref: 73
SOP Name: Marine Sediment
Measured by: socb1
Result Source: Measurement
Measured: Thursday, 22 September 2011 1:49:11 p.m.
Analysed: Thursday, 22 September 2011 1:49:12 p.m.

Particle Name: Marine Sediment	Accessory Name: None	Analysis model: General purpose	Sensitivity: Enhanced
Particle RI: 1.500	Absorption: 0.2	Size range: 0.020 to 2000.000 um	Obscuration: 16.04 %
Dispersant Name: Water	Dispersant RI: 1.330	Weighted Residual: 1.220 %	Result Emulation: Off
Concentration: 0.2913 %Vol	Span : 1.672	Uniformity: 0.532	Result units: Volume
Specific Surface Area: 0.0466 m ² /g	Surface Weighted Mean D[3,2]: 128.748 um	Vol. Weighted Mean D[4,3]: 351.950 um	

d(0.1): 136.684 um d(0.5): 300.062 um d(0.9): 638.319 um



38, Thursday, 22 September 2011 1:49:11 p.m.

Size (µm)	Volume In %	Size (µm)	Volume In %	Size (µm)	Volume In %	Size (µm)	Volume In %
0.050	0.45	3.900	3.39	63.000	96.16	2000.000	
3.900		63.000		2000.000			

Result Analysis Report

Sample Name: 39
Sample Source & type: Marine Sediment
Sample bulk lot ref: 74

SOP Name: Marine Sediment
Measured by: socb1
Result Source: Measurement

Measured: Thursday, 22 September 2011 1:54:43 p.m.
Analysed: Thursday, 22 September 2011 1:54:45 p.m.

Particle Name: Marine Sediment
Particle RI: 1.500
Dispersant Name: Water

Accessory Name: None
Absorption: 0.2
Dispersant RI: 1.330

Analysis model: General purpose
Size range: 0.020 to 2000.000 um
Weighted Residual: 0.639 %

Sensitivity: Enhanced
Obscuration: 19.03 %
Result Emulation: Off

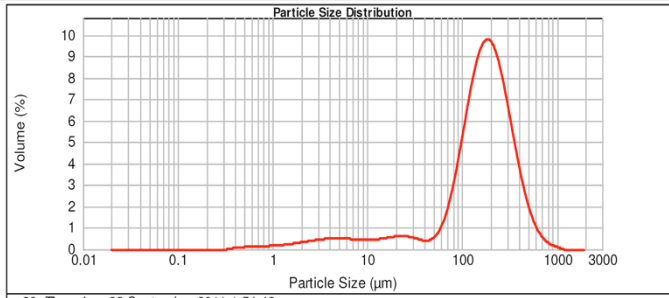
Concentration: 0.0751 %Vol
Specific Surface Area: 0.241 m²/g

Span : 1.983
Surface Weighted Mean D[3,2]: 24.927 um

Uniformity: 0.582
Vol. Weighted Mean D[4,3]: 192.465 um

Result units: Volume

d(0.1): 25.350 um d(0.5): 169.450 um d(0.9): 361.452 um



Size (µm)	Volume In %	Size (µm)	Volume In %	Size (µm)	Volume In %	Size (µm)	Volume In %
0.050	3.74	3.900	9.75	63.000	96.53	2000.000	
3.900		63.000		2000.000			

Result Analysis Report

Sample Name: 40
Sample Source & type: Marine Sediment
Sample bulk lot ref: 75

SOP Name: Marine Sediment
Measured by: socb1
Result Source: Measurement

Measured: Thursday, 22 September 2011 2:00:20 p.m.
Analysed: Thursday, 22 September 2011 2:00:21 p.m.

Particle Name: Marine Sediment
Particle RI: 1.500
Dispersant Name: Water

Accessory Name: None
Absorption: 0.2
Dispersant RI: 1.330

Analysis model: General purpose
Size range: 0.020 to 2000.000 um
Weighted Residual: 3.570 %

Sensitivity: Enhanced
Obscuration: 13.50 %
Result Emulation: Off

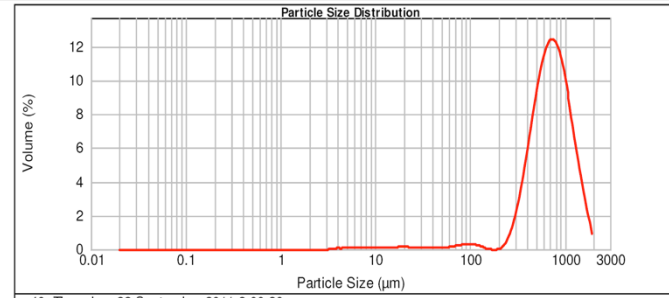
Concentration: 0.5930 %Vol
Specific Surface Area: 0.0191 m²/g

Span : 1.283
Surface Weighted Mean D[3,2]: 313.493 um

Uniformity: 0.405
Vol. Weighted Mean D[4,3]: 768.682 um

Result units: Volume

d(0.1): 371.628 um d(0.5): 708.930 um d(0.9): 1281.521 um



Size (µm)	Volume In %	Size (µm)	Volume In %	Size (µm)	Volume In %	Size (µm)	Volume In %
0.050	0.05	3.900	1.85	63.000	98.11	2000.000	
3.900		63.000		2000.000			



Department of Earth & Ocean Sciences
 School of Science and Engineering
 The University of Waikato
 Private Bag 3105
 Hamilton, New Zealand



Department of Earth & Ocean Sciences
 School of Science and Engineering
 The University of Waikato
 Private Bag 3105
 Hamilton, New Zealand

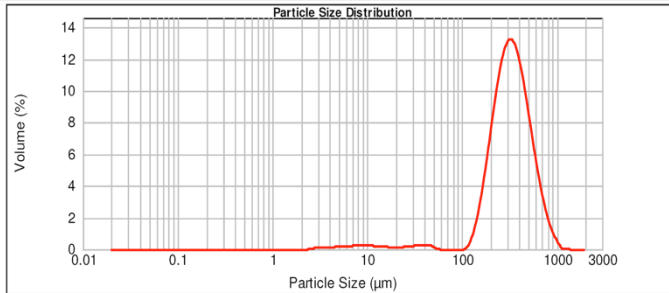
Result Analysis Report

Sample Name: 41
SOP Name: Marine Sediment
Measured: Thursday, 22 September 2011 2:05:47 p.m.
Sample Source & type: Measured by: socb1
Analysed: Thursday, 22 September 2011 2:05:48 p.m.
Sample bulk lot ref: 76
Result Source: Measurement

Particle Name: Marine Sediment
Accessory Name: None
Analysis model: General purpose
Sensitivity: Enhanced
Particle RI: 1.500
Absorption: 0.2
Size range: 0.020 to 2000.000 um
Obscuration: 12.90 %
Dispersant Name: Water
Dispersant RI: 1.330
Weighted Residual: 1.474 %
Result Emulation: Off

Concentration: 0.2601 %Vol
Span : 1.236
Uniformity: 0.398
Result units: Volume
Specific Surface Area: 0.0413 m²/g
Surface Weighted Mean D[3,2]: 145.136 um
Vol. Weighted Mean D[4,3]: 349.073 um

d(0.1): 176.917 um d(0.5): 320.333 um d(0.9): 572.950 um



41, Thursday, 22 September 2011 2:05:47 p.m.

Size (µm)	Volume In %	Size (µm)	Volume In %	Size (µm)	Volume In %	Size (µm)	Volume In %
0.050	0.28	3.900	3.29	63.000	96.45	2000.000	
3.900		63.000		2000.000			

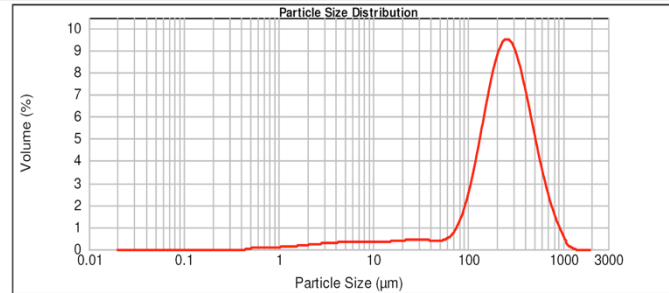
Result Analysis Report

Sample Name: 42
SOP Name: Marine Sediment
Measured: Thursday, 22 September 2011 2:11:04 p.m.
Sample Source & type: Measured by: socb1
Analysed: Thursday, 22 September 2011 2:11:05 p.m.
Sample bulk lot ref: 77
Result Source: Measurement

Particle Name: Marine Sediment
Accessory Name: None
Analysis model: General purpose
Sensitivity: Enhanced
Particle RI: 1.500
Absorption: 0.2
Size range: 0.020 to 2000.000 um
Obscuration: 16.43 %
Dispersant Name: Water
Dispersant RI: 1.330
Weighted Residual: 0.761 %
Result Emulation: Off

Concentration: 0.1041 %Vol
Span : 1.888
Uniformity: 0.584
Result units: Volume
Specific Surface Area: 0.141 m²/g
Surface Weighted Mean D[3,2]: 42.666 um
Vol. Weighted Mean D[4,3]: 277.601 um

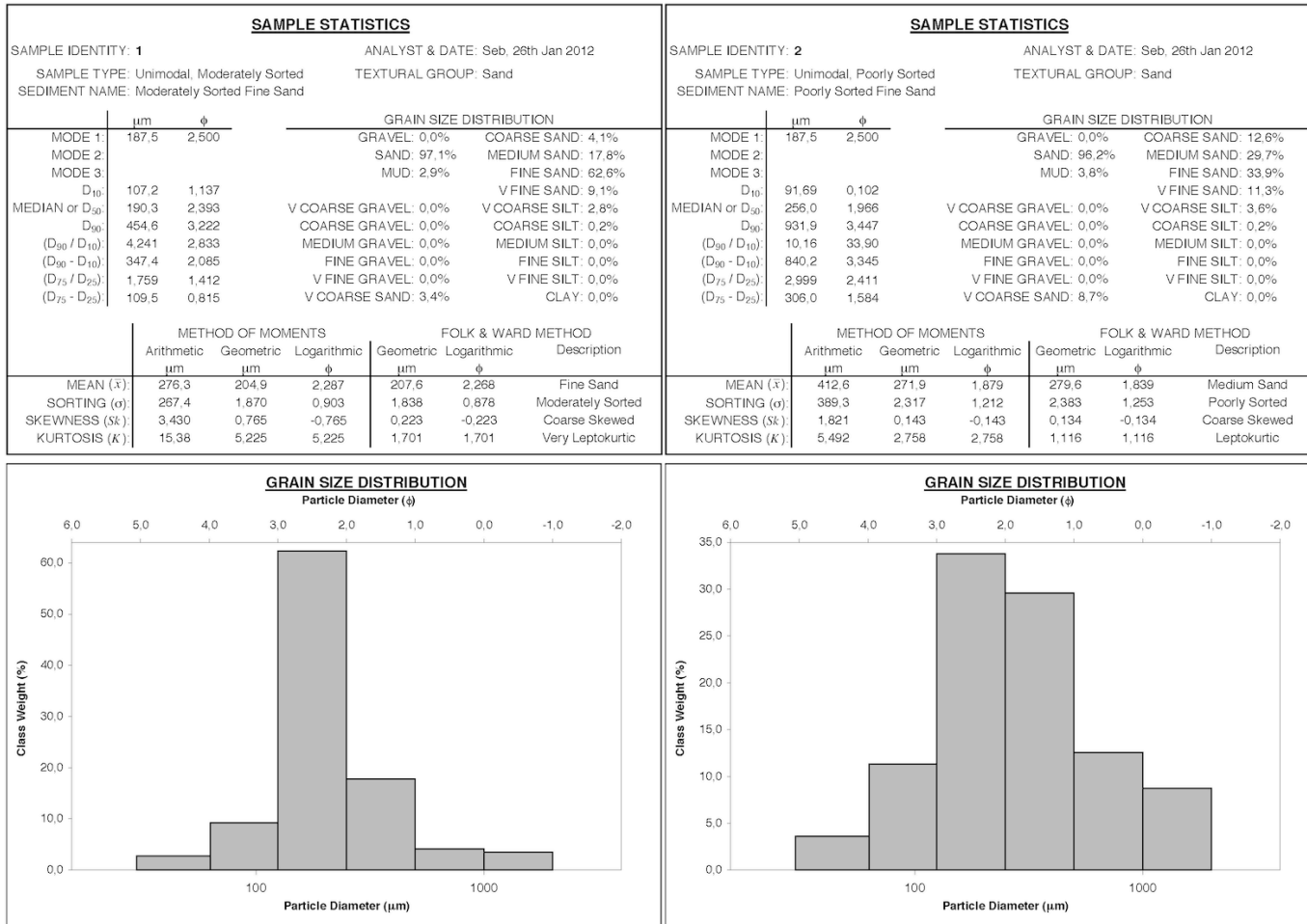
d(0.1): 75.321 um d(0.5): 239.972 um d(0.9): 528.472 um



42, Thursday, 22 September 2011 2:11:04 p.m.

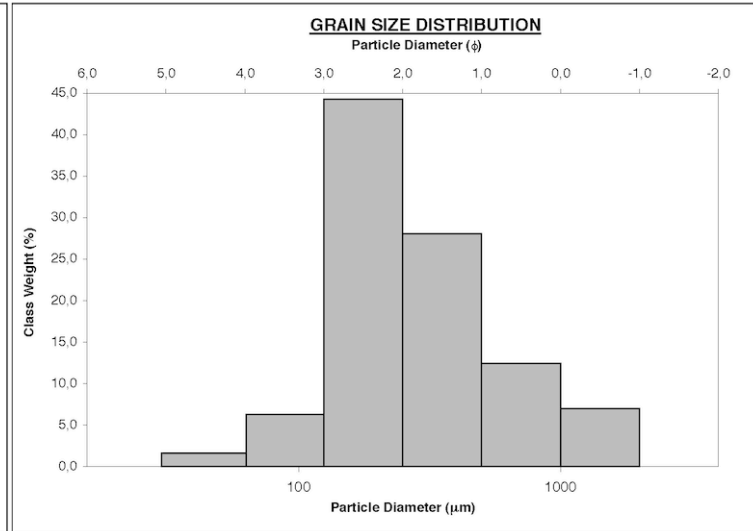
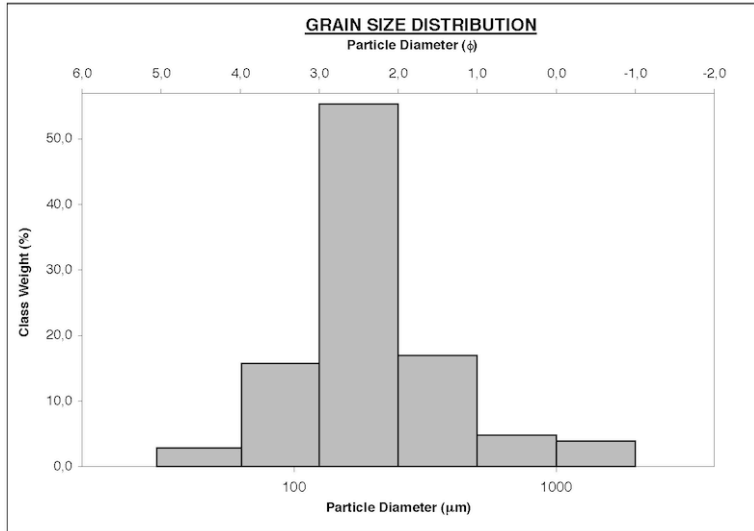
Size (µm)	Volume In %	Size (µm)	Volume In %	Size (µm)	Volume In %	Size (µm)	Volume In %
0.050	2.15	3.900	6.96	63.000	90.68	2000.000	
3.900		63.000		2000.000			

Grain Size Analysis, Sieving.



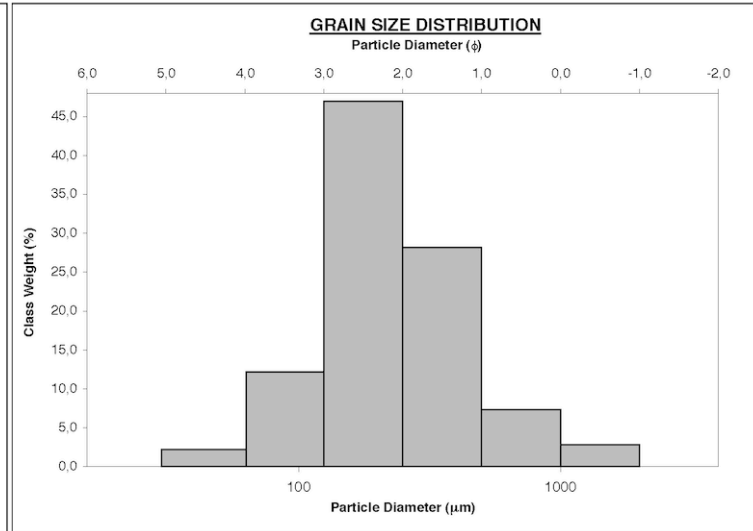
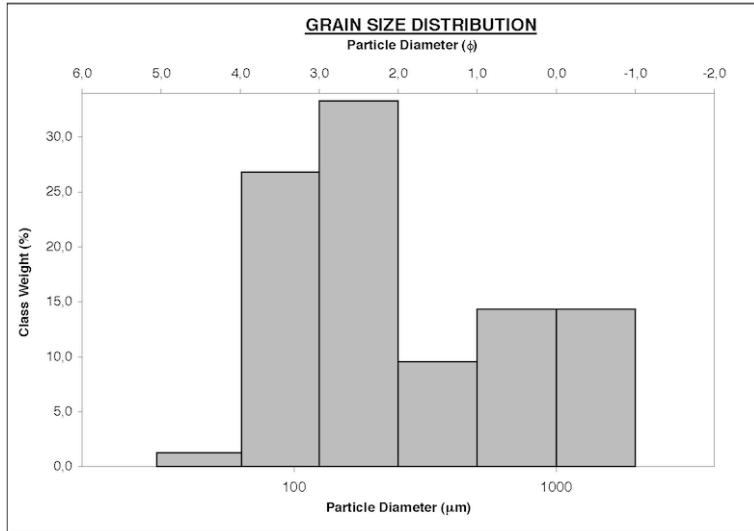
SAMPLE STATISTICS						
SAMPLE IDENTITY: 3		ANALYST & DATE: Seb, 26th Jan 2012				
SAMPLE TYPE: Unimodal, Moderately Sorted		TEXTURAL GROUP: Sand				
SEDIMENT NAME: Moderately Sorted Fine Sand						
	μm	ϕ	GRAIN SIZE DISTRIBUTION			
MODE 1:	187.5	2.500	GRAVEL: 0.0%	COARSE SAND: 4.8%		
MODE 2:			SAND: 97.0%	MEDIUM SAND: 17.0%		
MODE 3:			MUD: 3.0%	FINE SAND: 55.6%		
D ₁₀ :	85.52	1.079		V FINE SAND: 15.6%		
MEDIAN or D ₅₀ :	184.7	2.437	V COARSE GRAVEL: 0.0%	V COARSE SILT: 2.8%		
D ₉₀ :	473.4	3.548	COARSE GRAVEL: 0.0%	COARSE SILT: 0.2%		
(D ₉₀ / D ₁₀):	5.536	3.289	MEDIUM GRAVEL: 0.0%	MEDIUM SILT: 0.0%		
(D ₉₀ - D ₁₀):	387.9	2.469	FINE GRAVEL: 0.0%	FINE SILT: 0.0%		
(D ₇₅ / D ₂₅):	1.901	1.473	V FINE GRAVEL: 0.0%	V FINE SILT: 0.0%		
(D ₇₅ - D ₂₅):	122.0	0.927	V COARSE SAND: 3.9%	CLAY: 0.0%		
	METHOD OF MOMENTS		FOLK & WARD METHOD			
	Arithmetic	Geometric	Logarithmic	Geometric	Logarithmic	Description
	μm	μm	ϕ	μm	ϕ	
MEAN (\bar{x}):	278.5	198.3	2.334	196.8	2.345	Fine Sand
SORTING (σ):	286.2	1.974	0.981	1.979	0.985	Moderately Sorted
SKEWNESS (sk):	3.175	0.757	-0.757	0.186	-0.186	Coarse Skewed
KURTOSIS (K):	13.34	4.441	4.441	1.606	1.606	Very Leptokurtic

SAMPLE STATISTICS						
SAMPLE IDENTITY: 4		ANALYST & DATE: Seb, 26th Jan 2012				
SAMPLE TYPE: Unimodal, Poorly Sorted		TEXTURAL GROUP: Sand				
SEDIMENT NAME: Poorly Sorted Fine Sand						
	μm	ϕ	GRAIN SIZE DISTRIBUTION			
MODE 1:	187.5	2.500	GRAVEL: 0.0%	COARSE SAND: 12.4%		
MODE 2:			SAND: 98.3%	MEDIUM SAND: 28.1%		
MODE 3:			MUD: 1.7%	FINE SAND: 44.5%		
D ₁₀ :	129.1	0.238		V FINE SAND: 6.2%		
MEDIAN or D ₅₀ :	240.9	2.054	V COARSE GRAVEL: 0.0%	V COARSE SILT: 1.6%		
D ₉₀ :	847.9	2.953	COARSE GRAVEL: 0.0%	COARSE SILT: 0.1%		
(D ₉₀ / D ₁₀):	6.566	12.41	MEDIUM GRAVEL: 0.0%	MEDIUM SILT: 0.0%		
(D ₉₀ - D ₁₀):	718.8	2.715	FINE GRAVEL: 0.0%	FINE SILT: 0.0%		
(D ₇₅ / D ₂₅):	2.675	2.187	V FINE GRAVEL: 0.0%	V FINE SILT: 0.0%		
(D ₇₅ - D ₂₅):	273.3	1.420	V COARSE SAND: 7.0%	CLAY: 0.0%		
	METHOD OF MOMENTS		FOLK & WARD METHOD			
	Arithmetic	Geometric	Logarithmic	Geometric	Logarithmic	Description
	μm	μm	ϕ	μm	ϕ	
MEAN (\bar{x}):	394.4	276.5	1.855	274.7	1.864	Medium Sand
SORTING (σ):	358.6	2.087	1.062	2.133	1.093	Poorly Sorted
SKEWNESS (sk):	2.047	0.440	-0.440	0.260	-0.260	Coarse Skewed
KURTOSIS (K):	6.577	3.128	3.128	1.083	1.083	Mesokurtic



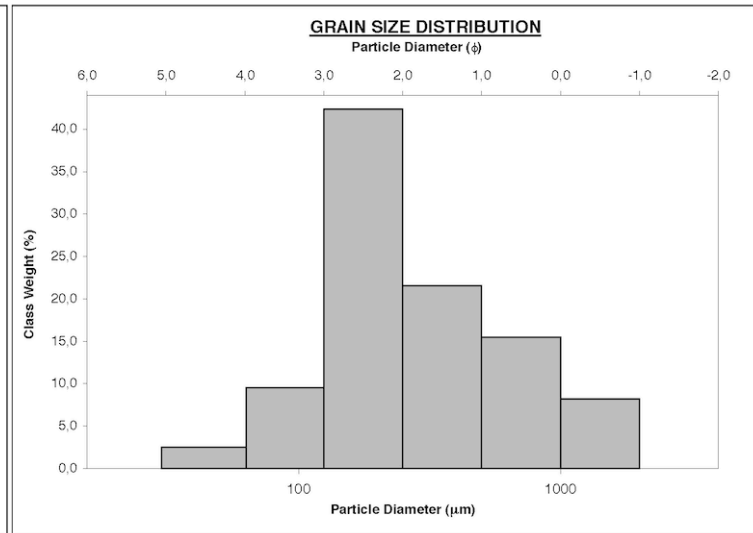
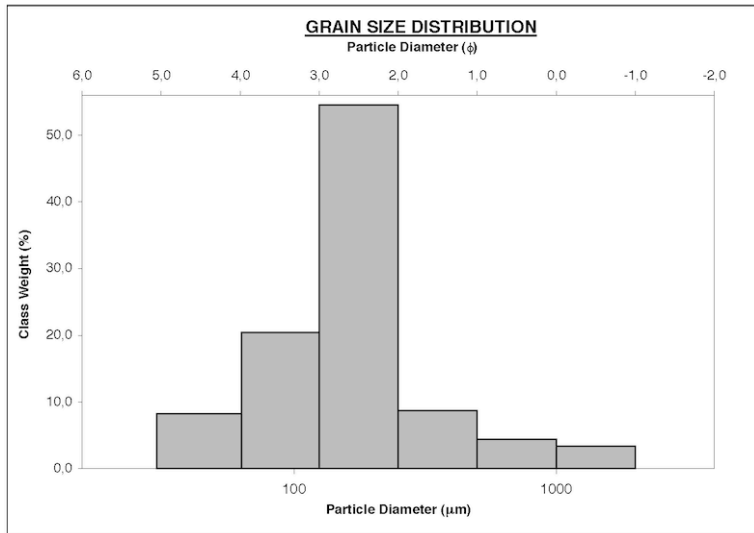
SAMPLE STATISTICS						
SAMPLE IDENTITY: 5		ANALYST & DATE: Seb, 26th Jan 2012				
SAMPLE TYPE: Bimodal, Poorly Sorted		TEXTURAL GROUP: Sand				
SEDIMENT NAME: Poorly Sorted Fine Sand						
	μm	ϕ	GRAIN SIZE DISTRIBUTION			
MODE 1:	187.5	2,500	GRAVEL: 0.0%		COARSE SAND: 14.4%	
MODE 2:	1500.0	-0,500	SAND: 98.7%		MEDIUM SAND: 9.6%	
MODE 3:			MUD: 1.3%		FINE SAND: 33.5%	
D ₁₀ :	78.68	-0,308			V FINE SAND: 26.7%	
MEDIAN or D ₅₀ :	196.9	2,345	V COARSE GRAVEL: 0.0%		V COARSE SILT: 1.3%	
D ₉₀ :	1237.6	3,668	COARSE GRAVEL: 0.0%		COARSE SILT: 0.1%	
(D ₉₀ / D ₁₀):	15,73	-11,925	MEDIUM GRAVEL: 0.0%		MEDIUM SILT: 0.0%	
(D ₉₀ - D ₁₀):	1158.9	3,975	FINE GRAVEL: 0.0%		FINE SILT: 0.0%	
(D ₇₅ / D ₂₅):	5.197	4,239	V FINE GRAVEL: 0.0%		V FINE SILT: 0.0%	
(D ₇₅ - D ₂₅):	485.5	2,378	V COARSE SAND: 14.4%		CLAY: 0.0%	
	METHOD OF MOMENTS		FOLK & WARD METHOD			
	Arithmetic	Geometric	Logarithmic	Geometric	Logarithmic	Description
	μm	μm	ϕ	μm	ϕ	
MEAN (\bar{x}):	449.1	254.3	1.975	255.9	1.966	Medium Sand
SORTING (σ):	481.5	2,675	1.419	2,862	1.517	Poorly Sorted
SKEWNESS (sk):	1,368	0,509	-0,509	0,335	-0,335	Very Coarse Skewed
KURTOSIS (K):	3,414	2,001	2,001	0,777	0,777	Platykurtic

SAMPLE STATISTICS						
SAMPLE IDENTITY: 6		ANALYST & DATE: Seb, 26th Jan 2012				
SAMPLE TYPE: Unimodal, Moderately Sorted		TEXTURAL GROUP: Sand				
SEDIMENT NAME: Moderately Sorted Fine Sand						
	μm	ϕ	GRAIN SIZE DISTRIBUTION			
MODE 1:	187.5	2,500	GRAVEL: 0.0%		COARSE SAND: 7.3%	
MODE 2:			SAND: 97.7%		MEDIUM SAND: 28.3%	
MODE 3:			MUD: 2.3%		FINE SAND: 47.1%	
D ₁₀ :	97.35	0,979			V FINE SAND: 12.1%	
MEDIAN or D ₅₀ :	210.9	2,245	V COARSE GRAVEL: 0.0%		V COARSE SILT: 2.2%	
D ₉₀ :	507.5	3,361	COARSE GRAVEL: 0.0%		COARSE SILT: 0.1%	
(D ₉₀ / D ₁₀):	5,212	3,434	MEDIUM GRAVEL: 0.0%		MEDIUM SILT: 0.0%	
(D ₉₀ - D ₁₀):	410.1	2,382	FINE GRAVEL: 0.0%		FINE SILT: 0.0%	
(D ₇₅ / D ₂₅):	2,379	1,820	V FINE GRAVEL: 0.0%		V FINE SILT: 0.0%	
(D ₇₅ - D ₂₅):	201.5	1,251	V COARSE SAND: 2.8%		CLAY: 0.0%	
	METHOD OF MOMENTS		FOLK & WARD METHOD			
	Arithmetic	Geometric	Logarithmic	Geometric	Logarithmic	Description
	μm	μm	ϕ	μm	ϕ	
MEAN (\bar{x}):	304.2	224.8	2,153	227.0	2,139	Fine Sand
SORTING (σ):	263.9	1,947	0,961	1,953	0,966	Moderately Sorted
SKEWNESS (sk):	2,860	0,356	-0,356	0,151	-0,151	Coarse Skewed
KURTOSIS (K):	12.58	3,661	3,661	1,138	1,138	Leptokurtic



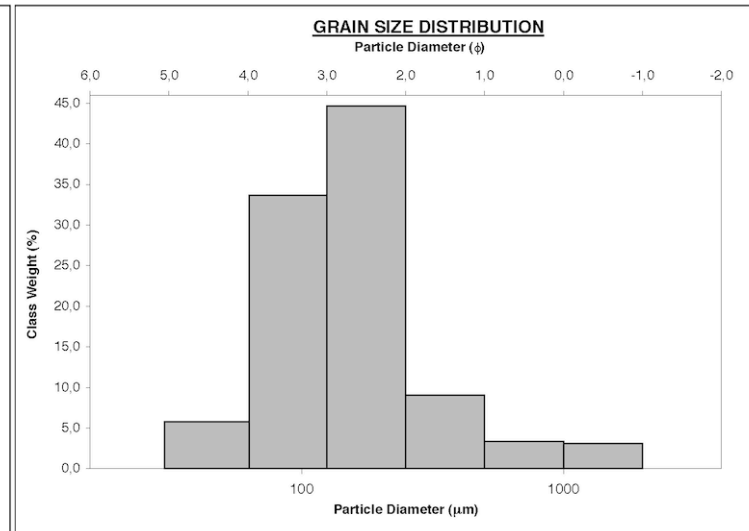
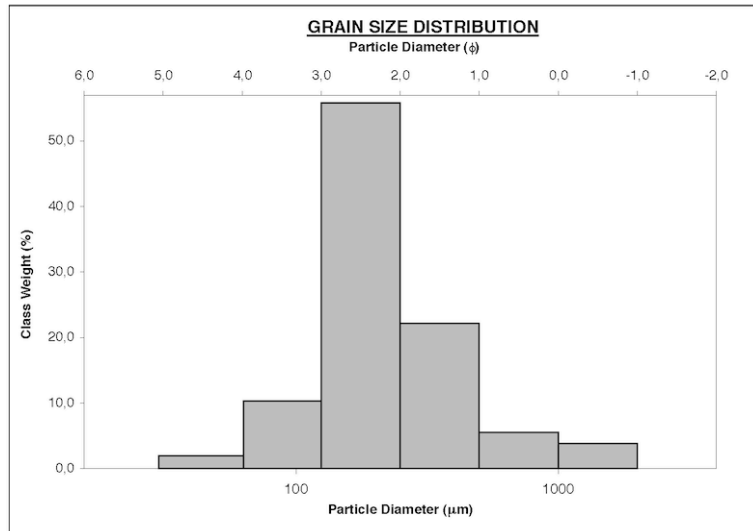
SAMPLE STATISTICS						
SAMPLE IDENTITY: 7		ANALYST & DATE: Seb, 26th Jan 2012				
SAMPLE TYPE: Unimodal, Poorly Sorted		TEXTURAL GROUP: Sand				
SEDIMENT NAME: Poorly Sorted Fine Sand						
	μm	ϕ	GRAIN SIZE DISTRIBUTION			
MODE 1:	187.5	2,500	GRAVEL: 0.0%	COARSE SAND: 4.4%		
MODE 2:			SAND: 91.3%	MEDIUM SAND: 8.7%		
MODE 3:			MUD: 8.7%	FINE SAND: 54.6%		
D ₁₀ :	65.64	1,265		V FINE SAND: 20.3%		
MEDIAN or D ₅₀ :	163.2	2,615	V COARSE GRAVEL: 0.0%	V COARSE SILT: 8.2%		
D ₉₀ :	416.2	3,929	COARSE GRAVEL: 0.0%	COARSE SILT: 0.5%		
(D ₉₀ / D ₁₀):	6,341	3,107	MEDIUM GRAVEL: 0.0%	MEDIUM SILT: 0.0%		
(D ₉₀ - D ₁₀):	350.6	2,665	FINE GRAVEL: 0.0%	FINE SILT: 0.0%		
(D ₇₅ / D ₂₅):	2,054	1,481	V FINE GRAVEL: 0.0%	V FINE SILT: 0.0%		
(D ₇₅ - D ₂₅):	115.0	1,038	V COARSE SAND: 3.3%	CLAY: 0.0%		
	METHOD OF MOMENTS		FOLK & WARD METHOD			
	Arithmetic	Geometric	Logarithmic	Geometric	Logarithmic	Description
	μm	μm	ϕ	μm	ϕ	
MEAN (\bar{x}):	240.7	164.4	2,605	150.2	2,735	Fine Sand
SORTING (σ):	273.3	2,075	1,053	2,051	1,036	Poorly Sorted
SKEWNESS (sk):	3,469	0,646	-0,646	-0,058	0,058	Symmetrical
KURTOSIS (K):	15,51	4,377	4,377	1,605	1,605	Very Leptokurtic

SAMPLE STATISTICS						
SAMPLE IDENTITY: 8		ANALYST & DATE: Seb, 26th Jan 2012				
SAMPLE TYPE: Unimodal, Poorly Sorted		TEXTURAL GROUP: Sand				
SEDIMENT NAME: Poorly Sorted Fine Sand						
	μm	ϕ	GRAIN SIZE DISTRIBUTION			
MODE 1:	187.5	2,500	GRAVEL: 0.0%	COARSE SAND: 15.5%		
MODE 2:			SAND: 97.4%	MEDIUM SAND: 21.7%		
MODE 3:			MUD: 2.6%	FINE SAND: 42.5%		
D ₁₀ :	107.5	0,114		V FINE SAND: 9.4%		
MEDIAN or D ₅₀ :	232.1	2,107	V COARSE GRAVEL: 0.0%	V COARSE SILT: 2.5%		
D ₉₀ :	924.1	3,217	COARSE GRAVEL: 0.0%	COARSE SILT: 0.1%		
(D ₉₀ / D ₁₀):	8,594	28,24	MEDIUM GRAVEL: 0.0%	MEDIUM SILT: 0.0%		
(D ₉₀ - D ₁₀):	816.5	3,103	FINE GRAVEL: 0.0%	FINE SILT: 0.0%		
(D ₇₅ / D ₂₅):	3,112	2,548	V FINE GRAVEL: 0.0%	V FINE SILT: 0.0%		
(D ₇₅ - D ₂₅):	326.0	1,638	V COARSE SAND: 8.2%	CLAY: 0.0%		
	METHOD OF MOMENTS		FOLK & WARD METHOD			
	Arithmetic	Geometric	Logarithmic	Geometric	Logarithmic	Description
	μm	μm	ϕ	μm	ϕ	
MEAN (\bar{x}):	410.9	272.9	1,873	279.6	1,838	Medium Sand
SORTING (σ):	387,2	2,263	1,178	2,343	1,228	Poorly Sorted
SKEWNESS (sk):	1,780	0,313	-0,313	0,272	-0,272	Coarse Skewed
KURTOSIS (K):	5,352	2,700	2,700	1,035	1,035	Mesokurtic



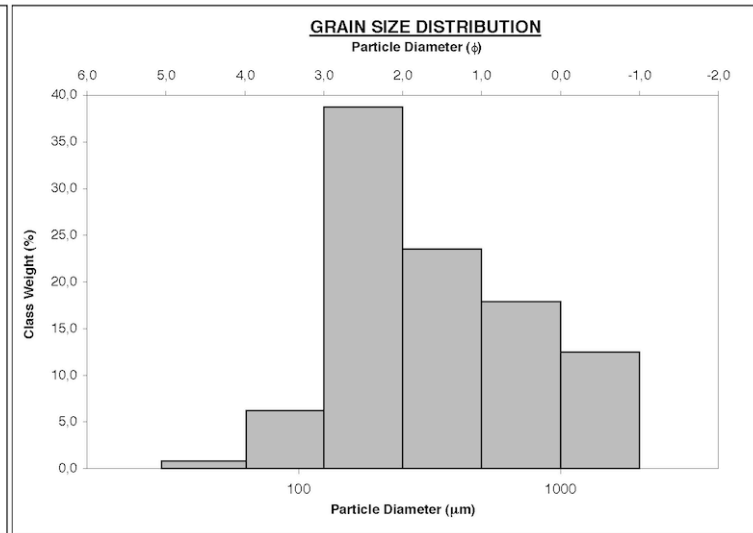
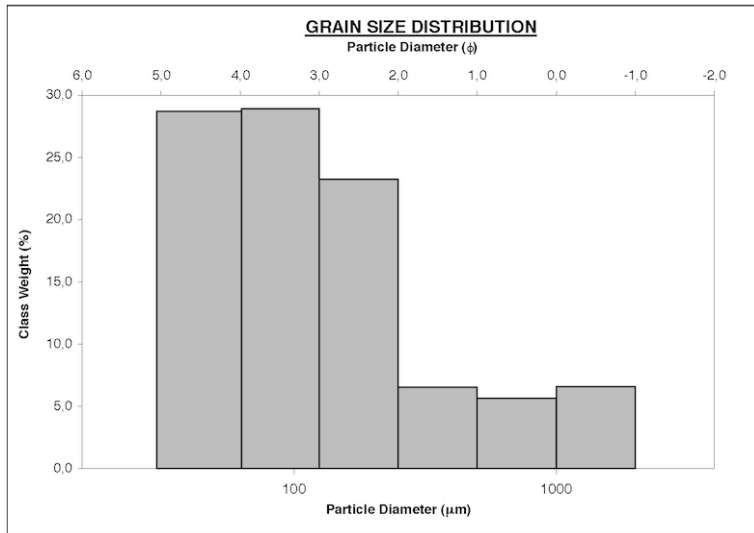
SAMPLE STATISTICS						
SAMPLE IDENTITY: 9		ANALYST & DATE: Seb, 26th Jan 2012				
SAMPLE TYPE: Unimodal, Moderately Sorted		TEXTURAL GROUP: Sand				
SEDIMENT NAME: Moderately Sorted Fine Sand						
GRAIN SIZE DISTRIBUTION						
	μm	ϕ				
MODE 1:	187.5	2,500				
MODE 2:						
MODE 3:						
D ₁₀ :	107.5	1,028				
MEDIAN or D ₅₀ :	199.3	2,327				
D ₉₀ :	490.5	3,217				
(D ₉₀ / D ₁₀):	4,562	3,131				
(D ₉₀ - D ₁₀):	383.0	2,190				
(D ₇₅ / D ₂₅):	2,101	1,629				
(D ₇₅ - D ₂₅):	161.0	1,071				
			GRAVEL: 0,0%	COARSE SAND: 5,6%		
			SAND: 98,0%	MEDIUM SAND: 22,2%		
			MUD: 2,0%	FINE SAND: 56,1%		
			V FINE SAND: 10,2%			
			V COARSE GRAVEL: 0,0%	V COARSE SILT: 1,9%		
			COARSE GRAVEL: 0,0%	COARSE SILT: 0,1%		
			MEDIUM GRAVEL: 0,0%	MEDIUM SILT: 0,0%		
			FINE GRAVEL: 0,0%	FINE SILT: 0,0%		
			V FINE GRAVEL: 0,0%	V FINE SILT: 0,0%		
			V COARSE SAND: 3,8%	CLAY: 0,0%		
METHOD OF MOMENTS						
			FOLK & WARD METHOD			
	Arithmetic	Geometric	Logarithmic	Geometric	Logarithmic	Description
	μm	μm	ϕ	μm	ϕ	
MEAN (\bar{x}):	297,9	218,4	2,195	219,8	2,186	Fine Sand
SORTING (σ):	282,4	1,915	0,937	1,914	0,937	Moderately Sorted
SKEWNESS (sk):	3,062	0,717	-0,717	0,235	-0,235	Coarse Skewed
KURTOSIS (K):	12,62	4,414	4,414	1,334	1,334	Leptokurtic

SAMPLE STATISTICS						
SAMPLE IDENTITY: 10		ANALYST & DATE: Seb, 26th Jan 2012				
SAMPLE TYPE: Unimodal, Moderately Sorted		TEXTURAL GROUP: Sand				
SEDIMENT NAME: Moderately Sorted Fine Sand						
GRAIN SIZE DISTRIBUTION						
	μm	ϕ				
MODE 1:	187.5	2,500				
MODE 2:						
MODE 3:						
D ₁₀ :	68,13	1,396				
MEDIAN or D ₅₀ :	146,8	2,768				
D ₉₀ :	380,1	3,876				
(D ₉₀ / D ₁₀):	5,579	2,777				
(D ₉₀ - D ₁₀):	312,0	2,480				
(D ₇₅ / D ₂₅):	2,329	1,552				
(D ₇₅ - D ₂₅):	123,2	1,220				
			GRAVEL: 0,0%	COARSE SAND: 3,4%		
			SAND: 93,9%	MEDIUM SAND: 9,1%		
			MUD: 6,1%	FINE SAND: 44,9%		
			V FINE SAND: 33,5%			
			V COARSE GRAVEL: 0,0%	V COARSE SILT: 5,8%		
			COARSE GRAVEL: 0,0%	COARSE SILT: 0,3%		
			MEDIUM GRAVEL: 0,0%	MEDIUM SILT: 0,0%		
			FINE GRAVEL: 0,0%	FINE SILT: 0,0%		
			V FINE GRAVEL: 0,0%	V FINE SILT: 0,0%		
			V COARSE SAND: 3,0%	CLAY: 0,0%		
METHOD OF MOMENTS						
			FOLK & WARD METHOD			
	Arithmetic	Geometric	Logarithmic	Geometric	Logarithmic	Description
	μm	μm	ϕ	μm	ϕ	
MEAN (\bar{x}):	223,5	153,1	2,708	141,0	2,826	Fine Sand
SORTING (σ):	263,0	2,027	1,020	1,957	0,969	Moderately Sorted
SKEWNESS (sk):	3,711	0,942	-0,942	0,054	-0,054	Symmetrical
KURTOSIS (K):	17,50	4,642	4,642	1,213	1,213	Leptokurtic



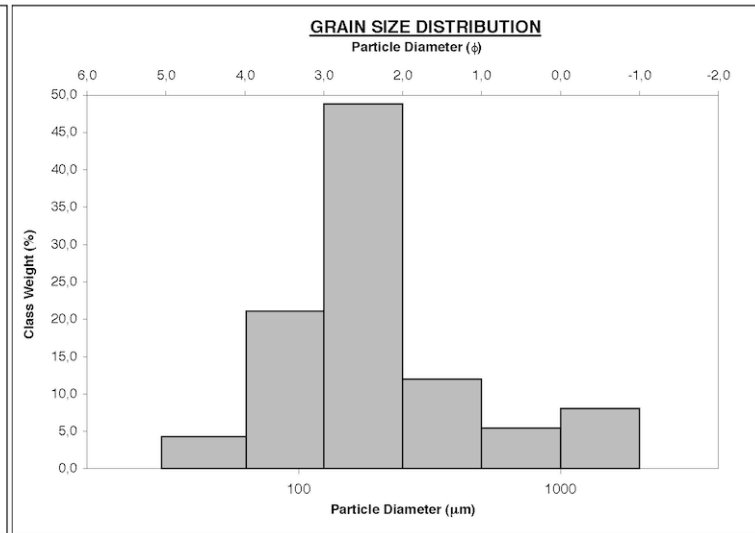
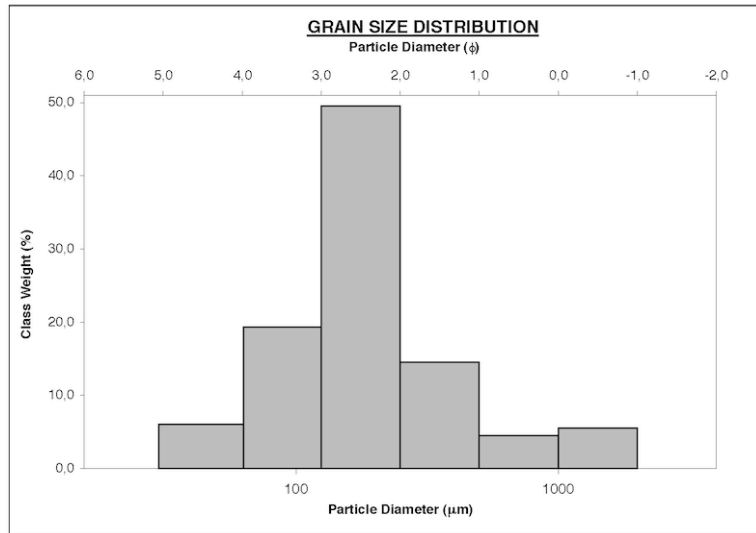
SAMPLE STATISTICS						
SAMPLE IDENTITY: 11		ANALYST & DATE: Seb, 26th Jan 2012				
SAMPLE TYPE: Bimodal, Poorly Sorted		TEXTURAL GROUP: Muddy Sand				
SEDIMENT NAME: Very Coarse Silty Very Fine Sand						
	μm	ϕ	GRAIN SIZE DISTRIBUTION			
MODE 1:	94,00	3,494	GRAVEL: 0,0%		COARSE SAND: 5,6%	
MODE 2:	1500,0	-0,500	SAND: 70,0%		MEDIUM SAND: 6,4%	
MODE 3:			MUD: 30,0%		FINE SAND: 22,9%	
D ₁₀ :	38,30	0,632	V FINE SAND: 28,6%			
MEDIAN or D ₅₀ :	101,5	3,301	V COARSE GRAVEL: 0,0%		V COARSE SILT: 28,4%	
D ₉₀ :	645,1	4,706	COARSE GRAVEL: 0,0%		COARSE SILT: 1,7%	
(D ₉₀ / D ₁₀):	16,84	7,443	MEDIUM GRAVEL: 0,0%		MEDIUM SILT: 0,0%	
(D ₉₀ - D ₁₀):	606,8	4,074	FINE GRAVEL: 0,0%		FINE SILT: 0,0%	
(D ₇₅ / D ₂₅):	3,715	1,829	V FINE GRAVEL: 0,0%		V FINE SILT: 0,0%	
(D ₇₅ - D ₂₅):	150,0	1,893	V COARSE SAND: 6,5%		CLAY: 0,0%	
	METHOD OF MOMENTS		FOLK & WARD METHOD			
	Arithmetic	Geometric	Logarithmic	Geometric	Logarithmic	Description
	μm	μm	ϕ	μm	ϕ	
MEAN (\bar{x}):	246,7	122,8	3,025	113,7	3,137	Very Fine Sand
SORTING (σ):	369,3	2,741	1,455	2,818	1,494	Poorly Sorted
SKEWNESS (sk):	2,604	0,956	-0,956	0,276	-0,276	Coarse Skewed
KURTOSIS (K):	8,811	3,163	3,163	1,106	1,106	Mesokurtic

SAMPLE STATISTICS						
SAMPLE IDENTITY: 12		ANALYST & DATE: Seb, 26th Jan 2012				
SAMPLE TYPE: Unimodal, Poorly Sorted		TEXTURAL GROUP: Sand				
SEDIMENT NAME: Poorly Sorted Fine Sand						
	μm	ϕ	GRAIN SIZE DISTRIBUTION			
MODE 1:	187,5	2,500	GRAVEL: 0,0%		COARSE SAND: 18,0%	
MODE 2:			SAND: 99,2%		MEDIUM SAND: 23,6%	
MODE 3:			MUD: 0,8%		FINE SAND: 38,9%	
D ₁₀ :	131,9	-0,202	V FINE SAND: 6,2%			
MEDIAN or D ₅₀ :	282,1	1,826	V COARSE GRAVEL: 0,0%		V COARSE SILT: 0,8%	
D ₉₀ :	1149,9	2,922	COARSE GRAVEL: 0,0%		COARSE SILT: 0,0%	
(D ₉₀ / D ₁₀):	8,716	-14,497	MEDIUM GRAVEL: 0,0%		MEDIUM SILT: 0,0%	
(D ₉₀ - D ₁₀):	1018,0	3,124	FINE GRAVEL: 0,0%		FINE SILT: 0,0%	
(D ₇₅ / D ₂₅):	3,585	3,652	V FINE GRAVEL: 0,0%		V FINE SILT: 0,0%	
(D ₇₅ - D ₂₅):	445,5	1,842	V COARSE SAND: 12,5%		CLAY: 0,0%	
	METHOD OF MOMENTS		FOLK & WARD METHOD			
	Arithmetic	Geometric	Logarithmic	Geometric	Logarithmic	Description
	μm	μm	ϕ	μm	ϕ	
MEAN (\bar{x}):	490,3	328,4	1,606	330,8	1,596	Medium Sand
SORTING (σ):	435,8	2,256	1,174	2,357	1,237	Poorly Sorted
SKEWNESS (sk):	1,406	0,322	-0,322	0,254	-0,254	Coarse Skewed
KURTOSIS (K):	3,775	2,294	2,294	0,872	0,872	Platykurtic



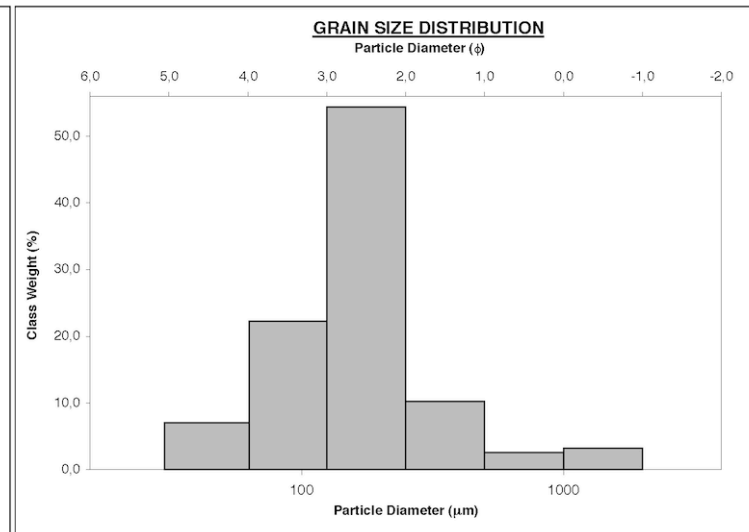
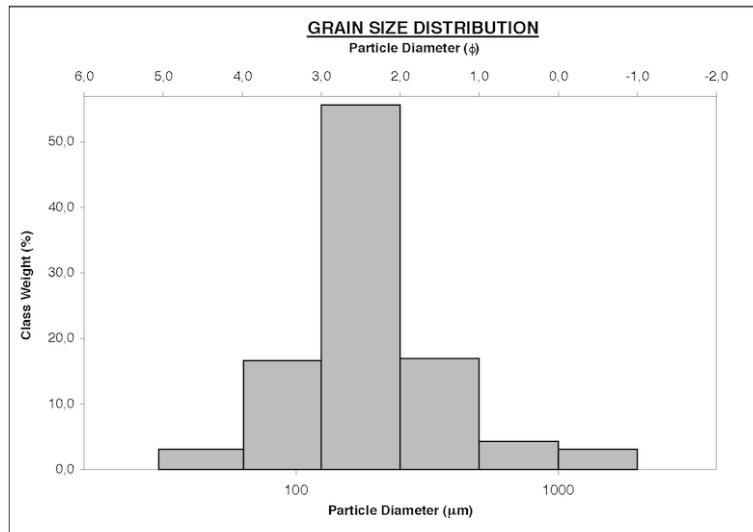
SAMPLE STATISTICS						
SAMPLE IDENTITY: 13		ANALYST & DATE: Seb, 26th Jan 2012				
SAMPLE TYPE: Unimodal, Poorly Sorted		TEXTURAL GROUP: Sand				
SEDIMENT NAME: Poorly Sorted Fine Sand						
	μm	ϕ	GRAIN SIZE DISTRIBUTION			
MODE 1:	187.5	2,500	GRAVEL: 0.0%		COARSE SAND: 4.5%	
MODE 2:			SAND: 93.6%		MEDIUM SAND: 14.5%	
MODE 3:			MUD: 6.4%		FINE SAND: 49.7%	
D ₁₀ :	71.40	0.979	V FINE SAND: 19.2%			
MEDIAN or D ₅₀ :	175.5	2,510	V COARSE GRAVEL: 0.0%		V COARSE SILT: 6.1%	
D ₉₀ :	507.4	3,808	COARSE GRAVEL: 0.0%		COARSE SILT: 0.4%	
(D ₉₀ / D ₁₀):	7,106	3,890	MEDIUM GRAVEL: 0.0%		MEDIUM SILT: 0.0%	
(D ₉₀ - D ₁₀):	436.0	2,829	FINE GRAVEL: 0.0%		FINE SILT: 0.0%	
(D ₇₅ / D ₂₅):	2,037	1,511	V FINE GRAVEL: 0.0%		V FINE SILT: 0.0%	
(D ₇₅ - D ₂₅):	126.6	1,026	V COARSE SAND: 5.6%		CLAY: 0.0%	
	METHOD OF MOMENTS		FOLK & WARD METHOD			
	Arithmetic	Geometric	Logarithmic	Geometric	Logarithmic	Description
	μm	μm	ϕ	μm	ϕ	
MEAN (\bar{x}):	286.2	187.0	2.419	180.3	2.471	Fine Sand
SORTING (σ):	329.4	2,188	1,130	2,266	1,180	Poorly Sorted
SKEWNESS (sk):	2,836	0,674	-0,674	0,130	-0,130	Coarse Skewed
KURTOSIS (K):	10,48	3,860	3,860	1,732	1,732	Very Leptokurtic

SAMPLE STATISTICS						
SAMPLE IDENTITY: 14		ANALYST & DATE: Seb, 26th Jan 2012				
SAMPLE TYPE: Bimodal, Poorly Sorted		TEXTURAL GROUP: Sand				
SEDIMENT NAME: Poorly Sorted Fine Sand						
	μm	ϕ	GRAIN SIZE DISTRIBUTION			
MODE 1:	187.5	2,500	GRAVEL: 0.0%		COARSE SAND: 5.5%	
MODE 2:	1500.0	-0,500	SAND: 95.5%		MEDIUM SAND: 12.0%	
MODE 3:			MUD: 4.5%		FINE SAND: 49.0%	
D ₁₀ :	75.35	0,356	V FINE SAND: 20.9%			
MEDIAN or D ₅₀ :	176.9	2,499	V COARSE GRAVEL: 0.0%		V COARSE SILT: 4.3%	
D ₉₀ :	781.4	3,730	COARSE GRAVEL: 0.0%		COARSE SILT: 0.3%	
(D ₉₀ / D ₁₀):	10,37	10,48	MEDIUM GRAVEL: 0.0%		MEDIUM SILT: 0.0%	
(D ₉₀ - D ₁₀):	706.0	3,374	FINE GRAVEL: 0.0%		FINE SILT: 0.0%	
(D ₇₅ / D ₂₅):	2,092	1,545	V FINE GRAVEL: 0.0%		V FINE SILT: 0.0%	
(D ₇₅ - D ₂₅):	134.7	1,065	V COARSE SAND: 8.1%		CLAY: 0.0%	
	METHOD OF MOMENTS		FOLK & WARD METHOD			
	Arithmetic	Geometric	Logarithmic	Geometric	Logarithmic	Description
	μm	μm	ϕ	μm	ϕ	
MEAN (\bar{x}):	320.6	199.1	2,328	191.6	2,383	Fine Sand
SORTING (σ):	381.1	2,289	1,195	2,327	1,219	Poorly Sorted
SKEWNESS (sk):	2,383	0,827	-0,827	0,239	-0,239	Coarse Skewed
KURTOSIS (K):	7,517	3,568	3,568	1,673	1,673	Very Leptokurtic



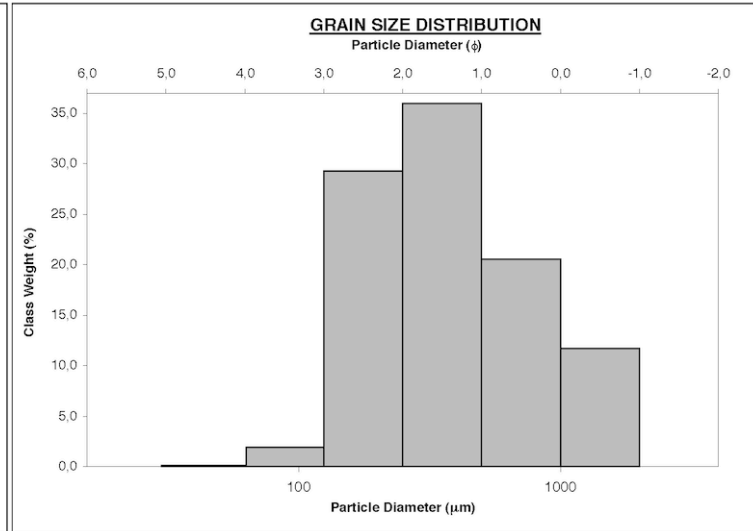
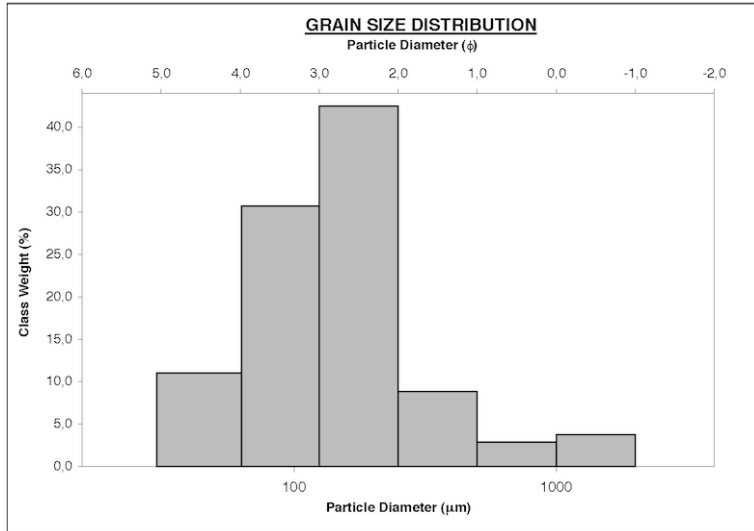
SAMPLE STATISTICS						
SAMPLE IDENTITY: 15		ANALYST & DATE: Seb, 26th Jan 2012				
SAMPLE TYPE: Unimodal, Moderately Sorted		TEXTURAL GROUP: Sand				
SEDIMENT NAME: Moderately Sorted Fine Sand						
		GRAIN SIZE DISTRIBUTION				
	μm	ϕ				
MODE 1:	187.5	2.500	GRAVEL: 0.0%		COARSE SAND: 4.3%	
MODE 2:			SAND: 96.8%		MEDIUM SAND: 17.0%	
MODE 3:			MUD: 3.2%		FINE SAND: 55.9%	
D ₁₀ :	83.30	1.158			V FINE SAND: 16.5%	
MEDIAN or D ₅₀ :	181.8	2.459	V COARSE GRAVEL: 0.0%		V COARSE SILT: 3.1%	
D ₉₀ :	448.0	3.585	COARSE GRAVEL: 0.0%		COARSE SILT: 0.2%	
(D ₉₀ / D ₁₀):	5.378	3.095	MEDIUM GRAVEL: 0.0%		MEDIUM SILT: 0.0%	
(D ₉₀ - D ₁₀):	364.7	2.427	FINE GRAVEL: 0.0%		FINE SILT: 0.0%	
(D ₇₅ / D ₂₅):	1.859	1.444	V FINE GRAVEL: 0.0%		V FINE SILT: 0.0%	
(D ₇₅ - D ₂₅):	114.5	0.894	V COARSE SAND: 3.0%		CLAY: 0.0%	
		METHOD OF MOMENTS			FOLK & WARD METHOD	
	Arithmetic	Geometric	Logarithmic	Geometric	Logarithmic	Description
	μm	μm	ϕ	μm	ϕ	
MEAN (\bar{x}):	263.1	191.6	2.384	189.6	2.399	Fine Sand
SORTING (σ):	260.7	1.928	0.947	1.928	0.947	Moderately Sorted
SKEWNESS (sk):	3.442	0.683	-0.683	0.136	-0.136	Coarse Skewed
KURTOSIS (K):	15.89	4.561	4.561	1.569	1.569	Very Leptokurtic

SAMPLE STATISTICS						
SAMPLE IDENTITY: 16		ANALYST & DATE: Seb, 26th Jan 2012				
SAMPLE TYPE: Unimodal, Moderately Sorted		TEXTURAL GROUP: Sand				
SEDIMENT NAME: Moderately Sorted Fine Sand						
		GRAIN SIZE DISTRIBUTION				
	μm	ϕ				
MODE 1:	187.5	2.500	GRAVEL: 0.0%		COARSE SAND: 2.6%	
MODE 2:			SAND: 92.6%		MEDIUM SAND: 10.2%	
MODE 3:			MUD: 7.4%		FINE SAND: 54.6%	
D ₁₀ :	68.17	1.415			V FINE SAND: 22.1%	
MEDIAN or D ₅₀ :	162.2	2.624	V COARSE GRAVEL: 0.0%		V COARSE SILT: 7.0%	
D ₉₀ :	375.1	3.875	COARSE GRAVEL: 0.0%		COARSE SILT: 0.4%	
(D ₉₀ / D ₁₀):	5.502	2.739	MEDIUM GRAVEL: 0.0%		MEDIUM SILT: 0.0%	
(D ₉₀ - D ₁₀):	306.9	2.460	FINE GRAVEL: 0.0%		FINE SILT: 0.0%	
(D ₇₅ / D ₂₅):	2.049	1.478	V FINE GRAVEL: 0.0%		V FINE SILT: 0.0%	
(D ₇₅ - D ₂₅):	114.1	1.035	V COARSE SAND: 3.2%		CLAY: 0.0%	
		METHOD OF MOMENTS			FOLK & WARD METHOD	
	Arithmetic	Geometric	Logarithmic	Geometric	Logarithmic	Description
	μm	μm	ϕ	μm	ϕ	
MEAN (\bar{x}):	231.9	162.6	2.621	149.4	2.743	Fine Sand
SORTING (σ):	261.2	2.001	1.001	1.936	0.953	Moderately Sorted
SKEWNESS (sk):	3.812	0.698	-0.698	-0.083	0.083	Symmetrical
KURTOSIS (K):	18.20	4.806	4.806	1.443	1.443	Leptokurtic



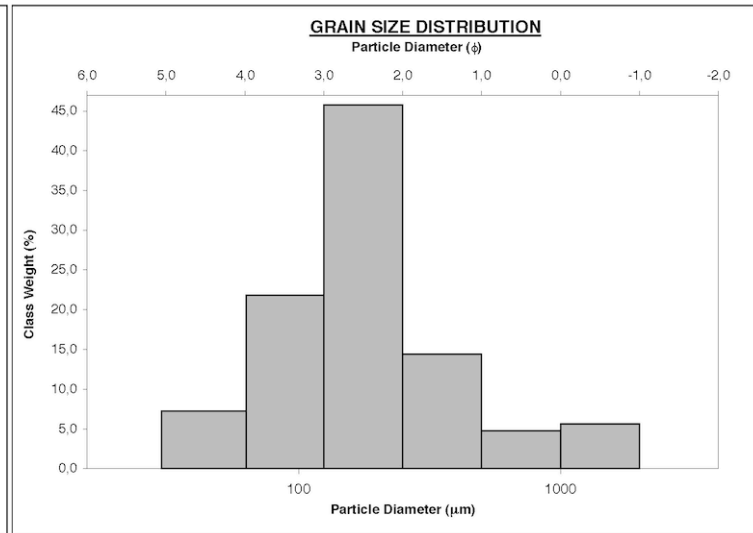
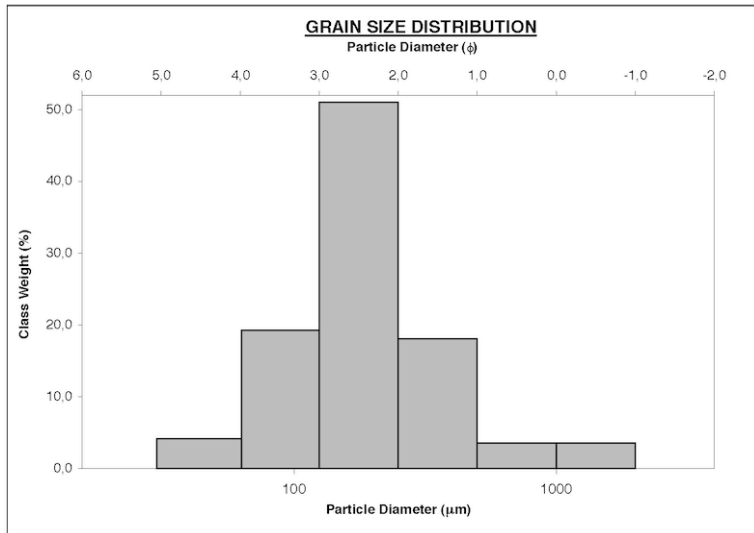
SAMPLE STATISTICS						
SAMPLE IDENTITY: 17		ANALYST & DATE: Seb, 26th Jan 2012				
SAMPLE TYPE: Unimodal, Poorly Sorted		TEXTURAL GROUP: Muddy Sand				
SEDIMENT NAME: Very Coarse Silty Fine Sand						
	μm	ϕ	GRAIN SIZE DISTRIBUTION			
MODE 1:	187.5	2,500	GRAVEL: 0.0%	COARSE SAND: 2.9%		
MODE 2:			SAND: 88.4%	MEDIUM SAND: 8.8%		
MODE 3:			MUD: 11.6%	FINE SAND: 42.5%		
D ₁₀ :	56.33	1,384		V FINE SAND: 30.4%		
MEDIAN or D ₅₀ :	142.2	2,814	V COARSE GRAVEL: 0.0%	V COARSE SILT: 11.0%		
D ₉₀ :	383.2	4,150	COARSE GRAVEL: 0.0%	COARSE SILT: 0.6%		
(D ₉₀ / D ₁₀):	6.803	2,999	MEDIUM GRAVEL: 0.0%	MEDIUM SILT: 0.0%		
(D ₉₀ - D ₁₀):	326.9	2,766	FINE GRAVEL: 0.0%	FINE SILT: 0.0%		
(D ₇₅ / D ₂₅):	2,517	1,599	V FINE GRAVEL: 0.0%	V FINE SILT: 0.0%		
(D ₇₅ - D ₂₅):	128.9	1,332	V COARSE SAND: 3.8%	CLAY: 0.0%		
	METHOD OF MOMENTS		FOLK & WARD METHOD			
	Arithmetic	Geometric	Logarithmic	Geometric	Logarithmic	Description
	μm	μm	ϕ	μm	ϕ	
MEAN (\bar{x}):	224.5	145.4	2.782	134.7	2.893	Fine Sand
SORTING (σ):	283.8	2,166	1,115	2,131	1,091	Poorly Sorted
SKEWNESS (sk):	3,549	0,815	-0,815	0,006	-0,006	Symmetrical
KURTOSIS (K):	15.72	4,228	4,228	1,283	1,283	Leptokurtic

SAMPLE STATISTICS						
SAMPLE IDENTITY: 18		ANALYST & DATE: Seb, 26th Jan 2012				
SAMPLE TYPE: Unimodal, Poorly Sorted		TEXTURAL GROUP: Sand				
SEDIMENT NAME: Poorly Sorted Medium Sand						
	μm	ϕ	GRAIN SIZE DISTRIBUTION			
MODE 1:	375.0	1,500	GRAVEL: 0.0%	COARSE SAND: 20.7%		
MODE 2:			SAND: 99.9%	MEDIUM SAND: 36.2%		
MODE 3:			MUD: 0.1%	FINE SAND: 29.4%		
D ₁₀ :	150.9	-0,150		V FINE SAND: 1.9%		
MEDIAN or D ₅₀ :	357.0	1,486	V COARSE GRAVEL: 0.0%	V COARSE SILT: 0.1%		
D ₉₀ :	1109.4	2,728	COARSE GRAVEL: 0.0%	COARSE SILT: 0.0%		
(D ₉₀ / D ₁₀):	7,350	-18,212	MEDIUM GRAVEL: 0.0%	MEDIUM SILT: 0.0%		
(D ₉₀ - D ₁₀):	958.5	2,878	FINE GRAVEL: 0.0%	FINE SILT: 0.0%		
(D ₇₅ / D ₂₅):	2,984	3,462	V FINE GRAVEL: 0.0%	V FINE SILT: 0.0%		
(D ₇₅ - D ₂₅):	426.4	1,577	V COARSE SAND: 11.8%	CLAY: 0.0%		
	METHOD OF MOMENTS		FOLK & WARD METHOD			
	Arithmetic	Geometric	Logarithmic	Geometric	Logarithmic	Description
	μm	μm	ϕ	μm	ϕ	
MEAN (\bar{x}):	524.0	380.6	1,394	377.6	1,405	Medium Sand
SORTING (σ):	409.5	2,032	1,023	2,152	1,106	Poorly Sorted
SKEWNESS (sk):	1,423	0,309	-0,309	0,146	-0,146	Coarse Skewed
KURTOSIS (K):	3,981	2,359	2,359	0,902	0,902	Mesokurtic



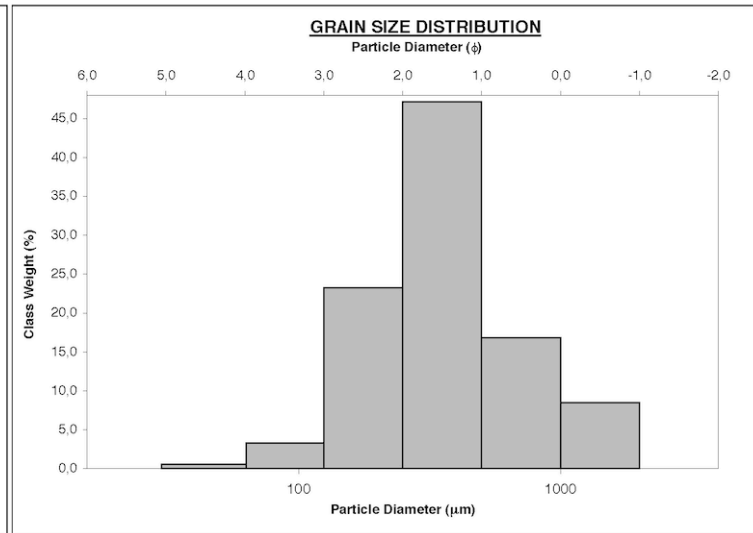
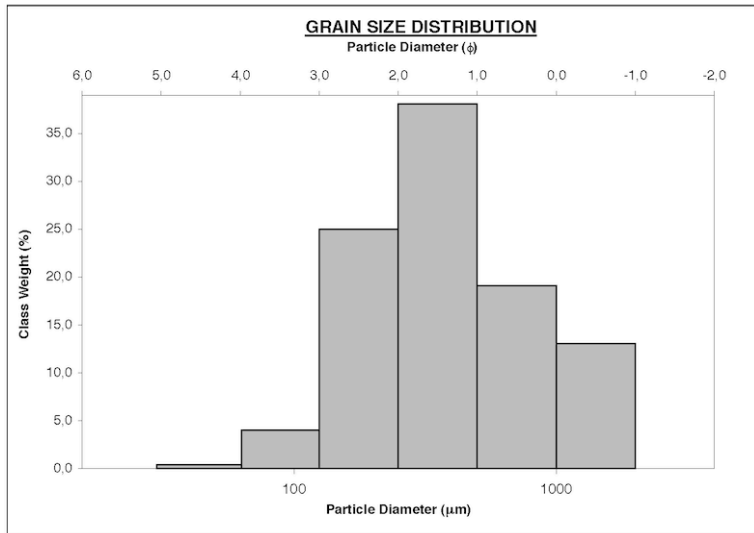
SAMPLE STATISTICS						
SAMPLE IDENTITY: 19		ANALYST & DATE: Seb, 26th Jan 2012				
SAMPLE TYPE: Unimodal, Poorly Sorted		TEXTURAL GROUP: Sand				
SEDIMENT NAME: Poorly Sorted Fine Sand						
	μm	ϕ	GRAIN SIZE DISTRIBUTION			
MODE 1:	187,5	2,500	GRAVEL: 0,0%		COARSE SAND: 3,6%	
MODE 2:			SAND: 95,5%		MEDIUM SAND: 18,1%	
MODE 3:			MUD: 4,5%		FINE SAND: 51,2%	
D ₁₀ :	76,74	1,160	V FINE SAND: 19,1%			
MEDIAN or D ₅₀ :	178,7	2,484	V COARSE GRAVEL: 0,0%		V COARSE SILT: 4,2%	
D ₉₀ :	447,6	3,704	COARSE GRAVEL: 0,0%		COARSE SILT: 0,2%	
(D ₉₀ / D ₁₀):	5,833	3,194	MEDIUM GRAVEL: 0,0%		MEDIUM SILT: 0,0%	
(D ₉₀ - D ₁₀):	370,9	2,544	FINE GRAVEL: 0,0%		FINE SILT: 0,0%	
(D ₇₅ / D ₂₅):	1,977	1,495	V FINE GRAVEL: 0,0%		V FINE SILT: 0,0%	
(D ₇₅ - D ₂₅):	124,5	0,984	V COARSE SAND: 3,5%		CLAY: 0,0%	
	METHOD OF MOMENTS		FOLK & WARD METHOD			
	Arithmetic	Geometric	Logarithmic	Geometric	Logarithmic	Description
	μm	μm	ϕ	μm	ϕ	
MEAN (\bar{x}):	263,6	186,5	2,422	182,3	2,456	Fine Sand
SORTING (σ):	274,1	2,006	1,004	2,019	1,013	Poorly Sorted
SKEWNESS (sk):	3,365	0,614	-0,614	0,106	-0,106	Coarse Skewed
KURTOSIS (K):	14,98	4,247	4,247	1,480	1,480	Leptokurtic

SAMPLE STATISTICS						
SAMPLE IDENTITY: 20		ANALYST & DATE: Seb, 26th Jan 2012				
SAMPLE TYPE: Unimodal, Poorly Sorted		TEXTURAL GROUP: Sand				
SEDIMENT NAME: Poorly Sorted Fine Sand						
	μm	ϕ	GRAIN SIZE DISTRIBUTION			
MODE 1:	187,5	2,500	GRAVEL: 0,0%		COARSE SAND: 4,7%	
MODE 2:			SAND: 92,3%		MEDIUM SAND: 14,4%	
MODE 3:			MUD: 7,7%		FINE SAND: 45,9%	
D ₁₀ :	67,62	0,931	V FINE SAND: 21,7%			
MEDIAN or D ₅₀ :	170,6	2,551	V COARSE GRAVEL: 0,0%		V COARSE SILT: 7,3%	
D ₉₀ :	524,6	3,886	COARSE GRAVEL: 0,0%		COARSE SILT: 0,4%	
(D ₉₀ / D ₁₀):	7,758	4,176	MEDIUM GRAVEL: 0,0%		MEDIUM SILT: 0,0%	
(D ₉₀ - D ₁₀):	457,0	2,956	FINE GRAVEL: 0,0%		FINE SILT: 0,0%	
(D ₇₅ / D ₂₅):	2,290	1,596	V FINE GRAVEL: 0,0%		V FINE SILT: 0,0%	
(D ₇₅ - D ₂₅):	140,3	1,196	V COARSE SAND: 5,6%		CLAY: 0,0%	
	METHOD OF MOMENTS		FOLK & WARD METHOD			
	Arithmetic	Geometric	Logarithmic	Geometric	Logarithmic	Description
	μm	μm	ϕ	μm	ϕ	
MEAN (\bar{x}):	283,5	181,0	2,466	174,5	2,519	Fine Sand
SORTING (σ):	332,9	2,250	1,170	2,351	1,233	Poorly Sorted
SKEWNESS (sk):	2,791	0,649	-0,649	0,115	-0,115	Coarse Skewed
KURTOSIS (K):	10,23	3,633	3,633	1,535	1,535	Very Leptokurtic



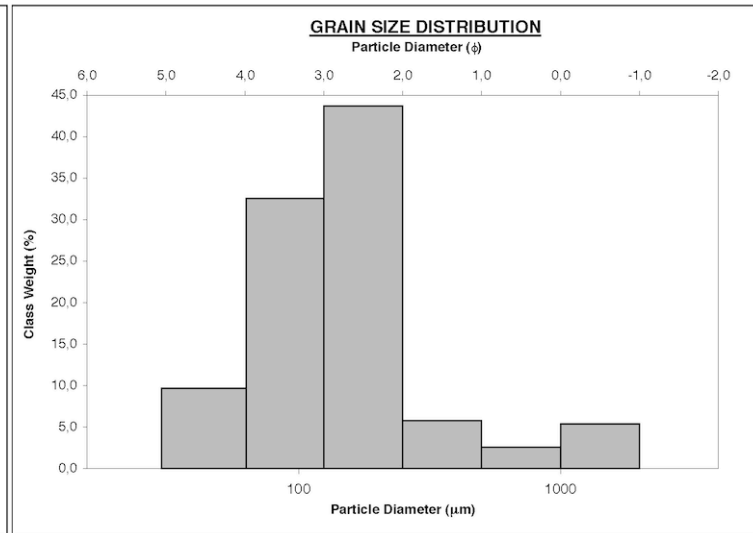
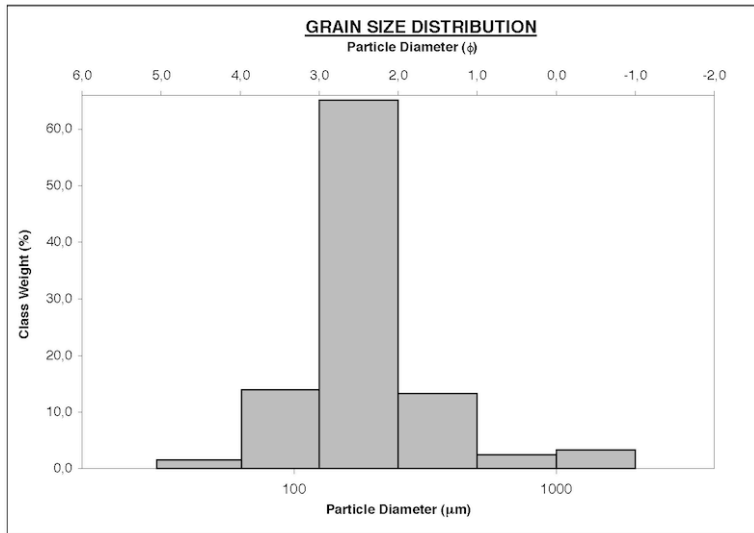
SAMPLE STATISTICS						
SAMPLE IDENTITY: 21		ANALYST & DATE: Seb, 26th Jan 2012				
SAMPLE TYPE: Unimodal, Poorly Sorted		TEXTURAL GROUP: Sand				
SEDIMENT NAME: Poorly Sorted Medium Sand						
	μm	ϕ	GRAIN SIZE DISTRIBUTION			
MODE 1:	375.0	1,500	GRAVEL: 0.0%		COARSE SAND: 19.2%	
MODE 2:			SAND: 99.6%		MEDIUM SAND: 38.2%	
MODE 3:			MUD: 0.4%		FINE SAND: 25.0%	
D ₁₀ :	146.1	-0.237			V FINE SAND: 4.0%	
MEDIAN or D ₅₀ :	363.0	1,462	V COARSE GRAVEL: 0.0%		V COARSE SILT: 0.4%	
D ₉₀ :	1178.8	2,775	COARSE GRAVEL: 0.0%		COARSE SILT: 0.0%	
(D ₉₀ / D ₁₀):	8,071	-11,692	MEDIUM GRAVEL: 0.0%		MEDIUM SILT: 0.0%	
(D ₉₀ - D ₁₀):	1032.8	3,013	FINE GRAVEL: 0.0%		FINE SILT: 0.0%	
(D ₇₅ / D ₂₅):	2,945	3,521	V FINE GRAVEL: 0.0%		V FINE SILT: 0.0%	
(D ₇₅ - D ₂₅):	430.3	1,558	V COARSE SAND: 13.1%		CLAY: 0.0%	
	METHOD OF MOMENTS		FOLK & WARD METHOD			
	Arithmetic	Geometric	Logarithmic	Geometric	Logarithmic	Description
	μm	μm	ϕ	μm	ϕ	
MEAN (\bar{x}):	535.2	382.3	1,387	383.5	1,383	Medium Sand
SORTING (σ):	423.9	2,102	1,072	2,205	1,141	Poorly Sorted
SKEWNESS (sk):	1,361	0,144	-0,144	0,129	-0,129	Coarse Skewed
KURTOSIS (K):	3,706	2,523	2,523	0,945	0,945	Mesokurtic

SAMPLE STATISTICS						
SAMPLE IDENTITY: 22		ANALYST & DATE: Seb, 26th Jan 2012				
SAMPLE TYPE: Unimodal, Poorly Sorted		TEXTURAL GROUP: Sand				
SEDIMENT NAME: Poorly Sorted Medium Sand						
	μm	ϕ	GRAIN SIZE DISTRIBUTION			
MODE 1:	375.0	1,500	GRAVEL: 0.0%		COARSE SAND: 16.9%	
MODE 2:			SAND: 99.4%		MEDIUM SAND: 47.4%	
MODE 3:			MUD: 0.6%		FINE SAND: 23.3%	
D ₁₀ :	150.0	0,087			V FINE SAND: 3.3%	
MEDIAN or D ₅₀ :	349.0	1,519	V COARSE GRAVEL: 0.0%		V COARSE SILT: 0.5%	
D ₉₀ :	941.7	2,737	COARSE GRAVEL: 0.0%		COARSE SILT: 0.0%	
(D ₉₀ / D ₁₀):	6,279	31,58	MEDIUM GRAVEL: 0.0%		MEDIUM SILT: 0.0%	
(D ₉₀ - D ₁₀):	791.7	2,650	FINE GRAVEL: 0.0%		FINE SILT: 0.0%	
(D ₇₅ / D ₂₅):	2,172	2,147	V FINE GRAVEL: 0.0%		V FINE SILT: 0.0%	
(D ₇₅ - D ₂₅):	274.3	1,119	V COARSE SAND: 8.5%		CLAY: 0.0%	
	METHOD OF MOMENTS		FOLK & WARD METHOD			
	Arithmetic	Geometric	Logarithmic	Geometric	Logarithmic	Description
	μm	μm	ϕ	μm	ϕ	
MEAN (\bar{x}):	479.4	359.2	1,477	358.4	1,480	Medium Sand
SORTING (σ):	363.7	1,949	0,963	2,027	1,019	Poorly Sorted
SKEWNESS (sk):	1,775	0,148	-0,148	0,103	-0,103	Coarse Skewed
KURTOSIS (K):	5,496	3,214	3,214	1,233	1,233	Leptokurtic



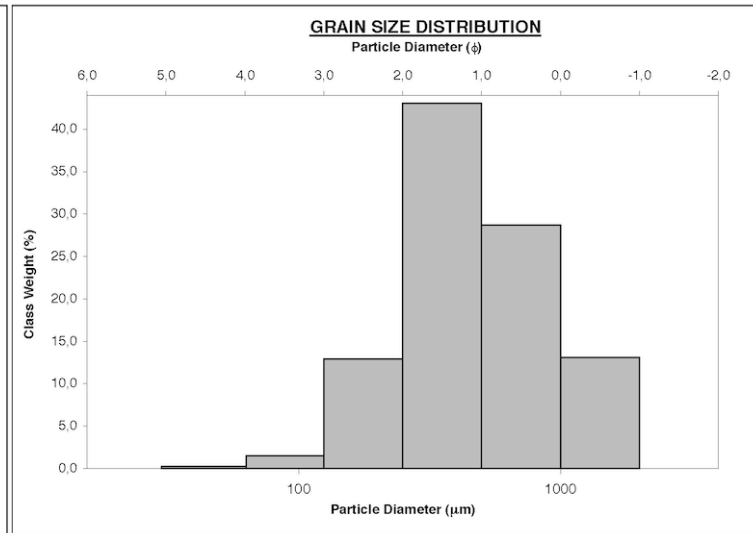
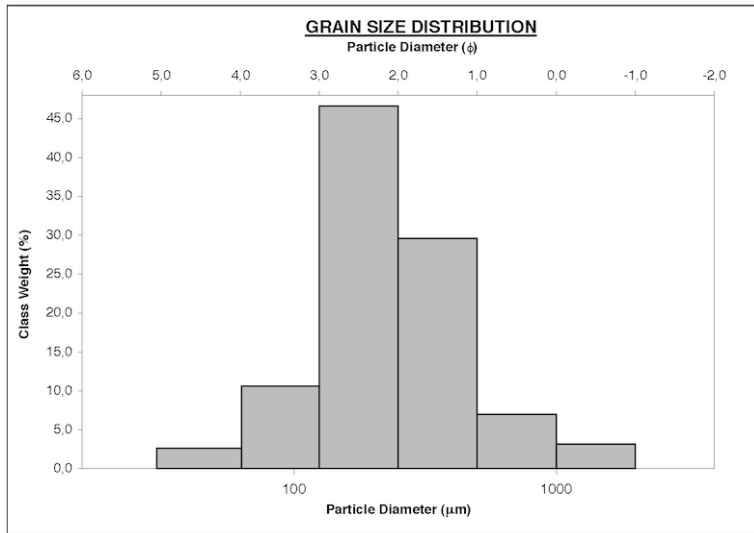
SAMPLE STATISTICS						
SAMPLE IDENTITY: 23		ANALYST & DATE: Seb, 26th Jan 2012				
SAMPLE TYPE: Unimodal, Moderately Sorted		TEXTURAL GROUP: Sand				
SEDIMENT NAME: Moderately Sorted Fine Sand						
GRAIN SIZE DISTRIBUTION						
	μm	ϕ				
MODE 1:	187.5	2,500				
MODE 2:						
MODE 3:						
D ₁₀ :	95.11	1,323				
MEDIAN or D ₅₀ :	180.0	2,474				
D ₉₀ :	399.6	3,394				
(D ₉₀ / D ₁₀):	4,201	2,565				
(D ₉₀ - D ₁₀):	304.5	2,071				
(D ₇₅ / D ₂₅):	1,698	1,365				
(D ₇₅ - D ₂₅):	96.40	0,764				
			GRAVEL: 0,0%	COARSE SAND: 2,4%		
			SAND: 98,4%	MEDIUM SAND: 13,3%		
			MUD: 1,6%	FINE SAND: 65,5%		
			V FINE SAND: 13,9%			
			V COARSE GRAVEL: 0,0%	V COARSE SILT: 1,6%		
			COARSE GRAVEL: 0,0%	COARSE SILT: 0,1%		
			MEDIUM GRAVEL: 0,0%	MEDIUM SILT: 0,0%		
			FINE GRAVEL: 0,0%	FINE SILT: 0,0%		
			V FINE GRAVEL: 0,0%	V FINE SILT: 0,0%		
			V COARSE SAND: 3,3%	CLAY: 0,0%		
METHOD OF MOMENTS						
			FOLK & WARD METHOD			
	Arithmetic	Geometric	Logarithmic	Geometric	Logarithmic	Description
	μm	μm	ϕ	μm	ϕ	
MEAN (\bar{x}):	253.9	190.6	2,392	187.6	2,414	Fine Sand
SORTING (σ):	257.2	1,800	0,848	1,700	0,765	Moderately Sorted
SKEWNESS (sk):	3,878	1,158	-1,158	0,154	-0,154	Coarse Skewed
KURTOSIS (K):	18,51	6,273	6,273	1,633	1,633	Very Leptokurtic

SAMPLE STATISTICS						
SAMPLE IDENTITY: 24		ANALYST & DATE: Seb, 26th Jan 2012				
SAMPLE TYPE: Unimodal, Poorly Sorted		TEXTURAL GROUP: Muddy Sand				
SEDIMENT NAME: Very Coarse Silty Fine Sand						
GRAIN SIZE DISTRIBUTION						
	μm	ϕ				
MODE 1:	187.5	2,500				
MODE 2:						
MODE 3:						
D ₁₀ :	61.40	1,366				
MEDIAN or D ₅₀ :	140.6	2,831				
D ₉₀ :	388.0	4,026				
(D ₉₀ / D ₁₀):	6,319	2,947				
(D ₉₀ - D ₁₀):	326.6	2,660				
(D ₇₅ / D ₂₅):	2,428	1,566				
(D ₇₅ - D ₂₅):	122.8	1,280				
			GRAVEL: 0,0%	COARSE SAND: 2,5%		
			SAND: 89,8%	MEDIUM SAND: 5,7%		
			MUD: 10,2%	FINE SAND: 43,8%		
			V FINE SAND: 32,3%			
			V COARSE GRAVEL: 0,0%	V COARSE SILT: 9,7%		
			COARSE GRAVEL: 0,0%	COARSE SILT: 0,6%		
			MEDIUM GRAVEL: 0,0%	MEDIUM SILT: 0,0%		
			FINE GRAVEL: 0,0%	FINE SILT: 0,0%		
			V FINE GRAVEL: 0,0%	V FINE SILT: 0,0%		
			V COARSE SAND: 5,4%	CLAY: 0,0%		
METHOD OF MOMENTS						
			FOLK & WARD METHOD			
	Arithmetic	Geometric	Logarithmic	Geometric	Logarithmic	Description
	μm	μm	ϕ	μm	ϕ	
MEAN (\bar{x}):	238.3	147.5	2,761	134.0	2,900	Fine Sand
SORTING (σ):	323.9	2,215	1,148	2,203	1,139	Poorly Sorted
SKEWNESS (sk):	3,230	1,048	-1,048	0,070	-0,070	Symmetrical
KURTOSIS (K):	12,56	4,601	4,601	1,477	1,477	Leptokurtic



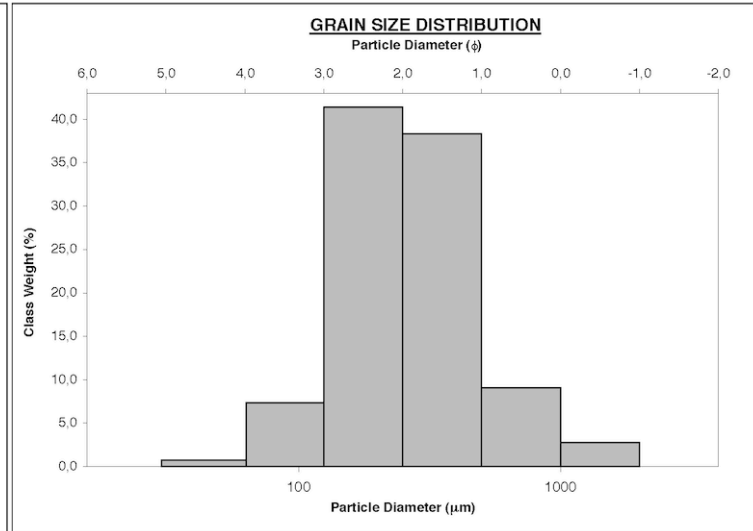
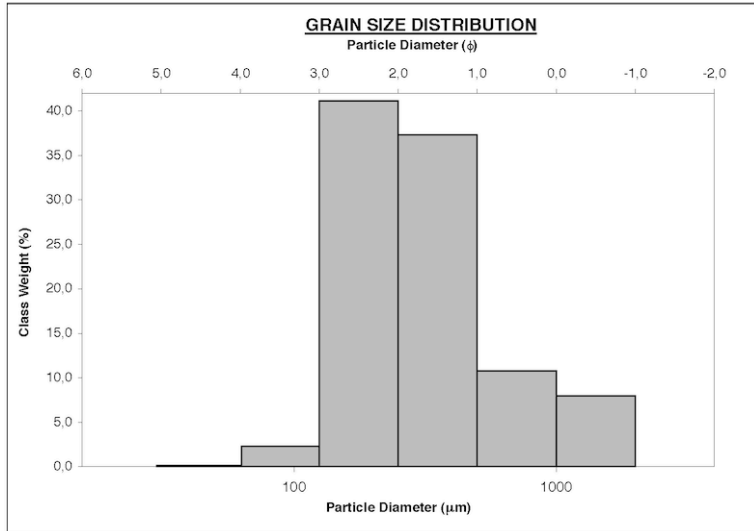
SAMPLE STATISTICS						
SAMPLE IDENTITY: 25		ANALYST & DATE: Seb, 26th Jan 2012				
SAMPLE TYPE: Unimodal, Moderately Sorted		TEXTURAL GROUP: Sand				
SEDIMENT NAME: Moderately Sorted Fine Sand						
	μm	ϕ	GRAIN SIZE DISTRIBUTION			
MODE 1:	187.5	2,500	GRAVEL: 0.0%		COARSE SAND: 7.0%	
MODE 2:			SAND: 97.2%		MEDIUM SAND: 29.7%	
MODE 3:			MUD: 2.8%		FINE SAND: 46.8%	
D ₁₀ :	100.9	0.983	V FINE SAND: 10.5%			
MEDIAN or D ₅₀ :	215.2	2,216	V COARSE GRAVEL: 0.0%		V COARSE SILT: 2.6%	
D ₉₀ :	505.8	3,310	COARSE GRAVEL: 0.0%		COARSE SILT: 0.2%	
(D ₉₀ / D ₁₀):	5.015	3,366	MEDIUM GRAVEL: 0.0%		MEDIUM SILT: 0.0%	
(D ₉₀ - D ₁₀):	405.0	2,326	FINE GRAVEL: 0.0%		FINE SILT: 0.0%	
(D ₇₅ / D ₂₅):	2,378	1,833	V FINE GRAVEL: 0.0%		V FINE SILT: 0.0%	
(D ₇₅ - D ₂₅):	204.8	1,250	V COARSE SAND: 3.1%		CLAY: 0.0%	
	METHOD OF MOMENTS		FOLK & WARD METHOD			
	Arithmetic	Geometric	Logarithmic	Geometric	Logarithmic	Description
	μm	μm	ϕ	μm	ϕ	
MEAN (\bar{x}):	309.9	228.5	2.130	230.2	2.119	Fine Sand
SORTING (σ):	270.2	1,958	0.969	1,957	0.968	Moderately Sorted
SKEWNESS (sk):	2.860	0.301	-0.301	0.139	-0.139	Coarse Skewed
KURTOSIS (K):	12.37	3.767	3.767	1.152	1.152	Leptokurtic

SAMPLE STATISTICS						
SAMPLE IDENTITY: 26		ANALYST & DATE: Seb, 26th Jan 2012				
SAMPLE TYPE: Unimodal, Moderately Sorted		TEXTURAL GROUP: Sand				
SEDIMENT NAME: Moderately Sorted Medium Sand						
	μm	ϕ	GRAIN SIZE DISTRIBUTION			
MODE 1:	375.0	1,500	GRAVEL: 0.0%		COARSE SAND: 28.8%	
MODE 2:			SAND: 99.7%		MEDIUM SAND: 43.2%	
MODE 3:			MUD: 0.3%		FINE SAND: 13.0%	
D ₁₀ :	193.6	-0,240	V FINE SAND: 1.5%			
MEDIAN or D ₅₀ :	439.8	1,185	V COARSE GRAVEL: 0.0%		V COARSE SILT: 0.3%	
D ₉₀ :	1180.9	2,369	COARSE GRAVEL: 0.0%		COARSE SILT: 0.0%	
(D ₉₀ / D ₁₀):	6.100	-9,875	MEDIUM GRAVEL: 0.0%		MEDIUM SILT: 0.0%	
(D ₉₀ - D ₁₀):	987.3	2,609	FINE GRAVEL: 0.0%		FINE SILT: 0.0%	
(D ₇₅ / D ₂₅):	2,555	4,295	V FINE GRAVEL: 0.0%		V FINE SILT: 0.0%	
(D ₇₅ - D ₂₅):	457.8	1,353	V COARSE SAND: 13.2%		CLAY: 0.0%	
	METHOD OF MOMENTS		FOLK & WARD METHOD			
	Arithmetic	Geometric	Logarithmic	Geometric	Logarithmic	Description
	μm	μm	ϕ	μm	ϕ	
MEAN (\bar{x}):	601.6	461.0	1.117	471.3	1.085	Medium Sand
SORTING (σ):	402.2	1,920	0.941	1,972	0.980	Moderately Sorted
SKEWNESS (sk):	1.223	-0.074	0.074	0.115	-0.115	Coarse Skewed
KURTOSIS (K):	3.518	2.940	2.940	1.022	1.022	Mesokurtic



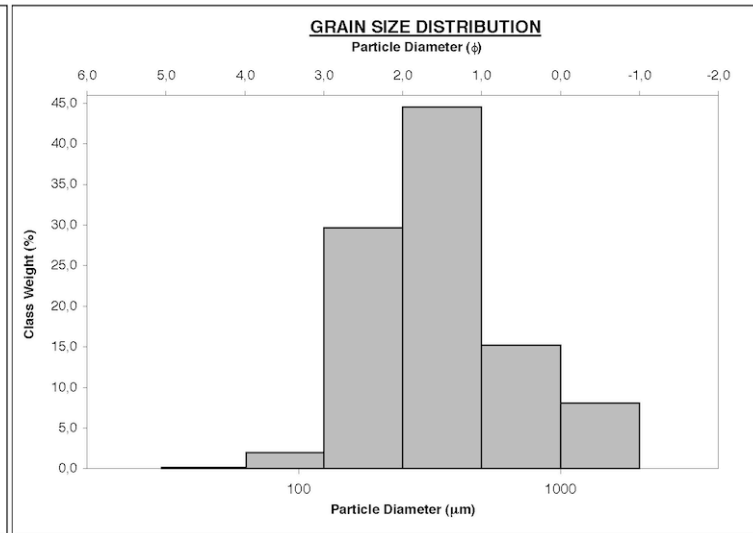
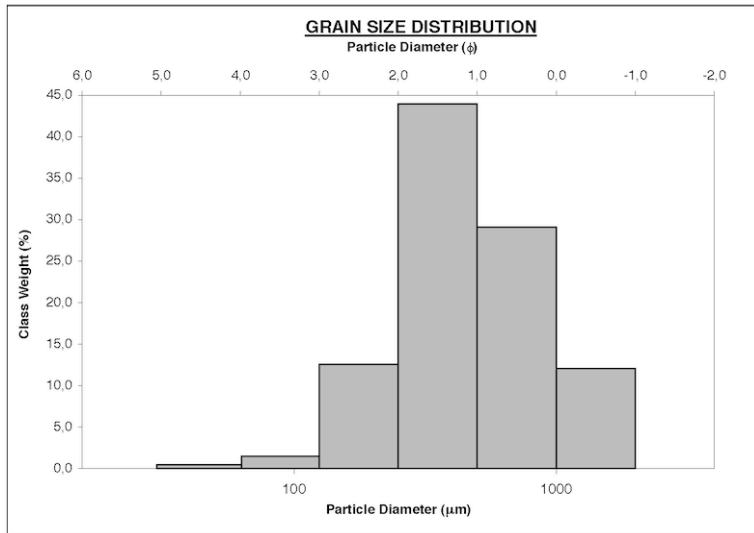
SAMPLE STATISTICS						
SAMPLE IDENTITY: 27		ANALYST & DATE: Seb, 26th Jan 2012				
SAMPLE TYPE: Unimodal, Moderately Sorted		TEXTURAL GROUP: Sand				
SEDIMENT NAME: Moderately Sorted Fine Sand						
	μm	ϕ	GRAIN SIZE DISTRIBUTION			
MODE 1:	187.5	2,500	GRAVEL: 0,0%		COARSE SAND: 10,8%	
MODE 2:			SAND: 99,8%		MEDIUM SAND: 37,5%	
MODE 3:			MUD: 0,2%		FINE SAND: 41,4%	
D ₁₀ :	142,0	0,188	V FINE SAND: 2,2%			
MEDIAN or D ₅₀ :	280,6	1,833	V COARSE GRAVEL: 0,0%		V COARSE SILT: 0,2%	
D ₉₀ :	878,0	2,816	COARSE GRAVEL: 0,0%		COARSE SILT: 0,0%	
(D ₉₀ / D ₁₀):	6,183	15,00	MEDIUM GRAVEL: 0,0%		MEDIUM SILT: 0,0%	
(D ₉₀ - D ₁₀):	736,0	2,628	FINE GRAVEL: 0,0%		FINE SILT: 0,0%	
(D ₇₅ / D ₂₅):	2,439	2,102	V FINE GRAVEL: 0,0%		V FINE SILT: 0,0%	
(D ₇₅ - D ₂₅):	262,8	1,286	V COARSE SAND: 8,0%		CLAY: 0,0%	
	METHOD OF MOMENTS		FOLK & WARD METHOD			
	Arithmetic	Geometric	Logarithmic	Geometric	Logarithmic	Description
	μm	μm	ϕ	μm	ϕ	
MEAN (\bar{x}):	420,8	308,7	1,696	297,3	1,750	Medium Sand
SORTING (σ):	361,3	1,934	0,952	1,976	0,983	Moderately Sorted
SKEWNESS (sk):	2,079	0,753	-0,753	0,232	-0,232	Coarse Skewed
KURTOSIS (K):	6,519	3,157	3,157	1,055	1,055	Mesokurtic

SAMPLE STATISTICS						
SAMPLE IDENTITY: 28		ANALYST & DATE: Seb, 26th Jan 2012				
SAMPLE TYPE: Unimodal, Moderately Sorted		TEXTURAL GROUP: Sand				
SEDIMENT NAME: Moderately Sorted Fine Sand						
	μm	ϕ	GRAIN SIZE DISTRIBUTION			
MODE 1:	187.5	2,500	GRAVEL: 0,0%		COARSE SAND: 9,1%	
MODE 2:			SAND: 99,2%		MEDIUM SAND: 38,5%	
MODE 3:			MUD: 0,8%		FINE SAND: 41,6%	
D ₁₀ :	129,2	0,795	V FINE SAND: 7,3%			
MEDIAN or D ₅₀ :	251,7	1,990	V COARSE GRAVEL: 0,0%		V COARSE SILT: 0,7%	
D ₉₀ :	576,3	2,953	COARSE GRAVEL: 0,0%		COARSE SILT: 0,0%	
(D ₉₀ / D ₁₀):	4,462	3,714	MEDIUM GRAVEL: 0,0%		MEDIUM SILT: 0,0%	
(D ₉₀ - D ₁₀):	447,2	2,158	FINE GRAVEL: 0,0%		FINE SILT: 0,0%	
(D ₇₅ / D ₂₅):	2,380	1,933	V FINE GRAVEL: 0,0%		V FINE SILT: 0,0%	
(D ₇₅ - D ₂₅):	228,9	1,251	V COARSE SAND: 2,8%		CLAY: 0,0%	
	METHOD OF MOMENTS		FOLK & WARD METHOD			
	Arithmetic	Geometric	Logarithmic	Geometric	Logarithmic	Description
	μm	μm	ϕ	μm	ϕ	
MEAN (\bar{x}):	339,4	261,1	1,938	255,5	1,969	Medium Sand
SORTING (σ):	260,6	1,849	0,886	1,873	0,905	Moderately Sorted
SKEWNESS (sk):	2,660	0,322	-0,322	0,070	-0,070	Symmetrical
KURTOSIS (K):	11,63	3,556	3,556	1,038	1,038	Mesokurtic



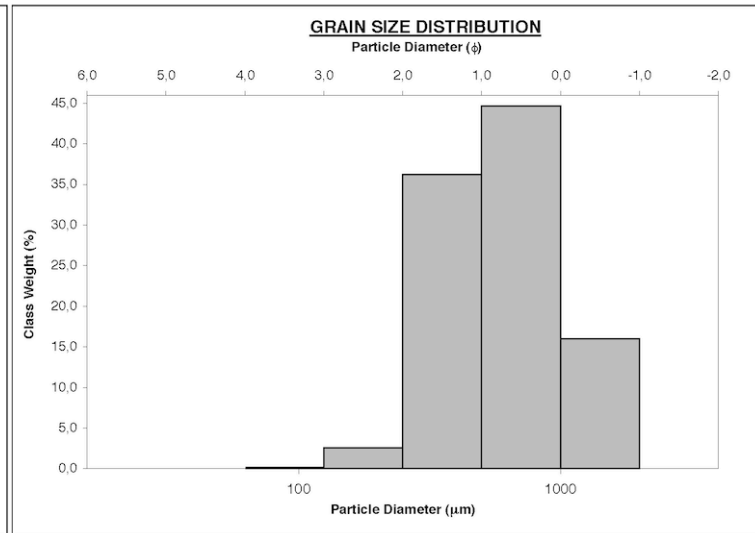
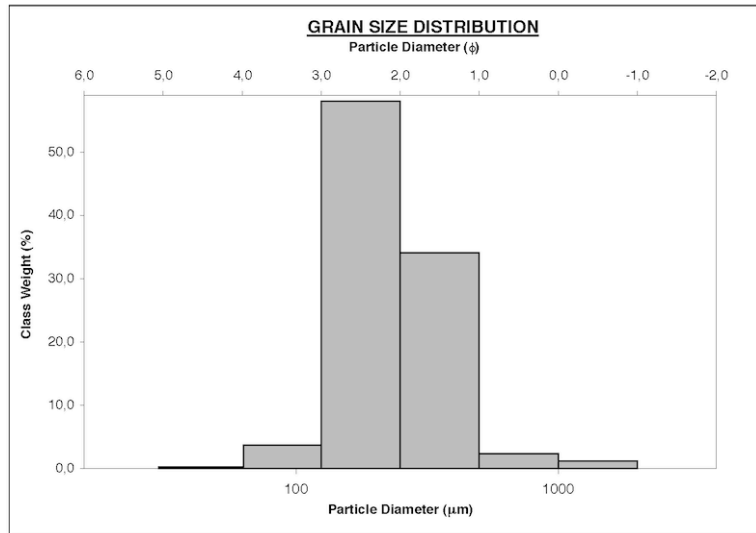
SAMPLE STATISTICS						
SAMPLE IDENTITY: 29		ANALYST & DATE: Seb, 26th Jan 2012				
SAMPLE TYPE: Unimodal, Moderately Sorted		TEXTURAL GROUP: Sand				
SEDIMENT NAME: Moderately Sorted Medium Sand						
GRAIN SIZE DISTRIBUTION						
	μm	ϕ				
MODE 1:	375.0	1,500				
MODE 2:						
MODE 3:						
D ₁₀ :	195.0	-0,173				
MEDIAN or D ₅₀ :	436.2	1,197				
D ₉₀ :	1127.2	2,359				
(D ₉₀ / D ₁₀):	5,781	-13,651				
(D ₉₀ - D ₁₀):	932.3	2,531				
(D ₇₅ / D ₂₅):	2,498	3,988				
(D ₇₅ - D ₂₅):	441.5	1,321				
			GRAVEL: 0,0%	COARSE SAND: 29,2%		
			SAND: 99,6%	MEDIUM SAND: 44,2%		
			MUD: 0,4%	FINE SAND: 12,6%		
			V FINE SAND: 1,5%			
			V COARSE GRAVEL: 0,0%	V COARSE SILT: 0,4%		
			COARSE GRAVEL: 0,0%	COARSE SILT: 0,0%		
			MEDIUM GRAVEL: 0,0%	MEDIUM SILT: 0,0%		
			FINE GRAVEL: 0,0%	FINE SILT: 0,0%		
			V FINE GRAVEL: 0,0%	V FINE SILT: 0,0%		
			V COARSE SAND: 12,1%	CLAY: 0,0%		
METHOD OF MOMENTS						
			FOLK & WARD METHOD			
	Arithmetic	Geometric	Logarithmic	Geometric	Logarithmic	Description
	μm	μm	ϕ	μm	ϕ	
MEAN (\bar{x}):	591,3	455,4	1,135	466,7	1,099	Medium Sand
SORTING (σ):	391,6	1,906	0,931	1,951	0,964	Moderately Sorted
SKEWNESS (sk):	1,275	-0,126	0,126	0,114	-0,114	Coarse Skewed
KURTOSIS (K):	3,751	3,178	3,178	1,036	1,036	Mesokurtic

SAMPLE STATISTICS						
SAMPLE IDENTITY: 30		ANALYST & DATE: Seb, 26th Jan 2012				
SAMPLE TYPE: Unimodal, Poorly Sorted		TEXTURAL GROUP: Sand				
SEDIMENT NAME: Poorly Sorted Medium Sand						
GRAIN SIZE DISTRIBUTION						
	μm	ϕ				
MODE 1:	375.0	1,500				
MODE 2:						
MODE 3:						
D ₁₀ :	150.1	0,126				
MEDIAN or D ₅₀ :	330.7	1,596				
D ₉₀ :	916.1	2,736				
(D ₉₀ / D ₁₀):	6,103	21,65				
(D ₉₀ - D ₁₀):	766.0	2,610				
(D ₇₅ / D ₂₅):	2,289	2,151				
(D ₇₅ - D ₂₅):	274,2	1,195				
			GRAVEL: 0,0%	COARSE SAND: 15,2%		
			SAND: 99,9%	MEDIUM SAND: 44,8%		
			MUD: 0,1%	FINE SAND: 29,8%		
			V FINE SAND: 2,0%			
			V COARSE GRAVEL: 0,0%	V COARSE SILT: 0,1%		
			COARSE GRAVEL: 0,0%	COARSE SILT: 0,0%		
			MEDIUM GRAVEL: 0,0%	MEDIUM SILT: 0,0%		
			FINE GRAVEL: 0,0%	FINE SILT: 0,0%		
			V FINE GRAVEL: 0,0%	V FINE SILT: 0,0%		
			V COARSE SAND: 8,1%	CLAY: 0,0%		
METHOD OF MOMENTS						
			FOLK & WARD METHOD			
	Arithmetic	Geometric	Logarithmic	Geometric	Logarithmic	Description
	μm	μm	ϕ	μm	ϕ	
MEAN (\bar{x}):	461,0	346,7	1,528	341,4	1,551	Medium Sand
SORTING (σ):	358,4	1,905	0,930	2,002	1,001	Poorly Sorted
SKEWNESS (sk):	1,886	0,470	-0,470	0,136	-0,136	Coarse Skewed
KURTOSIS (K):	5,898	2,960	2,960	1,127	1,127	Leptokurtic



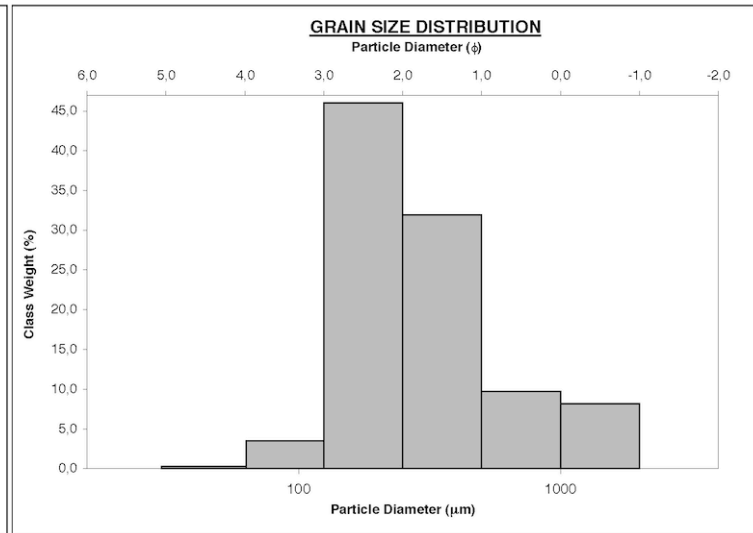
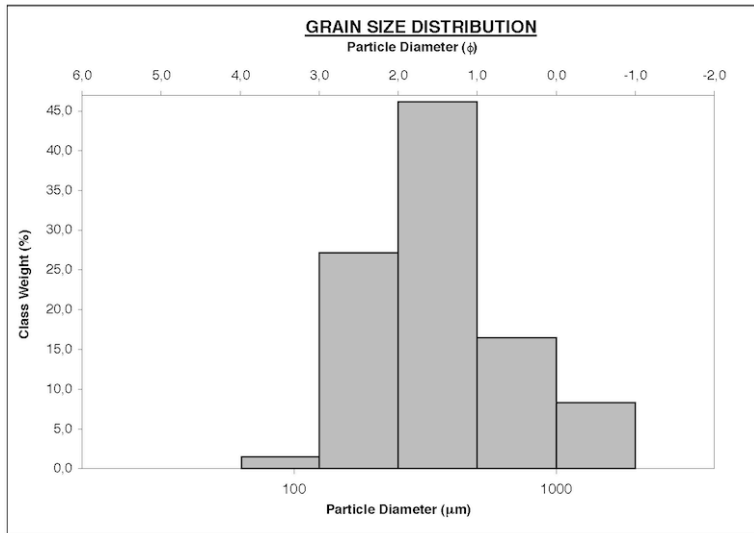
SAMPLE STATISTICS						
SAMPLE IDENTITY: 31		ANALYST & DATE: Seb, 26th Jan 2012				
SAMPLE TYPE: Unimodal, Moderately Well Sorted		TEXTURAL GROUP: Sand				
SEDIMENT NAME: Moderately Well Sorted Fine Sand						
	μm	ϕ	GRAIN SIZE DISTRIBUTION			
MODE 1:	187.5	2,500	GRAVEL: 0,0%	COARSE SAND: 2,4%		
MODE 2:			SAND: 99,7%	MEDIUM SAND: 34,2%		
MODE 3:			MUD: 0,3%	FINE SAND: 58,4%		
D ₁₀ :	134.4	1,189		V FINE SAND: 3,6%		
MEDIAN or D ₅₀ :	216.1	2,210	V COARSE GRAVEL: 0,0%	V COARSE SILT: 0,2%		
D ₉₀ :	438.5	2,895	COARSE GRAVEL: 0,0%	COARSE SILT: 0,0%		
(D ₉₀ / D ₁₀):	3,262	2,434	MEDIUM GRAVEL: 0,0%	MEDIUM SILT: 0,0%		
(D ₉₀ - D ₁₀):	304.1	1,706	FINE GRAVEL: 0,0%	FINE SILT: 0,0%		
(D ₇₅ / D ₂₅):	2,015	1,621	V FINE GRAVEL: 0,0%	V FINE SILT: 0,0%		
(D ₇₅ - D ₂₅):	163,0	1,011	V COARSE SAND: 1,1%	CLAY: 0,0%		
	METHOD OF MOMENTS		FOLK & WARD METHOD			
	Arithmetic	Geometric	Logarithmic	Geometric	Logarithmic	Description
	μm	μm	ϕ	μm	ϕ	
MEAN (\bar{x}):	276.2	230.5	2.117	229.7	2.122	Fine Sand
SORTING (σ):	177.4	1,583	0.663	1,570	0.650	Moderately Well Sorted
SKEWNESS (sk):	4,086	0,758	-0,758	0,194	-0,194	Coarse Skewed
KURTOSIS (K):	26,78	5,028	5,028	0,786	0,786	Platykurtic

SAMPLE STATISTICS						
SAMPLE IDENTITY: 32		ANALYST & DATE: Seb, 26th Jan 2012				
SAMPLE TYPE: Unimodal, Moderately Sorted		TEXTURAL GROUP: Sand				
SEDIMENT NAME: Moderately Sorted Coarse Sand						
	μm	ϕ	GRAIN SIZE DISTRIBUTION			
MODE 1:	750.0	0,500	GRAVEL: 0,0%	COARSE SAND: 44,9%		
MODE 2:			SAND: 100,0%	MEDIUM SAND: 36,4%		
MODE 3:			MUD: 0,0%	FINE SAND: 2,6%		
D ₁₀ :	287.3	-0,375		V FINE SAND: 0,1%		
MEDIAN or D ₅₀ :	591.8	0,757	V COARSE GRAVEL: 0,0%	V COARSE SILT: 0,0%		
D ₉₀ :	1296.8	1,799	COARSE GRAVEL: 0,0%	COARSE SILT: 0,0%		
(D ₉₀ / D ₁₀):	4,513	-4,799	MEDIUM GRAVEL: 0,0%	MEDIUM SILT: 0,0%		
(D ₉₀ - D ₁₀):	1009.5	2,174	FINE GRAVEL: 0,0%	FINE SILT: 0,0%		
(D ₇₅ / D ₂₅):	2,276	6,923	V FINE GRAVEL: 0,0%	V FINE SILT: 0,0%		
(D ₇₅ - D ₂₅):	487,9	1,186	V COARSE SAND: 16,0%	CLAY: 0,0%		
	METHOD OF MOMENTS		FOLK & WARD METHOD			
	Arithmetic	Geometric	Logarithmic	Geometric	Logarithmic	Description
	μm	μm	ϕ	μm	ϕ	
MEAN (\bar{x}):	718.3	590.9	0.759	575.5	0.797	Coarse Sand
SORTING (σ):	385.8	1,689	0.756	1,749	0.806	Moderately Sorted
SKEWNESS (sk):	1,002	0,035	-0,035	0,013	-0,013	Symmetrical
KURTOSIS (K):	3,026	2,537	2,537	0,906	0,906	Mesokurtic



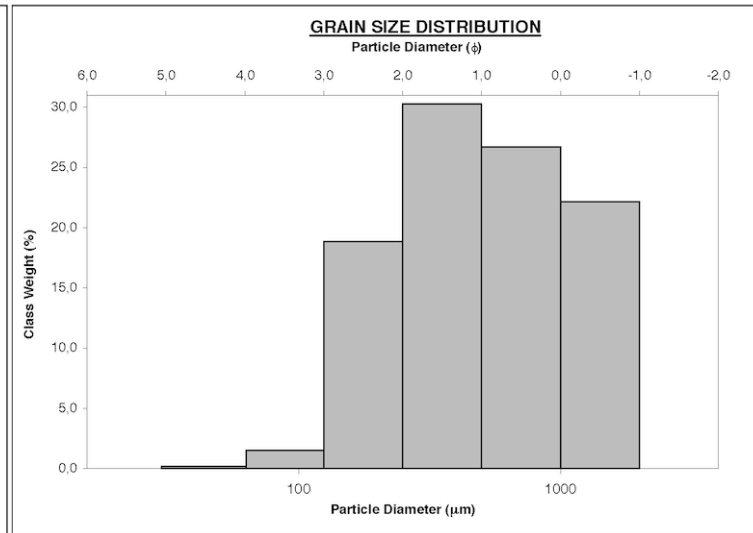
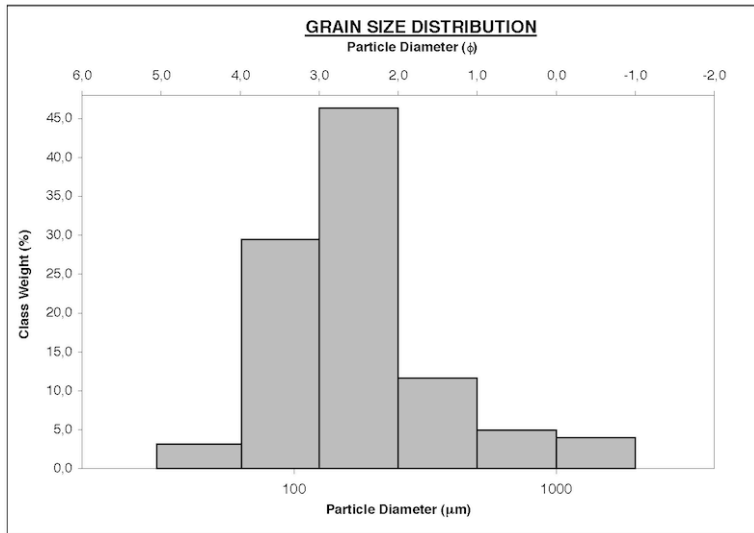
SAMPLE STATISTICS						
SAMPLE IDENTITY: 33		ANALYST & DATE: Seb, 26th Jan 2012				
SAMPLE TYPE: Unimodal, Moderately Sorted		TEXTURAL GROUP: Sand				
SEDIMENT NAME: Moderately Sorted Medium Sand						
	μm	ϕ	GRAIN SIZE DISTRIBUTION			
MODE 1:	375.0	1.500	GRAVEL: 0.0%	COARSE SAND: 16.5%		
MODE 2:			SAND: 100.0%	MEDIUM SAND: 46.4%		
MODE 3:			MUD: 0.0%	FINE SAND: 27.3%		
D ₁₀ :	155.3	0.104		V FINE SAND: 1.4%		
MEDIAN or D ₅₀ :	343.2	1.543	V COARSE GRAVEL: 0.0%	V COARSE SILT: 0.0%		
D ₉₀ :	930.5	2.687	COARSE GRAVEL: 0.0%	COARSE SILT: 0.0%		
(D ₉₀ / D ₁₀):	5.992	25.85	MEDIUM GRAVEL: 0.0%	MEDIUM SILT: 0.0%		
(D ₉₀ - D ₁₀):	775.2	2.583	FINE GRAVEL: 0.0%	FINE SILT: 0.0%		
(D ₇₅ / D ₂₅):	2.194	2.128	V FINE GRAVEL: 0.0%	V FINE SILT: 0.0%		
(D ₇₅ - D ₂₅):	271.2	1.133	V COARSE SAND: 8.3%	CLAY: 0.0%		
	METHOD OF MOMENTS		FOLK & WARD METHOD			
	Arithmetic	Geometric	Logarithmic	Geometric	Logarithmic	Description
	μm	μm	ϕ	μm	ϕ	
MEAN (\bar{x}):	474.8	350.6	1.471	355.4	1.493	Medium Sand
SORTING (σ):	359.0	1.878	0.909	1.993	0.995	Moderately Sorted
SKEWNESS (sk):	1.837	0.491	-0.491	0.131	-0.131	Coarse Skewed
KURTOSIS (K):	5.703	2.850	2.850	1.181	1.181	Leptokurtic

SAMPLE STATISTICS						
SAMPLE IDENTITY: 34		ANALYST & DATE: Seb, 26th Jan 2012				
SAMPLE TYPE: Unimodal, Moderately Sorted		TEXTURAL GROUP: Sand				
SEDIMENT NAME: Moderately Sorted Fine Sand						
	μm	ϕ	GRAIN SIZE DISTRIBUTION			
MODE 1:	187.5	2.500	GRAVEL: 0.0%	COARSE SAND: 9.8%		
MODE 2:			SAND: 99.7%	MEDIUM SAND: 32.0%		
MODE 3:			MUD: 0.3%	FINE SAND: 46.3%		
D ₁₀ :	137.3	0.184		V FINE SAND: 3.5%		
MEDIAN or D ₅₀ :	250.0	2.000	V COARSE GRAVEL: 0.0%	V COARSE SILT: 0.2%		
D ₉₀ :	880.2	2.865	COARSE GRAVEL: 0.0%	COARSE SILT: 0.0%		
(D ₉₀ / D ₁₀):	6.410	15.56	MEDIUM GRAVEL: 0.0%	MEDIUM SILT: 0.0%		
(D ₉₀ - D ₁₀):	742.9	2.680	FINE GRAVEL: 0.0%	FINE SILT: 0.0%		
(D ₇₅ / D ₂₅):	2.498	2.083	V FINE GRAVEL: 0.0%	V FINE SILT: 0.0%		
(D ₇₅ - D ₂₅):	257.5	1.321	V COARSE SAND: 8.2%	CLAY: 0.0%		
	METHOD OF MOMENTS		FOLK & WARD METHOD			
	Arithmetic	Geometric	Logarithmic	Geometric	Logarithmic	Description
	μm	μm	ϕ	μm	ϕ	
MEAN (\bar{x}):	406.5	291.5	1.778	278.4	1.845	Medium Sand
SORTING (σ):	368.6	1.981	0.986	1.991	0.994	Moderately Sorted
SKEWNESS (sk):	2.100	0.810	-0.810	0.331	-0.331	Very Coarse Skewed
KURTOSIS (K):	6.508	3.218	3.218	1.044	1.044	Mesokurtic



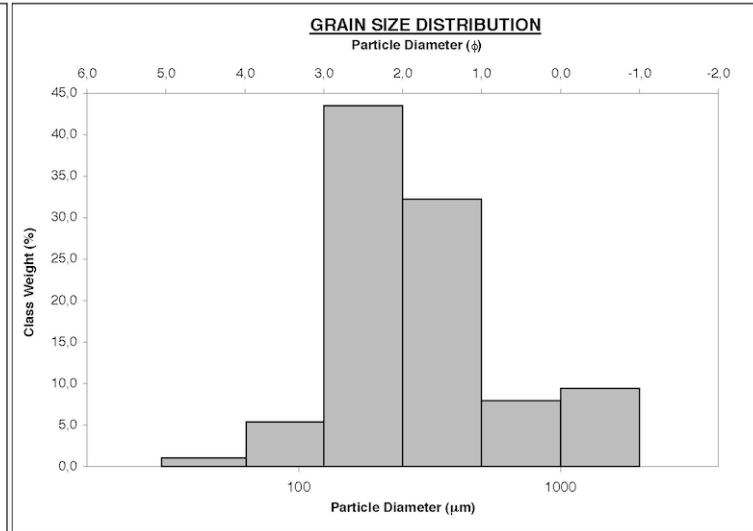
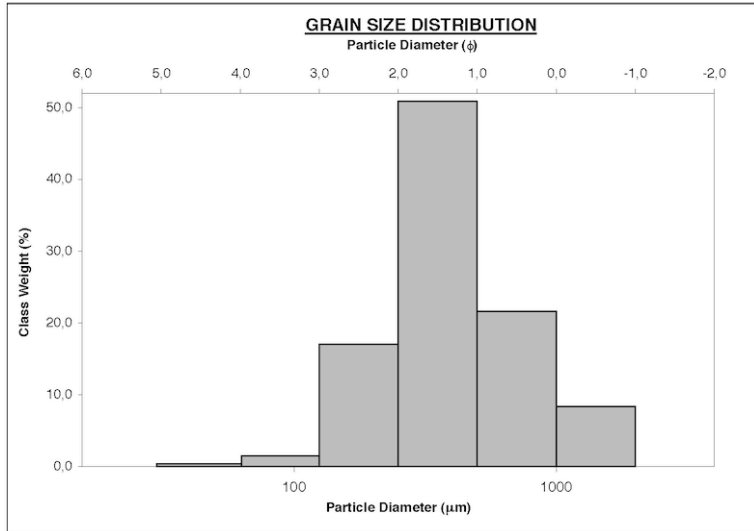
SAMPLE STATISTICS						
SAMPLE IDENTITY: 35		ANALYST & DATE: Seb, 26th Jan 2012				
SAMPLE TYPE: Unimodal, Poorly Sorted		TEXTURAL GROUP: Sand				
SEDIMENT NAME: Poorly Sorted Fine Sand						
		GRAIN SIZE DISTRIBUTION				
	μm	ϕ				
MODE 1:	187.5	2,500				
MODE 2:						
MODE 3:						
D ₁₀ :	73.53	1,085				
MEDIAN or D ₅₀ :	161.7	2,629				
D ₉₀ :	471.2	3,766				
(D ₉₀ / D ₁₀):	6,409	3,469				
(D ₉₀ - D ₁₀):	397.7	2,680				
(D ₇₅ / D ₂₅):	2,246	1,558				
(D ₇₅ - D ₂₅):	130.1	1,167				
			GRAIN SIZE DISTRIBUTION			
			GRAVEL: 0,0%	COARSE SAND: 5,0%		
			SAND: 96,6%	MEDIUM SAND: 11,7%		
			MUD: 3,4%	FINE SAND: 46,6%		
			V FINE SAND: 29,3%			
			V COARSE GRAVEL: 0,0%	V COARSE SILT: 3,2%		
			COARSE GRAVEL: 0,0%	COARSE SILT: 0,2%		
			MEDIUM GRAVEL: 0,0%	MEDIUM SILT: 0,0%		
			FINE GRAVEL: 0,0%	FINE SILT: 0,0%		
			V FINE GRAVEL: 0,0%	V FINE SILT: 0,0%		
			V COARSE SAND: 4,0%	CLAY: 0,0%		
			METHOD OF MOMENTS			
			FOLK & WARD METHOD			
	Arithmetic	Geometric	Logarithmic	Geometric	Logarithmic	Description
	μm	μm	ϕ	μm	ϕ	
MEAN (\bar{x}):	257,8	174,0	2,523	165,3	2,596	Fine Sand
SORTING (σ):	295,0	2,072	1,051	2,080	1,057	Poorly Sorted
SKEWNESS (sk):	3,152	0,950	-0,950	0,175	-0,175	Coarse Skewed
KURTOSIS (K):	12,98	4,183	4,183	1,310	1,310	Leptokurtic

SAMPLE STATISTICS						
SAMPLE IDENTITY: 36		ANALYST & DATE: Seb, 26th Jan 2012				
SAMPLE TYPE: Unimodal, Poorly Sorted		TEXTURAL GROUP: Sand				
SEDIMENT NAME: Poorly Sorted Medium Sand						
		GRAIN SIZE DISTRIBUTION				
	μm	ϕ				
MODE 1:	375.0	1,500				
MODE 2:						
MODE 3:						
D ₁₀ :	169.9	-0,550				
MEDIAN or D ₅₀ :	489.1	1,032				
D ₉₀ :	1464.2	2,558				
(D ₉₀ / D ₁₀):	8,620	-4,649				
(D ₉₀ - D ₁₀):	1294.3	3,108				
(D ₇₅ / D ₂₅):	3,364	17,92				
(D ₇₅ - D ₂₅):	654,1	1,750				
			GRAIN SIZE DISTRIBUTION			
			GRAVEL: 0,0%	COARSE SAND: 26,8%		
			SAND: 99,8%	MEDIUM SAND: 30,4%		
			MUD: 0,2%	FINE SAND: 18,9%		
			V FINE SAND: 1,5%			
			V COARSE GRAVEL: 0,0%	V COARSE SILT: 0,2%		
			COARSE GRAVEL: 0,0%	COARSE SILT: 0,0%		
			MEDIUM GRAVEL: 0,0%	MEDIUM SILT: 0,0%		
			FINE GRAVEL: 0,0%	FINE SILT: 0,0%		
			V FINE GRAVEL: 0,0%	V FINE SILT: 0,0%		
			V COARSE SAND: 22,2%	CLAY: 0,0%		
			METHOD OF MOMENTS			
			FOLK & WARD METHOD			
	Arithmetic	Geometric	Logarithmic	Geometric	Logarithmic	Description
	μm	μm	ϕ	μm	ϕ	
MEAN (\bar{x}):	685,4	496,2	1,011	500,9	0,997	Coarse Sand
SORTING (σ):	480,2	2,124	1,087	2,258	1,175	Poorly Sorted
SKEWNESS (sk):	0,761	-0,122	0,122	0,023	-0,023	Symmetrical
KURTOSIS (K):	2,151	2,109	2,109	0,842	0,842	Platykurtic



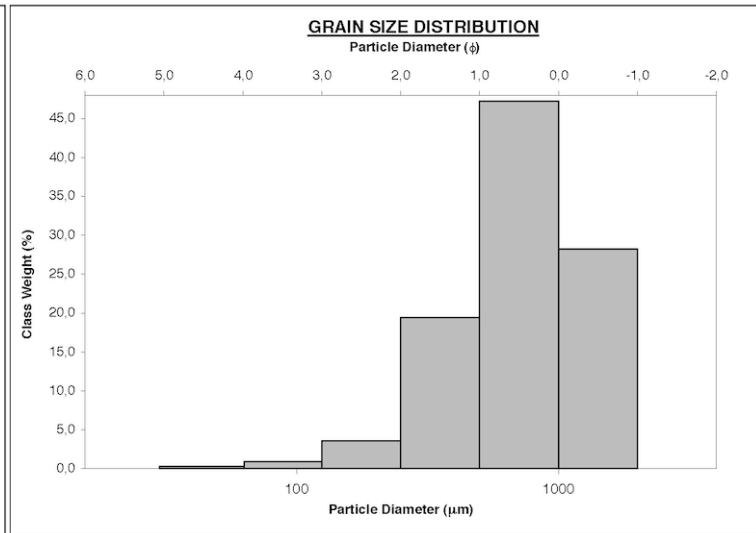
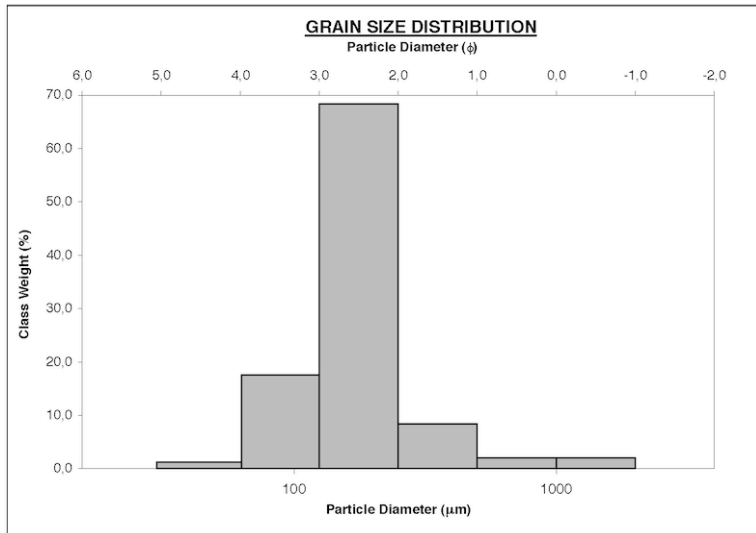
SAMPLE STATISTICS						
SAMPLE IDENTITY: 37		ANALYST & DATE: Seb, 26th Jan 2012				
SAMPLE TYPE: Unimodal, Moderately Sorted		TEXTURAL GROUP: Sand				
SEDIMENT NAME: Moderately Sorted Medium Sand						
	μm	ϕ	GRAIN SIZE DISTRIBUTION			
MODE 1:	375.0	1.500	GRAVEL: 0.0%	COARSE SAND: 21.7%		
MODE 2:			SAND: 99.6%	MEDIUM SAND: 51.1%		
MODE 3:			MUD: 0.4%	FINE SAND: 17.1%		
D ₁₀ :	174.2	0.076		V FINE SAND: 1.4%		
MEDIAN or D ₅₀ :	381.4	1.391	V COARSE GRAVEL: 0.0%	V COARSE SILT: 0.4%		
D ₉₀ :	948.9	2.521	COARSE GRAVEL: 0.0%	COARSE SILT: 0.0%		
(D ₉₀ / D ₁₀):	5.446	33.30	MEDIUM GRAVEL: 0.0%	MEDIUM SILT: 0.0%		
(D ₉₀ - D ₁₀):	774.6	2.445	FINE GRAVEL: 0.0%	FINE SILT: 0.0%		
(D ₇₅ / D ₂₅):	2.163	2.451	V FINE GRAVEL: 0.0%	V FINE SILT: 0.0%		
(D ₇₅ - D ₂₅):	316.0	1.113	V COARSE SAND: 8.4%	CLAY: 0.0%		
	METHOD OF MOMENTS		FOLK & WARD METHOD			
	Arithmetic	Geometric	Logarithmic	Geometric	Logarithmic	Description
	μm	μm	ϕ	μm	ϕ	
MEAN (\bar{x}):	513.1	398.5	1.327	405.0	1.304	Medium Sand
SORTING (σ):	353.3	1.849	0.887	1.920	0.941	Moderately Sorted
SKEWNESS (sk):	1.691	0.107	-0.107	0.129	-0.129	Coarse Skewed
KURTOSIS (K):	5.312	3.405	3.405	1.184	1.184	Leptokurtic

SAMPLE STATISTICS						
SAMPLE IDENTITY: 38		ANALYST & DATE: Seb, 26th Jan 2012				
SAMPLE TYPE: Bimodal, Poorly Sorted		TEXTURAL GROUP: Sand				
SEDIMENT NAME: Poorly Sorted Fine Sand						
	μm	ϕ	GRAIN SIZE DISTRIBUTION			
MODE 1:	187.5	2.500	GRAVEL: 0.0%	COARSE SAND: 8.0%		
MODE 2:	1500.0	-0.500	SAND: 98.9%	MEDIUM SAND: 32.3%		
MODE 3:			MUD: 1.1%	FINE SAND: 43.7%		
D ₁₀ :	132.2	0.070		V FINE SAND: 5.4%		
MEDIAN or D ₅₀ :	249.2	2.005	V COARSE GRAVEL: 0.0%	V COARSE SILT: 1.0%		
D ₉₀ :	952.9	2.920	COARSE GRAVEL: 0.0%	COARSE SILT: 0.1%		
(D ₉₀ / D ₁₀):	7.211	41.96	MEDIUM GRAVEL: 0.0%	MEDIUM SILT: 0.0%		
(D ₉₀ - D ₁₀):	820.8	2.850	FINE GRAVEL: 0.0%	FINE SILT: 0.0%		
(D ₇₅ / D ₂₅):	2.537	2.089	V FINE GRAVEL: 0.0%	V FINE SILT: 0.0%		
(D ₇₅ - D ₂₅):	257.6	1.343	V COARSE SAND: 9.4%	CLAY: 0.0%		
	METHOD OF MOMENTS		FOLK & WARD METHOD			
	Arithmetic	Geometric	Logarithmic	Geometric	Logarithmic	Description
	μm	μm	ϕ	μm	ϕ	
MEAN (\bar{x}):	410.5	285.4	1.809	273.8	1.869	Medium Sand
SORTING (σ):	387.7	2.079	1.056	2.082	1.058	Poorly Sorted
SKEWNESS (sk):	2.027	0.620	-0.620	0.265	-0.265	Coarse Skewed
KURTOSIS (K):	6.015	3.265	3.265	1.142	1.142	Leptokurtic



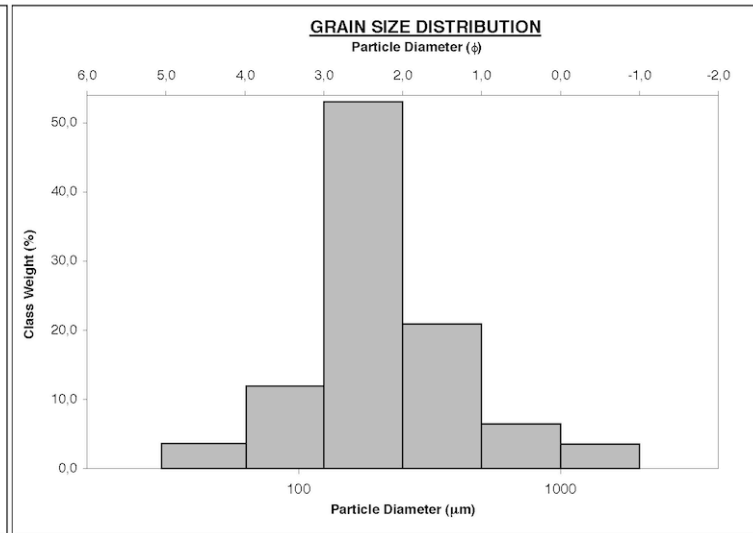
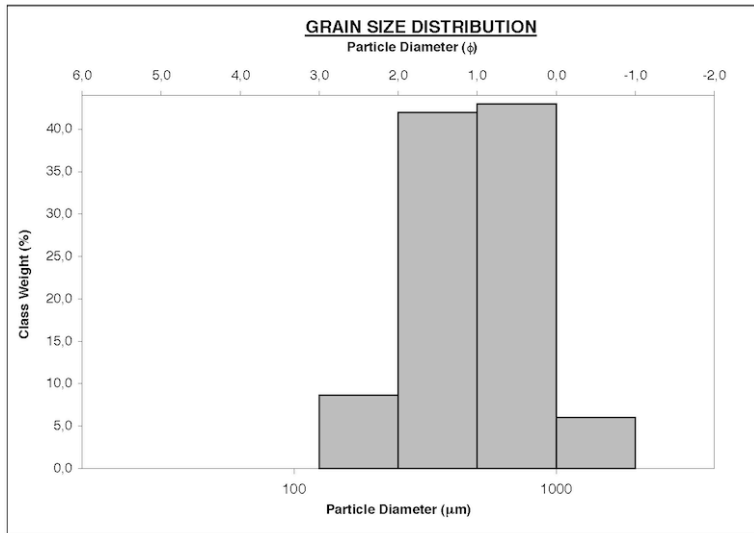
SAMPLE STATISTICS						
SAMPLE IDENTITY: 39		ANALYST & DATE: Seb, 26th Jan 2012				
SAMPLE TYPE: Unimodal, Moderately Well Sorted		TEXTURAL GROUP: Sand				
SEDIMENT NAME: Moderately Well Sorted Fine Sand						
	μm	ϕ	GRAIN SIZE DISTRIBUTION			
MODE 1:	187.5	2.500	GRAVEL: 0.0%		COARSE SAND: 2.0%	
MODE 2:			SAND: 98.8%		MEDIUM SAND: 8.5%	
MODE 3:			MUD: 1.2%		FINE SAND: 68.7%	
D ₁₀ :	88.67	1.705	V FINE SAND: 17.5%			
MEDIAN or D ₅₀ :	171.3	2.546	V COARSE GRAVEL: 0.0%		V COARSE SILT: 1.2%	
D ₉₀ :	306.8	3.495	COARSE GRAVEL: 0.0%		COARSE SILT: 0.1%	
(D ₉₀ / D ₁₀):	3.460	2.050	MEDIUM GRAVEL: 0.0%		MEDIUM SILT: 0.0%	
(D ₉₀ - D ₁₀):	218.1	1.791	FINE GRAVEL: 0.0%		FINE SILT: 0.0%	
(D ₇₅ / D ₂₅):	1.656	1.333	V FINE GRAVEL: 0.0%		V FINE SILT: 0.0%	
(D ₇₅ - D ₂₅):	87.29	0.728	V COARSE SAND: 2.0%		CLAY: 0.0%	
	METHOD OF MOMENTS		FOLK & WARD METHOD			
	Arithmetic	Geometric	Logarithmic	Geometric	Logarithmic	Description
	μm	μm	ϕ	μm	ϕ	
MEAN (\bar{x}):	222.8	175.0	2.515	166.7	2.585	Fine Sand
SORTING (σ):	210.2	1.687	0.755	1.602	0.680	Moderately Well Sorted
SKEWNESS (sk):	4.756	1.239	-1.239	-0.015	0.015	Symmetrical
KURTOSIS (K):	27.91	7.493	7.493	1.500	1.500	Very Leptokurtic

SAMPLE STATISTICS						
SAMPLE IDENTITY: 40		ANALYST & DATE: Seb, 26th Jan 2012				
SAMPLE TYPE: Unimodal, Moderately Sorted		TEXTURAL GROUP: Sand				
SEDIMENT NAME: Moderately Sorted Coarse Sand						
	μm	ϕ	GRAIN SIZE DISTRIBUTION			
MODE 1:	750.0	0.500	GRAVEL: 0.0%		COARSE SAND: 47.5%	
MODE 2:			SAND: 99.7%		MEDIUM SAND: 19.5%	
MODE 3:			MUD: 0.3%		FINE SAND: 3.6%	
D ₁₀ :	301.8	-0.647	V FINE SAND: 0.9%			
MEDIAN or D ₅₀ :	728.9	0.456	V COARSE GRAVEL: 0.0%		V COARSE SILT: 0.2%	
D ₉₀ :	1566.1	1.728	COARSE GRAVEL: 0.0%		COARSE SILT: 0.0%	
(D ₉₀ / D ₁₀):	5.189	-2.670	MEDIUM GRAVEL: 0.0%		MEDIUM SILT: 0.0%	
(D ₉₀ - D ₁₀):	1264.3	2.375	FINE GRAVEL: 0.0%		FINE SILT: 0.0%	
(D ₇₅ / D ₂₅):	2.145	-8.326	V FINE GRAVEL: 0.0%		V FINE SILT: 0.0%	
(D ₇₅ - D ₂₅):	579.3	1.101	V COARSE SAND: 28.3%		CLAY: 0.0%	
	METHOD OF MOMENTS		FOLK & WARD METHOD			
	Arithmetic	Geometric	Logarithmic	Geometric	Logarithmic	Description
	μm	μm	ϕ	μm	ϕ	
MEAN (\bar{x}):	861.9	697.7	0.519	716.8	0.480	Coarse Sand
SORTING (σ):	436.7	1.816	0.861	1.852	0.889	Moderately Sorted
SKEWNESS (sk):	0.411	-0.875	0.875	-0.064	0.064	Symmetrical
KURTOSIS (K):	1.914	4.352	4.352	1.045	1.045	Mesokurtic



SAMPLE STATISTICS						
SAMPLE IDENTITY: 41		ANALYST & DATE: Seb, 26th Jan 2012				
SAMPLE TYPE: Unimodal, Moderately Sorted		TEXTURAL GROUP: Sand				
SEDIMENT NAME: Moderately Sorted Coarse Sand						
	μm	ϕ	GRAIN SIZE DISTRIBUTION			
MODE 1:	750.0	0.500	GRAVEL: 0.0%	COARSE SAND: 43.2%		
MODE 2:			SAND: 100.0%	MEDIUM SAND: 42.1%		
MODE 3:			MUD: 0.0%	FINE SAND: 8.7%		
D ₁₀ :	255.5	0.092		V FINE SAND: 0.0%		
MEDIAN or D ₅₀ :	493.4	1.019	V COARSE GRAVEL: 0.0%	V COARSE SILT: 0.0%		
D ₉₀ :	938.2	1.969	COARSE GRAVEL: 0.0%	COARSE SILT: 0.0%		
(D ₉₀ / D ₁₀):	3.673	21.40	MEDIUM GRAVEL: 0.0%	MEDIUM SILT: 0.0%		
(D ₉₀ - D ₁₀):	682.8	1.877	FINE GRAVEL: 0.0%	FINE SILT: 0.0%		
(D ₇₅ / D ₂₅):	2.255	3.669	V FINE GRAVEL: 0.0%	V FINE SILT: 0.0%		
(D ₇₅ - D ₂₅):	410.4	1.173	V COARSE SAND: 6.0%	CLAY: 0.0%		
	METHOD OF MOMENTS		FOLK & WARD METHOD			
	Arithmetic	Geometric	Logarithmic	Geometric	Logarithmic	Description
	μm	μm	ϕ	μm	ϕ	
MEAN (\bar{x}):	588.4	488.1	1.035	491.2	1.026	Medium Sand
SORTING (σ):	307.4	1.667	0.737	1.731	0.792	Moderately Sorted
SKEWNESS (sk):	1.301	-0.079	0.079	-0.047	0.047	Symmetrical
KURTOSIS (K):	5.043	2.678	2.678	0.907	0.907	Mesokurtic

SAMPLE STATISTICS						
SAMPLE IDENTITY: 42		ANALYST & DATE: Seb, 26th Jan 2012				
SAMPLE TYPE: Unimodal, Moderately Sorted		TEXTURAL GROUP: Sand				
SEDIMENT NAME: Moderately Sorted Fine Sand						
	μm	ϕ	GRAIN SIZE DISTRIBUTION			
MODE 1:	187.5	2.500	GRAVEL: 0.0%	COARSE SAND: 6.5%		
MODE 2:			SAND: 96.2%	MEDIUM SAND: 21.0%		
MODE 3:			MUD: 3.8%	FINE SAND: 53.2%		
D ₁₀ :	90.06	0.989		V FINE SAND: 11.9%		
MEDIAN or D ₅₀ :	195.5	2.355	V COARSE GRAVEL: 0.0%	V COARSE SILT: 3.6%		
D ₉₀ :	503.8	3.473	COARSE GRAVEL: 0.0%	COARSE SILT: 0.2%		
(D ₉₀ / D ₁₀):	5.594	3.512	MEDIUM GRAVEL: 0.0%	MEDIUM SILT: 0.0%		
(D ₉₀ - D ₁₀):	413.8	2.484	FINE GRAVEL: 0.0%	FINE SILT: 0.0%		
(D ₇₅ / D ₂₅):	2.165	1.652	V FINE GRAVEL: 0.0%	V FINE SILT: 0.0%		
(D ₇₅ - D ₂₅):	164.5	1.114	V COARSE SAND: 3.6%	CLAY: 0.0%		
	METHOD OF MOMENTS		FOLK & WARD METHOD			
	Arithmetic	Geometric	Logarithmic	Geometric	Logarithmic	Description
	μm	μm	ϕ	μm	ϕ	
MEAN (\bar{x}):	293.8	210.5	2.248	216.1	2.210	Fine Sand
SORTING (σ):	282.5	2.001	1.001	1.978	0.984	Moderately Sorted
SKEWNESS (sk):	2.954	0.484	-0.484	0.208	-0.208	Coarse Skewed
KURTOSIS (K):	12.34	4.008	4.008	1.350	1.350	Leptokurtic



Groundtruthing data summary

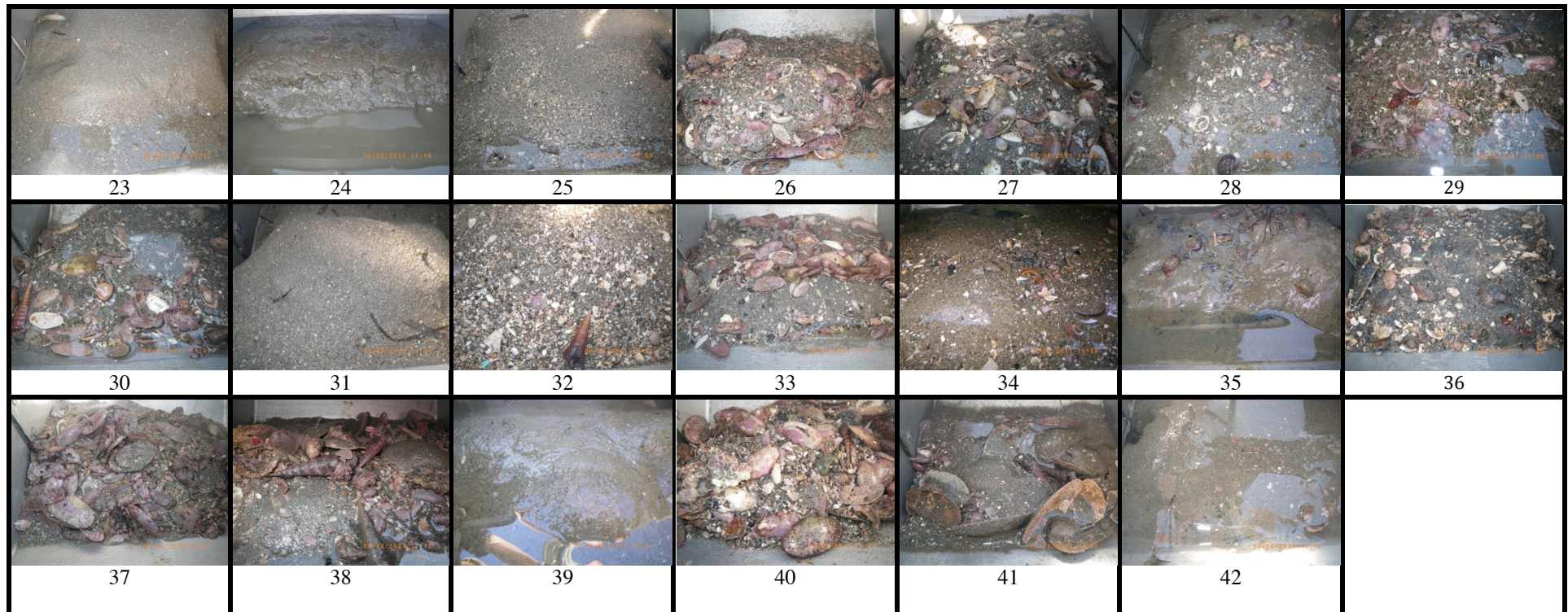
Site	X (NZTM)	Y (NZTM)	Water Depth (m)	Shell Coverage Class	Sediment Class	Sorting	Skewness	MALVERN Laser-size Percentage				Dry Sieving (excluding the gravel fraction) Percentage					
								Clay	Silt	Sand	Mean Grain Size	Very coarse sand	Coarse sand	Medium sand	Fine sand	Very fine sand	Silt and clay
1	1880197.937	5827259.754	-12.91	Rippled Sand	Fine Sand	Moderately Sorted	Coarse Skewed	2.42	6.60	90.97	0.449	3.40	4.15	17.84	62.57	9.09	2.95
2	1880347.936	5827253.349	-13.39	Shelly Sand	Medium Sand	Poorly Sorted	Coarse Skewed	17.43	38.57	44.00	0.542	8.72	12.63	29.67	33.90	11.24	3.84
3	1880497.935	5827246.943	-12.93	Sand	Fine Sand	Moderately Sorted	Coarse Skewed	2.59	7.17	90.24	0.51	3.90	4.76	17.05	55.65	15.61	3.04
4	1880116.533	5827112.958	-14.32	Shelly Sand	Medium Sand	Poorly Sorted	Coarse Skewed	0.79	3.81	95.40	0.707	7.04	12.44	28.13	44.47	6.22	1.69
5	1880266.531	5827106.552	-13.96	Shelly Sand	Medium Sand	Poorly Sorted	Very Coarse Skewed	13.07	35.68	51.25	0.409	14.44	14.38	9.62	33.54	26.67	1.35
6	1880416.53	5827100.147	-13.10	Sand	Fine Sand	Moderately Sorted	Coarse Skewed	1.59	4.85	93.56	0.558	2.82	7.34	28.28	47.15	12.10	2.32
7	1880566.529	5827093.742	-11.62	Sand	Fine Sand	Poorly Sorted	Symmetrical	3.76	11.07	85.17	0.35	3.31	4.39	8.70	54.60	20.21	8.79
8	1880185.127	5826959.756	-13.79	Shelly Sand	Medium Sand	Poorly Sorted	Coarse Skewed	1.49	5.24	93.27	0.702	8.23	15.51	21.70	42.49	9.39	2.67
9	1880335.125	5826953.351	-13.08	Sand	Fine Sand	Moderately Sorted	Coarse Skewed	2.07	5.86	92.07	0.491	3.78	5.61	22.24	56.13	10.20	2.04
10	1880485.124	5826946.945	-13.01	Sand	Fine Sand	Moderately Sorted	Symmetrical	2.27	7.55	90.18	0.365	3.05	3.36	9.09	44.92	33.40	6.18
11	1880103.722	5826812.961	-15.18	Sand	Very Fine Sand	Poorly Sorted	Coarse Skewed	5.36	26.12	68.52	0.354	6.47	5.58	6.43	22.93	28.23	30.36
12	1880253.72	5826806.555	-13.19	Shelly Sand	Medium Sand	Poorly Sorted	Coarse Skewed	0.68	3.06	96.26	0.855	12.52	17.96	23.63	38.91	6.16	0.81
13	1880403.719	5826800.149	-13.40	Sand	Fine Sand	Poorly Sorted	Coarse Skewed	2.28	7.90	89.82	0.455	5.56	4.53	14.54	49.71	19.15	6.50
14	1880553.718	5826793.743	-8.92	Sand	Fine Sand	Poorly Sorted	Coarse Skewed	7.41	25.61	66.98	0.266	8.05	5.47	12.02	49.04	20.86	4.55
15	1880172.315	5826659.759	-13.00	Sand	Fine Sand	Moderately Sorted	Coarse Skewed	0.73	4.09	95.18	0.466	3.02	4.28	17.02	55.92	16.48	3.28

Site	X (NZTM)	Y (NZTM)	Water Depth (m)	Shell Coverage Class	Sediment Class	Sorting	Skewness	MALVERN Laser-size Percentage				Dry Sieving (excluding the gravel fraction) Percentage					
								Clay	Silt	Sand	Mean Grain Size	Very coarse sand	Coarse sand	Medium sand	Fine sand	Very fine sand	Silt and clay
16	1880322.314	5826653.353	-12.94	Sand	Fine Sand	Moderately Sorted	Symmetrical	3.26	13.57	83.17	0.385	3.19	2.59	10.18	54.58	21.99	7.47
17	1880472.313	5826646.947	-13.30	Sand	Fine Sand	Poorly Sorted	Symmetrical	3.48	10.97	85.55	0.411	3.76	2.86	8.81	42.49	30.30	11.78
18	1880090.91	5826512.964	-5.95	Very Shelly Sand	Medium Sand	Poorly Sorted	Coarse Skewed	0.12	1.41	98.46	0.839	11.76	20.66	36.17	29.40	1.86	0.14
19	1880240.908	5826506.557	-9.03	Sand	Fine Sand	Poorly Sorted	Coarse Skewed	1.52	4.15	94.33	0.431	3.52	3.59	18.10	51.22	19.06	4.51
20	1880390.907	5826500.151	-12.41	Sand	Fine Sand	Poorly Sorted	Coarse Skewed	8.03	20.29	71.68	0.328	5.61	4.72	14.41	45.86	21.65	7.76
21	1880009.504	5826366.168	-7.08	Very Shelly Sand	Medium Sand	Poorly Sorted	Coarse Skewed	0.00	0.00	100.00	0.884	13.11	19.23	38.24	25.05	3.98	0.39
22	1880159.503	5826359.762	-4.32	Shell Lag	Medium Sand	Poorly Sorted	Coarse Skewed	0.26	2.17	97.57	0.914	8.54	16.87	47.39	23.34	3.28	0.59
23	1880309.501	5826353.356	-5.95	Sand	Fine Sand	Moderately Sorted	Coarse Skewed	0.83	3.51	95.67	0.486	3.29	2.41	13.28	65.48	13.87	1.66
24	1880459.5	5826346.949	-4.89	Sand	Fine Sand	Poorly Sorted	Symmetrical	4.19	10.93	84.88	0.309	5.38	2.52	5.73	43.78	32.22	10.36
25	1879928.099	5826219.373	-4.92	Rippled Sand	Fine Sand	Moderately Sorted	Coarse Skewed	0.00	1.00	99.00	0.715	3.13	6.98	29.75	46.85	10.51	2.78
26	1880078.097	5826212.967	-4.44	Shell Lag	Medium Sand	Moderately Sorted	Coarse Skewed	36.21	62.52	1.27	0.023	13.16	28.84	43.21	12.98	1.52	0.29
27	1880228.096	5826206.56	-2.99	Rippled Sand	Medium Sand	Moderately Sorted	Coarse Skewed	0.13	1.02	98.85	0.715	7.98	10.76	37.51	41.36	2.22	0.17
28	1880378.094	5826200.154	-6.39	Shelly Sand	Medium Sand	Moderately Sorted	Symmetrical	37.33	62.65	0.02	0.017	2.78	9.08	38.52	41.59	7.27	0.76
29	1879996.691	5826066.172	-4.66	Very Shelly Sand	Medium Sand	Moderately Sorted	Coarse Skewed	46.47	43.98	9.55	0.022	12.09	29.21	44.17	12.65	1.45	0.44
30	1880146.69	5826059.765	-3.34	Shell Lag	Medium Sand	Poorly Sorted	Coarse Skewed	51.54	48.46	0.00	0.011	8.08	15.22	44.76	29.81	1.99	0.14
31	1880294.572	5826035.366	-3.17	Rippled Sand	Fine Sand	Moderately Well Sorted	Coarse Skewed	54.08	37.71	8.04	0.043	1.12	2.39	34.23	58.37	3.63	0.25
32	1879915.285	5825919.377	-5.68	Sand	Coarse Sand	Moderately Sorted	Symmetrical	0.53	2.02	97.44	1.105	16.00	44.93	36.37	2.55	0.14	0.00
33	1880065.284	5825912.97	-3.84	Shell Lag	Medium Sand	Moderately Sorted	Coarse Skewed	0.05	0.76	99.19	0.841	8.28	16.50	46.45	27.32	1.45	0.00

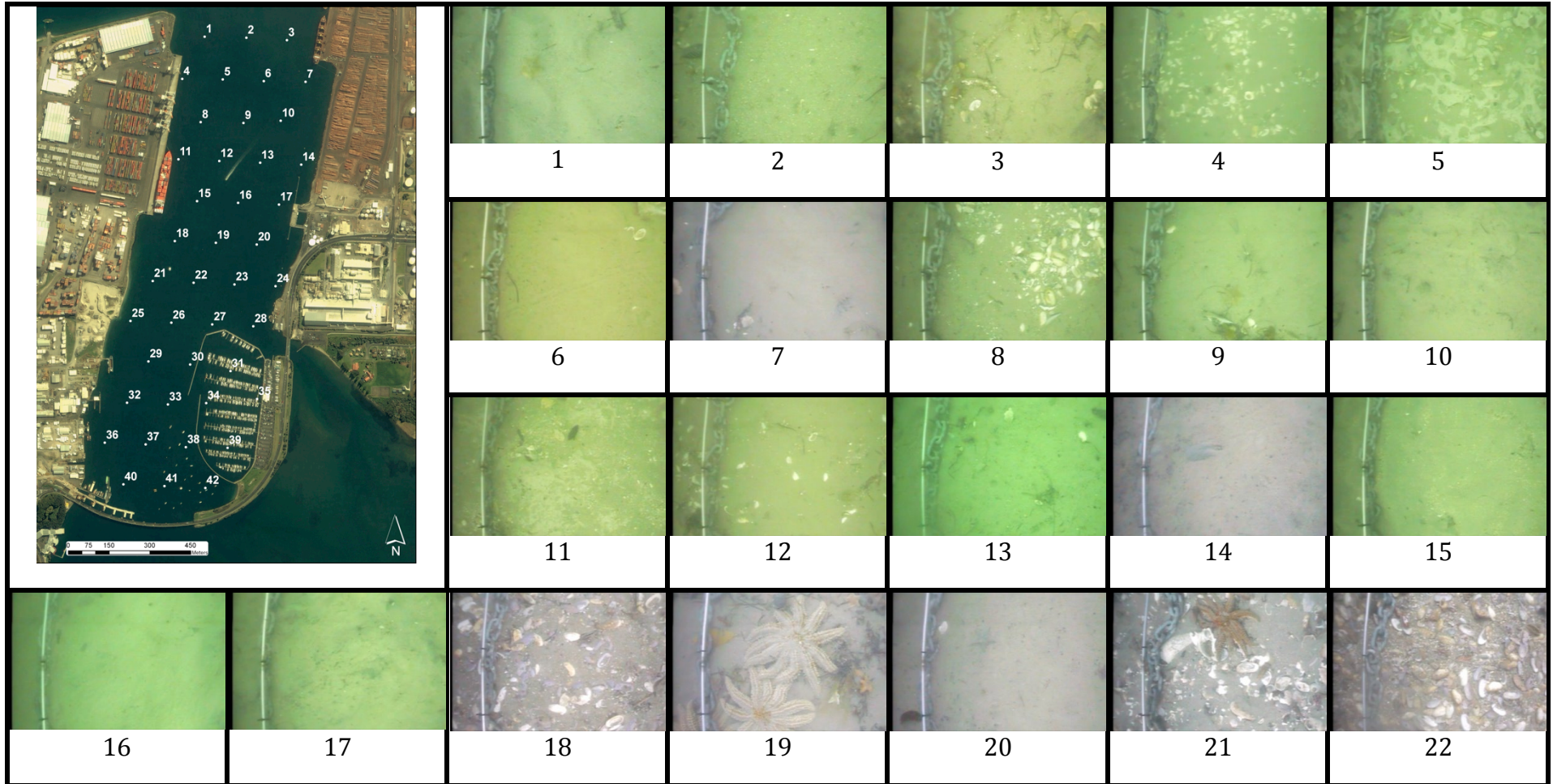
Site	X (NZTM)	Y (NZTM)	Water Depth (m)	Shell Coverage Class	Sediment Class	Sorting	Skewness	MALVERN Laser-size Percentage				Dry Sieving (excluding the gravel fraction) Percentage					
								Clay	Silt	Sand	Mean Grain Size	Very coarse sand	Coarse sand	Medium sand	Fine sand	Very fine sand	Silt and clay
34	1880205.757	5825918.204	-3.04	Rippled Sand	Medium Sand	Moderately Sorted	Very Coarse Skewed	0.26	2.41	97.34	0.601	8.20	9.76	32.03	46.27	3.47	0.26
35	1880392.401	5825933.229	-3.70	Sand	Fine Sand	Poorly Sorted	Coarse Skewed	6.30	12.24	81.46	0.401	3.99	5.01	11.71	46.59	29.30	3.39
36	1879833.879	5825772.582	-3.88	Very Shelly Sand	Coarse Sand	Poorly Sorted	Symmetrical	0.79	2.94	96.27	0.836	22.23	26.80	30.42	18.91	1.46	0.17
37	1879983.877	5825766.175	-3.86	Shell Lag	Medium Sand	Moderately Sorted	Coarse Skewed	0.75	2.58	96.68	0.861	8.36	21.69	51.06	17.07	1.40	0.42
38	1880133.876	5825759.768	-3.53	Shell Lag	Medium Sand	Poorly Sorted	Coarse Skewed	0.45	3.39	96.16	0.638	9.44	8.00	32.34	43.72	5.39	1.10
39	1880283.874	5825753.361	-2.64	Sand	Fine Sand	Moderately Well Sorted	Symmetrical	3.74	9.73	86.53	0.361	1.99	2.05	8.47	68.72	17.53	1.26
40	1879902.471	5825619.38	-5.43	Shell Lag	Coarse Sand	Moderately Sorted	Symmetrical	0.05	1.85	98.11	1.281	28.35	47.47	19.48	3.57	0.87	0.26
41	1880052.469	5825612.973	-4.99	Shell Lag	Medium Sand	Moderately Sorted	Symmetrical	0.26	3.29	96.45	0.572	6.03	43.16	42.13	8.68	0.00	0.00
42	1880202.468	5825606.566	-2.52	Sand	Fine Sand	Moderately Sorted	Coarse Skewed	2.15	6.96	90.88	0.528	3.56	6.51	21.02	53.25	11.83	3.83





















Sediment Grab Samples





Underwater Videos Snapshots



						
23	24	25	26	27	28	29
						
30	31	32	33	34	35	36
						
37	38	39	40	41	42	

